marine drugs

Special Issue Reprint

Bio-Active Products from Mangrove Ecosystems 2.0

Edited by
Jing Xu

mdpi.com/journal/marinedrugs

MDPI

Bio-Active Products from Mangrove Ecosystems 2.0

Bio-Active Products from Mangrove Ecosystems 2.0

Guest Editor

Jing Xu

MDPI

Basel • Beijing • Wuhan • Barcelona • Belgrade • Novi Sad • Cluj • Manchester

Guest Editor
Jing Xu
School of Marine Technology
and Equipment
Hainan University
Haikou
China

Editorial Office
MDPI AG
Grosspeteranlage 5
4052 Basel, Switzerland

This is a reprint of the Special Issue, published open access by the journal *Marine Drugs* (ISSN 1660-3397), freely accessible at: https://www.mdpi.com/journal/marinedrugs/special_issues/2C411Y6K8S.

For citation purposes, cite each article independently as indicated on the article page online and as indicated below:

Lastname, A.A.; Lastname, B.B. Article Title. *Journal Name* **Year**, *Volume Number*, Page Range.

ISBN 978-3-7258-8561-9 (Hbk)
ISBN 978-3-7258-8562-6 (PDF)
https://doi.org/10.3390/books978-3-7258-8562-6

Contents

About the Editor

Jing Xu

Jing Xu is currently a professor of School of Marine Technology and Equipment at Hainan University. She obtained her BS and MS degrees from Hainan University. Following since 2006, she has carried out doctoral research with Professor Huashi Guan at the College of Medicine and Pharmaceutics, Ocean University of China. Since 2007, she continued with a doctoral research in the group of Prof. Peter Proksch and received her PhD degree in 2010 at Heinrich-Heine-Universität Düsseldorf, Germany, where she sparked an interest in mangrove microbial natural products with a particular focus on bioactive molecules which has continued to this day. She joined the faculty of Hainan University after her graduation where she is currently a Professor on Pharmaceutical Chemistry. She undertook postdoctoral appointment in Nanjing University simultaneously, with Prof. Renxiang Tan during 2011–2014. 2016 was spent working with Prof. Dr. Peter Leadley at University of Cambridge as visiting scholar.

Preface

Following the resounding success of the first Special Issue, "Bio-active Products from Mangrove Ecosystems," this second volume, "Bio-Active Products from Mangrove Ecosystems 2.0," continues to explore the immense chemical and pharmaceutical potential harbored within these unique coastal environments. Mangrove ecosystems, positioned at the dynamic interface between terrestrial and marine realms, remain a vibrant tapestry of biodiversity. The ongoing emergence of drug-resistant pathogens and the relentless demand for novel therapeutic agents underscore the critical need to continually mine these ecological niches for structurally unique and pharmaceutically potent natural products. This new collection reaffirms the mangrove ecosystem as an inexhaustible reservoir for lead discovery and drug development, while also deepening our understanding of the chemical ecology and biosynthetic capabilities of its resident organisms.

This Special Issue presents six peer-reviewed articles, comprising two comprehensive reviews and four original research papers, that collectively showcase the remarkable progress made in the field up to mid-2024. The contributions highlight not only the isolation of new compounds with privileged scaffolds, such as polyketides, meroterpenoids, naphthalene derivatives, and macrolactins, but also delve into their potent bioactivities, including antimicrobial, cytotoxic, anti-proliferative, and enzyme inhibitory properties. Herein, we provide a brief overview of the main achievements contributed by the authors of this volume.

The review by Yu et al. offers a timely and systematic overview of novel secondary metabolites from mangrove-associated microorganisms, covering the period from January 2021 to May 2024. This comprehensive analysis examines 41 microbial strains that collectively yielded 165 distinct compounds. The authors underscore the predominant role of fungi as the primary contributors to this chemical diversity, highlighting the remarkable productivity and untapped potential of microbial populations within mangrove ecosystems for bioprospecting endeavors.

In a parallel review, Luo et al. meticulously compiled approximately 496 compounds derived from the Bruguiera genus and its associated endophytes. This extensive inventory includes terpenoids, steroids, alkaloids, quinones, polyketides, and flavonoids, among others. Notably, 201 of these compounds exhibited a spectrum of biological activities, including cytotoxic, antimicrobial, antioxidant, and anti-inflammatory effects. The review authors also discuss the intriguing phenomenon of similar compounds being present in both the host plants and their endophytes, providing valuable insights into their interaction relationships and offering promising lead compounds for drug discovery.

The original research articles included in this volume present exciting new discoveries from diverse mangrove-derived fungi. Xu et al. reported five new naphthalene derivatives, dalesconosides A–D and F, from the endophytic fungus Daldinia eschscholzii MCZ-18, isolated from the mangrove plant Ceriops tagal. These compounds feature rare structural moieties, such as a ribofuranoside substitution. Their findings revealed that several of these derivatives, alongside known compounds, exhibited broad-spectrum antimicrobial activity against clinically relevant pathogens, including methicillin-resistant Staphylococcus aureus and Candida albicans, providing fresh insights into structure–activity relationships for this compound class.

Wang et al. isolated two new meroterpenoids and a new α-pyrone derivative from the endophytic fungal strain *Aspergillus* sp. GXNU-Y85. The absolute configurations of these new isolates were rigorously established through extensive spectroscopic and ECD analyses. Pharmacological evaluation revealed that some known compounds co-isolated from this strain exhibited moderate

anti-proliferative activity against HeLa and A549 cancer cell lines, further expanding the chemical repertoire of mangrove-derived Aspergillus species.

Xu et al. employed the OSMAC (One Strain Many Compounds) strategy to explore the metabolic potential of a marine-derived *Bacillus subtilis* sp. 18, leading to the discovery of a new macrolactin antibiotic, macrolactin XY. This compound demonstrated superior antibacterial activity, particularly against Enterococcus faecalis. Mechanistic studies revealed that macrolactin XY disrupts bacterial cell membrane integrity and permeability, while also inhibiting genes associated with bacterial energy metabolism. This work provides a valuable theoretical foundation for the future development of macrolactins as antibacterial agents.

Chen et al. reported three new polyketides and a new natural benzoquinone derivative, embelin A, from the mangrove-derived fungus *Penicillium* sp. SCSIO 41411. Their findings highlighted the diverse bioactivities of these compounds, with one showing significant inhibition against phosphodiesterase 4 (PDE4), another displaying DPPH radical scavenging activity, and embelin A exhibiting cytotoxicity against prostate cancer cell lines. The X-ray single-crystal diffraction analysis of embelin A is described for the first time, firmly establishing its absolute configuration.

Collectively, the articles included in this Special Issue demonstrate that mangrove ecosystems continue to be an exceptionally attractive source of chemically diverse and biologically active natural products. The abundant microbial communities, particularly endophytic fungi, produce secondary metabolites with unusual skeletons and unique mechanisms of action, offering promising prospects for lead discovery. We extend our sincere gratitude to all the authors for their valuable contributions, which have significantly advanced our understanding of this unique ecological niche. We also hope that this collection will inspire further research into the biosynthesis of these fascinating molecules and the exploration of untapped microbial resources within mangrove habitats.

Funding: This work was co-financed by grants from the National Natural Science Foundation of China (No. 82160675) and the Collaborative Innovation Center Foundation of Hainan University (XTCX2022STB01).

Conflicts of Interest: The authors declare no conflicts of interest.

Jing Xu
Guest Editor

marine drugs

MDPI

Article

New Bioactive Polyketides from the Mangrove-Derived Fungus *Penicillium* sp. SCSIO 41411

Yi Chen [1,2,†], Jian Cai [1,2,†], Ziwei Xia [3], Chunmei Chen [1], Yonghong Liu [1,3], Lalith Jayasinghe [1,4], Xueni Wang [3,*] and Xuefeng Zhou [1,2,*]

[1] CAS Key Laboratory of Tropical Marine Bio-Resources and Ecology/Guangdong Key Laboratory of Marine Materia Medica, South China Sea Institute of Oceanology, Chinese Academy of Sciences, Guangzhou 510301, China; chenyi221@mails.ucas.ac.cn (Y.C.); caijian19@mails.ucas.ac.cn (J.C.); chenchunmei18@mails.ucas.ac.cn (C.C.); yonghongliu@scsio.ac.cn (Y.L.); lalith.ja@nifs.ac.lk (L.J.)
[2] University of Chinese Academy of Sciences, Beijing 100049, China
[3] Guangxi Zhuang Yao Medicine Center of Engineering and Technology, Institute of Traditional Chinese and Zhuang Yao Ethnic Medicine, Guangxi University of Chinese Medicine, Nanning 530200, China; xiaziwei1824@outlook.com
[4] National Institute of Fundamental Studies, Hantana Road, Kandy 200000, Sri Lanka
* Correspondence: wangxueni@gxtcmu.edu.cn (X.W.); xfzhou@scsio.ac.cn (X.Z.)
† These authors contributed equally to this work.

Abstract: Three new polyketides, including three ester derivatives (**1**, **3**, and **5**) and a new natural product, which was a benzoquinone derivative, embelin A (**4**), together with nine known ones (**2** and **6**–**13**), were isolated from the mangrove-derived fungus *Penicillium* sp. SCSIO 41411. Their structures were determined by detailed NMR and MS spectroscopic analyses. The X-ray single-crystal diffraction analysis of **4** was described for the first time. Compound **9** displayed obvious inhibition against PDE4 with an inhibitory ratio of 40.78% at 10 μM. Compound **12** showed DPPH radical scavenging activity, with an EC_{50} of 16.21 μg/mL, compared to the positive control (ascorbic acid, EC_{50}, 11.22 μg/mL). Furthermore, compound **4** exhibited cytotoxicity against PC-3 and LNCaP with IC_{50} values of 18.69 and 31.62 μM, respectively.

Keywords: mangrove-derived fungus; *Penicillium* sp.; polyketide; cytotoxicity

1. Introduction

Mangroves are a unique intertidal ecosystem located in tropical and subtropical regions, with nearly 60–70% of the world's tropical and subtropical coastlines covered by mangroves, widely regarded as one of the most productive ecosystems [1,2]. One of the key populations in this ecosystem is microbial diversity [2]. Fungi and bacteria make up 91% of the microbial biomass in tropical mangroves, which produce abundant marine natural products. As of December 2020, scientists have discovered at least 1387 new structures from mangrove-derived fungi, numerous of which demonstrated a variety of pharmacological activities [1–4].

Penicillium sp., as a representative of marine fungi, generates a wide range of bioactive secondary metabolites, mainly including polyketides, alkaloids, peptides, etc. [5–8]. Auroglaucin, isolated from an aciduric fungus strain, *Penicillium oxalicum* OUCMDZ-5207, exhibited strong selective inhibition on A549 cells, with an IC_{50} value of 5.67 μM [9]. Asperic acid, which was generated from the fungus *Penicillium polonicum* H175, displayed a noteworthy hypoglycemic impact comparable to that of the positive drug rosiglitazone (RSG) at 10 μM [10].

In our study, three new ester derivatives (**1**, **3**, and **5**) and one new natural product (**4**), together with nine known compounds (**2** and **6**–**13**) (Figure 1), were isolated from a mangrove sediment-derived fungus, *Penicillium* sp. SCSIO 41411. Herein, the specifics

of the isolation, structural elucidation, and bioactive assessments of isolated compounds were reported.

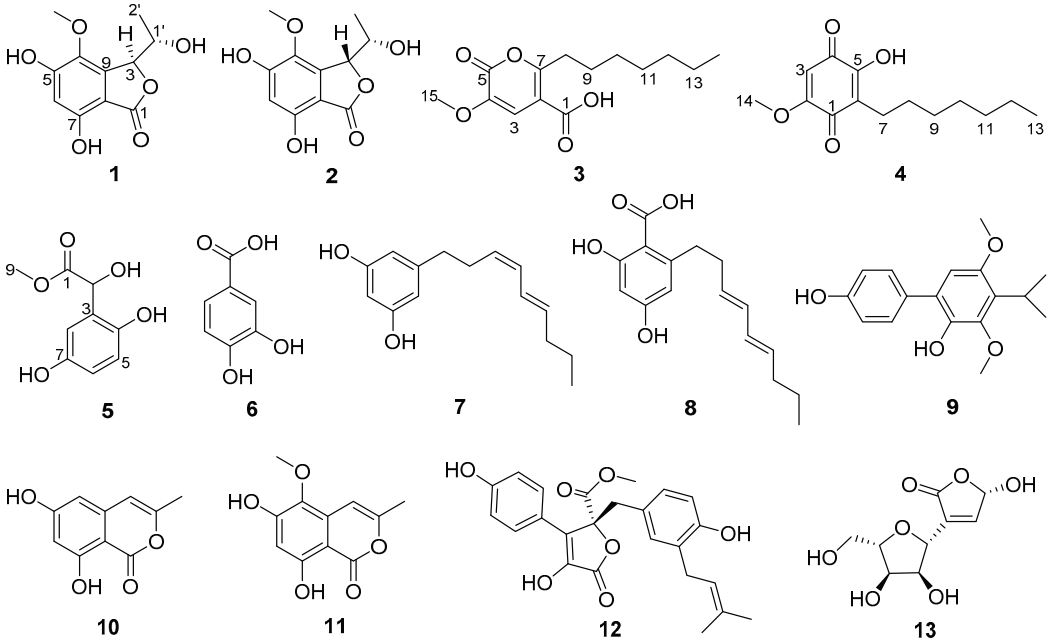

Figure 1. Structures of compounds **1**–**13**.

2. Results and Discussion

2.1. Structural Determination

Compound **1** was isolated as a brown oil, and its molecular formula of $C_{11}H_{12}O_6$ was determined by HRESIMS data at *m*/*z* 241.0709 $[M+H]^+$. The 1D NMR (Table 1) and HSQC spectra of **1** showed signals of one carbonyl carbon (δ_C 168.3), five unsaturated carbon signals (δ_C 157.3, 153.7, 134.3, 141.5, 103.4), one aromatic methine ($\delta_{H/C}$ 6.41/104.2), two oxygen-containing saturated methylenes ($\delta_{H/C}$ 5.26/81.5 and 4.18/65.1), and two methyls ($\delta_{H/C}$ 3.69/59.7 and 1.28/20.6) (one of them was methoxyl). These aforementioned data were similar to the 1D NMR data of the known compound embeurekol C (**2**), a polyketide derivative obtained from the fungus *Embellisia eureka* [11]. HMBC and COSY correlations (Figure 2) confirmed that the planar structures of **1** and **2** were consistent. To determine the absolute configuration of the secondary alcohol at C-1′ in **1** and **2**, we performed the Mosher ester analysis [12]. The (*R*)-MPA and (*S*)-MPA esters were prepared. Analysis of ^{1}H NMR data yielded $\Delta\delta_{RS}$ values (δ_R–δ_S), confirming that **1** and **2** had the same *S* configuration at C-1′ (Figure 3). Therefore, two theoretical configurations containing (3*S*, 1′*S*)-**1** and (3*R*, 1′*S*)-**1** were speculated for ECD calculation. Combined with the trend of the experimental curve of **1**, the absolute configuration of **1** was ultimately inferred to be 3*S*, 1′*S* (Figure 4). However, the experimental ECD spectra of **2** showed opposite trends with **1**, so it was speculated that the absolute configuration of C-3 in **2** was opposite to that of **1**, which was 3*R*. The specific optical rotation of **1** ($[\alpha]_D^{25}$ + 49.0 (*c* 0.1, CH_3OH)) and embeurekol C (**2**) ($[\alpha]_{20_D}$ − 17.0 (*c* 0.05, CH_3OH)) [11] further confirmed their opposite configurations at C-3. Consequently, compound **2** was identical to embeurekol C, and **1** was named embeurekol D.

Compound **3** was obtained as a red-brown solid. The molecular formula was determined as $C_{14}H_{20}O_5$ by HRESIMS data at *m*/*z* 269.1389 $[M+H]^+$. The one dimensional (1D) NMR (Table 2) and HSQC spectrum of **3** showed signals of two carbonyls (δ_C 172.7, 150.2), three nonprotonated sp^2 carbons (δ_C 160.0, 153.0, 144.2), one alkene methine ($\delta_{H/C}$ 6.96/115.6), six methylenes ($\delta_{H/C}$ 1.24/31.1, 1.30/28.4, 1.30/28.3, 2.68/27.5, 1.61/26.1, 1.24/22.0), and two methyls ($\delta_{H/C}$ 3.87/53.3, 0.85/13.9) (one of them was methoxyl). According to the HMBC correlation (Figure 2) of H-3/C-1, C-2, C-4, and C-5, compound **3**

was an unsaturated pentolactone derivative with a carboxyl group connected to C-2. The HMBC correlations of H_3-15/C-4 revealed that 15-OCH_3 was located at C-4. According to the molecular formula, the COSY-related signal indicated a spin-coupled system H_3-14/H_2-13/H_2-12/H_2-11/H_2-10/H_2-9/H_2-8, indicating the presence of heptane. The HMBC correlations of H_2-8/C-7, 2, and H_2-9/C-7 revealed that CH_2-8 was located at C-7. Compound **3** was unambiguously characterized, as shown in Figure 1. The structure of **3** was similar to that of dothydeopyron B [13], with the main difference being that **3** had a carboxyl group while dothydeopyron B had a methoxy group, and there was a hydroxyl group substituted at the branch. As a newly discovered natural product, the novelty of compound **3** lay in its presence of an aliphatic chain, which made it potentially more hydrophilic compared to compounds with longer chains. Finally, compound **3** was named 7-heptyl-4-methoxy-6-oxo-3*H*-pyran-2-carboxylic acid.

Compound **4** was obtained as a yellow solid and was determined to have the molecular formula $C_{14}H_{20}O_4$ from the HRESIMS data at m/z 253.1442 $[M+H]^+$. The 1D NMR (Table 2) and HSQC spectra of **4** showed signals of two carbonyl carbons (δ_C 184.5, 183.6), three alkene carbons (δ_C 161.9, 156.1, 120.1), one alkene methine ($\delta_{H/C}$ 5.88/104.0), six methylenes carbons ($\delta_{H/C}$ 1.29/33.0, 1.29/30.6, 1.32/30.2, 1.43/29.2, 1.32/23.7, 2.40/23.3), and two methyls ($\delta_{H/C}$ 3.83/57.2, 0.90/14.4) (one of them was methoxyl). The above data suggested that **4** had a benzoquinone skeleton and a fatty acid chain. The COSY correlations (Figure 2) of H_2-9/H_2-8/H_2-7 and H_2-12/H_3-13 and the HMBC correlations of H_3-13/CH_2-11 revealed that C-7–C-13 was a fatty acid chain. The HMBC correlations of H_2-7/C-1, C-5, C-6, and H_2-8/C-6 revealed that CH_2-7 was located at C-6. The HMBC correlations of H_3-14/C-2 indicated that the 14-OCH_3 was located at C-2. Furthermore, the X-ray crystal structure of **4** (CCDC 2363995, Figure 5) obtained by slow evaporation in CH_3OH at room temperature further confirmed the above elucidation of the planar structure. Compound **4** has been previously identified as a synthetic product, which was synthesized to illustrate the structure-activity relationship against α-glucosidase of the embelin derivatives [14]. Here we reported for the first time that this compound has been explored from nature and confirmed as a new natural product. Therefore, the compound was named embelin A.

Compound **5** was isolated as a brown oil and had the molecular formula $C_9H_{10}O_5$ as determined by HRESIMS data at m/z 221.0429 $[M+Na]^+$. The ^1H NMR of compound **5** shows a typical 1,2,4-trisubstituted benzene ring [δ_H 6.67 (1H, d, J = 3.0 Hz); 6.50 (1H, dd, J = 8.5, 3.0 Hz); 6.60 (1H, d, J = 8.5 Hz)]. The one-dimensional (1D) NMR (Table 1) and HSQC spectra of 5 showed signals of one carbonyl carbon (δ_C 173.3), three aromatic carbons (δ_C 149.7, 146.9, 126.6), three aromatic methines ($\delta_{H/C}$ 6.60/115.8, 6.50/115.2, and 6.67/114.2), one methine connected to hydroxyl group ($\delta_{H/C}$ 5.27/67.0), and one oxygenated methyl ($\delta_{H/C}$ 3.57/51.5). The HMBC correlations (Figure 2) of H_3-9/C-1 revealed that the oxygenated methyl group 9-OCH_3 was located at C-1. The HMBC correlations of H-2/C-1, 3, 4, and 8 indicated that C-2 was next to C-1 and C-3. Moreover, it indicated the location of the phenolic hydroxyl group (C-4) and the aromatic methine (C-8). The HMBC correlations of H-8/C-4, 6, and H-5/C-3, 7, and the COSY correlations of H-5/H-6 revealed the location of C-5, C-6, and C-7. The optical rotation of **5** was almost zero, suggesting that it was a racemate. Finally, compound **5** was named methyl α,2,5-trihydroxybenzeneacetate.

Meanwhile, the other eight known compounds were identified as protocatechuic acid (**6**) [15], 5-[(3*Z*,5*E*)-3,5-nonadienyl]-1,3-benzenediol (**7**) [16], 2,4-Dihydroxy-6-(3*E*,5*E*)-3,5-nonadien-1-ylbenzoic acid (**8**) [17,18], 3,5-Dimethoxy-4-(1-methylethyl)[1,1′-biphenyl]-2,4′-diol (**9**) [19], 3-Methyl-6,8-dihydroxyisocoumarin (**10**) [20], 6,8-dihydroxy-5-methoxy-3-methyl-1*H*-isochromen-1-one (**11**) [21], butyrolactone I (**12**) [22], polybotrin (**13**) [23], respectively, by comparing their NMR data (Supplementary Information) to previous reports. According to the literature, **11** exhibited *a*-glucosidase inhibitory activity with an IC_{50} value of 89.4 μM [24], and **12** had an acetylcholinesterase inhibiting effect [25].

Table 1. The ^{1}H and ^{13}C NMR data of compounds **1** and **5**.

Pos.	**1** [a]		**5** [b]	
	δ_C Type	δ_H (*J* in Hz)	δ_C Type	δ_H (*J* in Hz)
1	168.3, C		173.3, C	
2			67.0, CH	5.27, s
3	81.5, CH	5.26, br s	126.6, C	
4	134.3, C		146.9, C	
5	157.3, C		115.8, CH	6.60, d (8.5)
6	104.2, CH	6.41, s	115.2, CH	6.50, dd (8.5, 3.0)
7	153.7, C		149.7, C	
8	103.4, C		114.2, CH	6.67, d (3.0)
9	141.5, C		51.5, CH_3	3.57, s
10	59.7, CH_3	3.69, s		
1′	65.1, CH	4.18, q (5.9)		
2′	20.6, CH_3	1.28, d (6.5)		

[a] ^{1}H (500 MHz) and ^{13}C (125 MHz) measured in DMSO-d_6. [b] ^{1}H (700 MHz) and ^{13}C (175 MHz) measured in DMSO-d_6.

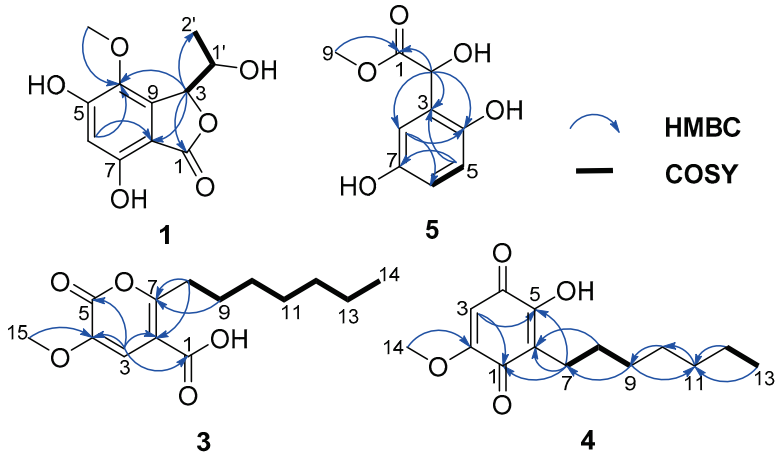

Figure 2. Key HMBC and COSY correlations of **1** and **3**–**5**.

Table 2. The ^{1}H and ^{13}C NMR data of compounds **3** and **4**.

Pos.	**3** [a]		**4** [b]	
	δ_C Type	δ_H (*J* in Hz)	δ_C Type	δ_H (*J* in Hz)
1	172.7, C		183.6, C	
2	144.2, C		161.9, C	
3	115.6, CH	6.96, s	104.0, CH	5.88, s
4	160.0, C		184.5, C	
5	150.2, C		156.1, C	
6			120.1, C	
7	153.0, C		23.3, CH_2	2.40, t (7.7)
8	27.5, CH_2	2.68, t (7.5)	29.2, CH_2	1.43, m
9	26.1, CH_2	1.61, m	30.2, CH_2	1.32, m
10	28.3, CH_2	1.30, m	30.6, CH_2	1.29, m
11	28.4, CH_2	1.30, m	33.0, CH_2	1.29, m
12	31.1, CH_2	1.24, m	23.7, CH_2	1.32, m
13	22.0, CH_2	1.24, m	14.4, CH_3	0.90, t (7.1)
14	13.9, CH_3	0.85, t (6.8)	57.2, CH_3	3.83, s
15	53.3, CH_3	3.87, s		

[a] ^{1}H (500 MHz) and ^{13}C (125 MHz) measured in DMSO-d_6. [b] ^{1}H (700 MHz) and ^{13}C (175 MHz) measured in CD_3OD.

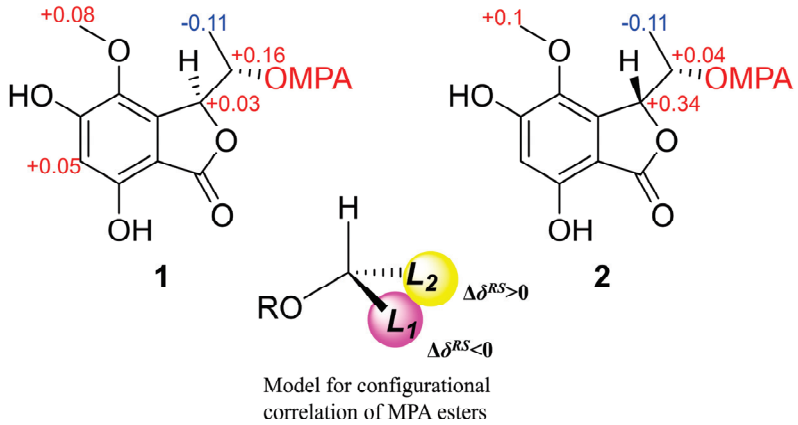

Figure 3. $\Delta\delta_{RS}$ (δ_R–δ_S) data for the MPA esters of **1**–**2**.

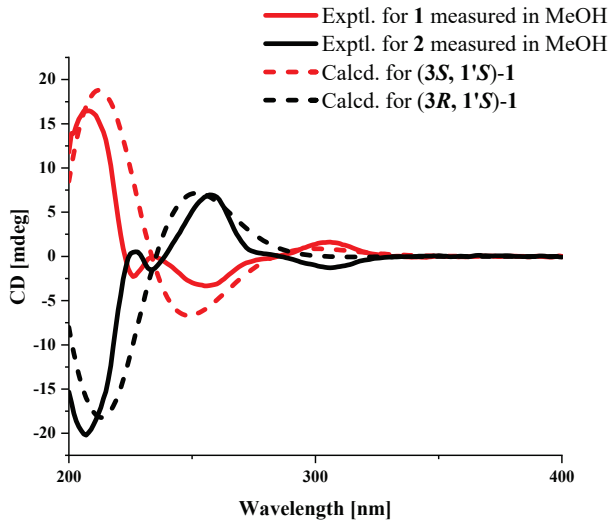

Figure 4. Experimental and calculated ECD spectrum of **1**.

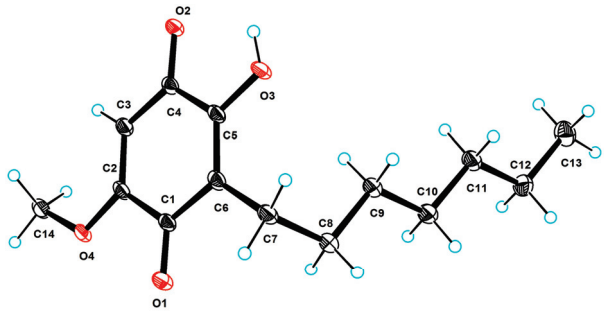

Figure 5. X-ray single-crystal structure of **4**.

As we can see, compounds **1/2** and **10/11** had similar parent nucleus structures, with the main difference being that **1/2** were five-membered lactone rings, while compounds **10/11** were six-membered lactone rings. The example of the development of furan and pyran rings in monoterpenoids illustrated the mechanism of biosynthesis. *Aspergillus niger* could be used to biotransformation linalool into both furanoid and pyranoid linalool oxide simultaneously [26]. The phenomena suggested that these two types of compounds had a certain biological relationship in the isolated strain.

2.2. Bioactivity Assay

The isolated compounds were evaluated for their antibacterial and cytotoxic activities (Table 3). Compounds **7** and **9** exhibited activities against *Staphylococcus aureus*, with the MIC values of 100 μg/mL. Compounds **3**, **7**, **8**, and **9** exhibited activities against *Streptococcus suis*, with MIC values of 100 μg/mL. In addition, compound **12** had a DPPH inhibitory activity with an EC_{50} of 16.21 μg/mL, compared to the positive control (ascorbic acid, with an EC_{50} of 11.22 μg/mL). Phosphodiesterase 4 (PDE4) is an important target for the treatment of inflammation [27]. In screening for PDE4 inhibitory activity, compounds **1**–**3** and **9**–**13** at 10 μM displayed inhibition against PDE4 with inhibitory ratios of 18.62%, 14.95%, 19.67%, 40.78%, 27.42%, 27.39%, 29.10%, and 26.22%, respectively. Among these, compound **9** exhibited moderate inhibitory activity against PDE4.

Table 3. Antibacterial and cytotoxicity activities of compounds.

Compounds	Antibacterial (MIC, μg/mL)		Cytotoxicity (IC_{50}, μM)		
	S. aureus	*S. suis*	PC-3	LNCaP	DU145
1	- [a]	-	-	-	-
3	-	100	-	-	-
4	-	-	18.69	31.62	>100
7	100	100	-	-	-
8	-	100	-	-	-
9	100	100	-	-	-
12	-	-	-	-	-
Positive	25 [b]	50 [c]	0.12 [d]	0.0018 [d]	0.0033 [d]

[a] "-" means no activity; [b] Streptomycin; [c] Penicillin; [d] Docetaxel.

Compounds **1**–**4** and **7**–**13** were tested at 10 μM in the cytotoxicity assay on two human prostate cancer cell lines, PC-3 and 22Rv1 (Figure 6). Compound **4** exhibited significant inhibition on PC-3, with an IC_{50} value of 18.69 μM. Furthermore, Compound **4** was evaluated against two additional prostate cancer cell lines, LNCaP and DU145. It effectively inhibited the LNCaP cell line with an IC_{50} value of 31.62 μM, while its IC_{50} value against the DU145 cell line was greater than 100 μM. The above results indicated that the cytotoxicity activity of **4** was selective, with the strongest activity against the PC-3 cell line. Among these three common prostate cancer cell lines, PC-3 was androgen-independent and had moderate metastatic potential [28]. Therefore, we speculated that compound **4** inhibited the mid-term stage of prostate cancer cell development. As a new natural product, **4** had a similar skeleton structure to auroglaucin-related analogs [29], both of which had a six-membered ring structure and a long chain. However, compounds **3** and **4** differed mostly in the characteristics of their six-membered rings. The cytotoxicity of **4** indicated that lengthy fatty chains had a minimal impact on the cytotoxicity of this kind of structure.

AKT1 (NP_005154.2) was involved in the growth, survival, and metabolism of cells [30]. Studies have shown that AKT1 protein could interact with UHRF1, but inhibited AKT1-induced phosphorylation of UHRF1 could induce degradation of UHRF1 protein, thereby reducing the interaction between UHRF1 and deubiquitinase USP7 and promoting its interaction with E3 ubiquitin-protein ligase BTRC, which is of great significance for the treatment of prostate cancer [31]. Therefore, AKT1 was selected as the docking target for further research. Compound **4** demonstrated a perfect interaction with the AKT1 protein (PDB ID: 3O96) with a docking score of −5.886. As shown in Figure 7, hydroxyl and ketone carbonyl groups of **4** formed two hydrogen bonds with the active site residues SER 205 and LYS 268.

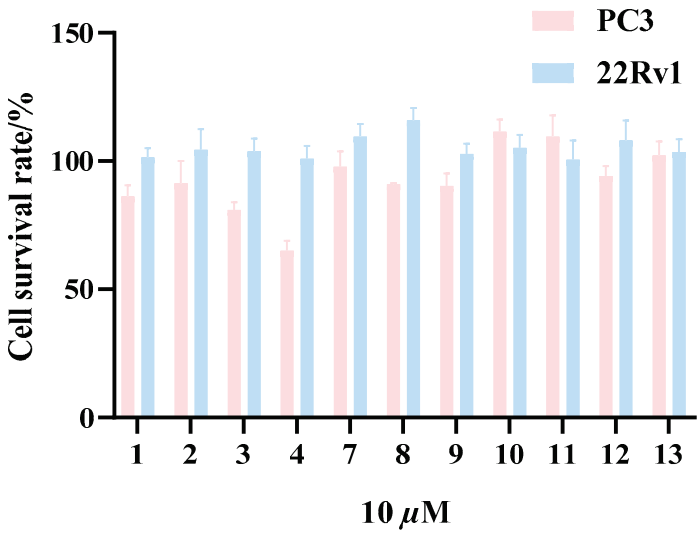

Figure 6. The cell survival rate of compounds **1**–**4** and **7**–**13** at 10 μM. All experiments were performed at least three times. The data are presented as the mean ± SD of representative experiments.

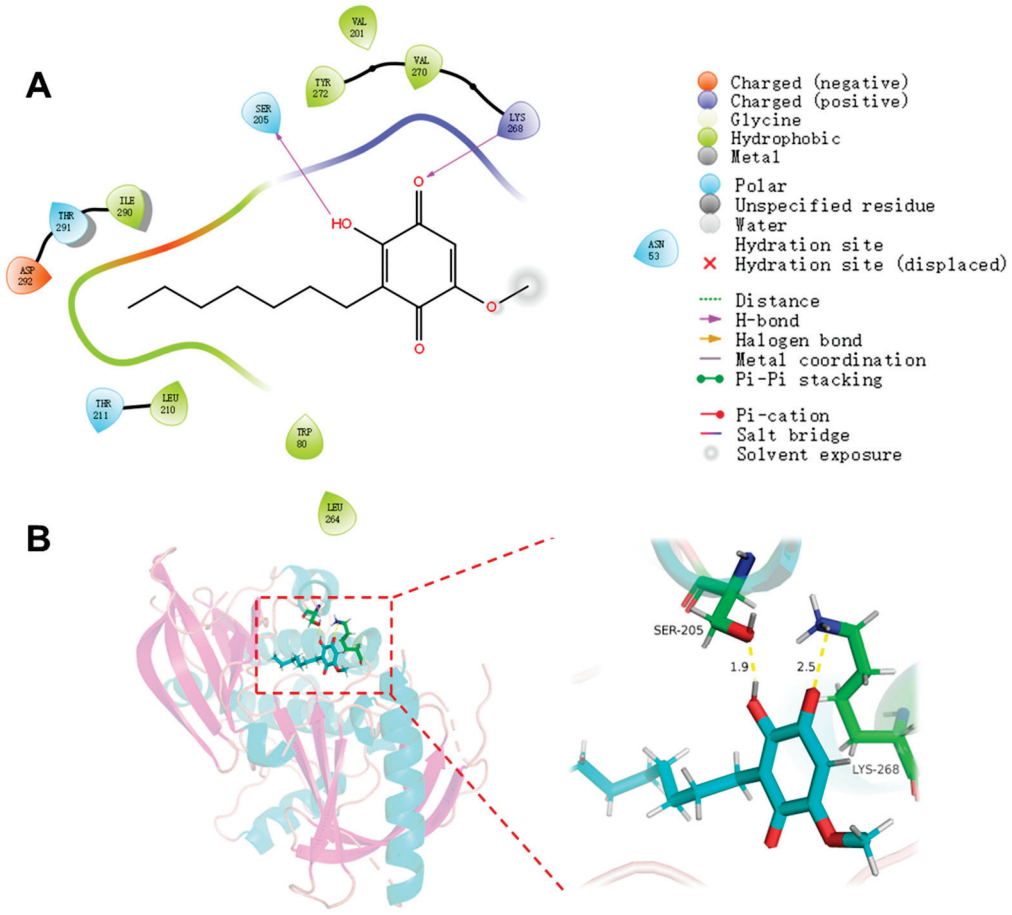

Figure 7. Molecular docking of **4** with AKT1 (PDB code: 3O96). (**A**) The two-dimensional (2D) interaction details of the predicted binding mode of **4** with the AKT1. The purple arrows in the Figure represent hydrogen bonds, indicating that **4** interacted with the active sites of the AKT1 protein pocket through hydrogen bonds. (**B**) The binding sites of molecule **4** with the AKT1 protein. On the left is the overall diagram of the interaction between **4** and AKT1, and on the right is the specific detail diagram. Among them, the distance between **4** and SER 205 is 1.9 Å, and the distance between **4** and LYS 268 is 2.5 Å.

3. Materials and Methods

3.1. General Experimental Procedures

Optical rotations were measured with an Anton Paar MPC500 (Anton, Graz, Austria) polarimeter. The UV spectra were recorded on a Shimadzu UV-2600 PC spectrometer (Shimadzu, Beijing, China), while the IR spectra were determined by an IR Affinity-1 spectrometer (Shimadzu). The ECD spectra were performed on a Chirascan circular dichroism spectrometer (Applied Photophysics, Leatherhead Surrey, UK). High-resolution electrospray ionization mass spectroscopy (HRESIMS) spectra were obtained on a Bruker maXis Q-TOF mass spectrometer (Bruker BioSpin International AG, Fällanden, Switzerland). The NMR spectra were collected on a Quantum-I Plus 500 MHz (Q-one Instrument Co., Ltd., Wuhan, China) operating at 500 MHz for ^{1}H NMR and 125 MHz for ^{13}C NMR and were collected on an AVANCE III HD 700 MHz (Bruker Switzerland AG, Fällanden, Switzerland) operating at 700 MHz for ^{1}H NMR and 175 MHz for ^{13}C NMR, which used tetramethylsilane as an internal standard. Semipreparative high-performance liquid chromatography (HPLC) was performed on the Hitachi Primaide with a DAD detector (Hitachi, Tokyo, Japan), using ODS columns (ChromCore 120 C18, 10 × 250 mm, 5 mm; YMC-pack ODS-A, 10 × 250 mm, 5 mm; COSMOSIL πNAP 10 × 250 mm; COSMOSIL 5C18-AR-II 10 × 250 mm). Column chromatography was detected by silica gel (200–300 mesh), and spots were detected on TLC (Qingdao Marine Chemical Factory, Qingdao, China) under 254 nm UV light, respectively. All solvents used were provided by Tianjin Fuyu Chemical and Industry Factory, Tianjin, China, and were of analytical grade.

3.2. Fungal Material

The strain *Penicillium* sp. SCSIO 41411 was isolated from the rhizosphere sediment sample of the mangrove *Aegiceras corniculatum* in Gaoqiao Mangrove, Zhanjiang. It was stored in the CAS Key Laboratory of Tropical Marine Bioresources and Ecology, South China Sea Institute of Oceanology, Chinese Academy of Sciences, Guangzhou, China. The strain was designated *Penicillium* sp. SCSIO 41411 is based on BLAST analysis of the ITS sequence (Supplementary Information) because it shared 99% of the similarities with *Penicillium brefeldianum* (NR_138263.1). Finally, the sequence was deposited in GenBank with the accession number OQ052995.

3.3. Fermentation and Extraction

The fungal strain *Penicillium* sp. SCSIO 41411 was statically cultivated on MA medium and then was cultured in 200 mL seed medium (1.5% malt extract, 2.0% sea salt) in 1 L Erlenmeyer flasks at 28 °C for 3 days on a rotary shaker (180 rpm). A large-scale fermentation was incubated at 26 °C for 28 days using a rice medium (200 g rice, 2% sea salt, 230 mL H_2O) in the 1 L flask (×80) under static conditions. The whole fermented culture was extracted with EtOAc three times to afford a brown extract (150 g).

3.4. Isolation and Purification

The whole ethyl acetate extract was subjected to a silica gel vacuum liquid chromatography using a step gradient elution of petroleum ether (PE)-dichloromethane (DCM) (*v*:*v* 1:0, 1:1, 0:1), DCM-methyl alcohol (CH_3OH) (*v*:*v* 100:1, 100:3, 50:3, 10:1, 5:1, 10:3, 5:2, 2:1, 10:7, 5:4, 10:9, 0:1), to yield 15 fractions (Frs. 1–15) in the light of TLC profiles. Fr. 2 was further purified by semipreparative HPLC (72% CH_3OH/H_2O, 3.0 mL/min) to afford 4 (2.4 mg, t_R 18.2 min). Fr. 4 to Fr. 6 were merged and then was divided into 18 subfractions (Frs. 4-1–4-18) by ODS silica gel eluting with CH_3OH/H_2O (5–100%). Based on this, Fr. 4–8 was directly separated by semipreparative HPLC (69% CH_3OH/H_2O, 3.0 mL/min) to offer 12 (37.4 mg, t_R 21.0 min). Compound **9** (6.3 mg, t_R 13.3 min) was further purified from Fr. 4–9 by semipreparative HPLC (60% CH_3CN/H_2O, 3.0 mL/min). Compound **3** (9.6 mg, t_R 13.3 min), compound **7** (25.0 mg, t_R 15.2 min), and Fr. 4-10-1 were further obtained from Fr. 4–10 by semipreparative HPLC (80% CH_3OH/H_2O, 2.0 mL/min; 60% CH_3CN/H_2O, 2.5 mL/min), respectively. Meanwhile, Fr. 4-10-1 was separated by semipreparative HPLC

(52% CH_3CN/H_2O, 0.04% formic acid, 3.0 mL/min) to gain 8 (9.7 mg, t_R 22.0 min). Fr. 4–2 to Fr. 4–7 were merged once again and then were divided into 15 subfractions (Frs. 4-2-1–4-2-15) by ODS silica gel eluting with CH_3OH/H_2O (5–100%). Compound **10** (2.3 mg, t_R 9.8 min) and 11 (12.7 mg, t_R 10.4 min) were further obtained from Fr. 4-2-5 by semipreparative HPLC (63% CH_3OH/H_2O, 2.5 mL/min), respectively. Compound **1** (6.83 mg, t_R 14.0 min), 5 (2.2 mg, t_R 9.7 min), 6 (4.5 mg, t_R 7.8 min) and Fr. 7-5 were firstly obtained from Fr. 7 by semipreparative HPLC (30% CH_3OH/H_2O, 2.5 mL/min; 5% CH_3OH/H_2O, 0.04% formic acid, 3.0 mL/min; 13% CH_3CN/H_2O, 0.04% formic acid, 3.0 mL/min, respectively. Meanwhile, Fr. 7-5 was further separated by semipreparative HPLC (12% CH_3CN/H_2O, 0.04% formic acid, 2.5 mL/min) to gain 2 (56.09 mg, t_R 12.0 min). Compound **13** (24.9 mg, t_R 7.4 min) was further purified from Fr. 9 by semipreparative HPLC (15% CH_3OH/H_2O, 2.5 mL/min).

3.5. Spectroscopic Data of Compounds

Embeurekol D (1): brown oil; $[\alpha]_D^{25}$ + 49.0 (*c* 0.1, CH_3OH); UV (CH_3OH) λ_{max} (logε) 214 (4.43), 257 (4.02), 302 (3.85) nm; ECD (0.83 mM, CH_3OH) λ_{max} 208 (+16.47), 226 (−2.28), 234 (−0.02), 256 (−3.33), 306 (+1.62); IR (film) ν_{max} 3370, 1732, 1616, 984 cm^{-1}; ^1H and ^{13}C NMR data, see Table 1; HRESIMS *m*/*z* 241.0709 $[M+H]^+$ (calculated for $C_{11}H_{13}O_6^+$, 241.0707).

7-heptyl-4-methoxy-6-oxo-3*H*-pyran-2-carboxylic acid (3): red brown solid; UV (CH_3OH) λ_{max} (logε) 226 (4.29), 312 (3.61) nm; IR (film) ν_{max} 3256, 2930, 1742, 1636, 1260, 1207 cm^{-1}; ^1H and ^{13}C NMR data, see Table 2; HRESIMS *m*/*z* 269.1389 $[M+H]^+$ (calculated for $C_{14}H_{21}O_5^+$, 269.1384).

Embelin A (4): yellow solid; UV (CH_3OH) λ_{max} (logε) 205 (4.05), 287 (4.27) nm; IR (film) ν_{max} 3339, 2924, 2853, 1663, 1634, 1593, 1204, 691 cm^{-1}; ^1H and ^{13}C NMR data, see Table 2; HRESIMS *m*/*z* 253.1442 $[M+H]^+$ (calculated for $C_{14}H_{21}O_4^+$, 253.1434).

Methyl α,2,5-trihydroxybenzeneacetate (5): brown oil; $[\alpha]_D^{25}$ 0.0 (*c* 0.1, CH_3OH); UV (CH_3OH) λ_{max} (logε) 205 (4.16), 301 (3.45) nm; IR (film) ν_{max} 3377, 2918, 2851, 1734, 1576, 1456, 1219, 762 cm^{-1}; ^1H and ^{13}C NMR data, see Table 1; HRESIMS *m*/*z* 221.0429 $[M+Na]^+$ (calculated for $C_9H_{10}NaO_5^+$, 221.0420).

3.6. X-ray Crystallographic Analysis

Compound **4** was dissolved in CH_3OH and slowly evaporated to obtain the clear light crystal. Crystallographic data for the structure that have been submitted to the Cambridge Crystallographic Data Centre (CCDC) can be seen and copies of which can be freely accessed applying to CCDC, 12 Union Road, Cambridge, CB2 1EZ, UK [P: +44 (0) 1223 336408].

Crystal data for 4: $C_{14}H_{20}O_4$, *M*r = 252.30, crystal size 0.3 × 0.05 × 0.05 mm^3, triclinic, *a* = 5.1888 (8) Å, *b* = 9.6297 (8) Å, *c* = 14.1355 (17) Å, α = 74.175 (9)°, β = 89.844 (12)°, γ = 79.330 (10)°, *V* = 666.93 (15) Å3, *Z* = 2, *T* = 99.98 (10) K, space group *P*-1, μ (Cu Kα) = 0.746 mm^{-1}, D_{calc} = 1.256 g/cm^3, 4793 reflections measured (6.508° ≤ 2Θ ≤ 151.438°), 2535 unique (R_{int} = 0.0620, R_{sigma} = 0.0720). The final R_1 was 0.0950 ($I > 2\sigma(I)$), and wR_2 was 0.2899 (all data). The goodness of fit on F^2 was 1.090 (CCDC 2363995).

3.7. ECD Computation Section

Compounds **1** and **2** were placed in Spartan'14, which used the MMFF molecular force field to perform a conformational search on the potential isomers separately. Then, the stable conformers of the first 5% in methanol solvent were optimized at the B3LYP/6-31+G (d) level via Gaussian 09 (D.01, Pittsburgh, PA, USA). A TDDFT polarizable continuum model at the level of B3LYP/6-311+G (d, p) was used to calculate the optimized low-energy conformations [32]. The calculated ECD spectra were generated from GaussView (6.0.16, Pittsburgh, PA, USA) and Origin 2021 with a half-bandwidth of 0.3–0.4 eV, wavelength corrected by the calculated UV curve with the measured curve and weighted by Boltzmann distribution to obtain the calculated ECD spectra.

3.8. Mosher's Method

Compound **1** (2.01 mg, 0.0084 mmol), followed by the addition of (*R*)-MPA (8.50 mg, 0.0512 mmol), DCC (0.3455 mg, 0.0017 mmol), and DMAP (0.2046 mg, 0.0017 mmol), was dissolved in chloroform-*d* (0.6 mL) and then stirred at room temperature for 6 h. The reaction was monitored by TLC detection [12]. (*R*)-MPA ester (1a) was purified by semipreparative HPLC (60% CH_3OH/H_2O, 3.0 mL/min) to yield 1a (0.7 mg). Compound **1b** (0.7 mg) was prepared using the same protocol as for 1a. The determination of the configuration of the hydroxyl group at C-1′ for 2 was performed the same way as for 1.

3.9. Antibacterial Activity Assay

Two bacteria (*Staphylococcus aureus* ATCC 25923, *Streptococcus suis* SC19) were assessed on 96-well plates. As positive controls against the two microorganisms, streptomycin and penicillin were employed, respectively. Then, compounds were assessed using a two-fold serial dilution approach on nutrient agar on a 96-well plate as previously described [33]. The medium's OD value was determined at 490 nm (OD_{490}) using a microplate reader (Thermo Scientific, Bremen, Germany) following a 24-h incubation period.

3.10. Antioxidant Activity Assay

The obtained compound **12** was evaluated for its antioxidant activities against DPPH. The effect of the compound on DPPH radical was estimated according to the method of Hatano et al. (1988) [34] and Yen et al. (1995) [35]. In summary, a methanolic DPPH solution was supplemented with compound **12** to obtain a final concentration of 2.5–250 μg/mL. After shaking the mixture and letting it stand for 30 min at room temperature in the dark, the OD_{517} values were measured using the PerkinElmer Enspire Multi-mode micro-orifice detector and enzyme labeling instrument (PerkinElmer, Waltham, MA, USA). Ascorbic acid was used as the positive control. Then, the free radical scavenging rate K (%) was computed based on the acquired OD_{517} value using the formula, and Origin 2021 was utilized to determine EC_{50}.

3.11. PDE4 Inhibitory Screening Assays

The PDE4D2 expression, purification, and enzymatic assay procedures were comparable to those we previously described [36]. In brief, the inhibition of PDE4D2 by **13** was measured using ^{3}H-cAMP as substrates (20,000–30,000 cpm/assay), and reactions took place in a mixture that also contained 50 mM Tris-HCl (pH 7.5), 10 mM $MgCl_2$, 0.5 mM (DTT) at room temperature (25°) for 15 min. Subsequently, the reaction was stopped with 0.2 M $ZnSO_4$, the unreacted ^{3}H-cAMP was precipitated out using 0.2 N $Ba(OH)_2$. The leftover supernatant was used to gauge the radioactivity in 2.5 mL of Ultima Gold liquid scintillation cocktails (PerkinElmer) by a liquid scintillation counter (PerkinElmer 2910) [36].

3.12. Cytotoxicity Bioassay

Human prostate cancer LNCaP, 22Rv1, PC-3, and DU145 cells were purchased from the Cell Bank/Stem Cell Bank of the Chinese Academy of Sciences (Shanghai, China). All cell lines were cultured in the medium according to the recommendations of the Chinese Academy of Sciences Cell Bank/Stem Cell Bank. The cells were incubated at 37 °C and 5% carbon dioxide. All culture media supplemented with 10% (*v*/*v*) fetal bovine serum (Biological Industries, Beit Haemek, Israel) and 1% penicillin/streptomycin. All cell lines were tested and found to be free of mycoplasma contamination. The MTT assay, which has been previously reported, was used to assess cytotoxicity [37]. To sum up, cells were treated with compounds after being seeded at a density of 5×10^3 per well on a 96-well plate overnight after 72 h incubation. Following drug treatment, 10 μL of MTT solution (5 mg/mL) was added to each well at the indicated timings, and the wells were then incubated for 4 h at 37 °C in a humidified 5% CO_2 incubator. After the supernatants were eliminated, DMSO (100 μL) was added. Then, the OD_{570} values after 10 min were measured

using a TECAN Infinite 200 PRO Nano Quant multimode microplate reader [37,38]. Three separate runs of the experiment were conducted.

3.13. Molecular Docking

Using the structure of AKT1 (PDB code: 3O96) [30], which was obtained from the Protein Data Bank as a starting model, it was then handled following the Protein Preparation Wizard workflow in Maestro 11.9. The optimized ligand was docked into the receptor with the default parameters, which were obtained from Receptor Grid Generation [39–42].

4. Conclusions

In conclusion, three new polyketides (**1**, **3**, and **5**) and one new natural product (**4**), together with nine known ones (**2** and **6**–**13**), were isolated from the mangrove sediment-derived fungus *Penicillium* sp. SCSIO 41411. Their structures were determined by extensive spectroscopic analyses, ECD calculations, and X-ray single-crystal diffraction. Compound **9** inhibited PDE4 with an inhibitory ratio of 40.78% at 10 μM. Compound **12** showed moderate antioxidant inhibitory activity with an EC_{50} of 16.21 μg/mL. Moreover, compound **4** demonstrated selective inhibitory activity against tumor cells, which provides a promising avenue for the development of anti-prostate cancer therapeutics.

Supplementary Materials: The following supporting information can be downloaded at https://www.mdpi.com/article/10.3390/md22090384/s1, physicochemical data of **2** and **6**–**13**; Figures S1–S55: The NMR, HRESIMS, UV, and IR spectra of **1**–**13**; ITS sequence data of the strain.

Author Contributions: Data curation, Y.C., J.C. and Z.X.; Funding acquisition, X.Z.; Investigation, Y.C., J.C., C.C. and L.J.; Project administration, Y.L. and X.Z.; Writing—original draft, Y.C.; Writing—review and editing, X.W. and X.Z. All authors have read and agreed to the published version of the manuscript.

Funding: This research was funded by the Special Project for Marine Economic Development of the Department of Natural Resources of Guangdong Province (GDNRC[2024]25).

Institutional Review Board Statement: Not applicable.

Informed Consent Statement: Not applicable.

Data Availability Statement: Data are contained within the article.

Acknowledgments: We are grateful to Z. Xiao, X. Zheng, A. Sun, Y. Zhang, and X. Ma in the analytical facility at SCSIO for recording spectroscopic data.

Conflicts of Interest: The authors declare no conflicts of interest.

References

1. Chen, S.; Cai, R.; Liu, Z.; Cui, H.; She, Z. Secondary metabolites from mangrove-associated fungi: Source, chemistry and bioactivities. *Nat. Prod. Rep.* **2022**, *39*, 560–595. [CrossRef] [PubMed]
2. Thatoi, H.; Behera, B.C.; Mishra, R.R.; Dutta, S.K. Biodiversity and biotechnological potential of microorganisms from mangrove ecosystems: A review. *Ann. Microbiol.* **2012**, *63*, 1–19. [CrossRef]
3. She, J.; Zhou, X. New insights into the antitumor potential of natural piericidins. *J. Holistic Integr. Pharm.* **2021**, *2*, 153–162.
4. Zhou, X. Mangrove soil-derived *Streptomyces*: An important resource of pharmaceutical active natural products. *J. Holistic Integr. Pharm.* **2022**, *3*, 300–314. [CrossRef]
5. Hafez Ghoran, S.; Taktaz, F.; Sousa, E.; Fernandes, C.; Kijjoa, A. Peptides from marine-derived fungi: Chemistry and biological activities. *Mar. Drugs* **2023**, *21*, 510. [CrossRef] [PubMed]
6. Huang, G.L.; Zhou, X.M.; Bai, M.; Liu, Y.X.; Zhao, Y.L.; Luo, Y.P.; Niu, Y.Y.; Zheng, C.J.; Chen, G.Y. Dihydroisocoumarins from the mangrove-derived fungus *Penicillium citrinum*. *Mar. Drugs* **2016**, *14*, 177. [CrossRef] [PubMed]
7. Wang, J.W.; Liu, Y.Y.; Chen, G.Y.; Zheng, C.J.; Nong, X.H. Alkaloid-metabolites from the mangrove-derived fungus *Penicillium robsamsonii* HNNU0006. *Fitoterapia* **2024**, *175*, 105906. [CrossRef]
8. Zhang, X.; Yin, Q.; Li, X.; Liu, X.; Lei, H.; Wu, B. Structures and bioactivities of secondary metabolites from *Penicillium* genus since 2010. *Fitoterapia* **2022**, *163*, 105349. [CrossRef]
9. Gao, H.; Wang, Y.; Luo, Q.; Yang, L.; He, X.; Wu, J.; Kachanuban, K.; Wilaipun, P.; Zhu, W.; Wang, Y. Bioactive metabolites from acid-tolerant fungi in a Thai mangrove sediment. *Front. Microbiol.* **2020**, *11*, 609952. [CrossRef]

10. Liu, S.Z.; Tang, X.X.; He, F.M.; Jia, J.X.; Hu, H.; Xie, B.Y.; Li, M.Y.; Qiu, Y.K. Two new compounds from a mangrove sediment-derived fungus *Penicillium polonicum* H175. *Nat. Prod. Res.* **2022**, *36*, 2370–2378. [CrossRef]
11. Ebrahim, W.; Aly, A.H.; Mandi, A.; Wray, V.; Essassi, E.M.; Ouchbani, T.; Bouhfid, R.; Lin, W.; Proksch, P.; Kurtan, T.; et al. O-heterocyclic embeurekols from *Embellisia eureka*, an endophyte of *Cladanthus arabicus*. *Chirality* **2013**, *25*, 250–256. [CrossRef]
12. Guo, X.; Meng, Q.; Niu, S.; Liu, J.; Guo, X.; Sun, Z.; Liu, D.; Gu, Y.; Huang, J.; Fan, A.; et al. Epigenetic Manipulation to Trigger Production of Guaiane-Type Sesquiterpenes from a Marine-Derived *Spiromastix* sp. Fungus with Antineuroinflammatory Effects. *J. Nat. Prod.* **2021**, *84*, 1993–2003. [CrossRef] [PubMed]
13. Chomcheon, P.; Wiyakrutta, S.; Sriubolmas, N.; Ngamrojanavanich, N.; Mahidol, C.; Ruchirawat, S.; Kittakoop, P. Metabolites from the endophytic mitosporic *Dothideomycete* sp. LRUB20. *Phytochemistry* **2009**, *70*, 121–127. [CrossRef] [PubMed]
14. Chen, X.; Gao, M.; Jian, R.; Hong, W.D.; Tang, X.; Li, Y.; Zhao, D.; Zhang, K.; Chen, W.; Zheng, X.; et al. Design, synthesis and α-glucosidase inhibition study of novel embelin derivatives. *J. Enzyme Inhib. Med. Chem.* **2020**, *35*, 565–573. [CrossRef]
15. Liu, D.S.; Liu, W.Z.; Lv, Z.H. Studies on secondary metabolites of *Aspergillus aculeatus* derived from coastal saline soil. *Chin. J. Mar. Drugs* **2014**, *33*, 28–32.
16. Wen, H.; Chen, C.; Sun, W.; Zang, Y.; Li, Q.; Wang, W.; Zeng, F.; Liu, J.; Zhou, Y.; Zhou, Q.; et al. Phenolic C-Glycosides and Aglycones from Marine-Derived Aspergillus sp. and Their Anti-Inflammatory Activities. *J. Nat. Prod.* **2019**, *82*, 1098–1106. [CrossRef] [PubMed]
17. Bringmann, G.; Lang, G.; Steffens, S.; Gunther, E.; Schaumann, K. Evariquinone, isoemericellin, and stromemycin from a sponge derived strain of the fungus *Emericella variecolor*. *Phytochemistry* **2003**, *63*, 437–443. [CrossRef]
18. Sun, W.; Zhuang, C.; Li, X.; Zhang, B.; Lu, X.; Zheng, Z.; Dong, Y. Varic acid analogues from fungus as PTP1B inhibitors: Biological evaluation and structure-activity relationships. *Bioorganic Med. Chem. Lett.* **2017**, *27*, 3382–3385. [CrossRef]
19. Hassan, H.A.; Abdelhafez, O.H.; Shady, N.H.; Yahia, R.; Mohamed, N.M.; Rateb, M.E.; Akil, L.; Khadra, I.; Glaeser, S.P.; Kampfer, P.; et al. The anti-infective potential of the endophytic fungi associated with Allium cepa supported by metabolomics analysis and docking studies. *Nat. Prod. Res.* **2023**, *37*, 4063–4068. [CrossRef]
20. Kumagai, H.; Amemiya, M.; Naganawa, H.; Sawa, T.; Ishizuka, M.; Takeuchi, T. Biosynthesis of antitumor antibiotic, cytogenin. *J. Antibiot.* **1993**, *47*, 440–446. [CrossRef]
21. Xu, Z.; Xiong, B.; Xu, J. Chemical Investigation of Secondary Metabolites Produced by Mangrove Endophytic Fungus *Phyllosticta capitalensis*. *Nat. Prod. Res.* **2021**, *35*, 1561–1565. [CrossRef] [PubMed]
22. Dewi, R.T.; Tachibana, S.; Fajriah, S.; Hanafi, M. α-Glucosidase inhibitor compounds from *Aspergillus terreus* RCC1 and their antioxidant activity. *Med. Chem. Res.* **2014**, *24*, 737–743. [CrossRef]
23. Zou, K.; Komatsu, K.; Zhu, S. A novel compound from *Hedysarum polybotrys*. *J. Asian Nat. Prod. Res.* **2007**, *9*, 699–703. [CrossRef] [PubMed]
24. Chen, S.; Liu, Y.; Liu, Z.; Cai, R.; Lu, Y.; Huang, X.; She, Z. Isocoumarins and benzofurans from the mangrove endophytic fungus *Talaromyces amestolkiae* possess α-glucosidase inhibitory and antibacterial activities. *RSC Adv.* **2016**, *6*, 26412–26420. [CrossRef]
25. Peng, Q.; Chen, W.; Lin, X.; Xiao, J.; Liu, Y.; Zhou, X. Butenolides from the coral-derived fungus *Aspergillius terreus* SCSIO41404. *Mar. Drugs* **2022**, *20*, 212. [CrossRef] [PubMed]
26. Demyttenaere, J.C.; Willemen, H.M. Biotransformation of linalool to furanoid and pyranoid linalool oxides by *Aspergillus niger*. *Phytochemistry* **1998**, *47*, 1029–1036. [CrossRef]
27. Song, Z.; Huang, Y.Y.; Hou, K.Q.; Liu, L.; Zhou, F.; Huang, Y.; Wan, G.; Luo, H.B.; Xiong, X.F. Discovery and structural optimization of toddacoumalone derivatives as novel PDE4 inhibitors for the topical treatment of psoriasis. *J. Med. Chem.* **2022**, *65*, 4238–4254. [CrossRef]
28. Duan, M.; Long, Y.; Yang, C.; Wu, X.; Sun, Y.; Li, J.; Hu, X.; Lin, W.; Han, D.; Zhao, Y.; et al. Selection and characterization of DNA aptamer for metastatic prostate cancer recognition and tissue imaging. *Oncotarget* **2016**, *7*, 36436–36446. [CrossRef] [PubMed]
29. Gao, J.; Leon, F.; Radwan, M.M.; Dale, O.R.; Husni, A.S.; Manly, S.P.; Lupien, S.; Wang, X.; Hill, R.A.; Dugan, F.M.; et al. Benzyl derivatives with in vitro binding affinity for human opioid and cannabinoid receptors from the fungus *Eurotium repens*. *J. Nat. Prod.* **2011**, *74*, 1636–1639. [CrossRef]
30. Wu, W.I.; Voegtli, W.C.; Sturgis, H.L.; Dizon, F.P.; Vigers, G.P.; Brandhuber, B.J. Crystal structure of human AKT1 with an allosteric inhibitor reveals a new mode of kinase inhibition. *PLoS ONE* **2010**, *5*, e12913. [CrossRef]
31. Fu, Y.; Cao, T.; Zou, X.; Ye, Y.; Liu, Y.; Peng, Y.; Deng, T.; Yin, L.; Li, X. AKT1 regulates UHRF1 protein stability and promotes the resistance to abiraterone in prostate cancer. *Oncogenesis* **2023**, *12*, 1. [CrossRef] [PubMed]
32. Luo, X.; Lin, X.; Tao, H.; Wang, J.; Li, J.; Yang, B.; Zhou, X.; Liu, Y. Isochromophilones A-F, Cytotoxic Chloroazaphilones from the Marine Mangrove Endophytic Fungus *Diaporthe* sp. SCSIO 41011. *J. Nat. Prod.* **2018**, *81*, 934–941. [CrossRef] [PubMed]
33. Wan, Z.; Fang, W.; Shi, L.; Wang, K.; Zhang, Y.; Zhang, Z.; Wu, Z.; Yang, Z.; Gu, Y. Novonestmycins A and B, two new 32-membered bioactive macrolides from *Streptomyces phytohabitans* HBERC-20821. *J. Antibiot.* **2015**, *68*, 185–190. [CrossRef] [PubMed]
34. Hatano, T.; Kagawa, H.; Yasuhara, T.; Okuda, T. Two new flavonoids and other constituents in licorice root: Their relative astringency and radical scavenging effects. *Chem. Pharm. Bull.* **1988**, *36*, 2090–2097. [CrossRef] [PubMed]
35. Yen, G.; Chen, H. Antioxidant activity of various tea extracts in relation to their antimutagenicity. *J. Agric. Food Chem.* **1995**, *43*, 27–32. [CrossRef]

36. Lin, T.T.; Huang, Y.Y.; Tang, G.H.; Cheng, Z.B.; Liu, X.; Luo, H.B.; Yin, S. Prenylated coumarins: Natural phosphodiesterase-4 inhibitors from *Toddalia asiatica*. *J. Nat. Prod.* **2014**, *77*, 955–962. [CrossRef] [PubMed]
37. Wang, X.; Zhu, J.; Yan, H.; Shi, M.; Zheng, Q.; Wang, Y.; Zhu, Y.; Miao, L.; Gao, X. Kaempferol inhibits benign prostatic hyperplasia by resisting the action of androgen. *Eur. J. Pharmacol.* **2021**, *907*, 174251. [CrossRef] [PubMed]
38. Miao, L.; Jiao, C.; Shao, R.; Qi, Y.; Fan, G.; Li, X.; Wang, Y.; Zhu, Y.; Zhang, J.; Gao, X. Bakuchiol suppresses oestrogen/testosterone-induced Benign Prostatic Hyperplasia development through up-regulation of epithelial estrogen receptor β and down-regulation of stromal aromatase. *Toxicol. Appl. Pharmacol.* **2019**, *381*, 114637. [CrossRef]
39. Liang, Z.; Gu, T.; Wang, J.; She, J.; Ye, Y.; Cao, W.; Luo, X.; Xiao, J.; Liu, Y.; Tang, L.; et al. Chromene and chromone derivatives as liver X receptors modulators from a marine-derived *Pestalotiopsis neglecta* fungus. *Bioorganic Chem.* **2021**, *112*, 104927. [CrossRef]
40. Long, J.; Chen, Y.; Chen, W.; Wang, J.; Zhou, X.; Yang, B.; Liu, Y. Cyclic peptides from the soft coral-derived fungus *Aspergillus sclerotiorum* SCSIO 41031. *Mar. Drugs* **2021**, *19*, 701. [CrossRef]
41. She, J.; Chen, Y.; Ye, Y.; Lin, X.; Yang, B.; Xiao, J.; Liu, Y.; Zhou, X. New carboxamides and a new polyketide from the sponge-derived fungus *Arthrinium* sp. SCSIO 41421. *Mar. Drugs* **2022**, *20*, 475. [CrossRef] [PubMed]
42. Wang, J.; Liang, Z.; Li, K.; Yang, B.; Liu, Y.; Fang, W.; Tang, L.; Zhou, X. Ene-yne hydroquinones from a marine-derived strain of the fungus *Pestalotiopsis neglecta* with effects on Liver X receptor alpha. *J. Nat. Prod.* **2020**, *83*, 1258–1264. [CrossRef] [PubMed]

marine drugs

MDPI

Article

Macrolactin XY, a Macrolactin Antibiotic from Marine-Derived *Bacillus subtilis* sp. 18

Yao Xu †, Yihao Song †, Yaodong Ning, Song Li, Yingxin Qu, Binghua Jiao * and Xiaoling Lu *

Department of Biochemistry and Molecular Biology, College of Basic Medical Sciences, Naval Medical University, Shanghai 200433, China; nmuxy@smmu.edu.cn (Y.X.); fcs032@163.com (Y.S.); ning_yd@sina.com (Y.N.); lisonglisong0716@163.com (S.L.); 1020609684@smmu.edu.cn (Y.Q.)

* Correspondence: jiaobh@live.cn (B.J.); luxiaoling80@126.com (X.L.)

† These authors contributed equally to this work.

Abstract: Two new compounds, macrolactin XY (**1**) and (5*R*, 9*S*, 10*S*)-5-(hydroxymethyl)-1,3,7-decatriene-9,10-diol (**2**), together with nine known compounds (**3**–**11**) were isolated from the marine *Bacillus subtilis* sp. 18 by the OSMAC strategy. These compounds were evaluated for antibacterial activity against six tested microorganisms. Compounds **1**–**5** and **7**–**10** showed varied antibacterial activity, with the minimum inhibitory concentration (MIC) ranging from 3 to 12 μg/mL. Macrolactin XY (**1**) was found to possess superior antibacterial activity, especially exhibiting significant effectiveness against *Enterococcus faecalis*. The antibacterial activity mechanism against *E. faecalis* was investigated. The mechanism may disrupt bacterial cell membrane integrity and permeability, and also inhibit the expression of genes associated with bacterial energy metabolism, as established by the experiments concerning cell membrane potential, SDS-PAGE electrophoresis, cell membrane integrity, and key gene expressions. This study offers valuable insights and serves as a theoretical foundation for the future development of macrolactins as antibacterial precursors.

Keywords: macrolactins; antibiotic; antibacterial mechanism; cell membrane integrity

1. Introduction

E. faecalis is a conditionally pathogenic bacterium that is commonly found in the normal flora of the intestinal tract and frequently implicated in hospital-acquired infections. Its clinical infections typically manifest as periodontitis, urinary tract infections, abdominal and pelvic trauma, and post-surgical infections [1–3]. Given its infectious nature and the extensive research conducted on its pathogenic mechanisms, *E. faecalis* serves as a valuable reference for diagnosing and treating various diseases. The current arsenal of medications used in treating *E. faecalis* infections primarily comprises penicillins and aminoglycoside antibiotics. Penicillins, the preferred drug for the treatment of *E. faecalis* infection, exhibit high sensitivity towards the pathogen, albeit with some resistance stemming from the bacterium's robust cell walls [4,5]. Moreover, prolonged antibiotic usage can perturb the intestinal flora balance, manifesting in gastrointestinal symptoms like anorexia, nausea, and dyspepsia. When penicillins are ineffective, aminoglycosides can be administered in tandem, albeit with the caveat of potential side effects such as ototoxicity and nephrotoxicity [6,7], necessitating cautious use. In light of the current scarcity of targeted therapeutic medications, it is beneficial to explore these therapeutic alternatives.

Macrolactins are natural compounds that feature three distinct diene structures embedded within a 24-membered lactone ring. So far, over 50 macrolactin analogs have been isolated [8]. These compounds exhibit diverse biological activities, including antibacterial, anti-inflammatory, antitumor, and antiviral effects [9–12], offering a vast array of potential avenues for novel drug development. Antibacterial activity is one of the most superior bioactivities of macrolactins, and they showed a strong effect on *Staphylococcus aureus*, *Bacillus subtilis*, and *Escherichia coli*, which might become new antibacterial lead compounds.

In this study, eleven compounds were obtained from *Bacillus subtilis* sp. 18 (Figure 1), including two new compounds (macrolactin XY (**1**) and (5*R*, 9*S*, 10*S*)-5-(hydroxymethyl)-1,3,7-decatriene-9,10-diol (**2**)) and nine known compounds (**3**–**11**). Subsequently, the antibacterial activity of all compounds was evaluated, and it was found that the new compound, macrolactin XY (**1**), showed significant activity against *E. faecalis*. Given the remarkable antibacterial activity of macrolactins, a preliminary investigation was conducted into its antibacterial mechanism using *E. faecalis* as an indicator bacterium.

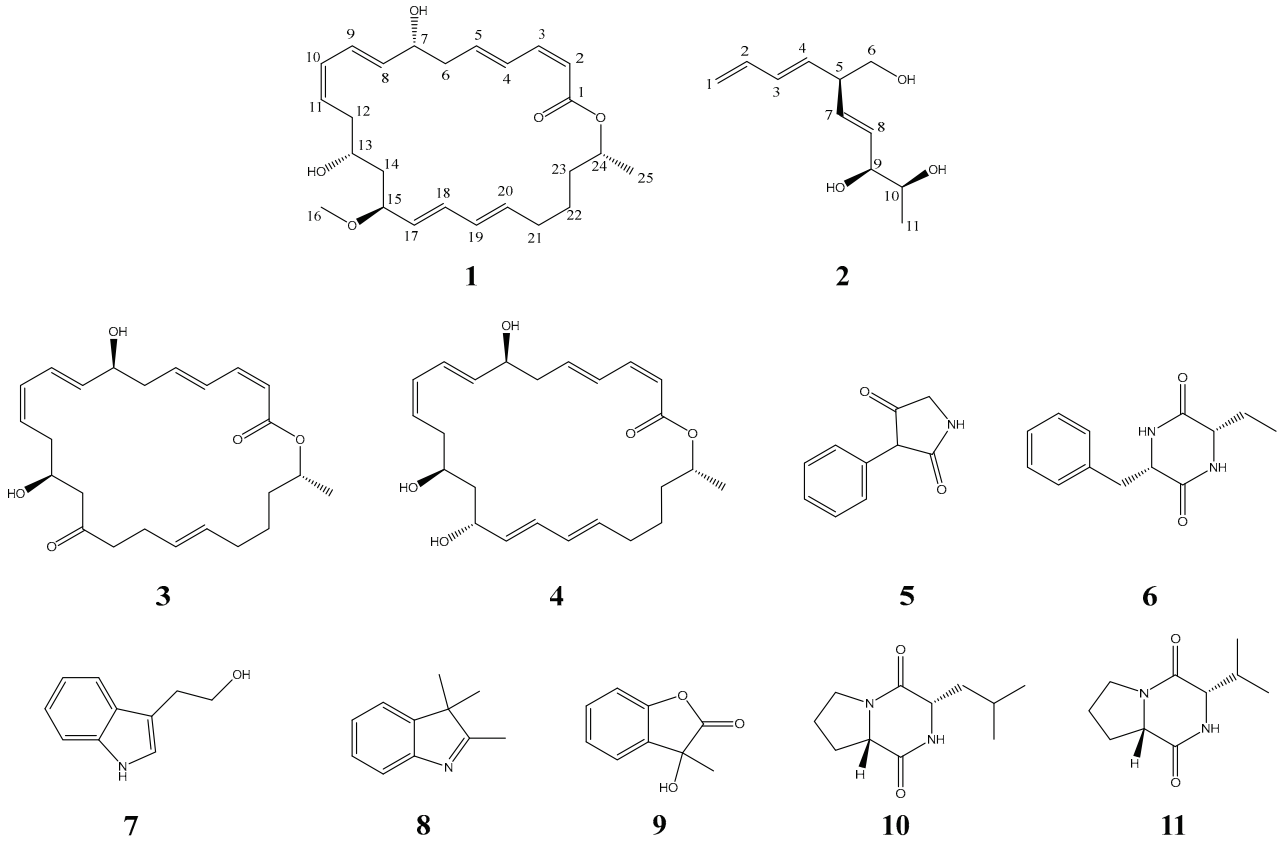

Figure 1. Structures of compounds **1**–**11**.

2. Results and Discussion

2.1. Structural Analysis of Compounds

Compound **1** was isolated as a white powder. The molecular formula was determined to be $C_{25}H_{36}O_5$ by HRESIMS, implying eight degrees of unsaturation. The UV spectrum exhibited absorption at λ_{max} 228 and 262 nm (Figure S1). The ^{1}H-NMR and ^{13}C-NMR data are shown in Table 1 (Figures S2 and S3). The ^{1}H-NMR data displayed two characteristic methyl proton signals at δ_H 3.27 (3H, s) and δ_H 1.28 (3H, d, J = 6.3 Hz). Analysis of the ^{13}C-NMR data and DEPT spectrum revealed a total of twenty-five carbons, including two methyls, six methylenes, sixteen methines, and one quaternary carbon signal. Twelve double-bond carbon signals were found at δc 118.2, 143.0, 130.0, 139.6, 135.8, 125.1, 130.0, 128.3, 130.1, 133.3, 129.9, and 135.5. Four carbons connecting oxygen atoms at δ_C 69.41, 71.16, 71.41, and 80.37, and one methoxyl carbon signal at δ_C 56.39 could be observed from the ^{13}C-NMR (Figures S4 and S6).

Table 1. ^{1}H and ^{13}C-NMR data of compounds **1** (in $CDCl_3$) and **2** (in CD_3OD).

Position	1 *		2 *	
	δc, Type	**δ_H, Mult. (*J* in Hz)**	**δc, Type**	**δ_H, Mult. (*J* in Hz)**
1a	166.4, C		116.2, CH_2	4.99, dd, (10.1, 1.8)
1b				5.13, dd, (14.3, 1.5)
2	118.2, CH	5.59, d, (11.6)	138.5, CH	6.35, dt, (14.2, 8.5)
3	143.0, CH	6.54, m	133.6, CH	6.15, dd, (13.0, 8.5)
4	130.0, CH	7.24, dd, (11.4, 15.2)	135.1, CH	5.67, m
5	139.6, CH	6.07, m	49.7, CH	2.98, t, (6.9)
6	41.7, CH_2	2.47, m	66.3, CH_2	3.53, d, (6.6)
7	71.4, CH	4.35, q, (6.9)	133.5, CH	5.62, m
8	135.8, CH	5.75, dd, (5.5, 15.1)	132.5, CH	5.58, dd, (5.5, 13.0)
9	125.1, CH	6.58, m	77.9, CH	3.86, m
10	130.0, CH	6.09, m	71.5, CH	3.65, m
11	128.3, CH	5.53, dt, (9.0, 9.0)	18.7, CH_3	1.14, d, (6.4)
12	35.4, CH_2	2.42, m		
13	69.4, CH	3.91, m		
14a	40.4, CH_2	1.77, m		
14b		1.71, m		
15	80.4, CH	3.96, m		
16	56.4, CH_3	3.27, s		
17	130.1, CH	5.43, dd, (8.0, 15.2)		
18	133.3, CH	6.15, dd, (10.4, 15.2)		
19	129.9, CH	6.02, m		
20	135.5, CH	5.68, dt, (7.0, 14.5)		
21a	32.1, CH_2	2.19, m		
21b		2.09, m		
22	24.6, CH_2	1.51, m		
23	35.0, CH_2	1.64, m		
24	71.2, CH	5.03, m		
25	20.0, CH_3	1.28, d, (6.3)		

* 500 MHz for ^{1}H-NMR and 125 MHz for ^{13}C-NMR.

The COSY correlations of H-2/H-3, H-4/H-5, H-6/H-7, H-7/H-8, H-8/H-9, H-12/H-13, H-13/H-14, H-14/H-15, H-15/H-17, H-20/H-21, H-21/H-22, H-22/H-23, H-23/H-24, and H-24/H-25 revealed the presence of five isolated spin systems: C-2/C-3, C-4 and C-6, C-6/C-7/C-8/C-9, C-12/C-13/C-14/C-15 and C-17, and C-20/C-21/C-22/C-23/C-24/C-25 (Figure 2 and Figure S5). The diagnostic HMBC correlations from H-25 to C-24, H-24 to C-1 and C-22/C-23, H-3 to C-1 and C-5, H-9 to C-7 and C-10, H-16 to C-15, H-12 to C-10/C-11 and C-13/C-14, and H-18 to C-15 and C-20 indicated a macrocycle with a 24-membered ring serving as its core structure (Figure S7). Due to the presence of three oxygenated carbon signals, the oxygenated carbons at C-7 and C-13 had to be substituted with a hydroxy group to satisfy the molecular formula, and the carbons at C-15 and C-24 were substituted with methoxyl and methyl, respectively (Figure 2). The ^{1}H coupling constant between H-2 and H-3 was 11.6 Hz, while the coupling constant between H-4 and H-5 was 15.2 Hz, indicating that the geometries of C-2 and C-4 were *Z* and *E* configurations. The ^{1}H coupling constant between H-8 and H-9 was 15.1 Hz, while the coupling constant between H-10 and H-11 was 9.0 Hz, indicating that the geometries of C-8 and C-10 were *E* and *Z* configurations. The ^{1}H coupling constant between H-17 and H-18 was 15.2 Hz, while the coupling constant between H-19 and H-20 was 14.5 Hz, indicating that the geometries of C-17 and C-19 were both *E* configurations. Thus, a planar structure was indicated.

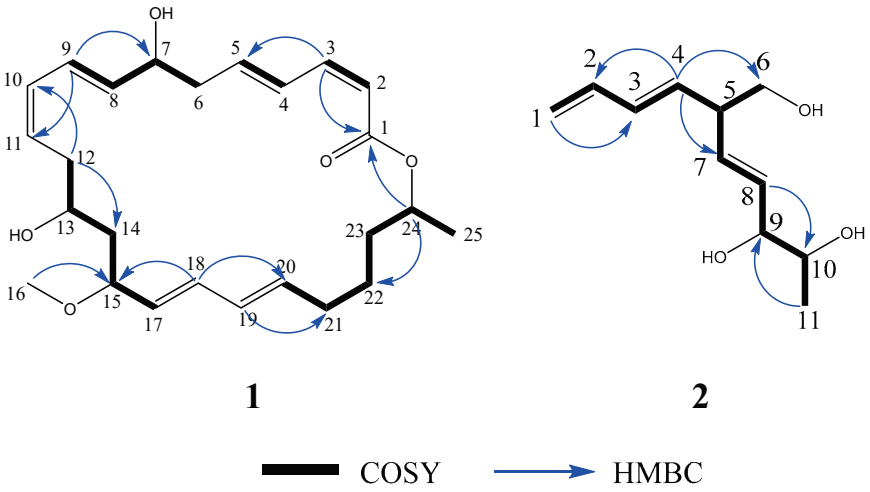

Figure 2. COSY and key HMBC correlations of compounds **1** and **2**.

Once the planar structure was established, its relative configuration was addressed by NOESY experiments (Figure 3). The NOESY cross-peaks of H-7/H-10, H-10/H-11, H-11/H-13 and H-10/H-24 indicated the same orientation of these protons. Therefore, the relative structure was determined (Figure S8).

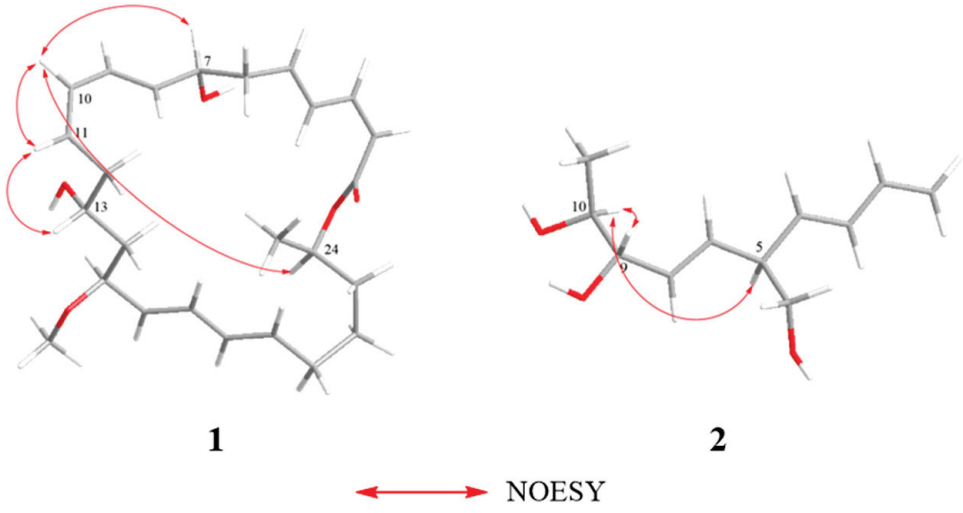

Figure 3. Key NOESY correlations of compounds **1** and **2**.

To ascertain the comprehensive absolute configurations of **1**, the quantum chemical electronic circular dichroism (ECD) calculation method was utilized. The negative Cotton effect (CE) at 260 nm and positive cotton effect at 233 nm in the calculated spectrum of the 7*R*, 13*R*, 15*S*, 24*R* enantiomer approximately matched the CE observed in the experimental ECD spectrum of **1** (Figure 4), enabling the assignment of the absolute configuration of **1**, as demonstrated. Finally, compound **1** was named as macrolactin XY. Compared to the other macrolactins, the main difference between macrolactin XY (**1**) and the others was that the latter were hydroxylated at C-15, whereas macrolactin XY (**1**) was methoxylated.

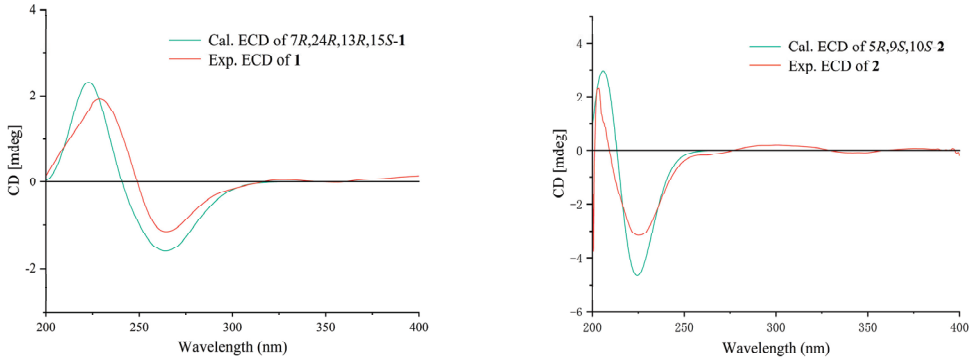

Figure 4. Calculated and experimental ECD spectra of compounds **1** and **2**.

Compound **2** was isolated as a yellow oil. The molecular formula was determined to be $C_{11}H_{18}O_3$ by HRESIMS, implying three degrees of unsaturation. The UV spectrum exhibited absorption at λ_{max} 226 nm (Figure S11). The ^{1}H-NMR and ^{13}C-NMR data are shown in Table 1 (Figures S12 and S13). The ^{1}H-NMR data displayed one characteristic methyl proton signal at δ_H 1.14 (3H, d, J = 6.4 Hz); seven olefinic protons signals at δ_H 6.35 (1H, dt, J = 14.2, 8.5 Hz), 6.15 (1H, dd, J = 13.0, 8.5 Hz), 5.67 (1H, m), 5.13 (1H, dd, J = 14.3, 1.5 Hz), 5.58 (1H, dd, J = 5.5, 13.0 Hz), 5.62 (1H, m), and 4.99 (1H, dd, J = 10.1, 1.8 Hz); one oxygen-bearing methylene proton signal at δ_H 3.53 (2H, d, J = 6.6 Hz); and three aliphatic methine signals, including two methine oxide signals at δ_H 3.86 (1H, m), 3.65 (1H, m), and one methine signal at δ_H 2.98 (1H, t, J = 6.9 Hz). Analysis of the ^{13}C-NMR data and DEPT spectrum revealed a total of eleven carbons, including six double-bond carbon signals at δc 116.2, 138.5, 133.6, 135.1, 133.5, and 132.5, three methine carbon signals, one methylene carbon signal, and one methyl carbon signal. Its structural characteristics mean that it is a precursor to terpene synthetic substances, suggesting the potential of producing some terpenes in this strain (Figures S14 and S16).

The COSY correlations of H-1/H-2, H-2/H-3, H-3/H-4, H-4/H-5, H-5/H-6, H-5/H-7, H-7/H-8, H-8/H-9, H-9/H-10, and H-10/H-11 revealed the presence of two isolated spin systems: C-1/C-2/C-3/C-4/C-5/C-6 and C-5/C-7/C-8/C-9/C-10/C-11 (Figure 2 and Figure S15). The diagnostic HMBC correlations from H-1 to C-2/C-3, H-4 to C-2/C-3 and C-5/C-6, H-4 to C-7, H-8 to C-9/C-10, and H-11 to C-9/C-10 indicated the presence of a terminal double bond conjugated with a trans double bond, confirming that an oxygen-bearing methylene is linked to this conjugated double bond via a methine group (Figure S17). Due to the presence of three oxygenated carbon signals, C-6 and C-9/C-10 had to be substituted with a hydroxyl group to satisfy the molecular formula. The ^{1}H coupling constant between H-3 and H-4 was 13.0 Hz, while the coupling constant between H-7 and H-8 was 13.0 Hz, indicating that the geometries of C-3 and C-7 were both *E* configurations. Thus, the planar structure was determined (Figure 2).

Once the planar structure was established, its relative configuration was addressed by NOESY experiments (Figure 3). The NOESY cross-peaks of H-9/H-10 and H-5/H-10 indicated the same orientation of these protons and that they were located on the same side of the molecule (Figure S18). Therefore, the relative structure was determined. To ascertain the comprehensive absolute configuration of **2**, the quantum chemical electronic circular dichroism (ECD) calculation method was utilized. The negative Cotton effect (CE) at 224 nm and positive CE at 204 nm in the calculated spectrum of the 5*R*, 9*S*, 10*S* enantiomer approximately matched the CE observed in the experimental ECD spectrum of **2** (Figure 4), enabling the assignment of the absolute configuration of **2**, as demonstrated. ECD analysis was also performed on six other isomers of compound **2** (Figure S21), however, the results indicated that none of them matched the experimental ECD spec-trum. Finally, compound **2** was named as (5*R*, 9*S*, 10*S*)-5-(hydroxymethyl)-1,3,7-decatriene-9,10-diol.

In addition, nine known compounds (**3**–**11**) were also isolated as metabolites of *Bacillus subtilis* sp. 18 (Figure 1). These compounds were identified through a comparison of

their spectral data with the spectroscopic data reported in the relevant literature, and all of them were classified as follows: macrolactin F (**3**), macrolactin A (**4**), 3-phenyl-2,4-pyrrolidinedione (**5**), cyclo (Phe-Thr) (**6**), tryptophol (**7**), 2,3,3-trimethylindolenine (**8**), 3-hydroxy-3-methyl-2(3H)-benzofuranone (**9**), L-leucyl-L-proline lactam (**10**), and cyclo (Pro-Val) (**11**).

2.2. Antibacterial Activity

2.2.1. Determination of MIC and MBC of Macrolactin XY against Test Microorganisms

Compounds **1–11** exhibited inhibitory activity against a range of microorganisms, including *S. aureus*, *B. subtilis*, *E. coli*, *E. faecalis*, *Vibrio traumaticus*, and *Vibrio parahaemolyticus*. As shown in Table 2, compounds **1–5** and **7–10** showed varied antibacterial activity, with MICs ranging from 3 to 12 μg/mL. Among them, macrolactin XY (**1**), macrolactin F (**3**), and macrolactin A (**4**) showed strong antibacterial effects, especially macrolactin XY (**1**), demonstrating a significant inhibitory effect (MIC 3 μg/mL and MBC 12 μg/mL) on *E. faecalis*.

Table 2. Antibacterial activity of compounds **1–11** against various indicator bacteria.

Compound	MIC (μg/mL)					
	E. coli	***E. faecalis***	***B. subtilis***	***S. aureus***	***V. traumaticus***	***V. parahaemolyticus***
1 *	6	3	6	6	-	-
2 *	6	-	-	6	-	-
3	-	-	6	6	-	-
4	-	-	6	6	-	-
5	-	-	-	12	-	-
6	6	-	-	-	-	-
7	-	-	-	-	-	-
8	-	-	12	-	-	-
9	12	-	-	6	-	-
10	12	-	-	-	-	-
11	-	-	-	-	-	-
Levofloxacin	0.5	0.5	0.5	0.5	0.5	0.5
Methanol	-	-	-	-	-	-

"*" indicates new compound; "-" indicates inactive.

Among the three isolated macrolactins, macrolactin XY (**1**) demonstrated superior activity compared to macrolactins A and F, particularly against *E. faecalis*. The analysis of known structure–activity relationships revealed that macrolactins exhibit great antibacterial activity when the C-15 position is linked to a hydroxyl group [8,13,14]. This suggests that the methoxyl group at the C-15 position contributes significantly to antibacterial effects, identifying the C-15 site as a crucial active site for the antibacterial activity of macrolactins.

2.2.2. Analysis of Bacterial Growth Curve

To further validate the antibacterial effect of macrolactin XY (**1**) against *E. faecalis*, a detailed investigation on the impact of macrolactin XY (**1**) on the specific growth rate of *E. faecalis* was conducted, as presented in Table 3. Additionally, a growth curve was plotted to illustrate the interaction between macrolactin XY (**1**) and *E. faecalis*, as depicted in Figure 5.

Table 3. Specific growth rate of *E. faecalis* in control and administered groups.

Time	Control Group	MIC Group
2 h	1.29 ± 0.02	0.31 ± 0.02
4 h	0.77 ± 0.03	0.39 ± 0.03
6 h	0.61 ± 0.01	0.35 ± 0.01
8 h	0.51 ± 0.02	0.29 ± 0.01
10 h	0.42 ± 0.03	0.25 ± 0.02
12 h	0.36 ± 0.02	0.22 ± 0.03
14 h	0.31 ± 0.03	0.19 ± 0.02
16 h	0.28 ± 0.01	0.18 ± 0.01
18 h	0.26 ± 0.02	0.17 ± 0.02
20 h	0.23 ± 0.02	0.16 ± 0.01
22 h	0.21 ± 0.01	0.15 ± 0.02
24 h	0.19 ± 0.01	0.14 ± 0.03

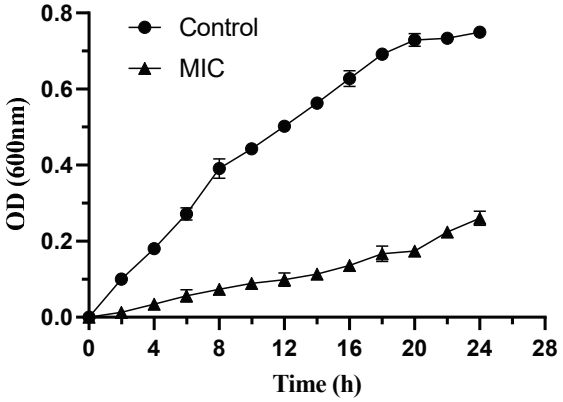

Figure 5. Growth curve of *E. faecalis*.

Upon examination of the growth curves, it became evident that the OD values of the control group exhibited a rapid increase, particularly in comparison to the treated group, and stabilized after approximately 20 h. This observation was primarily attributed to the bacteria's growth cycle. Notably, when the concentration of the sample solution was set at the MIC, bacterial growth was delayed over time. The resulting OD value was significantly lower than that of the control group ($p < 0.05$). Furthermore, the specific growth rate of *E. faecalis* decreased significantly ($p < 0.05$) with the effect of macrolactin XY (**1**), indicating its inhibitory effect on bacterial growth.

2.3. Antibacterial Mechanism

2.3.1. Effect on Bacterial Cell Membrane Potential

As depicted in Figure 6a, alterations in the membrane potential of *E. faecalis* exerted a profound influence on the metabolic activity of the bacteria [15]. Specifically, a decrease in fluorescence intensity served as an indicator of a reduced potential difference between the intracellular and extracellular environments [16]. Notably, the mean fluorescence intensity decreased by 23.9% when the concentration of macrolactin XY (**1**) approached the MIC level, compared to both the control and negative control groups. This decrement was statistically significant ($p < 0.0001$). In contrast, there was no significant difference between the control and negative control groups ($p > 0.05$), indicating that macrolactin XY (**1**) specifically targets bacterial membrane potential, ultimately affecting metabolic activity.

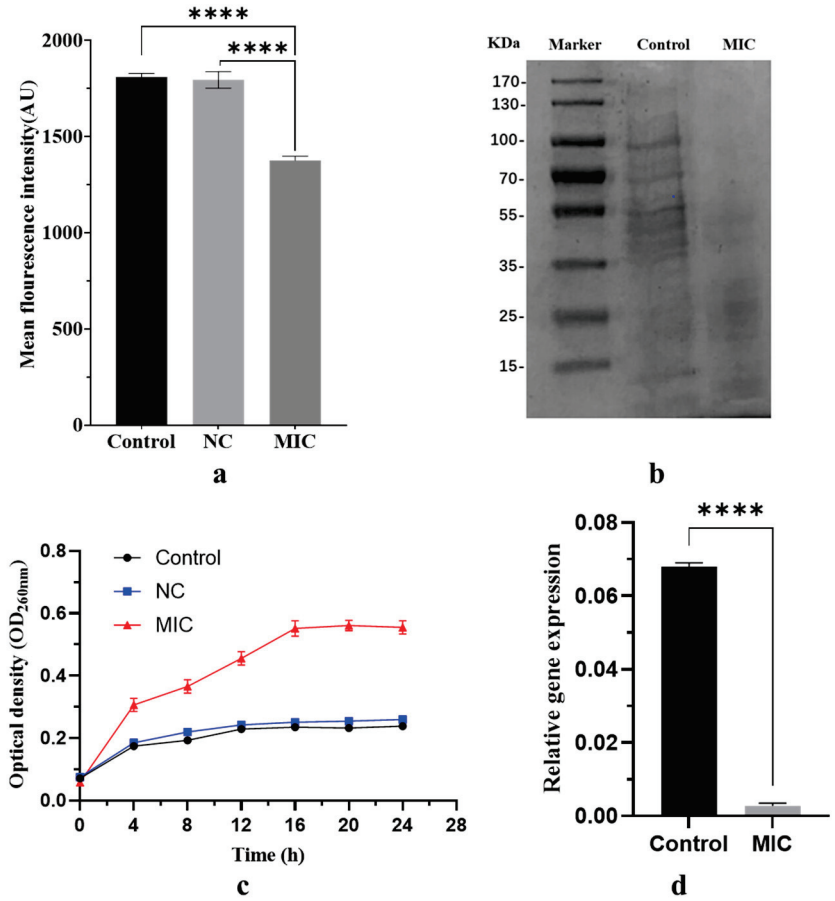

Figure 6. (**a**) Changes in fluorescence intensity of *E. faecalis* after addition of macrolactin XY. "****" represents $p < 0.0001$. (**b**) The gel electrophoresis picture of *E. faecalis* intracellular proteins. (**c**) Effect of macrolactin XY on cell membrane integrity of *E. faecalis*. (**d**) Relative expression of PK in *E. faecalis* following the action of macrolactin XY.

2.3.2. Results of SDS-PAGE Electrophoresis of Bacterial Proteins

Proteins serve as the fundamental building blocks of all life, and are essential for maintaining normal metabolic processes and facilitating the transportation of diverse substances throughout the body. The expression level of proteins provides a valuable indicator of the state of cellular life [17]. Bacteria harbour numerous crucial macromolecular proteins, such as glucose transporters, a class of transmembrane protein situated on the bacterial cell membrane. These are vital regulators of glucose's transmembrane transport, playing a pivotal role in bacteria's energy acquisition and metabolic processes [18]. Other enzymes that are integral to the biosynthesis of peptidoglycan in the bacterial cell wall, like penicillin-binding proteins, participate in the synthesis and maintenance of cell membrane stability [19]. The SDS-PAGE electrophoresis results, depicted in Figure 6b, revealed notable differences in protein profiles between the MIC group and the control group. In the control group, the protein bands of *E. faecalis* appeared distinct and abundant. Conversely, the protein bands in the MIC group exhibited fainter colours, with some bands disappearing altogether. The macrolactin XY-treated group showed predominantly lighter protein bands, indicating that macrolactin XY (**1**) interfered with protein synthesis. This resulted in a decrease in the overall protein content of the bacteria, particularly affecting protein bands above 55 kDa, which nearly vanished. These observations suggest that macrolactin XY (**1**) primarily impacted the synthesis of larger-molecular-weight proteins.

2.3.3. Effects on Cell Membrane Integrity

Cell membrane integrity is indicated by the leakage of nucleic acids from bacterial cells into the suspension [20]. As shown in Figure 6c, the nucleic acid content (measured as OD_{260nm}) remained relatively stable and did not exhibit significant changes ($p > 0.05$) over time in both blank group and the negative control groups. However, a significant increase ($p < 0.05$) in nucleic acid content (OD_{260nm}) was observed in the macrolactin XY-treated group, peaking at 0.563 in the 16th hour and remaining relatively unchanged.

2.3.4. The Impact on the Expression of Genes Involved in Bacterial Energy Metabolism

Pyruvate kinase (PK) plays an important role in bacterial energy metabolism, serving as a crucial enzyme in the glycolytic pathway. It can catalyse the conversion of phosphoenolpyruvate to pyruvate, the process of which generates ATP, providing the necessary energy for bacteria. Furthermore, PK is involved in regulating the balance between glycogenolysis and gluconeogenesis to ensure that bacteria can flexibly adapt to changes in energy demand and maintain their normal life activities and physiological functions.

As shown in Figure 6d, it became evident that the expression of PK in *E. faecalis* was significantly downregulated ($p < 0.0001$) in the macrolactin XY-treated group at the MIC compared to the control group. This reveals that macrolactin XY modulates the transcript levels of genes encoding enzymes and proteins that play crucial roles in ATP synthesis, glycolysis, and other energy-producing processes.

3. Materials and Methods

3.1. General Experimental Procedures

NMR spectra were acquired using a Bruker AMX-500 spectrometer (Bruker Biospin Corp., Billerica, MA, USA), operating at 500 MHz for ^{1}H-NMR and 125 MHz for ^{13}C-NMR to ensure high-resolution and accurate spectral data. For HRESIMS analysis, an Agilent 6210 LC/MSD TOF mass spectrometer (Agilent Technologies Inc., Lake Forest, CA, USA) was employed, providing precise mass measurements. UV spectra were recorded on a UV-8000 spectrophotometer (Shanghai Metash instruments Co., Shanghai, China), ensuring the accurate quantification of absorbance values. Optical rotations were measured precisely using an Anton Paar MCP 5500 instrument (Anton Paar Co., Graz, Austria). Chromatographic separations were carried out on a Waters 1525 HPLC system (Waters Corp., Milford, MA, USA) equipped with a Waters 2996 photodiode array detector, utilizing YMC-Pack Pro C18 RS columns (5 μm) from YMC Co., Ltd. (Kyoto, Japan). Purifications were performed using an Agilent LC1263 Infinity II purification system (Agilent Technologies Inc., CA, USA). Thin-layer chromatography analysis was conducted on HSGF254-precoated silica gel plates (10–40 mm) from Yantai Chemical Plant (Yantai, China), ensuring the high-quality separation of analytes.

3.2. Bacterial Strain

The strain *Bacillus subtilis* sp. 18 was isolated from a co-epidermal sample collected from a sponge dwelling in the waters of the South China Sea at a depth of 325 m. This strain was being maintained by the Department of Biochemistry and Molecular Biology at the Naval Military Medical University. To propagate the strain, individual colonies were inoculated into test tubes containing 10 mL of ISP_2 liquid medium (10 g/L of malt extract, 4 g/L of yeast, and 4 g/L of glucose). These cultures were then incubated for three days at a constant temperature of 28 °C with shaking at 180 rpm to generate seed cultures (OSMAC strategy in previous studies).

The Department of Biochemistry and Molecular Biology at the Naval Military Medical University generously provided us with a range of bacterial strains, including *E. faecalis* (ATCC 29212), *S. aureus* (ATCC 27217), *B. subtilis* (ATCC 21951), *E. coli* (ATCC 25922), *V. vulnificus* (ATCC 27562), and *V. parahaemolyticus* (ATCC 17802). To prepare these strains for subsequent experiments, 100 μL of each test strain was inoculated into test tubes containing 5 mL of nutrient broth medium (18 g/L of nutrient broth medium). The cultures

were then incubated at 28 °C with shaking at 180 rotations per minute for 12 h, ensuring optimal activation and proliferation before proceeding to the next step.

3.3. Fermentation

The seed culture was added to 500 mL of ISP_2 medium at a ratio of 10% (v/v) and incubated for eight days at 28 °C, with shaking at 180 rpm to allow for optimal growth and metabolism.

3.4. Extraction and Isolation

The fermentation broth underwent a separation process where it was filtered through eight layers of gauze, resulting in two distinct fractions. The filtrate was thoroughly mixed with an equal volume of ethyl acetate, while the bacterial material was thoroughly macerated with a combination of equal volumes of petroleum ether and ethyl acetate. Following stratification, the organic phase layer was collected, and this entire procedure was repeated three times. The combined organic phase layers from both the filtrate and the bacterial fraction were then evaporated using a rotary evaporator to obtain the fermentation product.

The crude extract (14 g) underwent vacuum liquid chromatography on a silica gel column, utilizing a gradient elution method with a mixed-solvent system of petroleum ether and ethyl acetate (from a 10:1 to 0:1) to obtain 10 fractions (A–Z). The fractions C, F, J, O, and Q underwent further elution on a forward silica gel column separately, employing a gradient of the same mixed-solvent system (from 50:1 to 0:1), yielding 13 subfractions for C (C1–C13), 10 subfractions for F (F1–F10), 4 subfractions for J (J1–J4), 12 subfractions for O (O1–O12), and 12 subfractions for Q (Q1–Q12). The fractions C12, C13, F2, F4, J2, O7, O9, Q7, and Q8 were then purified using HPLC ($MeOH/H_2O$, 2.0 mL/min) separately, resulting in the purification of compound **2** (1.3 mg in C12)**,** compound **10** (1.6 mg in C13)**,** compound **11** (2.1 mg in F2), compound **9** (1.3 mg in F4), compound **8** (1.3 mg in J2), compound **5** (1.3 mg in O7), compound **6** (1.1 mg in O9), compound **1** (1.1 mg in Q7), compound **3** (2.0 mg in Q7), compound **4** (1.1 mg in Q8), and compound **7** (1.2 mg in Q8). The detailed isolation process for the known compounds is omitted for brevity.

Macrolactin XY (**1**): white powder; $[\alpha]_D^{25}$-93.90 (*c* 0.1, MeOH); UV (MeOH) λmax (log ε) 228 (3.68), 262 (3.36) nm; CD (MeOH) ($\Delta\varepsilon$) 233 (+13.16), 260 (−6.40); ^{1}H-NMR and ^{13}C-NMR data, see Table 1; HRESIMS m/z 439.2458 $[M+Na]^+$ (calcd for $C_{25}H_{36}O_5Na$, 439.2455) (Figures S9 and S10).

(5*R*, 9*S*, 10*S*)-5-(hydroxymethyl)-1,3,7-decatriene-9,10-diol (**2**): yellow oil; $[\alpha]_D^{25}$-15.2785 (*c* 1.0, MeOH); UV (MeOH) λmax (log ε) 226 (3.89) nm; CD (MeOH) ($\Delta\varepsilon$) 204 (+10.46), 224 (−10.03); ^{1}H-NMR and ^{13}C-NMR data, see Table 1; HRESIMS m/z 221.1150 $[M+Na]^+$ (calcd for $C_{11}H_{18}O_3Na$, 221.11482) (Figures S19 and S20).

3.5. ECD Calculations

Initially, the conformational analyses for compounds **1** and **2** were conducted utilizing the Spartan'10 software (Wave-function, Inc., Irvine, CA, USA) within the MMFF94 force field. Later, conformers with a Boltzmann population of over 5% were refined at the B3LYP/6-31+G (d, p) level, employing the conductor-like polarizable continuum model (CPCM) in MeOH. The theoretical ECD calculations for compounds **1** and **2** were calculated using the time-dependent density functional theory (TDDFT) approach at the B3LYP/6-311++G (2d, 2p) level in MeOH, respectively. The ECD spectra were generated by SpecDis 1.6 (University of Würzburg, Germany) using a Gaussian band shape with an exponential half-width of 0.3 eV, derived from dipole-length dipolar and rotational strengths.

3.6. Antibacterial Activity

3.6.1. Determination of MIC and MBC in Macrolactin XY against Test Microorganisms

E. faecalis was activated according to the operation in 3.2 (to an optical density at OD_{600} of 0.6–0.8) and diluted with sterilized medium at a ratio of 1:1000. The sample was

dissolved in methanol and further diluted with sterile water to achieve a concentration of 64 μg/mL. This experiment was carried out using the micro-broth dilution method; first, a sterile 96-well plate was prepared by filling the outermost circle with 200 μL sterile water to prevent the bacterial solution from drying, and then the bacterial solution was added to the remaining wells. An amount of 10 μL sample solution (at a concentration of 64 μg/mL) was added to the first well, and then diluted to 0.5 μg/mL by the multiplicative dilution method to make the final concentration in the range of 0.5–64 μg/mL, and the negative (methanol) and positive controls (levofloxacin) were set. The 96-well plate was incubated in a constant-temperature incubator maintained at 28 °C for 12 h.

3.6.2. Analysis of Bacterial Growth Curve

E. faecalis was activated according to the operation in 3.2 (to an optical density at OD_{600} of 0.6–0.8) and the sample was dissolved in methanol and subsequently diluted with water to reach the MIC. To assess the growth curve, a sterile 96-well plate was prepared by leaving the outermost ring empty and filling each of the wells with 200 μL sterile water. In the remaining wells, 200 μL bacterial solution was dispensed, with 12 wells designated for each of the control and experimental groups. Then, 10 μL sample solution was received at the MIC of the experimental wells. The 9 plates were then incubated at 28 °C with agitation at 180 rpm. The optical density at 600 nm (OD_{600}) of the wells was measured every two hours. This process was repeated three times, and the average value was recorded. Subsequently, the specific growth rate was computed for the logarithmic growth period using the formula $\ln(N2/N1) = \mu t$ (N2 and N1 represent the bacterial counts at different time points and μ is the specific growth rate).

3.7. Antibacterial Mechanism

3.7.1. Bacterial Cell Membrane Potential

E. faecalis was activated according to the operation in 3.2 (to an optical density at OD_{600} of 0.6–0.8), and then transferred to a 1.5 mL EP tube for the next step. The MIC of compound **1** was added into the bacterial suspension, serving as the experimental treatment. Concurrently, a suspension lacking the sample solution was utilized as the blank control, while the solvent utilized to dissolve the sample represented the negative control. Following an incubation period of 10 h, the bacterial suspension was centrifuged at 4000 rpm for 10 min, yielding a bacterial pellet, which was washed twice with phosphate-buffered saline (PBS, 0.1 M, pH 7.2). Subsequently, a rhodamine 123 dye solution (rhodamine 123 powder was dissolved in methanol to form a solution of 1.0 g/mL and then diluted to 2.0 mg/mL with PBS) was added into the pellet, and then the mixture was incubated for 30 min in a dark area. All of the mixture was transferred to a 96-well plate, and the fluorescence intensity was measured using a fluorescence spectrophotometer (SpectraMax M2e, Molecular Devices, Sunnyvale, CA, USA).

3.7.2. SDS-PAGE Electrophoresis of Bacterial Proteins

E. faecalis was activated according to the operation in 3.2 (to an optical density at OD_{600} of 0.6–0.8), and the bacterial solution was divided into two groups. One group (1 mL) served as the untreated control, while the other (1 mL) received 200 μL compound **1** at its MIC. Both groups were incubated for 10 h. After the incubation was completed, centrifugation was performed to remove most of the supernatant, and then an ultrasonic crusher (80% of maximum power, running for 15 s at 10 s intervals for 15 min) was used to crush the cells and release the proteins. The SDS-PAGE Gel Rapid Preparation Kit (Shanghai Yase Biotechnology Co., Ltd., Shanghai, China) was used to prepare the gel (loaded 10 μL protein sample). After electrophoresis was completed, Coomassie brilliant blue was applied to visualize the separated protein bands obtained after decolorization.

3.7.3. Effects on Cell Membrane Integrity

The disruption of cell membrane integrity was demonstrated by quantifying the concentration of nucleic acids present in the bacterial suspension. *E. faecalis* was activated according to the operation in 3.2 (to an optical density at OD_{600} of 0.6–0.8), then dispensed into a 96-well plate (200 μL in each well), setting the blank control and negative control. For the experimental group, 20 μL sample solution containing an MIC was added, while the control group remained untreated. The incubation was carried out in an incubator at 28 °C, and 200 μL of the bacterial suspension was removed every 4 h. The OD_{260} value was determined using a UV–Vis spectrophotometer to indicate the nucleic acid content in the bacterial suspension.

3.7.4. The Impact on the Expression of Genes Involved in Bacterial Energy Metabolism

Pyruvate kinase (PK), a crucial enzyme involved in bacterial energy metabolism, was chosen for further analysis. To design primers, the PK sequence of *E. faecalis* was retrieved through a database query. Additionally, the 16s rRNA gene was employed as an internal reference gene. *E. faecalis* was activated according to the operation in 3.2 (to an optical density at OD_{600} of 0.6–0.8). An amount of 2 mL bacterial suspension was removed and added to two EP tubes, respectively. For the experimental group, 200 μL of sample solution was added at an MIC, while the control group remained untreated and was incubated for 10 h for the next step. RNA extraction was carried out using the TransStart RNA Extraction Kit (Beijing Quan's Gold Biological Company, Beijing, China), and reverse transcription was performed using the TransStart Top Green qPCR SuperMix Kit (Beijing Quan's Gold Biological Company). The resulting cDNA was stored at −80 °C. Real-time fluorescence quantitative PCR (QuantStudio 5, Thermo Fisher Scientific, Waltham, MA, USA) was utilized for the analysis, and the CT values obtained were employed to assess the expression of pertinent genes using the 2-ΔCT method. To guarantee the precision of the data, a minimum of three independent sets of experiments were conducted for each group.

3.8. Statistical Analysis

To ensure the accuracy and stability of the experimental data, all experiments were conducted in parallel groups and replicated three times. IBM SPSS Statistics 22.0 software (SPSS Inc., Armonk, NY, USA) was utilized for the analysis of the experimental data. One-way analysis of variance (ANOVA) was employed to determine significance levels, with *p*-values less than 0.05 considered statistically significant (* $p < 0.05$, ** $p < 0.01$, *** $p < 0.001$, **** $p < 0.0001$). To present the data in a more intuitive manner, GraphPad Prism was used for the statistical analysis of the experimental data.

4. Conclusions

In conclusion, eleven compounds, including two new compounds, were isolated from a fermentation broth of *Bacillus subtilis* sp. 18 through the OSMAC strategy in this study. Notably, a novel compound, macrolactin XY (**1**), demonstrated potent antibacterial activity against a diverse range of bacteria, particularly against *E. faecalis*, and its antibacterial mechanism was further investigated. Our findings suggest that the antibacterial mechanism of macrolactin XY (**1**) involves the disruption of the bacterial cell membrane, leading to the leakage of biomolecules such as nucleic acids and proteins, which disrupts the metabolic activity of the bacteria, ultimately leading to cell death (Figure 7). Furthermore, the mechanism also inhibited the expression of PK genes associated with bacterial energy metabolism, which disrupted the bacterial energy production pathway. Notably, a reduction in energy availability might adversely impact the functionality of ATP-reliant transporter proteins embedded in the bacterial cell membrane, particularly ion pumps and active transporters [21]. This, in turn, could disrupt the bacterial cell's material transport mechanisms and osmotic pressure regulation, potentially affecting its overall metabolic health and physiological state (Figure 7). Regrettably, owing to the limited quantity of our compounds, only a single pivotal gene pertaining to energy metabolism was analysed.

This work has laid a solid foundation for future studies on the antibacterial mechanism of macrolactin XY (**1**) and offers valuable insights for the development of macrolactins as potential antibacterial agents.

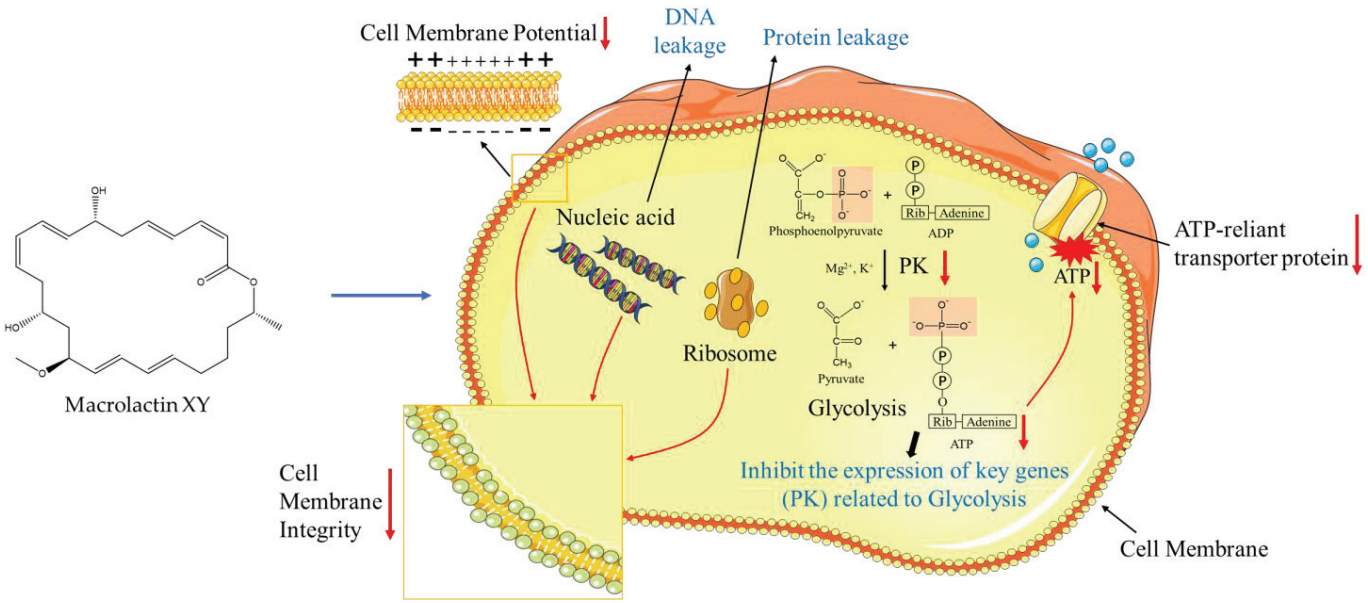

Figure 7. Possible antibacterial mechanism of action of macrolactin XY.

Supplementary Materials: The following supporting information can be downloaded at: https://www.mdpi.com/article/10.3390/md22080331/s1. Figure S1. UV spectrum of macrolactin XY (**1**); Figure S2. ^{1}H NMR of macrolactin XY (**1**) in $CDCl_3$; Figure S3. ^{13}C NMR of macrolactin XY (**1**) in $CDCl_3$; Figure S4. DEPT135 of macrolactin XY (**1**) in $CDCl_3$; Figure S5. COSY of macrolactin XY (**1**) in $CDCl_3$; Figure S6. HSQC of macrolactin XY (**1**) in $CDCl_3$; Figure S7. HMBC of macrolactin XY (**1**) in $CDCl_3$; Figure S8. NOESY of macrolactin XY (**1**) in $CDCl_3$; Figure S9. HR-ESI-MS of macrolactin XY (**1**); Figure S10. ORD of macrolactin XY (**1**); Figure S11. UV spectrum of (5*R*, 9*S*, 10*S*)-5-(hydroxymethyl)-1,3,7-decatriene-9,10-diol (**2**); Figure S12. ^{1}H NMR of (5*R*, 9*S*, 10*S*)-5-(hydroxymethyl)-1,3,7-decatriene-9,10-diol (**2**) in CD_3OD; Figure S13. ^{13}C NMR of (5*R*, 9*S*, 10*S*)-5-(hydroxymethyl)-1,3,7-decatriene-9,10-diol (**2**) in CD_3OD; Figure S14. DEPT135 of (5*R*, 9*S*, 10*S*)-5-(hydroxymethyl)-1,3,7-decatriene-9,10-diol (**2**) in CD_3OD; Figure S15. COSY of (5*R*, 9*S*, 10*S*)-5-(hydroxymethyl)-1,3,7-decatriene-9,10-diol (**2**) in CD_3OD; Figure S16. HSQC of (5*R*, 9*S*, 10*S*)-5-(hydroxymethyl)-1,3,7-decatriene-9,10-diol (**2**) in CD_3OD; Figure S17. HMBC of (5*R*, 9*S*, 10*S*)-5-(hydroxymethyl)-1,3,7-decatriene-9,10-diol (**2**) in CD_3OD; Figure S18. NOESY of (5*R*, 9*S*, 10*S*)-5-(hydroxymethyl)-1,3,7-decatriene-9,10-diol (**2**) in CD_3OD; Figure S19. HR-ESI-MS of (5*R*, 9*S*, 10*S*)-5-(hydroxymethyl)-1,3,7-decatriene-9,10-diol (**2**); Figure S20. ORD of (5*R*, 9*S*, 10*S*)-5-(hydroxymethyl)-1,3,7-decatriene-9,10-diol (**2**); Figure S21. ECD of (5*R*, 9*S*, 10*S*)-5-(hydroxymethyl)-1,3,7-decatriene-9,10-diol (**2**) (Six additional isomers).

Author Contributions: Conceptualization, methodology, and writing—original draft preparation, Y.X. and Y.S.; software and validation, Y.N. and S.L.; methodology, Y.Q. and Y.X.; investigation and resources, Y.X. and Y.S.; writing—review and editing, B.J.; writing—review and editing, funding acquisition, X.L. All authors have read and agreed to the published version of the manuscript.

Funding: This research was financially supported by the National Natural Science Foundation of China (82373786), Xiaoling Lu.

Institutional Review Board Statement: Not applicable.

Data Availability Statement: The data presented in this study are available on request from the corresponding author.

Conflicts of Interest: The authors declare no conflicts of interest.

References

1. Williamson, A.J.; Jacobson, R.; van Praagh, J.B.; Gaines, S.; Koo, H.Y.; Lee, B.; Chan, W.C.; Weichselbaum, R.; Alverdy, J.C.; Zaborina, O.; et al. *Enterococcus faecalis* promotes a migratory and invasive phenotype in colon cancer cells. *Neoplasia* **2022**, *27*, 100787. [CrossRef] [PubMed]
2. Abat, C.; Huart, M.; Garcia, V.; Dubourg, G.; Raoult, D. *Enterococcus faecalis* urinary-tract infections: Do they have a zoonotic origin? *J. Infect.* **2016**, *73*, 305–313. [CrossRef] [PubMed]
3. Ma, R.Y.; Deng, Z.L.; Du, Q.Y.; Dai, M.Q.; Luo, Y.Y.; Liang, Y.E.; Dai, X.Z.; Guo, S.M.; Zhao, W.H. *Enterococcus faecalis* Extracellular Vesicles Promote Apical Periodontitis. *J. Dent. Res.* **2024**, *103*, 672–682. [CrossRef] [PubMed]
4. Cusumano, J.A.; Daffinee, K.E.; Ugalde-Silva, P.; Peti, W.; Arthur, M.; Desbonnet, C.; Rice, L.B.; LaPlante, K.L.; García-Solache, M. Penicillin-Binding Proteins and Alternative Dual-Beta-Lactam Combinations for Serious *Enterococcus faecalis* Infections with Elevated Penicillin MICs. *Antimicrob. Agents Chemother.* **2023**, *67*, e00871-22. [CrossRef] [PubMed]
5. Herrera-Hidalgo, L.; Fernández-Rubio, B.; Luque-Márquez, R.; López-Cortés, L.E.; Gil-Navarro, M.V.; de Alarcón, A. Treatment of *Enterococcus faecalis* Infective Endocarditis: A Continuing Challenge. *Antibiotics* **2023**, *12*, 704. [CrossRef] [PubMed]
6. Rivetti, S.; Romano, A.; Mastrangelo, S.; Attinà, G.; Maurizi, P.; Ruggiero, A. Aminoglycosides-Related Ototoxicity: Mechanisms, Risk Factors, and Prevention in Pediatric Patients. *Pharmaceuticals* **2023**, *16*, 1353. [CrossRef]
7. Le, T.A.; Hiba, T.; Chaudhari, D.; Preston, A.N.; Palowsky, Z.R.; Ahmadzadeh, S.; Shekoohi, S.; Cornett, E.M.; Kaye, A.D. Aminoglycoside-Related Nephrotoxicity and Ototoxicity in Clinical Practice: A Review of Pathophysiological Mechanism and Treatment Options. *Adv. Ther.* **2023**, *40*, 1357–1365. [CrossRef] [PubMed]
8. Ortiz, A.; Sansinenea, E. Macrolactin Antibiotics: Amazing Natural Products. *Mini Rev. Med. Chem.* **2020**, *20*, 584–600. [CrossRef] [PubMed]
9. Ni, J.; Yu, L.; Li, F.; Li, Y.; Zhang, M.; Deng, Y.; Liu, X. Macrolactin R from *Bacillus siamensis* and its antifungal activity against Botrytis cinerea. *World J. Microbiol. Biotechnol.* **2023**, *39*, 117. [CrossRef]
10. Sohn, M.J.; Zheng, C.J.; Kim, W.G. Macrolactin, S, a New Antibacterial Agent with FabG inhibitory Activity from *Bacillus* sp. AT28. *J. Antibiot.* **2008**, *61*, 687–691. [CrossRef]
11. Dat, T.T.H.; Cuc, N.T.K.; Cuong, P.V.; Smidt, H.; Sipkema, D. Diversity and Antimicrobial Activity of Vietnamese Sponge-Associated Bacteria. *Mar. Drugs* **2021**, *19*, 353. [CrossRef] [PubMed]
12. Bharadwaj, K.K.; Sarkar, T.; Ghosh, A.; Baishya, D.; Rabha, B.; Panda, M.K.; Nelson, B.R.; John, A.B.; Sheikh, H.I.; Dash, B.P.; et al. Macrolactin A as a Novel Inhibitory Agent for SARS-CoV-2 M^{pro}: Bioinformatics Approach. *Appl. Biochem. Biotechnol.* **2021**, *193*, 3371–3394. [CrossRef]
13. Chakraborty, K.; Thilakan, B.; Raola, V.K. Polyketide Family of Novel Antibacterial 7-O-Methyl-5′-hydroxy-3′-heptenoate–Macrolactin from Seaweed-Associated *Bacillus subtilis* MTCC 10403. *J. Agric. Food Chem.* **2014**, *62*, 12194–12208. [CrossRef]
14. Gustafson, K.; Roman, M.; William, F. The macrolactins, a novel class of antiviral and cytotoxic macrolides from a deep-sea marine bacterium. *J. Am. Chem. Soc.* **1989**, *111*, 7519–7524. [CrossRef]
15. Novo, D.; Perlmutter, N.G.; Hunt, R.H.; Shapiro, H.M. Accurate flow cytometric membrane potential measurement in bacteria using diethyloxacarbocyanine and a ratiometric technique. *Cytometry* **1999**, *35*, 55–63. [CrossRef]
16. Lin, L.; Mao, X.; Sun, Y.; Rajivgandhi, G.; Cui, H. Antibacterial properties of nanofibers containing chrysanthemum essential oil and their application as beef packaging. *Int. J. Food Microbiol.* **2019**, *292*, 21–30. [CrossRef] [PubMed]
17. Wang, X.; Shen, Y.; Thakur, K.; Han, J.; Zhang, J.G.; Hu, F.; Wei, Z.J. Antibacterial Activity and Mechanism of Ginger Essential Oil against *Escherichia coli* and *Staphylococcus aureus*. *Molecules* **2020**, *25*, 3955. [CrossRef]
18. Ismail, A.; Tanasova, M. Importance of GLUT Transporters in Disease Diagnosis and Treatment. *Int. J. Mol. Sci.* **2022**, *23*, 8698. [CrossRef]
19. Martins, B.A.; Deffune, E.; Oliveira, O.N., Jr.; Moraes, M.L. Penicillin-binding proteins (PBPs) determine antibiotic action in Langmuir monolayers as nanoarchitectonics mimetic membranes of methicillin-resistant *Staphylococcus aureus*. *Colloids Surf. B Biointerfaces* **2022**, *214*, 112447. [CrossRef]
20. Luo, K.; Zhao, P.; He, Y.; Kang, S.; Shen, C.; Wang, S.; Guo, M.; Wang, L.; Shi, C. Antibacterial Effect of Oregano Essential Oil against *Vibrio vulnificus* and Its Mechanism. *Foods* **2022**, *11*, 403. [CrossRef]
21. S Hifnawy, M.; Hassan, H.M.; Mohammed, R.; M Fouda, M.; Sayed, A.M.; A Hamed, A.; F AbouZid, S.; Rateb, M.E.; Alhadrami, H.A.; Abdelmohsen, U.R. Induction of Antibacterial Metabolites by Co-Cultivation of Two Red-Sea-Sponge-Associated Actinomycetes *Micromonospora* sp. UR56 and *Actinokinespora* sp. EG49. *Mar. Drugs* **2020**, *18*, 243. [CrossRef] [PubMed]

marine drugs

MDPI

Communication

New Meroterpenoids and α-Pyrone Derivatives Isolated from the Mangrove Endophytic Fungal Strain *Aspergillus* sp. GXNU-Y85

Chungu Wang [1,†], Fanfan Wang [2,†], Pingfang Tao [2], Yuanling Shao [1], Qing Li [1], Minmin Gu [1], Zhixin Liao [1,*] and Feng Qin [2,*]

[1] Department of Pharmaceutical Engineering, School of Chemistry and Chemical Engineering, Southeast University, Nanjing 211189, China; cgwang0208@163.com (C.W.); 220203070@seu.edu.cn (Y.S.); liqing12018002134@163.com (Q.L.); 220213219@seu.edu.cn (M.G.)

[2] Guangxi Key Laboratory of Agricultural Resources Chemistry and Biotechnology, College of Chemistry and Food Science, Yulin Normal University, Yulin 537000, China; fanfanwang2020@163.com (F.W.); tpf005@126.com (P.T.)

* Correspondence: zxliao@seu.edu.cn (Z.L.); qinf1114@163.com (F.Q.)

† These authors contributed equally to this work.

Abstract: Two new meroterpenoids, aspergienynes O and P (**1** and **2**), one new natural compound, aspergienyne Q (**3**), and a new α-pyrone derivative named 3-(4-methoxy-2-oxo-2H-pyran-6-yl)butanoic acid (**4**) were isolated from the mangrove endophytic fungal strain *Aspergillus* sp. GXNU-Y85, along with five known compounds (**5**–**9**). The absolute configurations of those new isolates were confirmed through extensive analysis using spectroscopic data (HRESIMS, NMR, and ECD). The pharmacological study of the anti-proliferation activity indicated that isolates **5** and **9** displayed moderate inhibitory effects against HeLa and A549 cells, with the IC_{50} values ranging from 16.6 to 45.4 μM.

Keywords: *Aspergillus* sp.; meroterpenoids; α-pyrone derivatives; anti-proliferation activity

1. Introduction

Endophytic fungi, as a type of fungi, persist for an extended period in the healthy tissues and organs of plants, which can be regarded as a novel resource of microorganisms with high exploitation value and an important source of natural active substances [1, 2]. Therefore, the development and utilization of endophytic fungi can alleviate the shortage of resources and the destruction of ecological balance caused by extracting and separating a large number of beneficial bioactive products from plants, and also help protect rare and endangered plant resources [3]. Some secondary metabolites isolated from endophytic fungi have also drawn attention owing to their superior biological activities. Consequently, these secondary metabolites might be used as promising lead compounds for drug discovery [4].

In a continuous endeavour to identify the bioactive constituents derived from mangrove endophytic fungi [5,6], we isolated two new meroterpenoids, aspergienynes O and P (**1** and **2**), one new natural compound, aspergienyne Q (**3**), and a new α-pyrone derivative termed 3-(4-methoxy-2-oxo-2H-pyran-6-yl)butanoic acid (**4**), together with five previously reported compounds (**5**–**9**), from the secondary metabolites of *Aspergillus* sp. GXNU-Y85 derived from the fruits of the mangrove plant *Kandelia candel* in this study. Five kinds of human cancer cell lines were selected to detect the anti-proliferation activity of these isolates, and the separation and structure clarification process of **1**–**9** were described in detail (Figure 1).

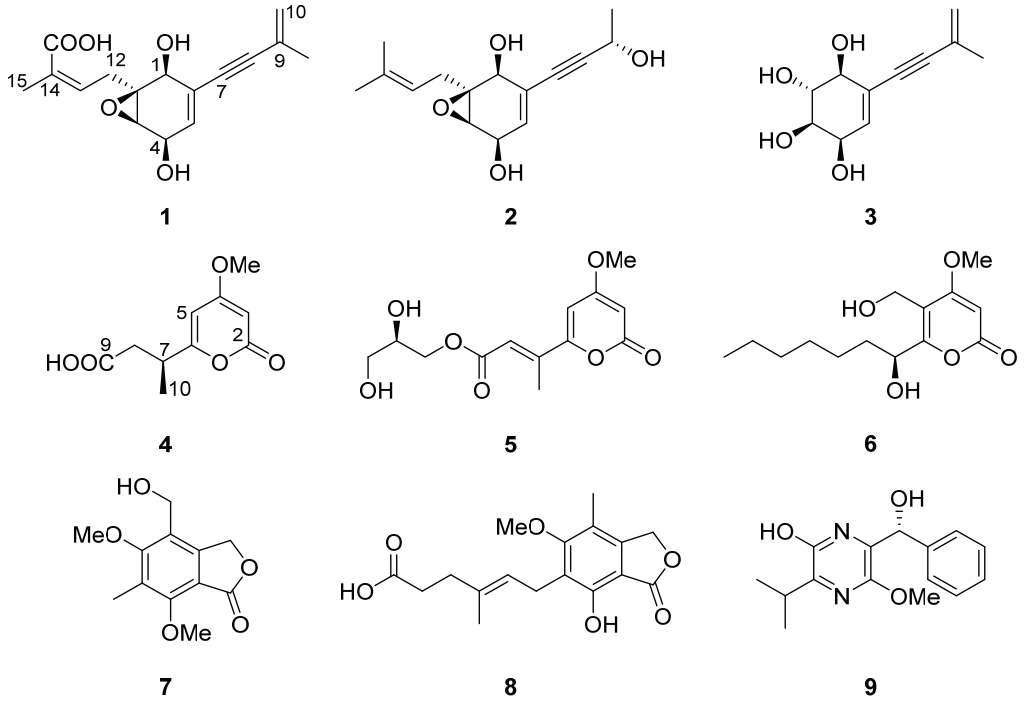

Figure 1. The chemical structures **1–9**.

2. Results and Discussion

2.1. Process of Structural Characterization of Isolates

Aspergienyne O (**1**) was acquired as a yellowish oil. Its HR-ESI-MS peak at m/z 313.1048 ([M + Na]$^+$, calcd for 313.1046) and the ^{13}C NMR data (Table 1) suggested a molecular formula of $C_{16}H_{18}O_5$ with eight degrees of unsaturation. The ^{1}H NMR and HSQC data of **1** (Table 1) exhibited four olefinic groups [δ_H 6.72 (m), 5.77 (dd, J = 5.0, 1.9 Hz), 5.28 (m) and 5.25 (m)], a methylene [δ_H 3.03 (dd, J = 15.1, 8.8 Hz), and 2.54 (dd, J = 15.1, 6.9 Hz)], three oxymethines [δ_H 4.46 (dd, J = 5.0, 2.5 Hz), 4.19 (t, J = 1.9 Hz), and 3.34 (t, J = 2.5 Hz)], and two methyls [δ_H 1.90 (s) and 1.87 (s)]. The ^{13}C NMR and HSQC data of **1** displayed sixteen carbons, such as a carbonyl carbon (δ_C 171.7), six sp^2 carbons (δ_C 141.1, 134.3, 132.6, 128.4, 124.3, and 122.3), two sp carbons (δ_C 91.7 and 87.5), three sp^3 methine carbons (δ_C 68.1, 66.1, and 60.3), one sp^3 nonprotonated carbon (δ_C 62.5), one sp^3 methylene group (δ_C 32.5), together with two methyl carbons (δ_C 23.5 and 12.9). The NMR data (Table 1) of **1** were highly similar to those of the previously reported biscognienyne D [7], except that the methyl group was replaced by the carboxyl group of **1**. The HMBC signals from H-15/H-13 to C-16 (δ_C 171.7) supported this speculation (Figure 2). Comprehensive analysis of its 2D NMR signals not only confirmed the above hypothesis but also verified the two-dimensional structure shown in Figure 1.

In the NOESY spectrum of **1** (Figure 3), there is a diagnostic association between the olefinic proton [δ_H 6.72 (m, H-13)] and the terminal methyl proton [δ_H 1.87 (s, H_3-15)], and thus the geometry of the $\Delta^{13,14}$ double bond was defined as *Z*. Furthermore, the NOESY signals of H-1/H-12β suggested that H-1 and H-12β were β-oriented. Meanwhile, the small value of $J_{H\text{-}3/H\text{-}4}$ (2.5 Hz) demonstrated a *cis*-orientation of these protons. The final configuration of **1** was elucidated as (1*S*,2*S*,3*R*,4*R*)-**1** by means of comparing its experimental ECD spectrum to those calculated (Figure 4).

Table 1. ^{1}H and ^{13}C NMR Data for **1** and **2** in CD_3OD.

No	1 [a]		2 [b]	
	δ_C, Type	δ_H (*J* in Hz)	δ_C, Type	δ_H (*J* in Hz)
1	68.1, CH	4.19, t (1.9)	67.6, CH	4.15, t (2.0)
2	62.5, C		63.2, C	
3	60.3, CH	3.34, t (2.5)	60.3, CH	3.3, s
4	66.1, CH	4.46, dd (5.0, 2.5)	66.1, CH	4.41, dd (4.9, 2.0)
5	134.3, CH	5.77, dd (5.0, 1.9)	134.2, CH	5.74, dd (4.9, 2.3)
6	124.3, C		124.1, C	
7	87.5, C		82.3, C	
8	91.7, C		92.7, C	
9	128.4, C		59.0, CH	4.57, q (6.6)
10	122.3, CH_2	5.28, m, 5.25, m	24.6, CH_3	1.41, d (6.6)
11	23.5, CH_3	1.90, s		
12	32.5, CH_2	3.03, dd (15.1, 8.8) 2.54, dd (15.1, 6.9)	32.2, CH_2	2.94, dd (14.6, 9.0) 2.14, dd (14.6, 6.2)
13	136.2, CH	6.72, m	119.0, CH	5.13, m
14	132.6, C		136.7, C	
15	12.9, CH_3	1.87, s	26.0, CH_3	1.73, s
16	171.7, C		18.1, CH_3	1.69, s

[a] ^{1}H NMR at 600 MHz, ^{13}C NMR at 150 MHz; [b] ^{1}H NMR at 400 MHz, ^{13}C NMR at 100 MHz.

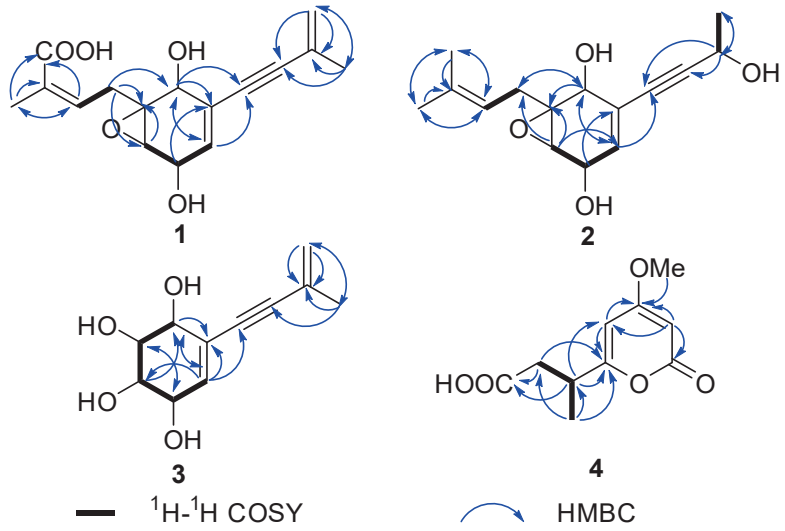

Figure 2. Key HMBC and ^{1}H-^{1}H COSY correlations of compounds **1**–**4**.

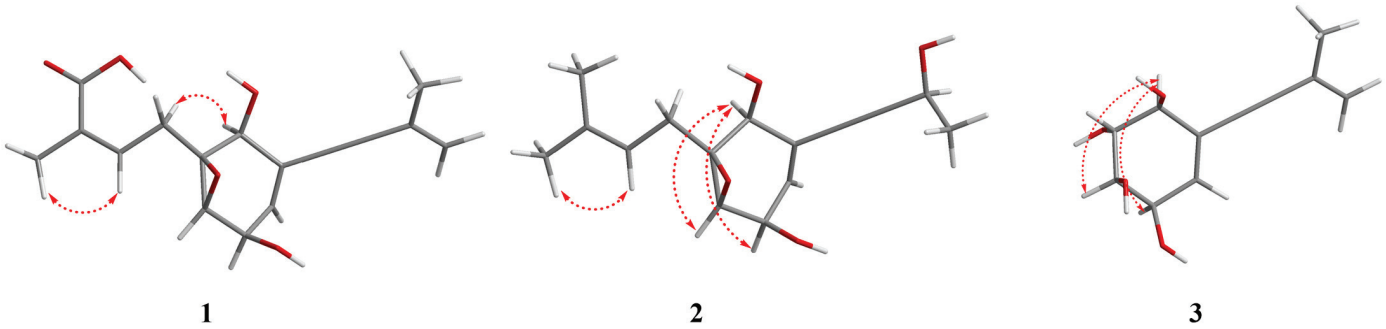

Figure 3. Key NOESY correlations for **1**–**3**.

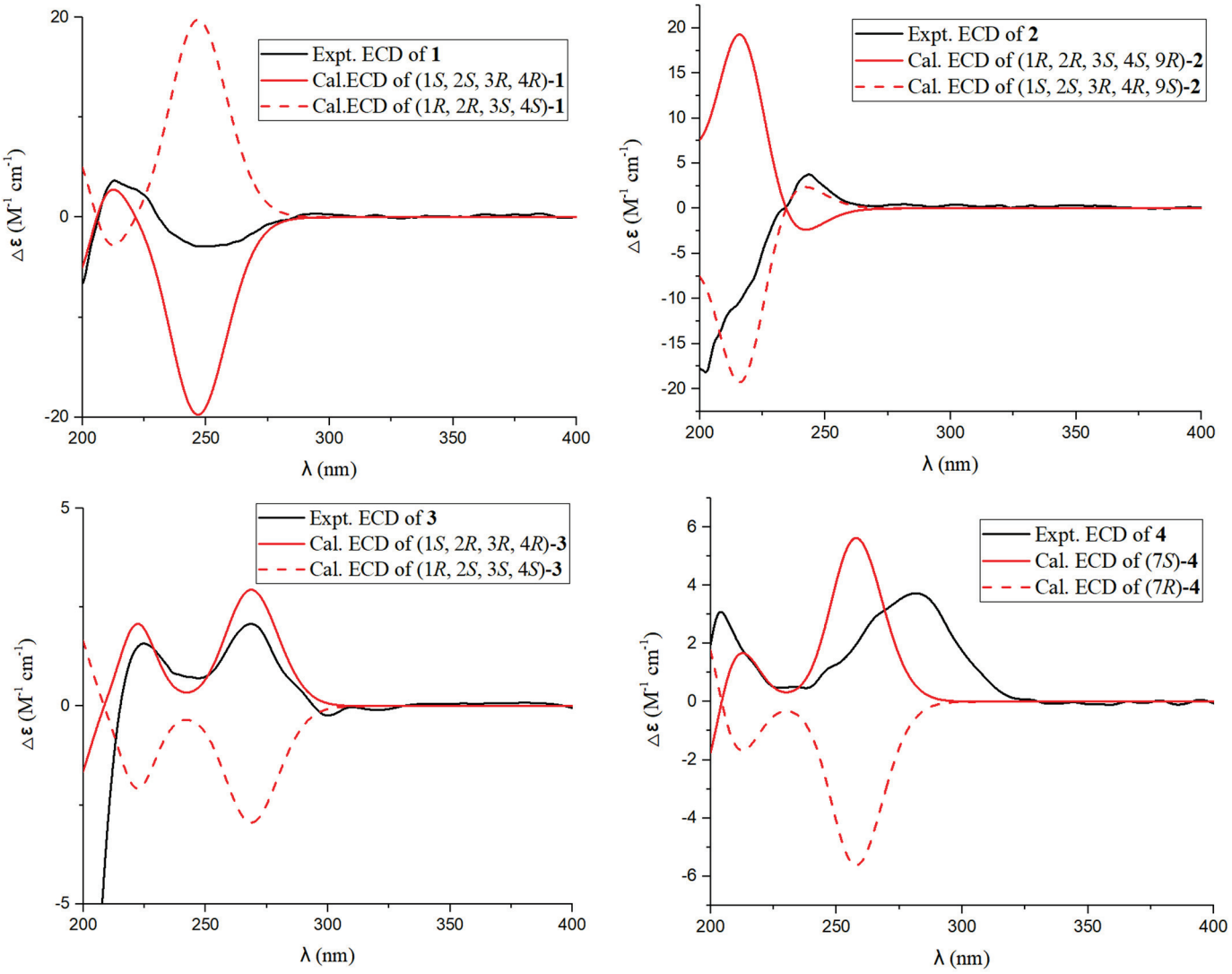

Figure 4. Calculated and experimental ECD spectra of **1**–**4**.

Aspergienyne P (**2**) was isolated as a yellowish oil. The analysis of the ion peak discovered at *m*/*z* 287.1255 ([M + Na]$^+$, calcd for 287.1259) in the HR-ESI-MS report combined with its ^{13}C NMR data gained the molecular formula $C_{15}H_{20}O_4$. Comprehensive analysis of 1D NMR information (Table 1) of **2** proposed that **2** and 1 are very similar in structure, except for the replacement of 16-COOH and the $\Delta^{9,10}$ double bond in **1** by a methyl group and a hydroxyl group in **2**, respectively, which was determined via the crucial HMBC signals from H-13/H-15 to C-16 (δ_C 18.1), H-16 (δ_H 1.69) to C-13/C-14/C-15, H-9 (δ_H 4.57) to C-7/C-8, H-10 to C-9 (δ_C 59.0), and the significant ^{1}H-^{1}H COSY signals (Figure 2) of H-9/H-10. The NOESY signals (Figure 3) of H-1/H-3 and H-1/H-4 suggested that H-1, H-3, and H-4 were on the same side. Consequently, (1*S**, 2*S**, 3*R**, 4*R**)-**2** was tentatively established. The ^{13}C NMR data of two potential isomers (**2a** and **2b**) (Figure 5) were calculated according to the GIAO method to determine the complete relative configuration of **2**. Due to the good correlation coefficient (R^2 = 0.9978) (Figure 6) and the high results of the DP4+ probability analysis (100%) (Table S2) between the calculated and experimental ^{13}C NMR chemical shifts, the (1*S**,2*S**,3*R**,4*R**,9*S**)-**2** was recommended. The absolute stereochemistry of **2** was determined as 1*S*, 2*S*, 3*R*, 4*R*, and 9*S* due to the coincidence of the calculated and experimental ECD spectral curves (Figure 4).

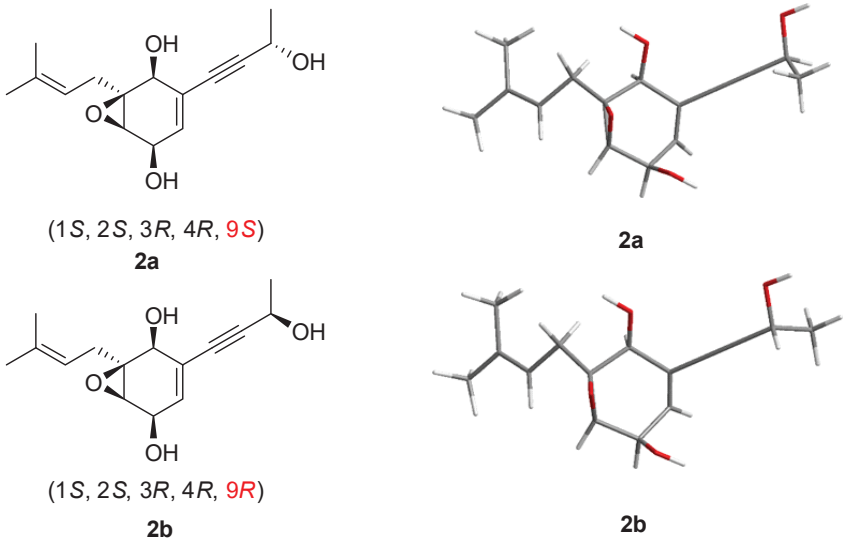

Figure 5. Conformations of low-energy conformers of structures **2a** and **2b** in MeOH.

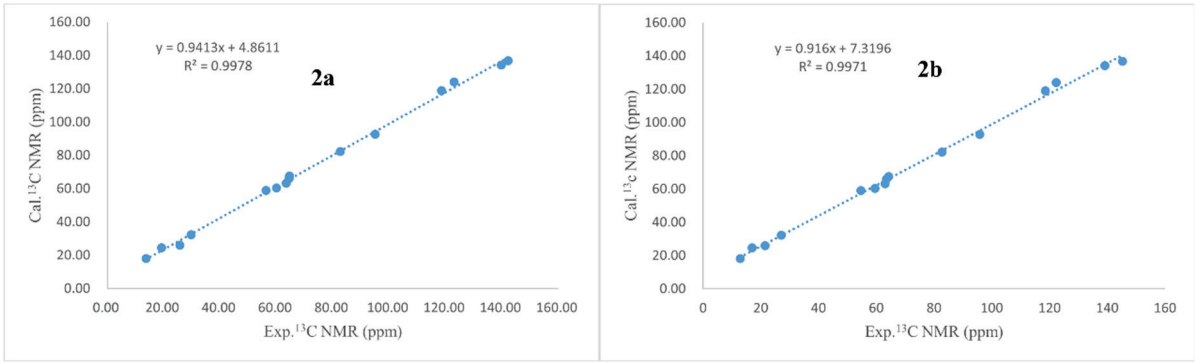

Figure 6. Regression analyses of experimental versus calculated ^{13}C NMR chemical shifts of model compounds **2a** and **2b**.

The $C_{11}H_{14}O_4$ of aspergienyne Q (**3**) was determined on the basis of HR-ESI-MS analysis, which exhibited a $[M+Na]^+$ ion at *m*/*z* 233.0785 (calcd for 233.0784). The NMR data (Table 2) of **3** was compared in detail with that of (1*R*,2*R*,3*R*,4*S*)-5-(3-Methylbut-3-en-1-yn-1-yl)-cyclohex-5-ene-1,2,3,4-tetraol [8], and combined with the HR-ESI-MS of **3**, and the structure of compound **3** was determined. Moreover, the absolute structure of **3** was further confirmed by 2D NMR and ECD spectroscopy (Figures 2–4). Thus, as shown in Figure 1, **3** is reported for the first time in this paper as a new natural product.

The molecular formula of 3-(4-methoxy-2-oxo-2H-pyran-6-yl)butanoic acid (**4**) was defined as $C_{10}H_{12}O_5$ according to the HR-ESI-MS ion peak discovered at *m*/*z* 213.0765 ($[M+H]^+$, calcd for 213.0763), implying five degrees of unsaturation. The ^{1}H NMR spectrum displayed the presence of two olefins [δ_H 6.04 (d, *J* = 2.2 Hz) and 5.54 (d, *J* = 2.2 Hz)], a methylene [δ_H 2.58 (dd, *J* = 14.6, 7.4 Hz) and 2.40 (dd, *J* = 14.6, 7.5 Hz)], one methine proton [δ_H 3.10 (m)], a methyl proton [δ_H 1.26 (d, *J* = 7.0 Hz)], and one methoxy [δ_H 3.85 (s)]. Subsequently, the carbon resonances of one methine group (δ_C 36.4), one methylene (δ_C 40.7), one methyl (δ_C18.3), and one methoxy (δ_C 56.9) were observed in its ^{13}C NMR spectrum, along with two carbonyl carbons (δ_C 176.0 and 167.4) and four olefin carbons (δ_C 173.0, 169.2, 100.7, and 88.4), as supported by its HSQC spectrum. The NMR data of **4** closely resembled those of pestalotiopyrone N [9], except for a $\Delta^{7,8}$ double bond in pestalotiopyrone N being replaced by one methine and one methylene present at C-7 and C-8 in **4**, which was proved on the basis of the key HMBC signals from H-7 to C-5/C-6/C-9, H-8 to C-6/C-9 and H-10 to C-6/C-7, and the key ^{1}H-^{1}H COSY signals (Figure 2) of H-7/H-8 and

H-7/H-10. Finally, the absolute configuration of (7*S*)-**4** was elucidated via ECD calculations (Figure 4).

Table 2. ^{1}H (400 MHz) and ^{13}C (100 MHz) NMR Data for **3** and **4** in CD_3OD.

No	3		No	4	
	δ_C, Type	δ_H (*J* in Hz)		δ_C, Type	δ_H (*J* in Hz)
1	74.4, CH	3.86, dd (7.2, 0.8)	2	167.4, C	
2	73.4, CH	3.71, dd (9.9, 7.2)	3	88.4, CH	5.54 d (2.2)
3	72.1, CH	3.48, dd (9.9, 4.3)	4	173.9, C	
4	67.6, CH	4.23, dd (5.2, 4.3)	5	100.7, CH	6.04 d (2.2)
5	134.1, CH	6.06, dd (5.2, 1.7)	6	169.2, C	
6	128.3, C		7	36.4, CH	3.10 m
7	87.5, C		8	40.7, CH_2	2.58 dd (14.6, 7.4), 2.40 dd (14.6, 7.5)
8	92.5, C		9	176.0, C	
9	128.3, C		10	18.3, CH_3	1.26 d (7.0)
10	122.5, CH_2	5.30, m; 5.28, m	4-OMe	56.9, CH_3	3.85 s
11	23.5, CH_3	1.91, m			

In addition to these four new isolates, five previously reported isolates were acquired, which were identified on the basis of comparing their spectral data with the reported data as pestalotiopyrone I (**5**) [10], ficipyrone A (**6**) [11], 4-(hydroxymethyl)-5,7-dimethoxy-6-methylisobenzofuran-1(3H)-one (**7**) [12], mycophenolic acid (**8**) [13], and terezine A (**9**) [14].

2.2. Results of Antiproliferative Activity

The MTT method was used to evaluate the anti-proliferative activity of all isolates on five human cancer cell lines. Among them, **9** displayed moderate anti-proliferation activity on HeLa cancer cells (IC_{50} =16.6 μM); moreover, **5** displayed anti-proliferation activity on the HeLa and A549 cancer cell lines (IC_{50} = 29.3 μM and IC_{50} = 45.4 μM, respectively). The other isolates displayed no notable anti-proliferation activity on five cancer cell lines (IC_{50} > 50 μM). The positive control was etoposide (IC_{50}: 15.7 μM for HeLa cells, 8.2 μM for A549 cells).

3. Materials and Methods

3.1. General Experimental Procedures

The NMR data were measured by Bruker 400 MHz and 600 MHz instruments (Bruker, Bremen, Germany). The HR-ESI-MS reports and the Optical rotations were collected using an LC-MS spectrometer (Agilent 6545 Q-TOF) and a JASCO P-2000 polarimeter (Jasco, Tokyo, Japan), respectively. The other instruments and materials employed in the experiments were the same as those in our previous reports [15].

3.2. Fungal Material

According to the sequence and morphology of the internal transcriptional spacer (ITS) of the strain, the fungal strain collected from fresh fruits of the mangrove plant *Kandelia candel* in the Beihai was identified and designated as GXNU-Y85. Subsequently, we obtained its registration number OR999402, as we submitted the ITSrDNA of GXNU-Y85 to GenBank.

3.3. Fermentation, Extraction, and Isolation

This target strain was fermented for 28 days at 25 °C, where the medium consisted of 80 mL H_2O (H_2O with 0.5% sea salt) and 80 g of rice. Mycelium was collected and soaked in methanol (3 × 10 L) for 2 days to collect the crude extract (21.4 g), which was subsequently extracted 3 times using ethyl acetate. The extract (11.1 g) was isolated via a silica gel column, and six fractions (Fr. 1-Fr. 6) were obtained using a ratio of PE-EtOAc solvent (50:1 to 1:1,

v/*v*). Fr. 5 (2.54 g) was further isolated through a Sephadex LH-20 column (100% methanol) to produce seven fractions (Fr. 5.1 to Fr. 5.7). Isolates **3** (5.6 mg), **8** (7.1 mg), and **5** (3.9 mg) were separated from Fr. 5.2 (0.84 g) based on semipreparative HPLC (50% MeOH–H_2O; 7 mL/min; YMC-column, 4.6 mm I.D. × 250 mm, S-5 μm, 12 nm). Isolates **2** (4.6 mg), **7** (6.3 mg), **1** (7.6 mg), and **6** (4.8 mg) were acquired from Fr. 5.4 (0.92 g) on the basis of semipreparative HPLC (MeCN–H_2O *v*/*v*, 40:60; 7 mL/min; YMC-column, 4.6 mm I.D. × 250 mm, S-5 μm, 12 nm). Fr. 5.7 (0.71 g) was further separated according to semipreparative HPLC (MeCN–H_2O *v*/*v*, 40:60; 7 mL/min; YMC-column, 4.6 mm I.D. × 250 mm, S-5 μm, 12 nm) to yield **4** (5.2 mg) and **9** (6.1 mg).

3.3.1. Aspergienyne O (**1**)

Yellowish oil; $[\alpha]_D^{22}$ −13.75 (*c* 0.37, MeOH); UV (MeOH) λ_{max} (log ε) 259.5 (3.25) nm; IR (KBr) ν_{max} 3357, 2977, 2930, 2195, 1671, 1448, and 1039 cm^{-1}; HR-ESI-MS *m*/*z* $[M + Na]^+$ (313.1048); ECD (MeOH) λmax (Δε) 213.50 (+3.769), 247.74 (−2.965) nm; NMR data (in CD_3OD) at Table 1.

3.3.2. Aspergienyne P (**2**)

Yellowish oil; $[\alpha]_D^{22}$ −41.26 (*c* 0.30, MeOH); UV (MeOH) λ_{max} (log ε) 258.1 (3.15) nm; IR (KBr) ν_{max} 3421, 1719, 1609, 1430, 1384, 1247, 830, and 787 cm^{-1}; HR-ESI-MS *m*/*z* $[M + Na]^+$ (287.1255); ECD (MeOH) λmax (Δε) 202.50 (−18.463), 243.09 (+4.011) nm; NMR data (in CD_3OD) at Table 1.

3.3.3. Aspergienyne Q (**3**)

Yellowish oil; $[\alpha]_D^{22}$ +16.89 (*c* 0.69, MeOH); UV (MeOH) λ_{max} (log ε) 259.2 (3.02) nm; IR (KBr) ν_{max} 3428, 2955, 2870, 1656, 1459, 1382, 1370, 1038, 967, and 834 cm^{-1}; HR-ESI-MS *m*/*z* $[M + Na]^+$ (233.0785); ECD (MeOH) λmax (Δε) 224.76 (+1.570), 268.54 (+2.080) nm; NMR data (in CD_3OD) at Table 2.

3.3.4. 3-(4-Methoxy-2-oxo-2H-pyran-6-yl)butanoic Acid (**4**)

Yellowish oil; $[\alpha]_D^{22}$ −15.03 (*c* 0.28, MeOH); UV (MeOH) λ_{max} (log ε) 212.7 (3.08), 264.4 (3.31) nm; IR (KBr) ν_{max} 3411, 2933, 1638, 1464, 1371, 1034, and 886 cm^{-1}; HR-ESI-MS *m*/*z* $[M + H]^+$ (213.0765); ECD (MeOH) λmax (Δε) 203.65 (+3.078), 281.71 (+3.744) nm; NMR data (in CD_3OD) at Table 2.

3.4. ECD and NMR Calculations

The absolute stereochemistry of the new isolates was defined through the ECD and NMR calculations described in previous reports [16,17]. The Supporting Information provides a detailed description of the process.

3.5. Anti-Proliferative Activity Test

The anti-proliferative activity of **1**–**9** against five cancer cell lines (A549, MCF-7, Hela, 5-8F, and T24 cells) was evaluated by MTT assay as previously reported [18]. The positive control was etoposide.

4. Conclusions

In the present study, three new compounds (**1**, **2**, and **4**), one new natural compound (**3**), and five previously reported isolates (**5**–**9**) were acquired from the fungal strain *Aspergillus* sp. GXNU-Y85 by various chromatographic techniques. Extensive spectroscopic data (HRESIMS, NMR, and ECD) and quantum chemical calculations were used to determine the structures of these new compounds. Biological activity studies revealed that compounds **5** and **9** showed moderate anti-proliferative activity against HeLa and A549 cells (IC_{50} = 16.6–45.4 μM).

Supplementary Materials: The following supporting information can be downloaded at: https://www.mdpi.com/article/10.3390/md22060277/s1, NMR, IR, UR and HRESIMS spectra of **1**–**4**. NMR spectra of **5**–**9**.

Author Contributions: Z.L. and F.Q. conceived and designed the experiments. C.W. performed the experiments. F.W., P.T., Y.S., Q.L. and M.G. analyzed the data. C.W., F.Q. and Z.L. wrote the paper. All authors have read and agreed to the published version of the manuscript.

Funding: This study was supported by the Natural Science Foundation of Guangxi Province (2024GXNSFBA010005), and Basic Ability Improvement Project of Young and Middle-Aged Teachers in Guangxi Colleges (2024KY0597), the PhD Start-up Fund of Yulin Normal University (G2023ZK22).

Data Availability Statement: The authors declare that all data of this study are available within the article and its Supplementary Materials file or from the corresponding authors upon request.

Conflicts of Interest: The authors declare no conflicts of interest.

References

1. Ancheeva, E.; Daletos, G.; Proksch, P. Bioactive secondary metabolites from endophytic fungi. *Curr. Med. Chem.* **2020**, *27*, 1836–1854. [CrossRef] [PubMed]
2. Wang, Z.; Wang, L.; Pan, Y.; Zheng, X.; Liang, X.; Sheng, L.; Zhang, D.; Sun, Q.; Wang, Q. Research advances on endophytic fungi and their bioactive metabolites. *Bioprocess Biosyst. Eng.* **2023**, *46*, 165–170. [CrossRef] [PubMed]
3. Kouipou Toghueo, R.M.; Boyom, F.F. Endophytic fungi from terminalia species: A comprehensive review. *J. Fungi* **2019**, *5*, 43. [CrossRef] [PubMed]
4. Zheng, R.; Li, S.; Zhang, X.; Zhao, C. Biological activities of some new secondary metabolites isolated from endophytic fungi: A review study. *Int. J. Mol. Sci.* **2021**, *22*, 959. [CrossRef] [PubMed]
5. Qin, F.; Luo, L.; Liu, Y.C.; Bo, X.L.; Wu, F.R.; Wang, F.F.; Tan, M.J.; Wei, Y.Q.; Dou, X.B.; Wang, C.Y.; et al. Diisoprenyl-cyclohexene-type meroterpenoids from a mangrove endophytic fungus *Aspergillus* sp. GXNU-Y65 and their anti-nonalcoholic steatohepatitis activity in AML12 cells. *Phytochemistry* **2024**, *218*, 113955. [PubMed]
6. Qin, F.; Song, Z.S.; Luo, L.; Bo, X.L.; Wu, F.R.; Tan, M.J.; Wang, F.F.; Huang, X.S.; Wang, H.S. Diisoprenyl cyclohexene-type meroterpenoids with cytotoxic activity from a mangrove endophytic fungus *Aspergillus* sp. GXNU-Y85. *Mar. Drugs* **2024**, *22*, 58. [CrossRef]
7. Akone, S.H.; Wang, H.; Mouelle, E.N.M.; Mándi, A.; Kurtán, T.; Koliye, P.R.; Hartmann, R.; Bhatia, S.; Yang, J.; Müller, W.E.; et al. Prenylated cyclohexene-type meroterpenoids and sulfur-containing xanthones produced by *Pseudopestalotiopsis* theae. *Phytochemistry* **2022**, *197*, 113124. [CrossRef]
8. Buckler, J.N.; Meek, T.; Banwell, M.G.; Carr, P.D. Total synthesis of the cyclic carbonate-containing natural product aspergillusol B from D-(-)-tartaric acid. *J. Nat. Prod.* **2017**, *80*, 2088–2093. [CrossRef] [PubMed]
9. Wang, J.J.; Peng, Q.Y.; Yao, X.G.; Liu, Y.H.; Zhou, X.F. New pestallic acids and diphenylketone derivatives from the marine alga-derived endophytic fungus *Pestalotiopsis* neglecta SCSIO41403. *J. Antibiot.* **2020**, *73*, 585588. [CrossRef] [PubMed]
10. Rönsberg, D.; Debbab, A.; Mándi, A.; Wray, V.; Dai, H.F.; Kurtán, T.; Proksch, P.; Aly, A.H. Secondary metabolites from the endophytic fungus *Pestalotiopsis* virgatula isolated from the mangrove plant *Sonneratia* caseolaris. *Tetrahedron Lett.* **2013**, *54*, 3256–3259. [CrossRef]
11. Liu, S.C.; Liu, X.Y.; Guo, L.D.; Che, Y.S.; Liu, L. 2H-pyran-2-one and 2H-furan-2-one derivatives from the plant endophytic fungus *Pestalotiopsis* fici. *Chem. Biodivers.* **2013**, *10*, 2007–2013. [CrossRef] [PubMed]
12. Peng, J.Y.; Chen, P.W.; Li, C.W.; Liu, J.T.; Sun, Y.J.; Yang, M.Z.; Ding, B.; Huang, H.B.; Tao, Y.W. Phthalide metabolites produced by mangrove endophytic fungus *Pestalotiopsis* sp. SAS4. *Magn. Reson. Chem.* **2022**, *60*, 525–529. [CrossRef] [PubMed]
13. Siebert, A.; Cholewinski, G.; Trzonkowski, P.; Rachon, J. Immunosuppressive properties of amino acid and peptide derivatives of mycophenolic acid. *Eur. J. Med. Chem.* **2020**, *189*, 112091. [CrossRef] [PubMed]
14. Wang, Y.; Gloer, J.B.; Scott, J.A.; Malloch, D. Terezines A-D: New amino acid-derived bioactive metabolites from the coprophilous fungus *Sporormiella* teretispora. *J. Nat. Prod.* **1995**, *58*, 93–99. [CrossRef] [PubMed]
15. Qin, F.; Wang, C.Y.; Kim, D.; Wang, H.S.; Zhu, Y.K.; Lee, S.K.; Yao, G.Y.; Liang, D. Nitidumpeptins A and B, cyclohexapeptides isolated from *Zanthoxylum nitidum* var. tomentosum: Structural elucidation, total synthesis, and antiproliferative activity in cancer cells. *J. Org. Chem.* **2021**, *86*, 1462–1470. [CrossRef] [PubMed]
16. Qin, F.; Wang, C.Y.; Wang, C.G.; Chen, Y.; Li, J.J.; Li, M.S.; Zhu, Y.K.; Lee, S.K.; Wang, H.S. Undescribed isoquinolines from *Zanthoxylum nitidum* and their antiproliferative effects against human cancer cell lines. *Phytochemistry* **2023**, *205*, 113476. [CrossRef] [PubMed]

17. Qin, F.; Wang, C.Y.; Hu, R.; Wang, C.G.; Wang, F.F.; Zhou, M.M.; Liang, D.; Liao, H.B.; Lee, S.K.; Wang, H.S. Anti-infammatory activity of isobutylamides from *Zanthoxylum nitidum* var. Tomentosum. *Fitoterapia* **2020**, *142*, 104486. [CrossRef] [PubMed]
18. Huang, R.Z.; Jin, L.; Wang, C.G.; Xu, X.J.; Du, Y.; Liao, N.; Ji, M.; Liao, Z.X.; Wang, H.S. A pentacyclic triterpene derivative possessing polyhydroxyl ring A suppresses growth of HeLa cells by reactive oxygen species-dependent NF-κB pathway. *Eur. J. Pharmacol.* **2018**, *838*, 157–169. [CrossRef] [PubMed]

marine drugs

MDPI

Article

New Naphthalene Derivatives from the Mangrove Endophytic Fungus *Daldinia eschscholzii* MCZ-18

Zhiyong Xu [1,2], Ting Feng [1], Zhenchang Wen [1], Qing Li [1], Biting Chen [1], Pinghuai Liu [1,3] and Jing Xu [1,*]

[1] Collaborative Innovation Center of Ecological Civilization, School of Chemistry and Chemical Engineering, Hainan University, Haikou 570228, China; xuzhiyong@jxas.ac.cn (Z.X.); 20081700210004@hainanu.edu.cn (T.F.); wenzc789@126.com (Z.W.); 22210710000026@hainan.edu.cn (Q.L.); cbt688228@163.com (B.C.); twlph@163.com (P.L.)
[2] Institute of Applied Chemistry, Jiangxi Academy of Sciences, Nanchang 330096, China
[3] Institute Research and Utilization on Seaweed Biological Resources, Key Laboratory of Haikou, Hainan University, Haikou 570228, China
* Correspondence: happyjing3@163.com; Tel.: +86-898-6627-9226; Fax: +86-898-6627-9010

Abstract: Five new naphthalene derivatives dalesconosides A–D, F (**1**–**4**, **6**), a known synthetic analogue named dalesconoside E (**5**), and eighteen known compounds (**7**–**24**) were isolated from *Daldinia eschscholzii* MCZ-18, which is an endophytic fungus obtained from the Chinese mangrove plant *Ceriops tagal*. Differing from previously reported naphthalenes, compounds **1** and **2** were bearing a rare ribofuranoside substituted at C-1 and the 5-methyltetrahydrofuran-2,3-diol moiety, respectively. Their structures were determined by detailed nuclear magnetic resonance (NMR) and mass spectroscopic (MS) analyses, while the absolute configurations were established by theoretical electronic circular dichroism (ECD) calculation. Compounds **1**, **3**, **13**–**17** and **19** showed broad ranges of antimicrobial spectrum against five indicator test microorganisms (*Enterococcus faecalis*, Methicillin-resistant *Staphylococcus aureus*, *Escherichia coli*, *Pseudomonas aeruginosa* and *Candida albicans*); especially, **1**, **16** and **17** were most potent. The variations in structure and attendant biological activities provided fresh insights concerning structure−activity relationships for the naphthalene derivatives.

Keywords: mangrove endophytic fungus; *Daldinia eschscholzii*; naphthalenes; antimicrobial activity; cytotoxicity

1. Introduction

Microorganisms from special ecological niches such as the mangrove endosymbionts have been demonstrated to be a reliable source of structurally novel and pharmacologically potent natural products (NPs) and have likewise drawn the attention of NP researchers [1,2]. Mangrove-associated fungi produce a larger number of bioactive secondary metabolites compared to any other mangrove-derived microbes; more than 70% were isolated from endophyte fungi [3,4]. Filamentous fungi of the species *Daldinia eschscholtzii* is known as an endophyte commonly found in multiple hosts such as dead trees [5], insects [6], alga [7], broad-leaved forest [8] and mangroves [9,10]. It has been demonstrated to be a prolific source of bioactive polyketides including immunosuppressive dalesconols A and B, acetodalmanols A and B, (+)-daeschol A, dalmanol A, 2,16-dihydroxyl-benzo[j]fluoranthene [6,11], free radical scavengers (±)-daeschol A [11], cytotoxic (±)-acetodalmanol B, 2,16-dihydroxyl-benzo[j]fluoranthene [11], fungistatic helicascolide C [7], stem cell differentiation inducer selesconol [12], NLRP3 inflammasome activation inhibitors spirodalesol [13] and α-glucosidase inhibitors chromones, naphthoquinones, and naphthofurans [14,15]. As part of our ongoing investigations on mangrove endophytic fungi [16–18], *Daldinia eschscholtzii*-Mcz18 was isolated from a fresh branch of the mangrove plant *Ceriops tagal*. Five new aromatic polyketide dalesconosides A–D, F (**1**–**4**, **6**), a known

synthetic analogue named dalesconoside E (**5**) (this is the first isolation from a natural source), as well as 18 known compounds (**7**–**24**) (Figure 1) were isolated and identified from the mangrove endophytic fungus *Daldinia eschscholzii* MCZ-18. These compounds were examined for antimicrobial and cytotoxic activities. Details of the isolation, structure elucidation, and antimicrobial and cytotoxic activities of these compounds are reported herein.

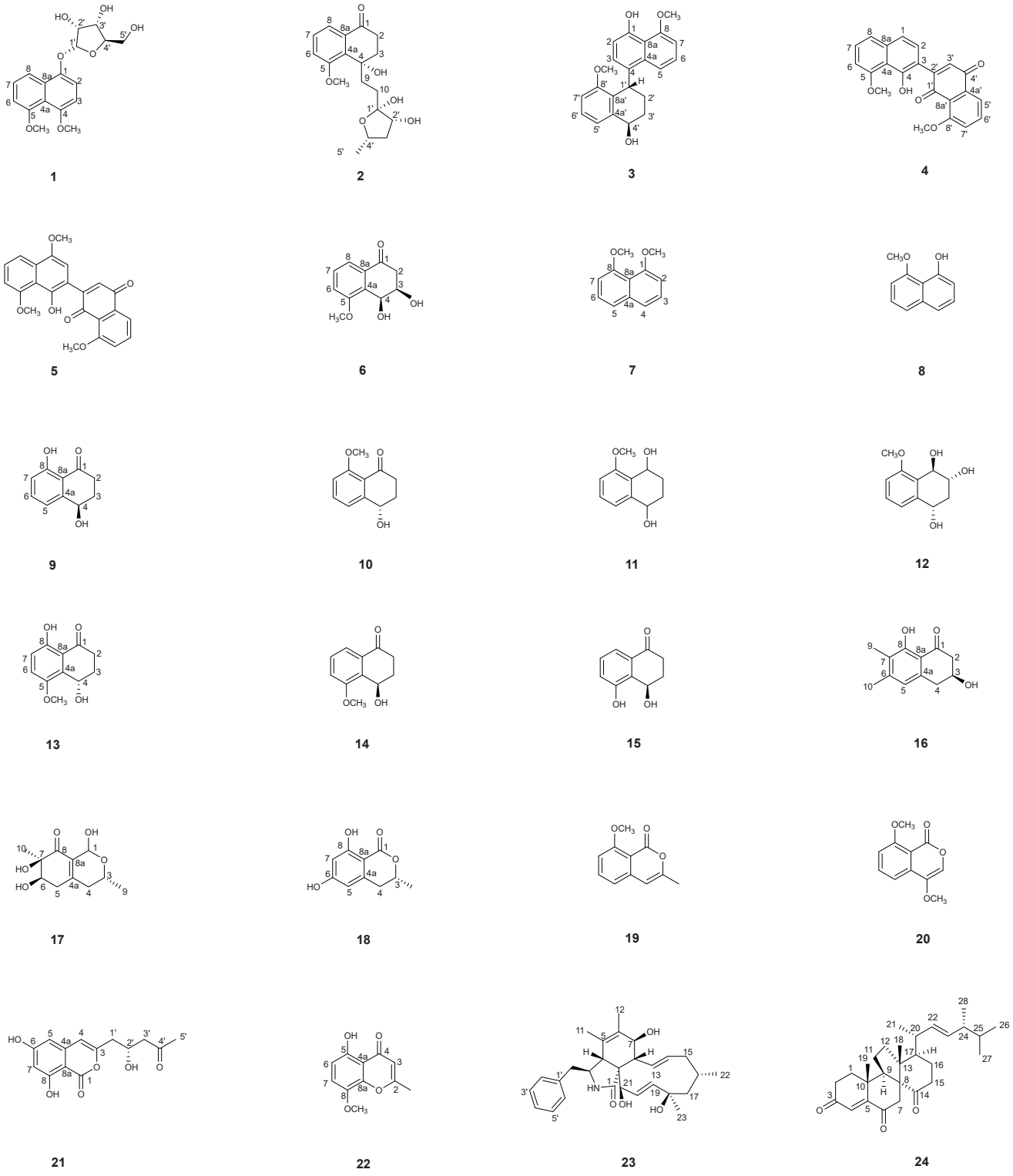

Figure 1. Chemical structures of compounds **1**–**24**.

2. Results and Discussion

2.1. Structure Elucidation

Dalesconoside A (**1**) was isolated as yellow needles with the molecular formula $C_{17}H_{20}O_7$ established by HR-ESIMS (*m*/*z* 337.1289, calcd for $[M+H]^+$ 337.1282). Consequently, **1** had eight degrees of unsaturation. The ^1H and ^{13}C NMR data (Tables 1 and 2) of **1** indicated that seven out of eight degrees of unsaturation are derived from a naphthalene moiety. Therefore, the last unsaturation degree was attributed to an additional ring system. The ^1H and ^{13}C NMR in combination with the ^1H-^1H COSY and HSQC spectra showed that the compound had five signals of aromatic protons at [δ_H 8.00 (d, *J* = 6.4 Hz), δ_C 116.5, d, CH-8; δ_H 7.39 (t, *J* = 6.5, 6.4 Hz), δ_C 127.2, d, CH-7; 7.18 (d, *J* = 6.8 Hz), δ_C 113.1, d, CH-3; δ_H 6.96 (d, *J* = 6.1 Hz), δ_C 108.4, d, CH-6; 6.84 (d, *J* = 6.8 Hz), δ_C 108.2, d, CH-2], an anomeric proton [δ_H 5.63 (d, *J* = 3.6 Hz), δ_C 103.9, d, CH-1′], two methoxy groups [δ_H 3.92, s, δ_C 56.9, q, 5-OCH_3; δ_H 3.87, s, δ_C 57.7, q, 4-OCH_3], and signals of a furanoside moiety at δ_H 3.65–4.24. Comparison of the ^1H and ^{13}C NMR data with those of 1,8-dimethoxynaphthalene (**7**) co-isolated in the culture medium and isotorachrysone-6-*O*-α-D-ribofuranoside [19] revealed that **1** was a 1,8-dimethoxynaphthalene ribofuranoside. The HMBC correlations (Figure 2) observed from H-1′ (δ_H 5.63) to C-1 (δ_C 156.6) established that the connection of the furanoside and naphthalene moieties were through the ether bridge. The relative configuration of **1** was interpreted by the diagnostic NOE interactionsH-1′/H-2′, H-2′/H-3′, H-1′/H_2-5′, and H-3′/ H_2-5, which revealed their co-facial relationship (Figure 3). The α configuration of ribose was confirmed by the chemical shifts (δ_H 5.63, δ_C 103.9, CH-1′) and coupling constant of the anomeric proton $J_{1',2'}$ value 3.6 Hz. The sample limitations precluded further acid hydrolysis to study the absolute configuration of the α-ribofuranoside in **1**, whereas the calculated ECD spectrum method can be used to predict the absolute configuration of C-1′ (Figure 4, Tables S1 and S2). Consequently, the absolute configuration of C-1′ was assigned to be *R*, and the sugar moiety was assigned as α-D-ribofuranoside. Thus, compound **1** was elucidated as 4,5-dimethoxynaphthalen-1-*O*-α-D-ribofuranoside and named dalesconoside A (Figures S1–S8).

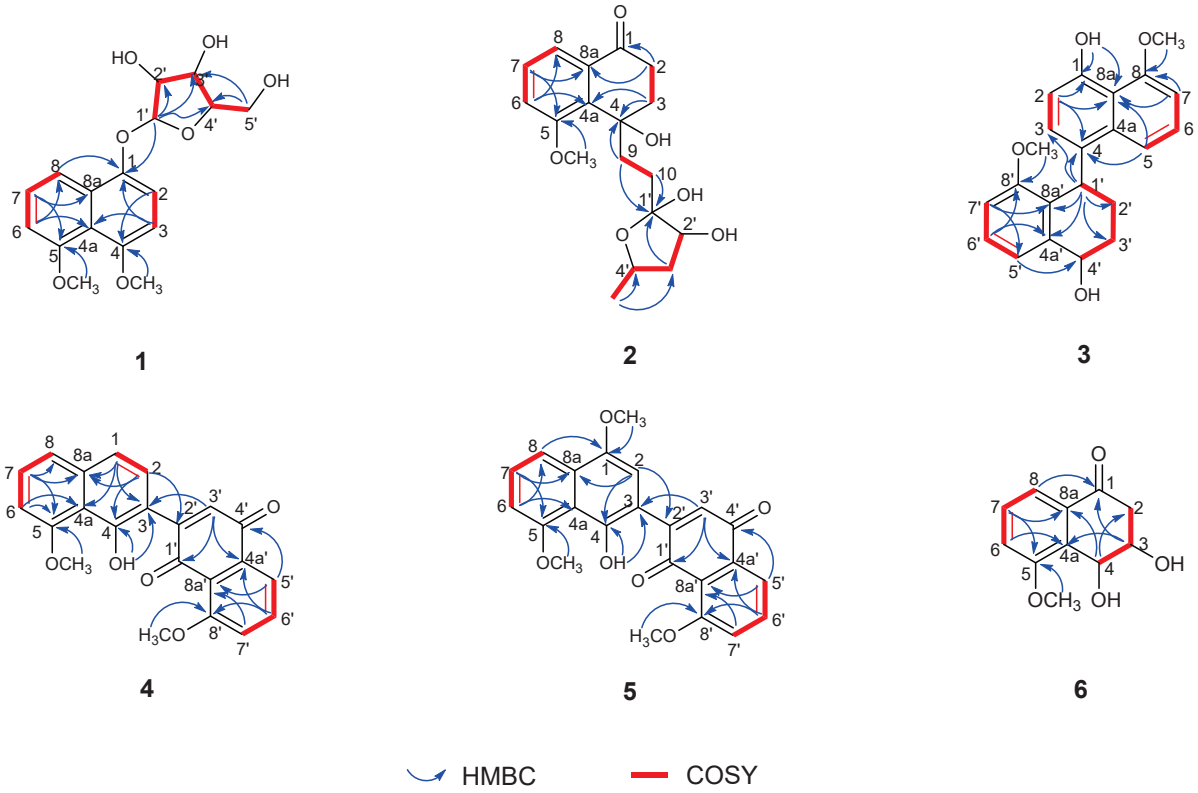

Figure 2. Key COSY and HMBC correlations of compounds **1**–**6**.

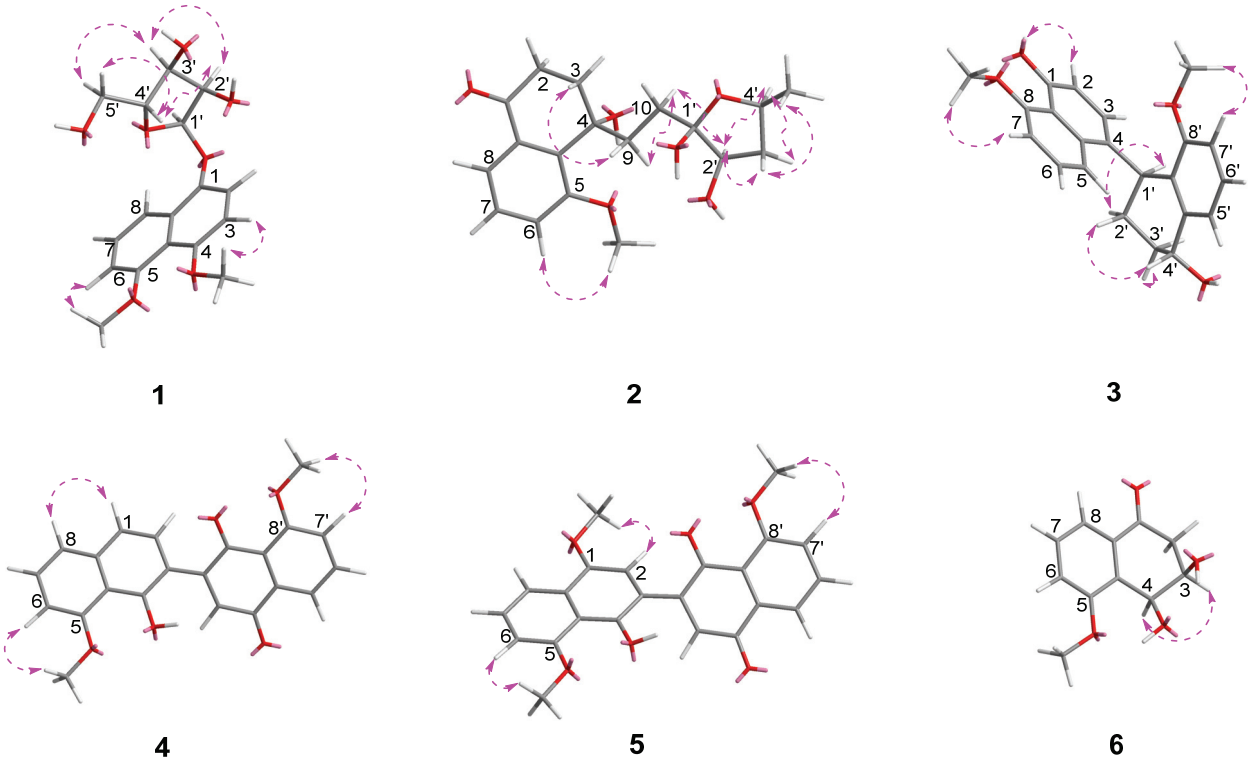

Figure 3. Key NOESY correlations of compounds **1–6**.

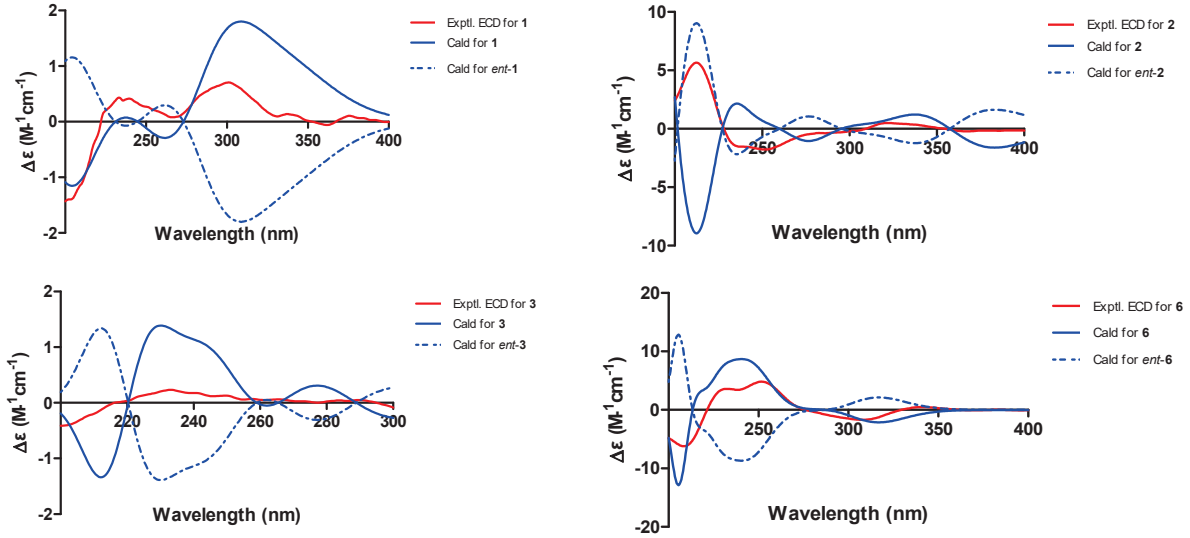

Figure 4. Experimental and calculated electronic circular dichroism (ECD) spectra of **1–3** and **6**.

Table 1. ^{1}HNMR data of **1–6**.

Position	1 [a,d]	2 [a,c]	3 [b,c]	4 [b,c]	5 [b,c]	6 [a,c]
1				7.33, d (7.6)		
2	6.84, d (6.8)	2.46, m	6.59, d (8.0)	7.35, d (7.6)	6.72, s	H_a 3.18, dd (16.9, 2.8) H_b 2.64, dd (16.9, 3.2)
3	7.18, d (6.8)	H_a 2.76, m H_b 2.63, m	6.37, d (8.0)			4.37, dd (3.2, 2.8)
4						5.13, d (2.8)

Table 1. *Cont.*

Position	1 [a,d]	2 [a,c]	3 [b,c]	4 [b,c]	5 [b,c]	6 [a,c]
5			7.91, d (8.7)			
6	6.96, d (6.1)	7.32, dd (8.1, 1.0)	7.45, t (8.4, 7.7)	6.82, d (7.6)	6.87, d (7.7)	7.29, d (8.1)
7	7.39, t (6.5, 6.4)	7.42, t (8.1, 7.8)	6.86, d (7.7)	7.37, t (7.8)	7.39, t (8.3, 8.0)	7.42, t (8.1, 7.8)
8	8.00, d (6.4)	7.60, dd (7.8, 1.0)		7.43, d (7.6)	7.87, d (7.9)	7.56, d (7.8)
9		H_a 2.54, m H_b 2.33, m				
10		H_a 2.56, m H_b 2.23, m				
1′	5.63, d (3.6)					
2′	4.24, m (overlap)	4.15, t (7.5)	H_a 2.38, m; H_b 1.86, m			
3′	4.15, dd (6.6, 3.1)	H_a 2.00,m H_b 1.83, m	H_a 1.83, m; H_b 1.78, m	7.06, s	7.05, s	
4′	4.23, m (overlap)	4.29, m	4.87, t (2.7)			
5′	H_a 3.71, dd (9.7, 3.8) H_b 3.65, dd (9.7, 3.2)	1.21, d (6.3)	7.11, d (7.6)			
6′			7.32, t (7.9)	7.78, dd (7.6, 2.9)	7.77, dd (7.6, 1.0)	
7′			6.79, d (8.0)	7.68, t (8.2, 7.8)	7.68, t (8.3, 7.7)	
8′				7.31, d (8.2)	7.32, d (8.1)	
1-OCH_3					3.96, s	
4-OCH_3	3.87, s					
5-OCH_3	3.92, s	3.89, s		4.05, s	4.03, s	3.93, s
8-OCH_3			4.08, s			
8′-OCH_3			3.49, s	4.01, s	4.01, s	
4-OH				9.82, s	9.42, s	

[a] In CD_3OD. [b] In $CDCl_3$.[c] ^1H (400 MHz). [d] ^1H (500 MHz).

Dalesconoside B (**2**) was obtained as a colorless oil, and it possessed the same molecular formula of $C_{18}H_{24}O_6$ as **1** with seven degrees of unsaturation as determined by HRESIMS (*m*/*z* 359.1464, calcd for [M+Na] $^+$359.1465). The ^1H NMR spectrum of **1** (Table 1) exhibited resonances for three aromatic protons [δ_H 7.60 (dd, *J* = 7.8, 1.0 Hz), H-8; δ_H 7.42 (dd, *J* = 8.1, 7.8 Hz), H-7; δ_H 7.32 (dd, *J* = 8.1, 1.0 Hz), H-6], which indicated the presence of a trisubstituted benzene ring. The ^1H NMR spectrum further showed signals for 12 aliphatic protons, six oxygenated protons, including two oxygenated methines (δ_H 4.15 (t, *J* = 7.5 Hz), H-2′; δ_H 4.29, m, H-4′), one methoxy group (δ_H 3.89, s, 5-OCH_3) and one secondary methyl group [δ_H 1.21 (d, *J* = 6.3 Hz), H_3-5′]. The ^{13}C NMR spectrum disclosed 18 carbon resonances, including two sp^3 methyls, five sp^3 methylenes, two sp^3 methines, two sp^3 quaternary carbons (including a dioxysubstituted sp^3 carbon at δ_C 115.8 (C-1′)), three sp^2 olefinic methines, and four sp^2 nonprotonated carbons (including one ketone carbonyl), as supported by the DEPT and HSQC spectra. ^1H–^1H COSY spectrum (Figure 2) suggested the presence of fragments of –CH_2(2)–CH_2(3)–, –CH(5)–CH(6)–CH(7)–, –CH_2(9)–CH_2(10)–, and –CH(2′)–CH_2(3′)–CH(4′)–CH_3(5′), suggesting that **2** contains a tetralone skeleton and a 5-methyltetrahydrofuran-2,3-diol moiety. This was confirmed by the HMBC correlations from H_2-2 (δ_H 2.46, m) and H-7 (δ_H 7.42) to C-8a (δ_C 134.7); H_2-3 (δ_H 2.76, m; δ_H 2.63, m) and H-6 (δ_H 7.32) to C-4a (δ_C 134.6); and H_2-3 and H_2-9 (δ_H 2.54, m; δ_H 2.33, m) to C-4 (δ_C 84.8). Other correlations in the HMBC spectrum from H_2-9, H_2-10 (δ_H 2.56, m; δ_H 2.23, m) and H_2-3′ (δ_H 2.00, m; δ_H 1.83, m) to C-1′ (δ_C 115.8); 5-OCH_3 (δ_H 3.89) to C-5 (δ_C 159.3)

further supported the atom connectivity in compound **2**. The relative configuration of **2** was assigned by analysis of the NOESY spectrum (Figure 3). There were observed correlations between H-2′/ H-4′, H-2′/ H_b-3′, H_a-3′/ H_3-5′, H-2′/ H_a-10, H_a-10/ H_b-9, and H_a-9/ H_b-3, indicating that H-2′, H_b-3′, H-4′, H_b-9 and H_a-10 are on the same face and H_a-3′, H_3-5′, H_a-9 and H_b-3 are on the other face, which is consistent with a 4*S**,1′*R**,2′*S**,4′*R** relative configuration. The absolute configuration of **2** was then determined by comparing experimental and calculated ECD spectra using time-dependent density-functional theory (TDDFT) as shown in Figure 4, Tables S3 and S4. However, theoretical computations with the expected structure provided an ECD spectrum that was an excellent fit with the mirror image of the measured spectrum of **2**. Finally, the structure of **2** was assigned to be (*R*)-4-(2-((1′*S*,2′*R*,4′*S*)-1′,2′-dihydroxy-4′-methyltetrahydrofuran-1′-yl)ethyl)-4-hydroxy-5-methoxy-3,4-dihydronaphthalen-1(2H)-one (Figures S9–S16).

Table 2. ^{13}C NMR data of **1**–**6**.

Position	1 [a,d]	2 [a,c]	3 [b,c]	4 [b,c]	5 [b,c]	6 [a,c]
1	148.6, C	199.8, C	152.8, C	118.7, CH	147.9, C	198.9, C
2	108.2, CH	38.6, CH_2	109.4, CH	128.8, CH	107.2, CH	41.8, CH_2
3	113.1, CH	36.6, CH_2	126.6, CH	116.2, C	114.9, C	71.4, CH
4	153.6, C	84.8, C	131.5, C	152.8, C	146.4, C	65.1, CH
4a	131.7, C	134.6, C	134.1, C	114.8, C	115.4, C	131.2, C
5	158.0, C	159.3, C	117.9, CH	156.7, C	156.5, C	160.1, C
6	108.4, CH	118.6, CH	125.5, CH	104.6, CH	105.6, CH	117.3, CH
7	127.2, CH	130.3, CH	103.8, CH	126.8, CH	126.4, CH	130.4, CH
8	116.5, CH	120.1, CH	156.9, C	121.9, CH	116.0, CH	118.7, CH
8a	119.7, C	134.7, C	115.6, C	137.4, C	129.0, C	133.8, C
9		36.1, CH_2				
10		35.1, CH_2				
1′	103.9, CH	115.8, C	33.7, CH	183.3, C	183.3, C	
2′	73.7, CH	75.0, CH	23.5, CH_2	150.4, C	151.0, C	
3′	71.2, CH	40.4, CH_2	26.7, CH_2	134.5, CH	134.5, CH	
4′	87.6, CH	73.3, CH	67.3, CH	185.4, C	185.4, C	
4a′			140.4, C	134.5, C	134.4, C	
5′	63.3, CH_2	22.4, CH_3	121.6, CH	118.7, CH	118.7, CH	
6′			127.2, CH	134.6, CH	134.5, CH	
7′			110.2, CH	117.8, CH	117.8, CH	
8′			157.2, C	159.7, C	159.7, C	
8a′			128.2, C	121.0, C	121.2, C	
1-OCH_3					56.0, CH_3	
4-OCH_3	57.7, CH_3					
5-OCH_3	56.9, CH_3	56.1, CH_3		56.2, CH_3	56.2, CH_3	56.5, CH_3
8-OCH_3			56.2, CH_3			
8′-OCH_3			55.6, CH_3	56.5, CH_3	56.5, CH_3	

[a] In CD_3OD. [b] In $CDCl_3$.[c] ^{13}C (100 MHz). [d] ^{13}C (125 MHz).

Dalesconoside C (**3**) was obtained as yellow needles, which has the molecular formula $C_{22}H_{22}O_4$ established by HR-ESIMS (*m*/*z* 351.1597, calcd for $[M+H]^+$ 351.1591). Consequently, **3** had 12 degrees of unsaturation. The ^{1}H and ^{13}C NMR data of **3** (Tables 1 and 2) indicated that 11 of the 12 units of unsaturation come from a naphthalene moiety and an aromatic ring. Thus, the last remaining degree of unsaturation must be attributed to an additional ring system. The 1D NMR spectroscopic data indicated the presence of a structure with two units, one of which is identical with those of 8-methoxy-1-naphthol (**8**), which was isolated from the same source. The second part showed signals corresponding to 1,2,3,4-tetrahydro-5-methoxynaphthalene with the substitution at C-4. The ^{1}H-^{1}H COSY and HSQC spectra of **3** allowed the assignments of the fragments –CH(2)–CH(3)–, –CH(5)–CH(6)–CH(7)–, –CH(1′)–CH_2(2′)–CH_2(3′)–CH(4′)– and –CH(5′)–CH(6′)–CH(7′)–. The HMBC correlations from H-1′ (δ_H 5.04) to C-3 (δ_C 126.6), C-4 (δ_C 131.5), C-2′ (δ_C 23.5), C-3′ (δ_C 26.7), C-4a′ (δ_C 140.4) and C-8a′ (δ_C 128.2); from 1-OH (δ_H 9.37) to C-1 (δ_C 152.8),

C-2 (δ_C 109.4) and C-8a (δ_C 115.6); from 8-OCH_3 (δ_H 4.08) to C-8 (δ_C 156.9); and from 8′-OCH_3 (δ_H 3.49) to C-8′ (δ_C 157.2) enable the establishment of the planer structure of **3**. The relative configuration of **3** was based on the NOESY correlations as indicated in Figure 3. The NOESY correlations observed of H-1′/H_b-2′(δ_H 1.86), H-1′/H-5 (δ_H 7.91), H_b-2′/H-5 and H_b-2′/H-4′ (δ_H 4.87) indicated that H-1′ and H-4′ were on the same side of the 1,2,3,4-tetrahydronaphthalene moiety. The absolute configuration of **1** were also determined by comparing experimental and calculated electronic circular dichroism (ECD) spectra for the truncated model (1′*S*, 4′*S*) -**3a** and the truncated model (1′*R*, 4′*R*) -**3b** using time-dependent density-functional theory (TDDFT) (Tables S5 and S6). The calculated electronic circular dichroism (ECD) curve for 1a was in good agreement with the experimental ECD spectrum of **3** (Figure 4). Therefore, the absolute configuration of **3** was firmly assigned as 1′*S*, 4′*S*. Thus, the complete structure of **3** was established (Figures S17–S24).

Dalesconoside D (**4**) was obtained as a red amorphous powder. Its molecular formula, $C_{22}H_{16}O_5$ (15 degrees of unsaturation), was established by HR-ESI-MS (*m*/*z* 361.1071, calcd for $[M+H]^+$ 361.1071). Using the ^1H and ^{13}C NMR (Tables 1 and 2) combined with the HSQC spectra of **4**, a phenolic hydroxyl signal at δ_H 9.82 (s, 4-OH), the signals for nine aromatic signals at [δ_H 7.78 (dd, *J* = 7.6, 2.9 Hz), δ_C 118.8, d, CH-5′; δ_H 7.68 (t, *J* = 8.2, 7.8 Hz), δ_C 134.6, d, CH-6′; 7.43 (d, *J* = 7.6 Hz), δ_C 121.9, d, CH-8; δ_H 7.37 (t, *J* = 7.8 Hz), δ_C 126.8, d, CH-7; δ_H 7.35 (d, *J* = 7.6 Hz), δ_C 118.7, d, CH-1; δ_H 7.33, s, δ_C 128.8, d, CH-2; δ_H 7.31 (d, *J* = 8.2 Hz), δ_C 117.8, d, CH-7′; δ_H 7.06, s, δ_C 134.5, d, CH-3′; 6.82 (d, *J* = 7.6 Hz), δ_C 104.6, d, CH-6], and signals of two methoxy groups [δ_H 4.05, s, δ_C 56.2, q, 5-OCH_3; δ_H 4.01, s, δ_C 56.5, q, 8′-OCH_3] were observed. The coupling constants and ^1H-^1H COSY spectrum showed the presence of three ^1H-^1H spin systems from –CH(1)–CH(2)–, –CH(6)–CH(7)–CH(8)– and –CH(5′)–CH(6′)–CH(7′)–. The NMR spectroscopic data indicated that **4** comprised one 7-hydroxy-1-methoxyanthracene-9,10-dione subunit and one 8-methoxy-1-naphthol (**8**) subunit [20]. The HMBC spectrum (Figure 2) and NOESY correlations (Figure 3) supported the assignments of the methoxy groups 5-OCH_3 at C-5 (δ_C 156.7) and 8′-OCH_3 at C-8′ (δ_C 159.7). Moreover, HMBC correlations of 4-OH with C-4 (δ_C 152.8) and C-3(δ_C 116.2), H-2 with C-3(δ_C 116.2) and C-2 (δ_C 150.4), H-2 with C-2′(δ_C 150.4), and H-3′ with C-3 (δ_C 116.2) provided evidence for the C-3-C-2′ linkage of **4**. On the basis of the above results, the structure of dalesconoside D (**4**) was identified as 1′-hydroxy-8,8′-dimethoxy-[2,2′-binaphthalene]-1,4-dione (Figures S25–S32).

Dalesconoside E (**5**) was obtained as a red amorphous powder. Its molecular formula $C_{23}H_{18}O_6$ (i.e., differing from that of **4** by an additional OCH_3 group) was established from HRESIMS at *m*/*z* 391.1177 $[M+H]^+$. The ^1H and ^{13}C NMR data (Tables 1 and 2) of **5** were similar to those of **4** except for the significant downfield shift of C-1(δ_C 147.9) and the presence of a methoxy signal (δ_H 3.96, s, δ_C 56.0, q, 1-OCH_3) indicative of **5** was a methoxylated analogue of **4**. The HMBC correlations (Figure 2) of 1-OCH_3 with C-1 revealed that the extra methoxy group is bound to C-1. Hence, **5** was 1-methoxydalesconoside D (Figures S33–S40). Compound **5** is here reported for the first time as a natural product. It was previously prepared via a two-step sequence involving the oxidative dimerization of hydroquinone monomethyl ethers [21].

Dalesconoside F (**6**) was isolated as a colorless amorphous powder. Its molecular formula $C_{11}H_{12}O_4$ was deduced from HRESIMS at *m*/*z* 209.0806 $[M+H]^+$, indicating six degrees of unsaturation. The planer structure of **6** was determined as 3,4-dihydroxy-5-methoxy-3,4-dihydronaphthalen-1(2H)-one [22], which was chemically synthesized from 3,4,5-trihydroxy-1-tetralone with diazomethane, on the basis of ^1H and ^{13}C NMR observations, including 2D ^1H-^1H COSY and HSQC and HMBC spectral data (Figure 2). However, the observed NOESY correlations (Figure 3) of H-3 with H-4 suggested that these protons were on the same spatial orientation. Furthermore, the theoretical ECD spectrum (Figure 4, Tables S7 and S8) was also calculated by a quantum chemical method at the [B3LYP/ 6-311+G(2d,p)] level, and the predicted ECD curve of (3*R*,4*S*)-**6** was in good agreement with that of the experimental one. Finally, the absolute configuration of **6**, named dalesconoside F, was unambiguously determined to be 3*R*,4*S* (Figures S41–S48).

By comparing physical and spectroscopic data with those reported in the literature, the known compounds were elucidated as 1,8-dimethoxynaphthalene (**7**), 8-methoxy-1-naphthol (**8**) [23], regiolone (**9**) [24], nodulisporone (**10**) [25], nodulisporol (**11**) [25], xylariol A (**12**) [26], (4*R*)-4,8-dihydroxy- 3-hydro-5-methoxy-1-naphthalenone (**13**) [27], (4R)-O-methylsclerone (**14**) [28], (4*R*)-3,4-dihydro-4,5-dihydroxynaphthalen-1(2H)-one (**15**) [29], (3*S*)-3,8-dihydroxy-6,7-dimethyl-a-tetralone (**16**) [9], fusaraisochromenone (**17**) [30], 3*R*-3,4-dihydro-6,8-dihydroxy-3-methylisocoumarin (**18**) [31], 2-acetyl-7-methoxybenzofuran (**19**) [32], 4,8-dimethoxy-1H-isochromen-1-one (**20**) [22], (+)-citreoisocoumarin (**21**) [33], 5-hydroxy-8-methoxy-2-methyl-4H-1-benzopyran-4-one(**22**) [34], cytochalasin O (**23**) [35], and dankasterone A (**24**) [36].

2.2. Biological Activity

Compounds **1**–**24** were tested for antimicrobial activity against *Pseudomonas aeruginosa*, *Enterococcus faecalis*, methicillin-resistant *Staphylococcus aureus* and *Escherichia coli* as well as antifungal activity against *Candida albicans*. As shown in Table 3, all metabolites showed antimicrobial activity against at least one of the five tested indicator pathogens at the selected concentration of 50 μg/mL, but all of the antimicrobial activities were weaker than that of the positive control. Compounds **1**, **3**, **13**–**17** and **19** exhibited a wide range of antimicrobial activities; especially, **1** (against *P. aeruginosa* and *E. coli*), **16** (against *E. coli*) and **17** (against MRSA) were most potent, and their resistant strain with MIC values reached 6.25 μg/mL. The comparison between compounds **1** and **7** approved that the substitution of additional furanose was the critical structural component for its antimicrobial activity. The antibacterial results of the comparison of **2**–**16** suggested that the dihydronaphthalen-1-one nucleus may not be sensitive to the tested microbes in some cases, but the extra auxochromes, e.g., -OCH_3, -OH or CH_3 enhanced the antibacterial effect of the compound against the tested bacteria and fungi. Meanwhile, when the hydroxyl group is oxidized to a carbonyl group to a certain extent, the antibacterial activity of the metabolite against some indicator bacteria is weakened. Comparing the antimicrobial activities of compounds **17**–**22** indicated that the *O*-containing heterocyclic substructure may increase the compound's effect on *P. aeruginosa*, *E. faecalis*, *MRSA* and *E. coli*. When the -OH and -OCH_3 groups are differently substituted on the benzene ring or the lactone/quionone of metabolites' isocoumarin backbone, different indicator bacteria have different promotion and inhibition. In general, the broad antimicrobial activities of these naphthalene derivatives support their continued investigation so as to develop a deeper understanding of structure−activity relationships and mechanism of antimicrobial action.

Table 3. Antimicrobial activities of isolated compounds **1**–**24**.

	MIC(μg/mL)				
Compound	***P. aeruginosa***	***E. faecalis***	**MRSA**	***E.coli***	***C. albicans***
1	6.25	25	12.5	6.25	25
2	50	>50	50	>50	>50
3	25	25	25	12.5	>50
4	25	50	50	>50	>50
5	12.5	50	25	>50	50
6	>50	>50	50	50	>50
7	12.5	50	25	25	50
8	25	>50	25	50	12.5
9	>50	25	>50	>50	25
10	50	>50	50	50	>50
11	50	25	50	50	>50
12	25	25	25	>50	25
13	25	12.5	12.5	25	25
14	25	25	25	25	25
15	50	25	50	25	25
16	12.5	25	12.5	6.25	50

Table 3. *Cont.*

Compound	MIC(μg/mL)				
	P. aeruginosa	***E. faecalis***	**MRSA**	***E.coli***	***C. albicans***
17	12.5	12.5	6.25	12.5	25
18	>50	>50	12.5	25	>50
19	12.5	25	25	12.5	>50
20	>50	>50	50	50	>50
21	50	>50	50	50	>50
22	>50	>50	25	50	>50
23	>50	>50	25	25	>50
24	50	>50	>50	>50	>50
Ciprofloxacin	0.78	0.625	0.3125	0.625	
Amphotericin B					0.78

3. Materials and Methods

3.1. General Experimental Procedure

Optical rotation was recorded at 20 °C using a WYA-2S digital Abbe polarimeter (Shanghai Physico-optical Instrument Factory, Shanghai, China). UV spectral data were obtained from online UV spectra acquired on a Shimadzu UV-2401 PC spectrophotometer. NMR spectra were recorded on a Bruker AV-400 and AV-500 (Bruker Corporation, Fällanden, Switzerland) instrument with TMS as an internal standard. ESI-MS spectra were recorded on a VG Auto Spec-3000 mass spectrometer (VG, Manchester, UK). High-resolution ESI-MS were recorded on an Agilent 6210 mass spectrometer (Agilent Technologies, Waldbronn, Germany) employing peak matching. The ECD spectra were measured on a JASCO J-715 spectra polarimeter (Japan Spectroscopic, Tokyo, Japan). SephadexLH-20 (Beijing Biotopped Science & Technology Co., Ltd., Beijing, China), SiliaSphere C18 (SiliCycle, Quebec, Canada) and Silica gel (200–300 mesh, Qingdao Marine Chemical Factory, Qingdao, China) were used for column chromatography (CC). Thin-layer chromatography (TLC) was performed on precoated silica gel GF254 plates (Qingdao Marine Chemical Factory, Qingdao, China).

3.2. Fungal Material

The strain MCZ-18 was isolated from a fresh, healthy branch of *Ceriops tagal* collected from the Dong Zhai Gang-Mangrove Garden on Hainan Island, China. The fungus was isolated under sterile conditions from the inner tissue of the flower following an isolation protocol described previously [37] and identified as *Daldinia eschscholzii* (GenBank accession no. MH712260) by morphologic traits and molecular identification. A voucher strain was deposited in the School of Chemical Engineering and Technology, Hainan University, Haikou, China.

3.3. Fermentation, Extraction and Isolation

The *Daldinia eschscholzii* MCZ-18 strain was cultivated on an autoclaved rice solid-substrate medium, consisting of 80 1 L Erlenmeyer flasks. Each flask included 80 g of rice, 0.24 g of sea salt and 80 mL of water. The culture was maintained at a temperature of 25 °C. Following a fermentation period of 29 days, the mycelia and rice were subjected to three extractions using EtOAc. The extracts underwent filtration and evaporation under decreased pressure to yield a crude extract of 75 g. The crude extracts were then submitted to vacuum liquid chromatography (VLC) on silica gel employing a step gradient of petroleum ether/ethyl acetate (1:0–0:1, *v*/*v*) to obtain five fractions (Fr.1–Fr.5). Fr.1 was eluted equivalently with petroleum ether to give **8** (200 mg). Fr.2 was eluted equivalently with petroleum ether / ethyl acetate (50:1, *v*/*v*) to obtain **7** (150 mg). Fr.3 was eluted with a step gradient of petroleum ether/ethyl acetate (20:1, 10:1, 5:1, 3:1, 1:1, *v*/*v*) to give 3 fractions (Fr.3.1–Fr.3.3). Subsequently, Fr.3.1 was further separated by Sephadex LH-20 chromatography (CH_2Cl_2/MeOH, 1:1, *v*/*v*) and finally by an ODS column eluting with

MeOH-H_2O (70:30, 80:20, 90:10, 100:0, *v*/*v*) giving **24** (4.5 mg) and **22** (20 mg). Fr.3.2 was eluted equivalently with petroleum ether/ethyl acetate (5:1, *v*/*v*) to give 3 subfractions (Fr.3.2.1–Fr.3.2.3). Fr.3.2.2 was further purified by preparative TLC (developing solvents: CH_2Cl_2/MeOH, 100: 3, *v*/*v*) to obtain **14** (12 mg) and **16** (24 mg). Fr.3.2.3 was purified by Sephadex LH-20 CC (CH_2Cl_2/MeOH, 1:1, *v*/*v*) and finally by an ODS column eluting with MeOH-H_2O (60:40, 70:30, *v*/*v*) to obtain **3** (2 mg), **19** (6 mg), **11** (1.0 mg), **5** (2.6 mg), **4** (1.2 mg) and **9** (2 mg). **2** (1.8 mg) and **6** (2.2 mg) was acquired by Sephadex LH-20 chromatography (CH_2Cl_2/MeOH, 1:1, *v*/*v*) and C-18 ODS column (MeOH/H_2O, 60:40, 70:30, *v*/*v*). Fr.3.3 was eluted with a step gradient of petroleum ether/ethyl acetate (3:1, 2:1, 1:1, *v*/*v*) to give 3 fractions (Fr.3.3.1–Fr.3.3.3). Fr.3.3.2 was purified by Sephadex LH-20 CC (CH_2Cl_2/MeOH, 1:1, *v*/*v*) and finally by an ODS column eluting with MeOH-H_2O (60:40, *v*/*v*) to obtain **13** (3 mg), **18** (3.2 mg) and **12** (2 mg). Fr.3.3.3 was purified by Sephadex LH-20 CC (MeOH) and finally by an ODS column eluting with MeOH-H_2O (45:55, *v*/*v*) to obtain **21** (3.3 mg), **10** (3.6 mg) and **17** (4.4 mg). Fr.4 was purified by an ODS column eluting with MeOH-H_2O (40:60, 50:50, 60:40, 70:30, 80:20, 90:10, 100:0, *v*/*v*) to obtain 3 subfractions (Fr 4.1–Fr 4.3) and **23** (3.8 mg). Fr.4.2 was purified by Sephadex LH-20 CC (MeOH) and finally by an ODS column eluting with MeOH-H_2O (45:55, *v*/*v*) to obtain **15** (3 mg), **20** (2.6 mg) and **1** (5.5 mg).

Dalesconoside A (**1**): yellow needles; $[\alpha]^{20}_D$ +100 (*c* 0.0001, MeOH); UV (MeOH) λ_{max} 226 nm; ^1H and ^{13}C NMR data, see Tables 1 and 2; (+)-HRESIMS at *m*/*z* 337.1289 $[M+H]^+$ (calcd for $C_{17}H_{21}O_7$ 337.1282).

Dalesconoside B (**2**): colorless oil; $[\alpha]^{20}_D$ +10 (*c* 0.0001, MeOH); UV (MeOH) λ_{max} 205 nm; ^1H and ^{13}C NMR data, see Tables 1 and 2; (+)-HRESIMS at *m*/*z* 359.1464 $[M+Na]^+$ (calcd for $C_{18}H_{24}O_6Na$ 359.1465).

Alesconoside C (**3**): yellow needles; $[\alpha]^{20}_D$ +80 (*c* 0.0001, MeOH); UV (MeOH) λ_{max} 202 nm; ^1H and ^{13}C NMR data, see Tables 1 and 2; (+)-HRESIMS at *m*/*z* 351.1597 $[M+H]^+$ (calcd for $C_{22}H_{23}O_4$ 351.1591).

Dalesconoside D (**4**): red amorphous solid; UV (MeOH) λ_{max} 201 nm; ^1H and ^{13}C NMR data, see Tables 1 and 2; (+)-HRESIMS at *m*/*z* 361.1071 $[M+H]^+$ (calcd for $C_{22}H_{17}O_5$ 361.1071).

Dalesconoside E (**5**): red amorphous solid; UV (MeOH) λ_{max} 202 nm; $[\alpha]^{20}_D$ +70 (*c* 0.0001, MeOH); UV (MeOH) λ_{max} 201 nm; ^1H and ^{13}C NMR data, see Tables 1 and 2; (+)-HRESIMS at *m*/*z* 391.1177 $[M+H]^+$ (calcd for $C_{23}H_{19}O_6$ 391.1176).

Dalesconoside F (**6**): colorless solid; $[\alpha]^{20}_D$ +80 (*c* 0.0001, MeOH); UV (MeOH) λ_{max} 221 nm; ^1H and ^{13}C NMR data, see Tables 1 and 2; (+)-HRESIMS at *m*/*z* 209.0806 $[M+H]^+$ (calcd for $C_{11}H_{13}O_4$ 209.0808).

3.4. ECD Calculations

The Monte Carlo conformational searches were carried out by means of the Spartan's 14 software (v1.1.4) using a Merck Molecular Force Field (MMFF). The conformers of **1**–**3** and **6** with a Boltzmann population of over 5% were chosen for ECD calculations, and then the conformers were initially optimized at B3LYP/6-31g (d, p) in gas. The theoretical calculation of ECD was conducted in MeOH using time-dependent density functional theory (TD-DFT) at the B3LYP/6-31+g (d, p) level for all conformers of compounds. Rotatory strengths for a total of 30 excited states were calculated. ECD spectra were generated using the program SpecDis 1.6 (University of Würzburg, Würzburg, Germany) and GraphPad Prism 5 (University of California San Diego, CA, USA) from dipole-length rotational strengths by applying Gaussian band shapes with sigma = 0.3 eV.

3.5. Antimicrobial Activity Assay

The microplate assay method was used to assess the antimicrobial activities of compounds **1**–**24** against four terrestrial pathogenic bacteria (*Pseudomonas aeruginosa*, *Methicillin-resistant Staphylococcus aureus*, *Bacillus subtilis* and *Escherichia coli*) and one pathogenic fungus (*Candida albicans*) (Guangdong Microbial Culture Collection Center,

China, CDMCC) according to previously reported methods [38]. Ciprofloxacin and amphotericin B were used as a positive control.

4. Conclusions

In conclusion, five new naphthalene derivatives (**1**–**4**, **6**), a new natural product (**5**) and eighteen known compounds (**7**–**24**) were isolated from mangrove endophytic fungus *Daldinia eschscholzii* MCZ-18. Compounds **1** and **2** are naphthalenes bearing a rare ribofuranoside substituted at C-1 and the 5-methyltetrahydrofuran-2,3-diol moiety, respectively. This is the first report of these naphthalene subtypes being isolated from mangrove-derived fungal sources. All the isolated metabolites showed more or less antimicrobial activities. Several naphthalene derivatives (**1**, **3**, **13**–**17** and **19**) showed broad ranges of antimicrobial spectrum. Based on the structure–activity relationship analysis, oxygen heterocyclic rings such as ribofuranoside and tetrahydropyran moieties, auxochromes, e.g., -OCH_3, -OH or CH_3 were considered as the pharmacophores. The results presented herein reinforce the importance of the mangrove microbial environment as a source of antimicrobial compounds with remarkably varied applications.

Supplementary Materials: The following supporting information can be downloaded at https://www.mdpi.com/article/10.3390/md22060242/s1, Figures S1–S48; Tables S1–S8. The 1D, 2D NMR and HRESIMS spectra for **1**–**24** are available online at Figures S1–S48.

Author Contributions: J.X. designed and supervised this research, structured the elucidation, and wrote the draft and final revision of the manuscript. Z.X. performed the isolation. T.F. and B.C. helped organize and test compound data. Z.W. measured the NMR spectra. Q.L. and P.L. carried out the biological activity. The final revision of the manuscript was revised by all the authors. All authors have read and agreed to the published version of the manuscript.

Funding: The National Natural Science Foundation of China (No. 82160675/81973229), the Key Research Program of Hainan Province (ZDYF2021SHFZ108), the Collaborative Innovation Center Foundation of Hainan University (XTCX2022STB01) and the Guangdong Key Laboratory of Marine Materia Medica Open Fund (LMM2021-4) are gratefully acknowledged for the grants that co-financed this project.

Institutional Review Board Statement: Not applicable.

Data Availability Statement: The original data presented in the study are included in the article/Supplementary Materials; further inquiries can be directed to the corresponding author.

Conflicts of Interest: The authors declare no conflicts of interest.

References

1. Lin, W.; Li, G.; Xu, J. Bio-Active Products from Mangrove Ecosystems. *Mar. Drugs* **2023**, *21*, 239. [CrossRef] [PubMed]
2. Wu, M.J.; Xu, B.; Guo, Y.W. Unusual Secondary Metabolites from the Mangrove Ecosystems: Structures, Bioactivities, Chemical, and Bio-Syntheses. *Mar. Drugs* **2022**, *20*, 535. [CrossRef] [PubMed]
3. Xu, J. Biomolecules Produced by Mangrove-Associated Microbes. *Curr. Med. Chem.* **2011**, *18*, 5224–5266. [CrossRef] [PubMed]
4. Xu, J. Bioactive Natural Products Derived from Mangrove-Associated Microbes. *RSC Adv.* **2015**, *5*, 841–892. [CrossRef]
5. Karnchanatat, A.; Petsom, A.; Sangvanich, P.; Piapukiew, J.; Whalley, A.J.S.; Reynolds, C.D.; Gadd, G.M.; Sihanonth, P. A Novel Thermostable Endoglucanase from the Wood-Decaying Fungus *Daldinia eschscholzii* (Ehrenb.:Fr.) Rehm. *Enzym. Microb. Technol.* **2008**, *42*, 404–413. [CrossRef]
6. Zhang, Y.L.; Ge, H.M.; Zhao, W.; Dong, H.; Xu, Q.; Li, S.H.; Li, J.; Zhang, J.; Song, Y.C.; Tan, R.X. Unprecedented Immunosuppressive Polyketides from *Daldinia eschscholzii*, a Mantis-Associated Fungus. *Angew. Chem. Int. Ed.* **2008**, *47*, 5823–5826. [CrossRef] [PubMed]
7. Tarman, K.; Palm, G.J.; Porzel, A.; Merzweiler, K.; Arnold, N.; Wessjohann, L.A.; Unterseher, M.; Lindequist, U. Helicascolide C, a New Lactone from an Indonesian Marine Algicolous Strain of *Daldinia eschscholzii* (Xylariaceae, Ascomycota). *Phytochem. Lett.* **2012**, *5*, 83–86. [CrossRef]
8. Luo, Y.; Qiu, L.; Deng, Y.; Yuan, X.-H.; Gao, P. A New Chromone and a New Aliphatic Ester Isolated from *Daldinia eschscholtzii*. *J. Asian Nat. Prod. Res.* **2018**, *20*, 883–888. [CrossRef] [PubMed]
9. Kongyen, W.; Rukachaisirikul, V.; Phongpaichit, S.; Sakayaroj, J. A New Hydronaphthalenone from the Mangrove-Derived *Daldinia eschscholtzii* PSU-STD57. *Nat. Prod. Res.* **2015**, *29*, 1995–1999. [CrossRef]

10. Yang, L.-J.; Liao, H.-X.; Bai, M.; Huang, G.-L.; Luo, Y.-P.; Niu, Y.-Y.; Zheng, C.-J.; Wang, C.-Y. One New Cytochalasin Metabolite Isolated from a Mangrove-Derived Fungus *Daldinia eschscholtzii* HJ001. *Nat. Prod. Res.* **2018**, *32*, 208–213. [CrossRef]
11. Zhang, Y.L.; Zhang, J.; Jiang, N.; Lu, Y.H.; Wang, L.; Xu, S.H.; Wang, W.; Zhang, G.F.; Xu, Q.; Ge, H.M.; et al. Immunosuppressive Polyketides from Mantis-Associated *Daldinia eschscholzii*. *J. Am. Chem. Soc.* **2011**, *133*, 5931–5940. [CrossRef] [PubMed]
12. Zhang, A.H.; Tan, R.; Jiang, N.; Yusupu, K.; Wang, G.; Wang, X.L.; Tan, R.X. Selesconol, a Fungal Polyketide That Induces Stem Cell Differentiation. *Org. Lett.* **2016**, *18*, 5488–5491. [CrossRef] [PubMed]
13. Zhang, A.H.; Liu, W.; Jiang, N.; Wang, X.L.; Wang, G.; Xu, Q.; Tan, R.X. Sequestration of Guest Intermediates by Dalesconol Bioassembly Lines in *Daldinia eschscholzii*. *Org. Lett.* **2017**, *19*, 2142–2145. [CrossRef] [PubMed]
14. Liao, H.-X.; Shao, T.-M.; Mei, R.-Q.; Huang, G.-L.; Zhou, X.-M.; Zheng, C.-J.; Wang, C.-Y. Bioactive Secondary Metabolites from the Culture of the Mangrove-Derived Fungus *Daldinia eschscholtzii* HJ004. *Mar. Drugs* **2019**, *17*, 710. [CrossRef] [PubMed]
15. Liao, H.-X.; Zheng, C.-J.; Huang, G.-L.; Mei, R.-Q.; Nong, X.-H.; Shao, T.-M.; Chen, G.-Y.; Wang, C.-Y. Bioactive Polyketide Derivatives from the Mangrove-Derived Fungus *Daldinia eschscholtzii* HJ004. *J. Nat. Prod.* **2019**, *82*, 2211–2219. [CrossRef]
16. Feng, Z.; Zhang, X.; Wu, J.; Wei, C.; Feng, T.; Zhou, D.; Wen, Z.; Xu, J. Immunosuppressive cytochalasins from the mangrove endophytic fungus *Phomopsis asparagi* DHS-48. *Mar. Drugs* **2022**, *20*, 526. [CrossRef] [PubMed]
17. Feng, T.; Wei, C.; Deng, X.; Chen, D.; Wen, Z.; Xu, J. Epigenetic manipulation induced production of immunosuppressive chromones and cytochalasins from the mangrove endophytic fungus *Phomopsis asparagi* DHS-48. *Mar. Drugs* **2022**, *20*, 616. [CrossRef]
18. Wu, J.; Chen, D.; Li, Q.; Feng, T.; Xu, J. Metabolomics-Guided Discovery of New Dimeric Xanthones from Co-Cultures of Mangrove Endophytic Fungi *Phomopsis asparagi* DHS-48 and *Phomopsis* sp. DHS-11. *Mar. Drugs* **2024**, *22*, 102. [CrossRef] [PubMed]
19. Huang, H.; Lin, Y.; Zhou, S.; Vrijmoed, L.L.P. Metabolites of Mangrove Endophytic Fungus 3920 from the South China Sea. *Acta Sci. Nat. Univ. Sunyatseni* **2005**, *6*, 137–138.
20. Lu, M.M.; Chen, Y.C.; Liu, H.X.; Li, S.N.; Li, H.H.; Tao, M.H.; Hao, Z.B.; Zhang, W.M. Secondary Metabolites of Endophytic *Daldinia eschscholtzii* A630 from *Pogostemon cablin* and Their Cytotoxic Activities. *Nat. Prod. Res. Dev.* **2018**, *30*, 1176–1180. [CrossRef]
21. Takeya, T.; Kondo, H.; Otsuka, T.; Tomita, K.; Okamoto, I.; Tamura, O. A Novel Construction of Dibenzofuran-1,4-Diones by Oxidative Cyclization of Quinone-Arenols. *Org. Lett.* **2007**, *9*, 2807–2810. [CrossRef] [PubMed]
22. Fujimoto, Y.; Yokoyama, E.; Takahashi, T.; Uzawa, J.; Morooka, N.; Tsunoda, H.; Tatsuno, T. Studies on the Metabolites of Penicillium Diversum Var. Aureum. I. *Chem. Pharm. Bull.* **1986**, *34*, 1497–1500. [CrossRef] [PubMed]
23. Nadeau, A.K.; Sorensen, J.L. Polyketides Produced by *Daldinia loculata* Cultured from Northern Manitoba. *Tetrahedron Lett.* **2011**, *52*, 1697–1699. [CrossRef]
24. Deng, Q.; Li, G.; Sun, M.; Yang, X.; Xu, J. A New Antimicrobial Sesquiterpene Isolated from Endophytic Fungus *Cytospora* sp. from the Chinese Mangrove Plant *Ceriops tagal*. *Nat. Prod. Res.* **2020**, *34*, 1404–1408. [CrossRef]
25. Kamisuki, S.; Ishimaru, C.; Onoda, K.; Kuriyama, I.; Ida, N.; Sugawara, F.; Yoshida, H.; Mizushina, Y. Nodulisporol and Nodulisporone, Novel Specific Inhibitors of Human DNA Polymerase λ from a Fungus, *Nodulisporium* sp. *Bioorganic Med. Chem.* **2007**, *15*, 3109–3114. [CrossRef] [PubMed]
26. Guo, Z.-L.; Zheng, J.-J.; Cao, F.; Wang, C.; Wang, C.-Y. Chemical Constituents of the Gorgonian-Derived Fungus *Chaetomium globosum*. *Chem. Nat. Compd.* **2017**, *53*, 199–202. [CrossRef]
27. Buchanan, M.S.; Hashimoto, T.; Takaoka, S.; Kan, Y.; Asakawa, Y. A 10-Phenyl-[11]-Cytochalasan from a Species of *Daldinia*. *Phytochemistry* **1996**, *42*, 173–176. [CrossRef]
28. Chang, C.; Chang, H.; Cheng, M.; Liu, T.; Hsieh, S.; Yuan, G.; Chen, I. Inhibitory Effects of Constituents of an Endophytic Fungus *Hypoxylon investiens* on Nitric Oxide and Interleukin-6 Production in RAW264.7 Macrophages. *Chem. Biodivers.* **2014**, *11*, 949–961. [CrossRef] [PubMed]
29. Couché, E.; Fkyerat, A.; Tabacchi, R. Stereoselective Synthesis of *cis*- and *trans*-3,4-Dihydro-3,4,8-trihydroxynaphthalen-1(2*H*)-one. *Helv. Chim. Acta* **2009**, *92*, 903–917. [CrossRef]
30. Boonyaketgoson, S.; Trisuwan, K.; Bussaban, B.; Rukachaisirikul, V.; Phongpaichit, S. Isochromanone Derivatives from the Endophytic Fungus *Fusarium* sp. PDB51F5. *Tetrahedron Lett.* **2015**, *56*, 5076–5078. [CrossRef]
31. Krohn, K.; Bahramsari, R.; Flörke, U.; Ludewig, K.; Kliche-Spory, C.; Michel, A.; Aust, H.-J.; Draeger, S.; Schulz, B.; Antus, S. Dihydroisocoumarins from Fungi: Isolation, Structure Elucidation, Circular Dichroism and Biological Activity. *Phytochemistry* **1997**, *45*, 313–320. [CrossRef] [PubMed]
32. Wen, L.; Guo, Z.; Li, Q.; Zhang, D.; She, Z.; Vrijmoed, L.L.P. A New Griseofulvin Derivative from the Mangrove Endophytic Fungus *Sporothrix* Sp. *Chem. Nat. Compd.* **2010**, *46*, 363–365. [CrossRef]
33. Youssef, D.T.A.; Shaala, L.A.; Genta-Jouve, G. Asperopiperazines A and B: Antimicrobial and Cytotoxic Dipeptides from a Tunicate-Derived Fungus *Aspergillus* sp. DY001. *Mar. Drugs* **2022**, *20*, 451. [CrossRef] [PubMed]
34. Sun, Y.; Liu, G.; Huang, H.; Yu, P. Chromone Derivatives from *Halenia elliptica* and Their Anti-HBV Activities. *Phytochemistry* **2012**, *75*, 169–176. [CrossRef] [PubMed]
35. Zhang, S.; Liao, H.; Liang, D. Chemical constitutes from *Clerodendrum japonicum*. *China J. Chin. Mater. Medica* **2018**, *43*, 2732–2739. [CrossRef] [PubMed]

36. Amagata, T.; Tanaka, M.; Yamada, T.; Doi, M.; Minoura, K.; Ohishi, H.; Yamori, T.; Numata, A. Variation in Cytostatic Constituents of a Sponge-Derived *Gymnascella dankaliensis* by Manipulating the Carbon Source. *J. Nat. Prod.* **2007**, *70*, 1731–1740. [CrossRef] [PubMed]
37. Zhou, J.; Li, G.; Deng, Q.; Zheng, D.; Yang, X.; Xu, J. Cytotoxic Constituents from the Mangrove Endophytic *Pestalotiopsis* sp. Induce G_0/G_1 Cell Cycle Arrest and Apoptosis in Human Cancer Cells. *Nat. Prod. Res.* **2018**, *32*, 2968–2972. [CrossRef]
38. Wei, C.W.; Sun, C.X.; Feng, Z.; Zhang, X.X.; Xu, J. Four New Chromones from the Endophytic Fungus *Phomopsis asparagi* DHS-48 Isolated from the Chinese Mangrove Plant *Rhizophora mangle*. *Mar. Drugs* **2021**, *19*, 348. [CrossRef]

marine drugs

MDPI

Review

New Secondary Metabolites of Mangrove-Associated Strains

Yunxia Yu [1,2], Zimin Wang [2], Dingmi Xiong [2], Liman Zhou [2], Fandong Kong [2,*] and Qi Wang [1,*]

[1] Department of Pediatric Intensive Care Medicine, Hainan Women and Children's Medical Center, Haikou 570206, China; yuyunxia2023@163.com

[2] Key Laboratory of Chemistry and Engineering of Forest Products, State Ethnic Affairs Commission, Guangxi Key Laboratory of Chemistry and Engineering of Forest Products, Guangxi Collaborative Innovation Center for Chemistry and Engineering of Forest Products, Guangxi Minzu University, Nanning 530006, China; wzm55802023@163.com (Z.W.); xdm7026@163.com (D.X.); zhouliman88@126.com (L.Z.)

* Correspondence: kongfandong0127@126.com (F.K.); wqi1220@163.com (Q.W.)

Abstract: Positioned at the dynamic interface between terrestrial and marine realms, mangroves embody a vibrant tapestry of biodiversity, encompassing an array of plants, animals, and microorganisms. These microbial inhabitants of mangrove habitats have emerged as a pivotal resource for antimicrobials and a plethora of pharmaceutically valuable compounds, spanning enzymes, antineoplastic agents, pesticides, immunosuppressants, and immunomodulators. This review delves into the recent landscape (January 2021 to May 2024, according to the time of publication) of novel secondary metabolites isolated from mangrove-associated microorganisms, analyzing 41 microbial strains that collectively yielded 165 distinct compounds. Our objective is to assess the productivity and potential of natural products derived from microbial populations within mangrove ecosystems in recent times. Notably, fungi stand out as the preeminent contributors to the emergence of these novel natural products, underscoring their pivotal role in the bioprospecting endeavors within these unique environments.

Keywords: mangrove ecosystems; microorganisms; secondary metabolites; new compounds

1. Introduction

Despite their fragility and sporadic distribution, mangrove ecosystems worldwide exhibit remarkable productivity [1]. These unique environments are marked by periodic tidal inundation, leading to significant fluctuations in environmental factors such as salinity and nutrient availability, thereby imparting specific and distinguishing traits [2]. The abundance of carbon and other essential nutrients within these ecosystems fosters the proliferation of diverse microbial communities, which have evolved remarkable resilience to moderate salinity levels and the unpredictable nature of their surroundings [3]. This microbial diversity encompasses a broad spectrum of organisms, including bacteria, fungi, cyanobacteria, microalgae, macroalgae, and fungus-like protists, all of which have been documented within mangrove habitats [4].

Natural products (NPs), encompassing the secondary metabolites extracted from animals, plants, marine organisms, and microorganisms, have garnered immense attention since the discovery of their unique physiological activities. This groundbreaking revelation has paved the way for the development of numerous therapeutic and healthcare drugs [5]. Notably, some of these natural products serve as lead compounds, undergoing strategic structural modifications to emerge as novel generations of drugs [6]. Furthermore, they boast significant economic value, finding applications in pesticides, food additives, daily chemicals, and other fine chemical products.

The exploration of bioactive lead compounds from mangrove microorganisms has emerged as a vibrant frontier within natural product chemistry research [7]. Mangrove-derived microbes represent a promising reservoir of bioactive natural products, yielding

structurally unparalleled compounds with therapeutic potential [8,9]. However, the challenge remains for drug developers to effectively harness this abundant source of natural products. In recent years, particularly after 2013, Blunt and his colleagues have underscored the distinction between mangrove-associated fungi and marine fungi, driven by the proliferation of reported compounds originating from fungi inhabiting mangrove plants and soils [10–13]. This distinction underscores the uniqueness and potential of mangrove-derived microorganisms.

Recently, many researchers have reviewed mangrove-associated natural products from different aspects. Chen et al. summarized the discovery relating to the source and characteristics of metabolic products isolated from mangrove-associated fungi from 1989 to 2020, focusing on bioactivity and the unique chemical diversity of these natural products [3]. Braga et al. reviewed antibacterial, antifungal, and antiviral chemicals produced by soil/sediment-derived mangrove fungi from 1990 to 2022 [14]. Wu et al. collected 134 secondary metabolites and classified them into two major families in terms of the biological sources and 15 subfamilies according to the chemical structures, highlighting the structural diversity and bioactivities of the mangrove ecosystem-associated secondary metabolites [15]. Law et al. highlighted research on mangrove-derived streptomycetes and the production of anticancer-related compounds from these microorganisms (2008–2019) [16]. Collectively, these reviews underscore the immense untapped potential of mangrove microbial secondary metabolites as a rich source for the development of novel therapeutic agents in the medical realm. In this comprehensive review, we delve into the diverse strains sourced from mangroves, the myriad of compounds they produce, and the biological activities associated with these compounds. By examining the latest advancements and trends in this field, we aim to provide insights that may inspire future research endeavors and facilitate the discovery of novel bioactive natural products with significant therapeutic and economic implications.

2. Strains

Herein, 41 strains were reviewed, including 39 strains of fungi and 2 strains of actinomycetes, of which 27 strains of endophytic fungi accounted for 69.2% of the total fungi (Figure 1).

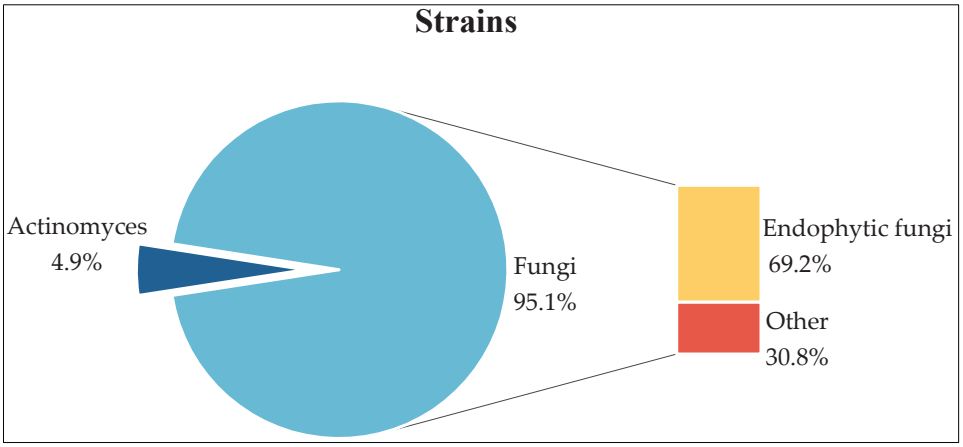

Figure 1. The types of strains.

2.1. Fungi

Mangrove forests are biodiversity 'hotspots' for marine fungi [17]. Fungi are essential to the survival of this ecosystem. They participate in the synthesis of enzymes required for the decomposition of organic matter in this environment, converting it into nutrients available for its metabolism or that of other organisms, as well as allowing subsequent colonization by bacteria and yeasts to supplement the decomposition process, thereby contributing to the cycling and flow of nutrients to higher trophic levels [14,18–20]. The mangrove environment is an important target for bioprospection of secondary metabolite-

producing fungi because it contributes to the development of several fungal species with potential biotechnological applications. After all, fungal secondary metabolites are typically produced in response to biotic or abiotic environmental influences. The organisms present in these areas are expected to be sources of unusual compounds due to the mangrove's unique characteristics [21,22]. Currently, research on the secondary metabolites of fungi associated with mangroves has grown significantly. In this paper, the secondary metabolites of 39 strains of fungi were reviewed. Among these fungi, there were 11 strains of *Penicillium*, 9 strains of *Aspergillus*, and 3 strains of *Phomopsis*. There are 17 genera in total (Figure 2).

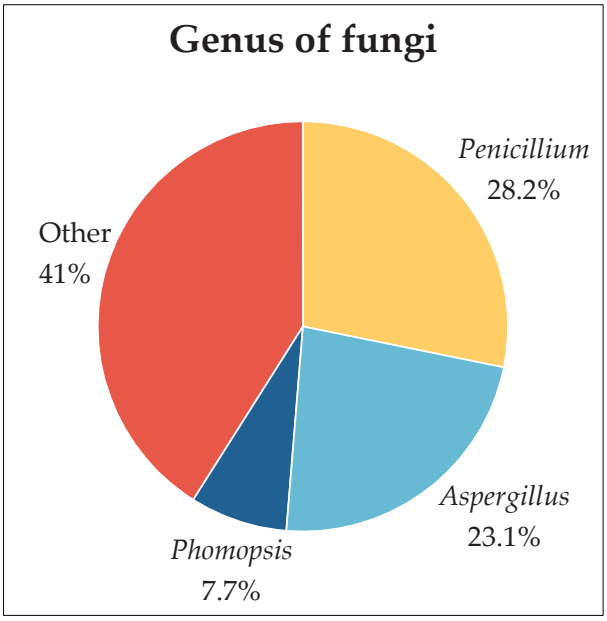

Figure 2. Genus of 39 strains of fungi.

2.2. Actinomycetes

Actinomycetes are a potential source of bioactive substances and the most abundant source of secondary metabolites. Several reports from different geographical locations around the world have described the occurrences of actinomycetes in different mangrove habitats [23,24]. This relatively large distribution of actinomycete species in mangrove ecosystems worldwide seems to indicate that mangroves are a treasure trove of actinomycetes.

2.3. Endophytic Fungi

Endophytic fungi refer to fungi that live within plant tissues and spend part of their life cycle in plant systems without causing any obvious pathogenic symptoms [25]. Most endophytic fungi belong to the genus Ascomycetes and are a multi-class group [3]. Endophytic fungi are an important class of mangrove fungi, and mangrove endophytic fungi are the second largest group of marine fungi, and the study of secondary metabolites is a promising new field [26,27]. Mangrove endophytic fungi have evolved in symbiosis with host plants, forming a unique bioactive substance synthesis pathway or metabolic pathway, from which a wealth of novel structures and/or bioactive substances with special functions can be metabolized, such as antitumor, antibiotic, neuroprotective, antioxidant, anti-inflammatory, antiviral and immunomodulator compounds [3,25]. Herein, 112 secondary metabolites isolated from 27 strains of endophytic fungi and their biological activities were reviewed (Table 1) (Figures 3 and 4).

Table 1. Secondary metabolites isolated from endophytic fungi and their activities.

Sr. No.	Endophytic Fungus	Host Plant(s)	Sources	Compound Isolated	Bioactivity and IC_{50}/EC_{50}/Inhibition	Reference
1	*Phomopsis* sp. DHS-11	the living root of the mangrove plant *Rhizophora mangle*	Dong Zhai Gang mangrove garden on Hainan Island, China	**1**	HeLa cells (11.49 ± 1.64 μmol L^{-1})	[28]
				2		
				3	HeLa cells (8.70 ± 0.94 μmol L^{-1})	
				4	HepG 2 (34.10 ± 2.92 μmol L^{-1})	
				5		[29]
2	*Cytospora heveae* NSHSJ-2	the fresh stem of mangrove plant *Sonneratia caseolaris*	the Nansha Mangrove National Nature Reserve in Guangdong Province, China	**6**	DPPH radical scavenging activity (11.5 ± 0.1 μmol L^{-1})	[30]
				7	DPPH radical scavenging activity (21.5 ± 1.0 μmol L^{-1})	
				8	DPPH radical scavenging activity (19.7 ± 1.8 μmol L^{-1})	
				9	DPPH radical scavenging activity (16.6 ± 0.4 μmol L^{-1})	
				10	DPPH radical scavenging activity (9.5 ± 0.1 μmol L^{-1})	
				11		
				12		
3	*Colletotrichum* sp. SCSIO KcB3-2	a mangrove plant, *Kandelia candel*	Dayawan, Shenzhen, Guangdong Province, China	**13**	AChE inhibitory activity (2.2 ± 0.18 μmol L^{-1})	[31]
4	*Phomopsis asparagi* DHS-48	a healthy tree root of the mangrove plant *Rhizophora mangle*	Dong Zhai Gang-Mangrove Garden in Hainan Province	**14**		[32]
				15	normal splenocytes (111.7 ± 1.1 μmol L^{-1}) ConA-Induced T-Cell Proliferation (21.6 ± 1.7 μmol L^{-1}) LPS-Induced B-Cell Proliferation (78.5 ± 1.3 μmol L^{-1})	
				16		
				17	ConA-Induced T-Cell Proliferation (42.35 ± 2.49 μmol L^{-1}) LPS-Induced B-Cell Proliferation (88.19 ± 2.59 μmol L^{-1})	[33]
				18	HepG2 (59.14 ± 15.79 μmol L^{-1}) Hela (5.82 ± 0.82 μmol L^{-1})	
5	*Pestalotiopsis* sp. HQD-6	fresh, healthy leaf of Chinese mangrove plant *Rhizophora mucronata*	Dong Zhai Gang-Mangrove Garden on Hainan Island, China	**19**		[34]
				20	Hela (50.42 ± 0.07 μmol L^{-1})	
6	*Talaromyces flavus* TGGP35	the stem of the mangrove plant *Acanthus ilicifolius*	Dongzhai Port, Haikou, Hainan Province	**21**		[35]
				22		
				23		
				24		
				25		
				26	antioxidant activity (0.14 mmol L^{-1})	
				27		[36]
				28		
				29	Hela (62.23 ± 0.23 μmol L^{-1})	
				30		
				31	antioxidant activity (0.40 mmol L^{-1})	
				32	Hela (57.14 ± 0.15 μmol L^{-1})	
				33	anti-insect activity against newly hatched larvae of Helicoverpa armigera Hubner (50–200 μgmL^{-1})	
7	*Fusarium* sp. 2ST2	healthy leaves of *Kandelia candel*	the South China Sea, Dong Zhai Harbor Mangrove Nature Reserve Area, Hainan Province, China	**34**	A549 (8.7 μmol L^{-1})	[37]
				35	A550 (4.38 μmol L^{-1})	
				36		
				37		
				38		
				39		
				40		
				41		
8	*Aspergillus fumigatus* HQD24	the flower of the Chinese mangrove plant *Rhizophora mucronata*		**42**	decreased ACAT2 inhibitory activity (12.0 mmol L^{-1})	[38]

Table 1. *Cont.*

Sr. No.	Endophytic Fungus	Host Plant(s)	Sources	Compound Isolated	Bioactivity and IC_{50}/EC_{50}/Inhibition	Reference
9	*Nigrospora camelliae-sinensis* S30	mangrove *Lumnitzera littorea*		**43**		[39]
				44		
10	*Penicillium crustosum* SCNU-F0006	*Acanthus ilicifolius* L. mangrove plant	the Yangjiang Mangrove Nature Reserve in Guangdong Province	**45**	RAW 264.7 cells (above 50 μmol L^{-1}) anti-inflammatory activity (42.22 ± 2.26 μmol L^{-1}) DPPH radical scavenging activity (180.2 μmol L^{-1}) antimicrobial activities against *Bacillus subtilis*, *Penicillium italicum*, and *Pseudomonas aeruginosa*	[40]
11	*Diaporthe* sp. ZJHJYZ-1	a fresh leaf of the semi-mangrove plant *Hibiscus tiliaceus* L.	Zhanjiang Mangrove National Nature Reserve in Guangdong Province, China	**46**		[41]
				47		
12	*Penicillium sclerotiorum* ZJHJJ-18	the stems of the mangrove plant *Hibiscus tiliaceus*	the shore of the Zhanjiang Mangrove Nature Reserve in Guangdong Province, China	**48**	inhibit LPS-induced NO production in RAW264.7 macrophage cells	[42]
				49	inhibit LPS-induced NO production in RAW264.8 macrophage cells	
				50	inhibit LPS-induced NO production in RAW264.9 macrophage cells	
				51	inhibit LPS-induced NO production in RAW264.10 macrophage cells	
				52	inhibit LPS-induced NO production in RAW264.11 macrophage cells	
				53	inhibit LPS-induced NO production in RAW264.12 macrophage cells	
				54		
				55		
				56		
13	*Penicillium herquei* JX4	the mangrove *Ceriops tagal*	the South China Sea	**57**	anti-inflammatory activities	[43]
				58	anti-inflammatory activities	
				59	anti-inflammatory activities	
14	*Phomopsis* sp. QYM-13	healthy leaves of *Kandelia candel*	the South China Sea, Dongzhai Harbor Mangrove Nature Reserve Area, Hainan Province, China	**60**		[44]
				61	MDA-MB-435 (4.9–8.2 μmol L^{-1})	
				62		
				63		
				64		
				65		
				66		
				67		
				68		
				69		
				70		
				71		
15	*Daldinia eschscholtzii* KBJYZ-1	the root of *Pluchea indica* Less	Zhanjiang Mangrove National Nature Reserve in Guangdong Province, China	**72**	anti-inflammatory activities (19.3 μmol L^{-1})	[45]
				73		
				74		
				75		
				76	anti-inflammatory activities (12.9 μmol L^{-1})	
16	*Aspergillus sydowii* #2B	the leaves of the mangrove plant *Aricennia marina*		**77**	inhibit the production of nitric oxide (NO) in lipopolysaccharide (LPS)-induced RAW 246.7 cells (40.15 μmol L^{-1})	[46]
				78	VCaP (20.06 ± 2.01 μmol L^{-1})	
17	*Aspergillus fumigatus* SAI12	leaves of mangrove plant *Sonneratia apetala* Buch.-Ham.	Dongzhaigang National Nature Reserve in south China's Hainan Province	**79**		[47]
				80		

Table 1. *Cont.*

Sr. No.	Endophytic Fungus	Host Plant(s)	Sources	Compound Isolated	Bioactivity and IC_{50}/EC_{50}/Inhibition	Reference
18	*Aspergillus* sp. GXNU-A9	a leaf of mangrove *Acanthus ilicifolius* L.	Qinzhou City, China	**81**	moderate inhibitory activity against nitric oxide (NO) production anti-inflammatory activity	[48]
19	*Aspergillus* sp. GXNU-Y65	fresh fruit of the mangrove plant *Kandelia candel*	Beihai, China	**82**		[49]
				83		
				84	anti-nonalcoholic steatohepatitis activity	
				85		
				86		
				87		
				88		
				89		
				90		
20	*Aspergillus* sp. GXIMD00016	Fresh leaves of *Kandelia candel*	Beihai Golden Bay Mangrove Reserve	**91**		[50]
21	*Aspergillus* QG1a	the mangrove *Kandelia candel*	the seaside of Qinzhou, Guangxi Province, China	**92**	A549 (59.283 μmol L^{-1}) A2780 (46.197 μmol L^{-1}) MIA PACA-2 (42.664 μmol L^{-1})	[51]
				93	A2780 (6.808 μmol L^{-1}) MIA PACA-2 (15.400 μmol L^{-1})	
22	*Aspergillus* sp. GXNU-4QQY1a	healthy leaves of *Acanthus ilicifolius* L.		**94**	insecticidal activity against citrus psyllids (lethality values of 92.31 ± 6.20%)	[52]
				95	exhibited good insecticidal activity against citrus psyllids (lethality values of 87.80 ± 9.32%)	
23	*Didymella* sp. CYSK-4	a fresh branch of the mangrove plant *Pluchea indica*	Shankou Mangrove Na ture Reserve in Guangxi Province, China	**96**	A549 (11.0 μmol L^{-1})	[53]
				97	A549 (2.8 μmol L^{-1}) KYSE 150 (5.9 μmol L^{-1})	
				98		
				99		
24	*Fusarium. proliferatum* NSD-1	a fresh twig from mangrove plant *Kandelia candel*	a Mangrove of Nansha District of Guangzhou in Guangdong Province, China	**100**	A549 (75.9 ± 10.4 μmol L^{-1}) SW480 (37.5 ± 8.0 μmol L^{-1})	[54]
				101		
				102		
				103	moderate IL-1β inhibitory activity	
				104	A549 (24.9 ± 10.1 μmol L^{-1}) SW480 (77.7 ± 3.6 μmol L^{-1})	
25	*Penicillium verruculosum* TGM14	mangrove *Xylocarpus granatum* Koenig	the South China Sea	**105**		[55]
26	*Penicillium* sp. GXIMD 03001	the rhizophoraceous mangrove *Kandelia candel*	the Beibu Gulf	**106**		[56]
				107		
27	*Amorosia* sp. SCSIO 41026	the leaf of *Avicennia marina* (Forsk.) Vierh.	the mangrove wetland in Zhanjiang, Guangdong province, China	**108**	inhibit LPS-induced NO production in RAW264.7 macrophage cells	[57]
				109		
				110		
				111	inhibit LPS-induced NO production in RAW264.7 macrophage cells	
				112		

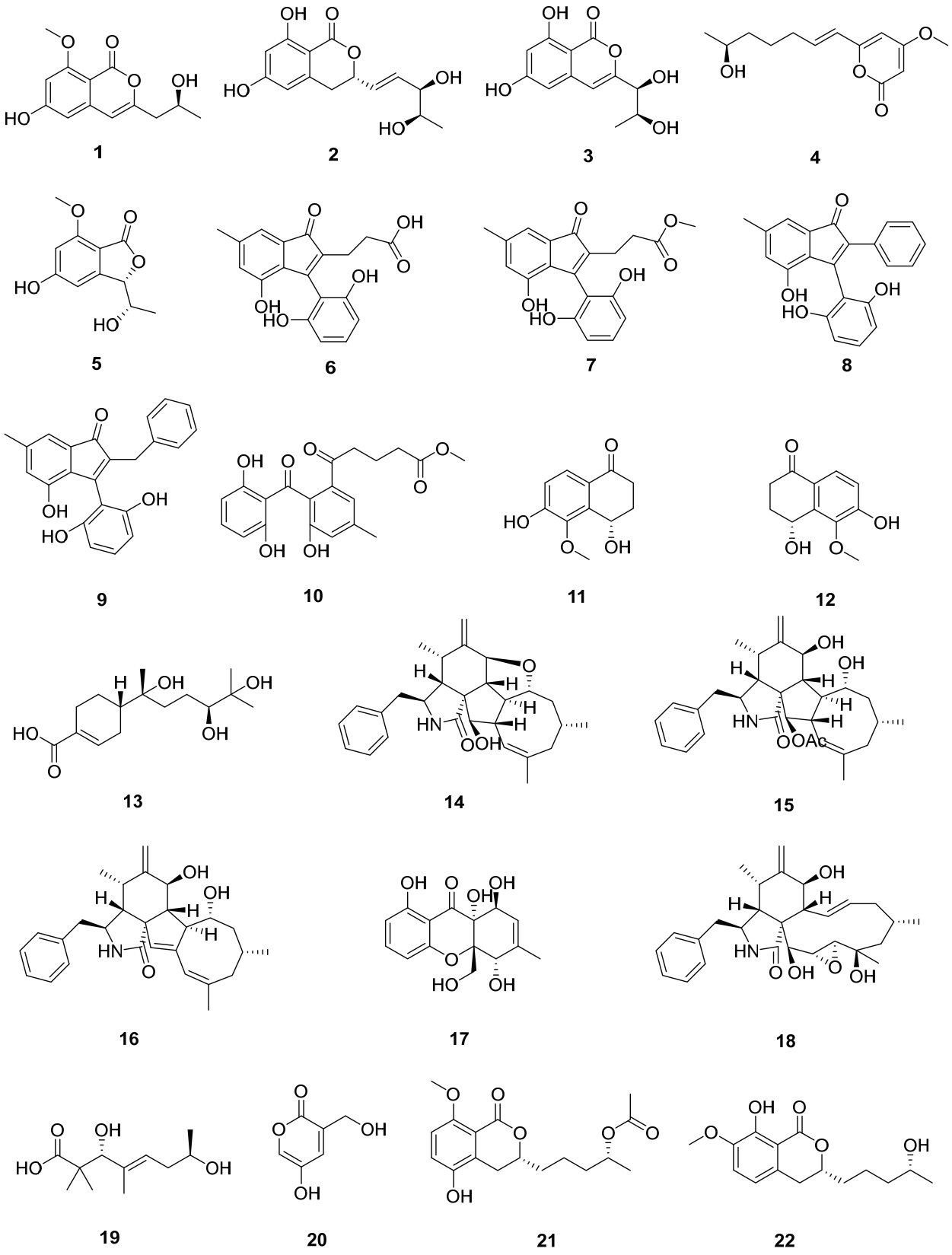

Figure 3. *Cont.*

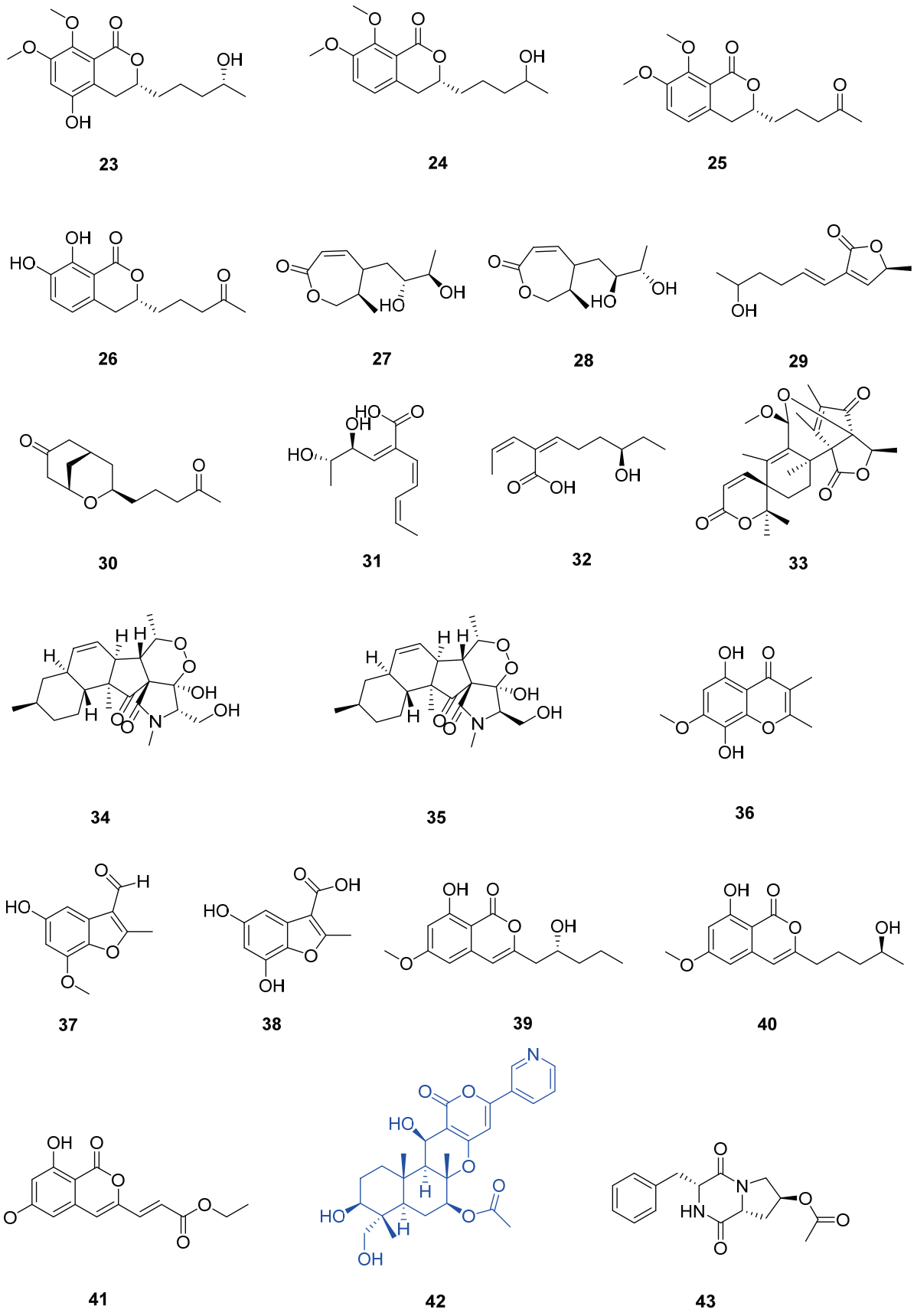

Figure 3. *Cont.*

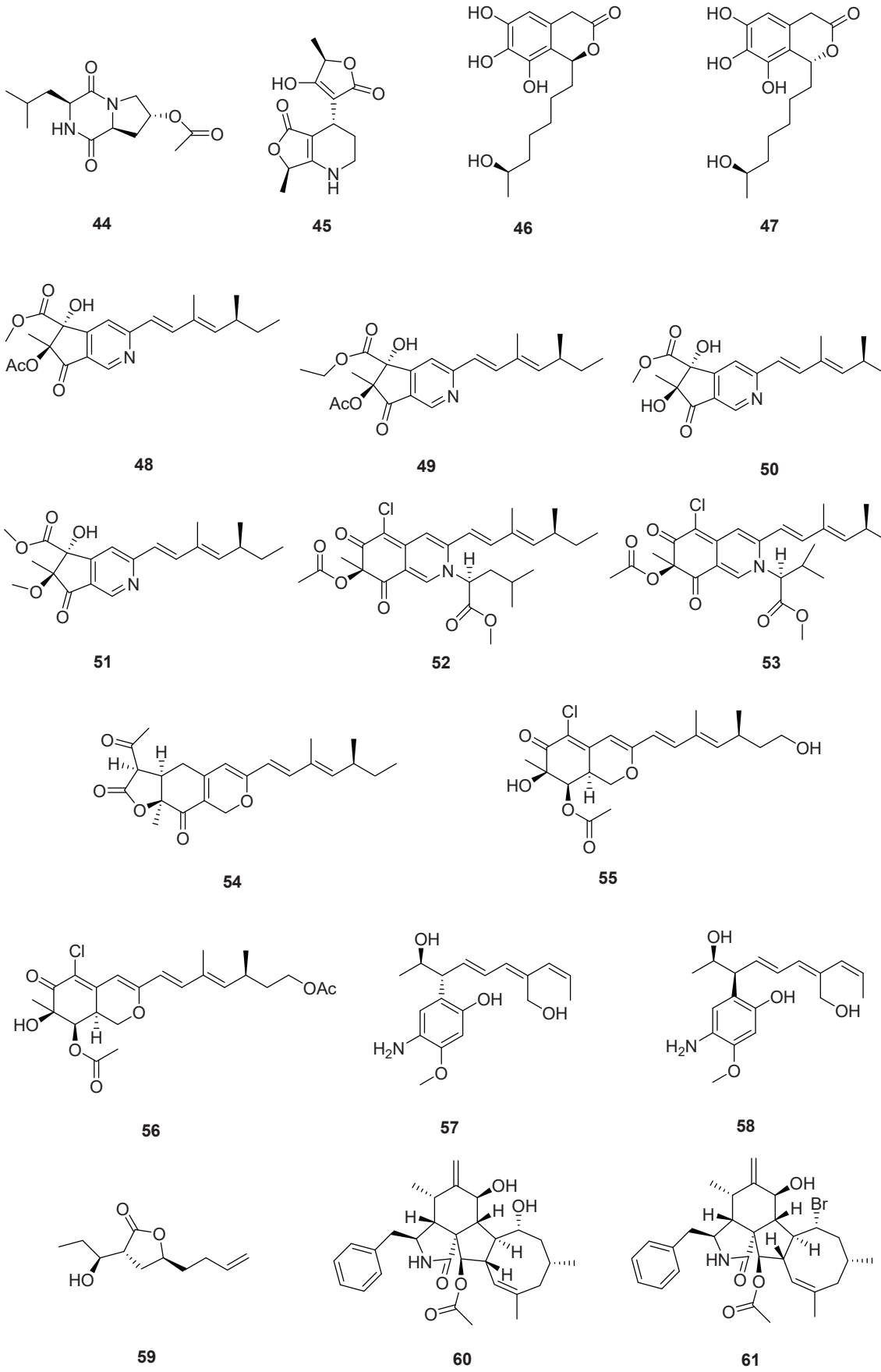

Figure 3. *Cont.*

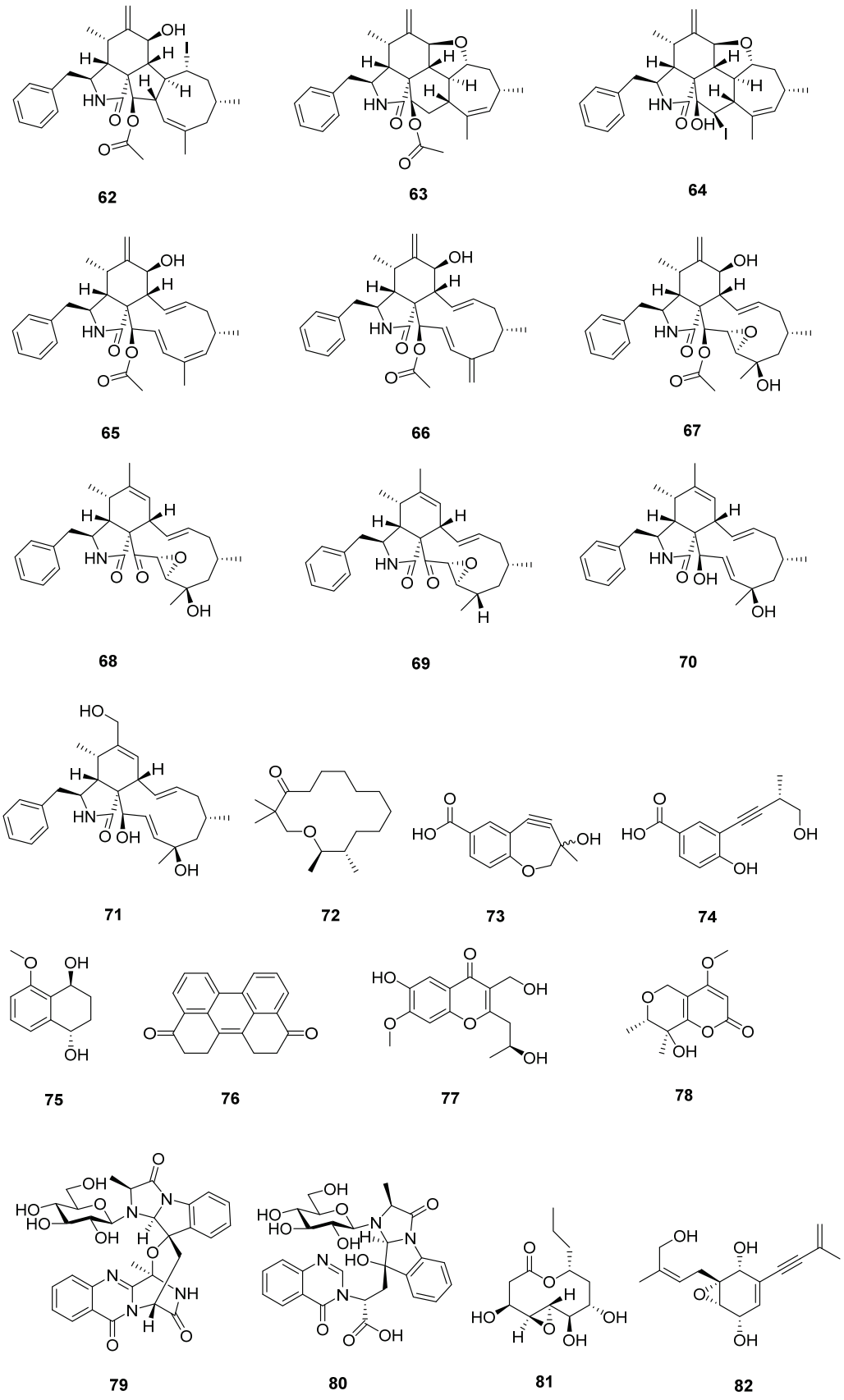

Figure 3. *Cont*.

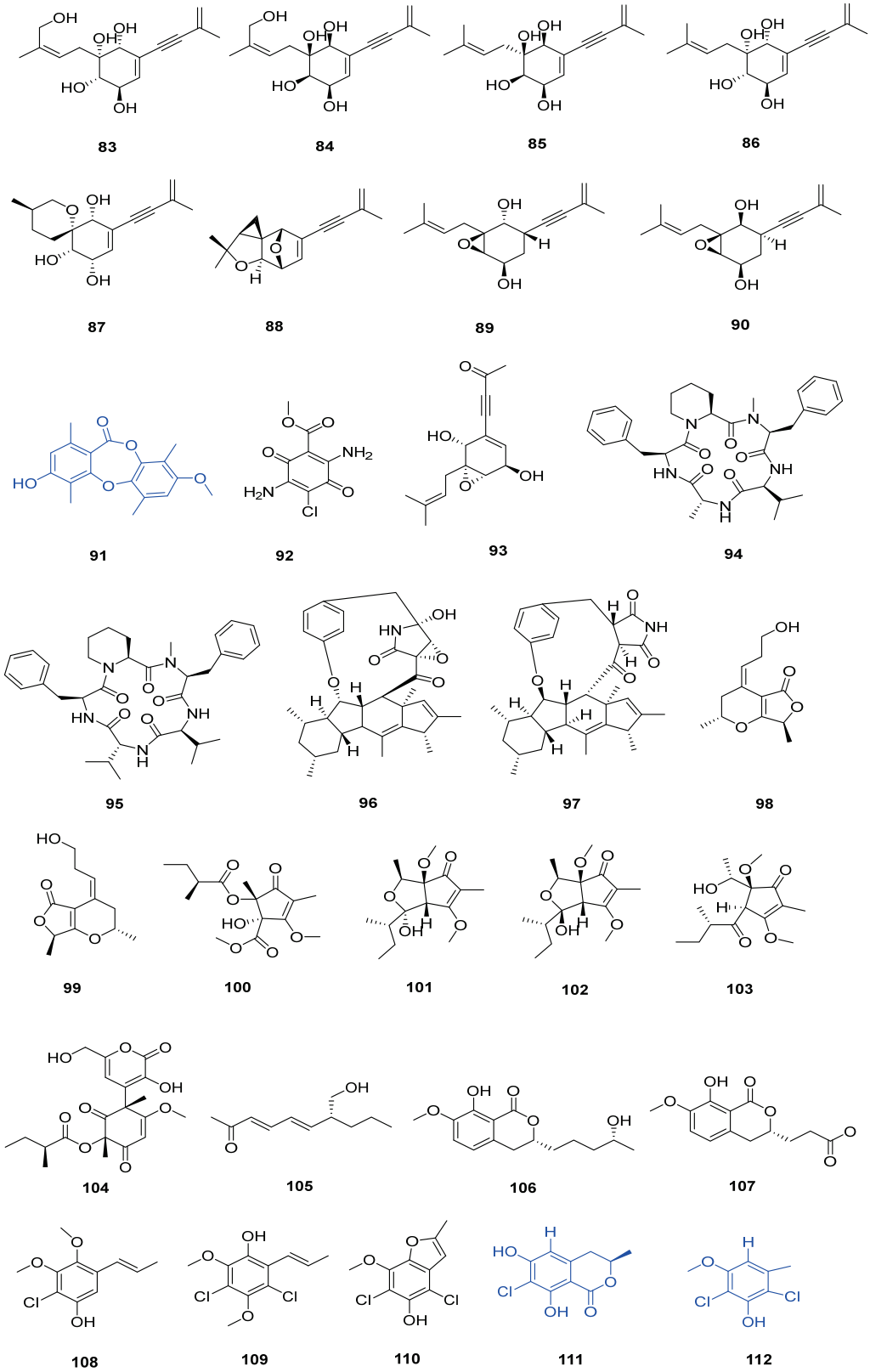

Figure 3. Compounds isolated from endophytic fungi. Note: new compounds are marked in black; the blue ones are new natural products.

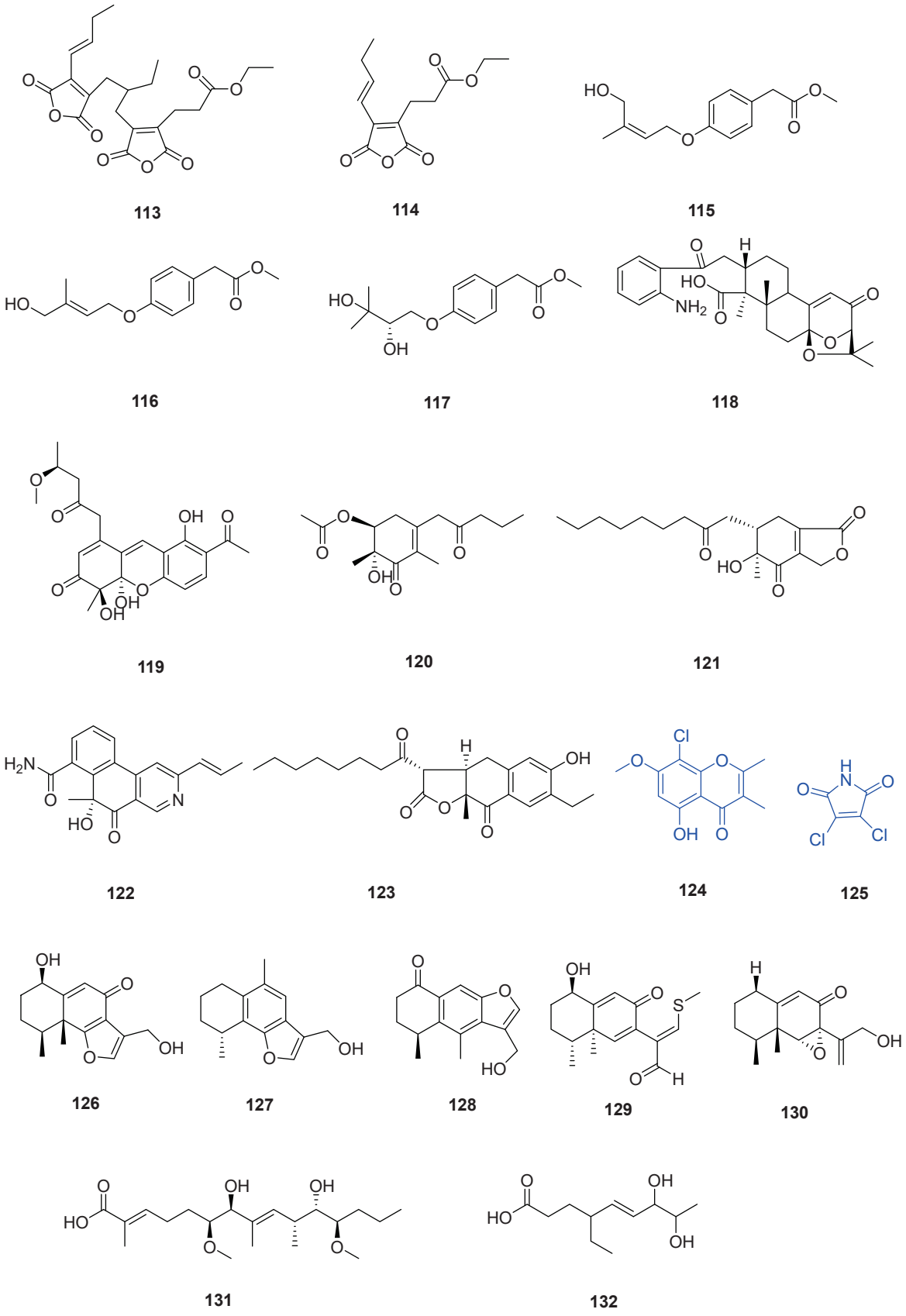

Figure 4. *Cont.*

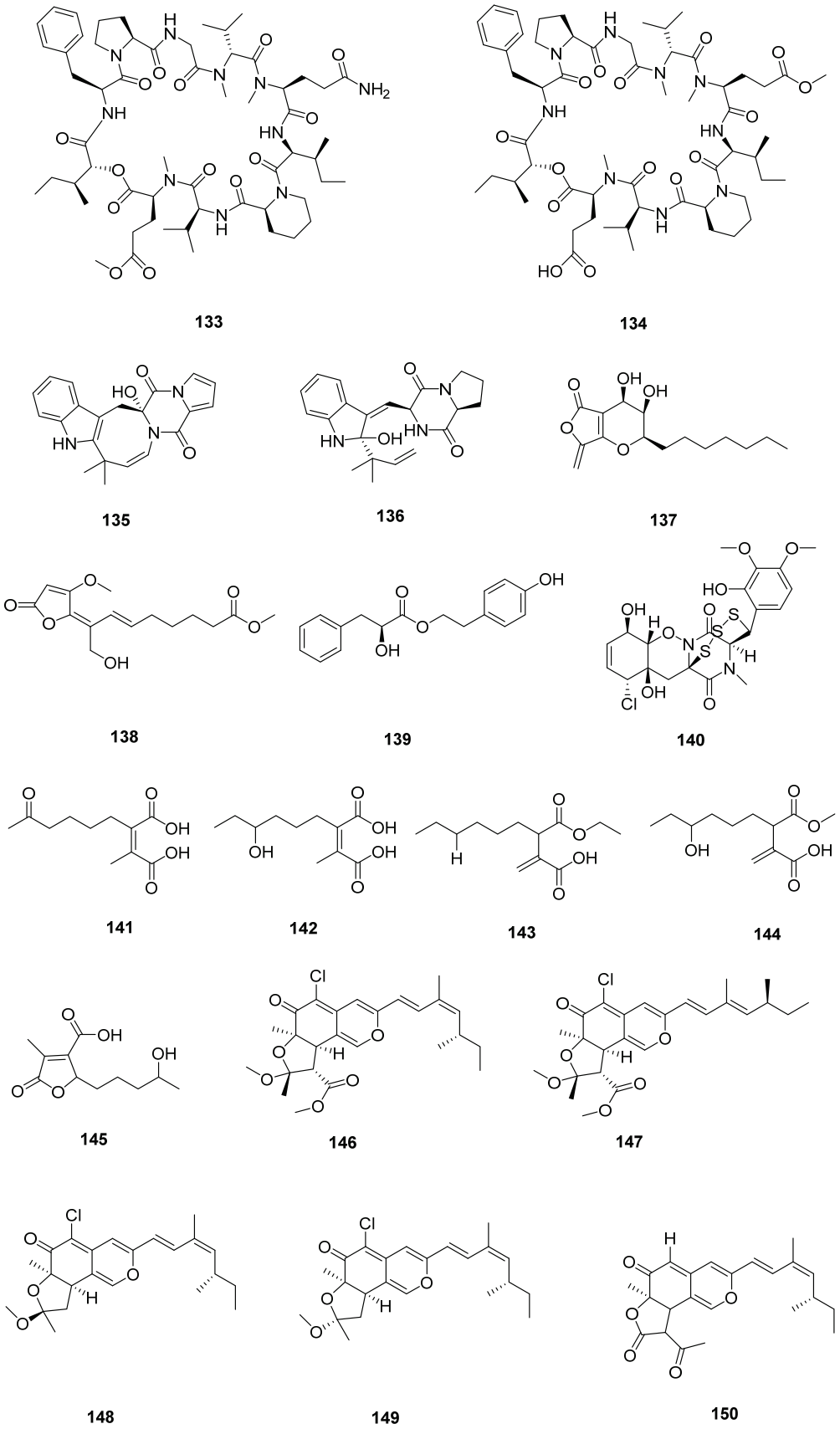

Figure 4. *Cont*.

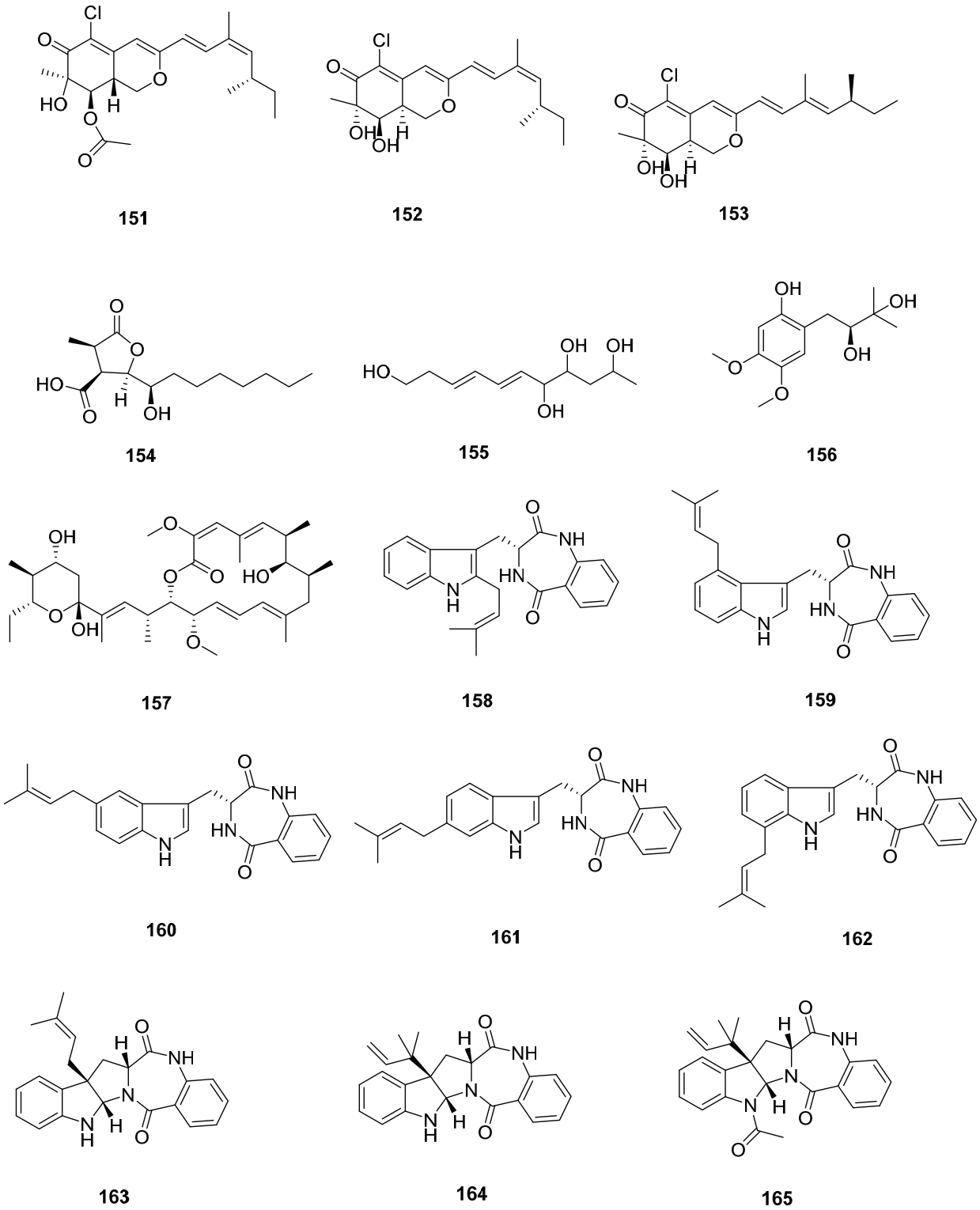

Figure 4. Compounds from other sources. Note: new compounds are marked in black; the blue ones are new natural products.

3. Compounds

Among the 165 new natural products, there are mainly polyketides, nitrogen-containing compounds, halogenated compounds, and terpenoids, including a pair of tetralone enantiomers, a pair of mutually converting epimers and a pair of new enantiomers (+) and

(−) didymetone (among these compounds, some nitrogen-containing and halogenated compounds are also polyketides) (Figure 5).

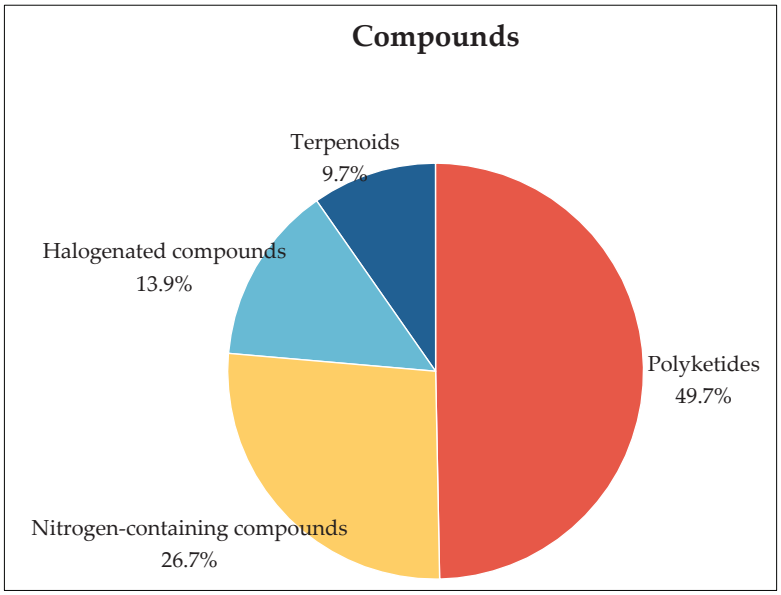

Figure 5. Types of all compounds.

3.1. Polyketides

Polyketides represent a highly diverse group of natural products with structurally intriguing carbon skeletons, which comprise polyphenols, macrolides, polyenes, enediynes, and polyethers [58].

Three new isocoumarins (**1**–**3**) and one new pyrone derivative (**4**) were isolated from the ethyl acetate extract of the fermentation broth of the mangrove endophytic fungus *Phomopsis* sp. DHS-11 [28]. And a novel benzofuranone compound (**5**) was discovered for the first time from its fermented extract [29]. Seven new polyketides, including four indenone derivatives, cytoindenones A–C (**6**, **8**–**9**), 3′-methoxycytoindenone A (**7**), a benzophenone derivative, cytorhizophin J (**10**), and a pair of tetralone enantiomers, (±)-4,6-dihydroxy-5-methoxy-α-tetralone (**11** and **12**) were obtained from the endophytic fungus *Cytospora heveae* NSHSJ-2 isolated from the fresh stem of the mangrove plant *Sonneratia caseolaris* [30]. A mangrove endophytic fungus *Phomopsis asparagi* DHS-48 was found to be particularly productive, and one new compound named phaseolorin J (**17**) was isolated from the culture treated with sodium butyrate [32,33]. Two new polyketides, pestalotiopin B (**19**) and pestalotiopyrone N (**10**) were obtained from the ethyl acetate extracts of the rice solid cultures of the mangrove endophytic fungus *Pestalotiopsis* sp. HQD-6 [34]. Six new isocoumarin derivatives talaromarins A–F (**21**–**26**) were isolated from the mangrove-derived fungus *Talaromyces flavus* TGGP35 [35]. Six new polyketides, which included three new lactones (talarotones A–C) (**27**–**29**), one new polyketide (talarotide A) (**30**), and two new polyenes (talaroyenes A and B) (**31**, **32**), were isolated from the mangrove-derived fungus *Talaromyces flavus* TGGP35 [36]. One new chromone fusarimone A (**36**), two new benzofurans fusarifurans A (**37**) and B (**38**), and three new isocoumarins fusarimarins A–C (**39**–**41**) were isolated from the mangrove endophytic fungus *Fusarium* sp. 2ST2 [37]. Two new octaketides, cytosporones W (**46**) and X (**47**), were isolated from the mangrove endophytic fungus *Diaporthe* sp. ZJHJYZ-1. Compounds **46** and **47** were a pair of epimers, whose configuration of C-1 could mutually convert, causing racemization of the lactone ring [41]. One undescribed azaphilone derivative (**54**) was obtained and identified from the fermented rice cultures of a mangrove endophytic fungus *Penicillium sclerotiorum* ZJHJJ-18 [42]. One new long-chain polyene pinophol G (**59**) was obtained from EtOAc extract of the mangrove-derived fungus *Penicillium herquei* JX4 [43]. Five

new polyketide derivatives, eschscholin B (**72**), dalditone A and B (**73** and **74**), (1R,4R)-5-methoxy-1,2,3,4-tetrahydronaphthalene-1,4-dio (**75**), and daldilene A (**76**), were isolated from the mangrove endophytic fungus *Daldinia eschscholtzii* KBJYZ-1 [45]. Two new pyrone derivatives, 2-(12S-hydroxypropyl)-3-hydroxy-methyl-6-hydroxy-7-methoxychromone (**77**) and (±)-pyrenocine S (**78**), were obtained from the mangrove endophytic fungus *Aspergillus sydowii* #2B [46]. A new lactone, asperlactone A (**81**), was isolated from the mangrove endophytic fungus *Aspergillus* sp. GXNU-A9 [48]. The mangrove endophytic fungus *Aspergillus* sp. GXIMD00016 was fermented by using rice medium. The metabolites were isolated by chromatography technology and 2,7-didechlorovicanic (**91**) were obtained [50]. A new diisoprenyl-cyclohexene-type meroterpenoid, biscognienyne M (**93**), was isolated from the mangrove endophytic fungus *Aspergillus* QG1a [51]. A pair of new enantiomers (+) and (−) didymetone (**98** and **99**) were purified from the mangrove endophytic fungus *Didymella* sp. CYSK-4 [53]. Five undescribed polyketides, including two talaketide derivatives (**100** and **101**), two asperpentenone derivatives (**102** and **103**), and one phomaligol derivative (**104**), were obtained from the mangrove endophytic fungus *Fusarium proliferatum* NSD-1 [54]. A new compound, named penicillquei C (**105**), was isolated from the fermentation broth of the mangrove-derived fungus *Penicillium verruculosum* TGM14 [55]. Two new isocoumarins named peniciisocoumarins I and J (**106** and **107**) were obtained from *Penicillium* sp. GXIMD 03001, an endophytic fungus derived from the rhizophoraceous mangrove *Kandelia candel* [56].

To discover bioactive natural products from mangrove sediment-derived microbes, a chemical investigation of the two Beibu Gulf-derived fungal strains, *Talaromyces* sp. SCSIO 41050 and *Penicillium* sp. SCSIO 41411, led to the isolation of 23 natural products. Five of them were identified as new ones, including two polyketide derivatives with unusual acid anhydride moieties named cordyanhydride A ethyl ester (**113**) and maleicanhydridane (**114**), and three hydroxyphenylacetic acid derivatives named stachylines H–J (**115**–**117**) [59]. Through the thorough investigation into the chemical constituents of *M. purpureus* wmd2424, five previously undescribed compounds, monascuspurins A–E (**119**–**123**), were isolated from the EtOAc extract of the mangrove-derived fungus *Monascus purpureus* wmd2424 cultured in RGY medium [60]. Two previously undescribed linear polyketides **131**–**132** were identified by spectroscopic methods from the culture broth of the mangrove-derived actinomycete *Streptomyces* sp. WHUA03072 [61]. Three new polyketides penicinones A–C (**137**–**139**) were isolated and identified from the culture extract of the mangrove-derived fungus *Penicillium* sp [62]. Five new alkane derivatives (**141**–**145**) were isolated from the mangrove sediment-derived fungus *Penicillium ludwigii* SCSIO 41408 [63]. Ochlephilone **150** was isolated from the culture broth of the mangrove-derived fungus *Penicillium sclerotiorum* HY5 [64]. Chemical investigation of the fungus *Xylariaceae* sp. SCSIO41212 has led to the isolation of two new compounds, xylaolide B (**154**) and xylaolide C (**155**) [65]. A novel tetrasubstituted benzene derivative peniprenylphenol A (**156**) was isolated from a scaled-up culture of the Indonesian mangrove sediment-derived fungus *Penicillium chrysogenum* ZZ1151 in rice medium [66]. An active compound **157** was isolated from the fermentation broth of *Streptomyces* sp. MCCG218 [67].

3.2. Nitrogen-Containing Compounds

Nitrogen-containing compounds are core parts not only of natural and synthetic medicines but also of biologically active compounds including natural products [68].

Three new cytochalasins, phomoparagins A–C (**14**–**16**), were isolated from *Phomopsis asparagi* DHS-48, a mangrove-derived endophytic fungus [32,33]. Compound phomoparagin D (**18**) was isolated from the culture treated with sodium butyrate of the fungus [32,33]. Two new 3-decalinoyltetramic acid derivatives with peroxide bridge fusarisetins E (**34**) and F (**35**) were isolated from the mangrove endophytic fungus *Fusarium* sp. 2ST2 [37]. Chemical investigation of endophytic fungus *Aspergillus fumigatus* HQD24, isolated from the flower of *Rhizophora mucronata*, led to the isolation of eight alkaloids, in which compound **42** was known as a synthetic product and isolated as a natural product for the first

time [38]. Two new 2,5-diketopiperazines derivatives (**43**–**44**) were isolated from a culture broth of an endophytic fungus *Nigrospora camelliae-sinensis* S30, derived from mangrove *Lumnitzera littorea* [39]. One previously undescribed alkaloid, named penifuranone A (**45**), was isolated from the mangrove endophytic fungus *Penicillium crustosum* SCNU-F0006 [40]. Four undescribed azaphilone derivatives, sclerazaphilones A–D (**48**–**51**) were obtained and identified from the fermented rice cultures of a mangrove endophytic fungus *Penicillium sclerotiorum* ZJHJJ-18 [42]. One new epimer pair of long-chain polyenes penicilqueis E (**57**) and F (**58**) was obtained from EtOAc extract of the mangrove-derived fungus *Penicillium herquei* JX4 [43]. Nine new cytochalasins (**60**, **63**, **65**–**71**) were isolated from the mangrove-derived fungus *Phomopsis* sp. QYM-13 [44]. Two new glucosidated indole-containing quinazoline alkaloids designated fumigatosides G (**79**) and H (**80**) were isolated from the mangrove-derived fungus *Aspergillus fumigatus* SAl12 [47]. An investigation on bioactive metabolites from the mangrove endophytic fungus *Aspergillus* sp. GXNU-4QQY1a led to the isolation of two undescribed cyclic peptides, guaspertide A (**94**) and guaspertide B (**95**) [52]. Two new 12- or 13-membered-ring macrocyclic alkaloids ascomylactam D and E (**96**, **97**) were purified from the mangrove endophytic fungus *Didymella* sp. CYSK-4 [53].

An unprecedented di-*seco*-indole diterpenoid, peniditerpenoid A (**118**), was obtained from the mangrove-sediment-derived fungus *Penicillium* sp. SCSIO 41411 [69]. Chemical examination of the fermented broth of the mangrove-derived fungus *Phaeosphaeriopsis* sp. S296 resulted in the isolation of two new cyclodecadepsipeptides, namely phaeosphamides A (**133**) and B (**134**) [70]. Two new prenylated indole diketopiperazine alkaloids (PIDAs) penicamides A and B (**135** and **136**) were isolated and identified from the culture extract of the mangrove-derived fungus *Penicillium* sp. [62]. Four new alkaloid compounds asperkaloids A–D (**158**–**161**) and four new indole-benzodiazepine-2,5-dione derivatives asperdinones E–H (**162**–**165**) were isolated from the culture extracts of the mangrove-derived fungus *Aspergillus spinosus* WHUF0344 [71].

3.3. Terpenoids

Terpenoids are the most abundant class of compounds in natural substances. There are many terpenoids with strong physiological or biological activity that have been used in clinical practice, and the well-known anti-malarial drug artemisinin and the antitumor drug paclitaxel belong to this family. At the same time, they are also an important class of natural flavors, which are indispensable raw materials for the cosmetics and food industries.

A new polychiral bisabolane sesquiterpene, bisabolanoic acid A (**13**), was isolated from the mangrove-derived fungus *Colletotrichum* sp. SCSIO KcB3–2 [31]. One new meroterpenoid (talaropenoid A) (**33**) was isolated from the mangrove-derived fungus *Talaromyces flavus* TGGP35 [36]. Nine previously undescribed diisoprenyl-cyclohexene-type meroterpenoids, aspergienynes A–I (**82**–**90**), were obtained from the mangrove endophytic fungal strain *Aspergillus* sp. GXNU-Y65 [49].

Five new sesquiterpenoids, citreobenzofuran D–F (**126**–**128**) and phomenone A–B (**129**–**130**), were isolated from the culture of the mangrove-derived fungus *Penicillium* sp. HDN13-494 [72].

3.4. Halogenated Compounds

Marine halogenated compounds comprise a varied assembly of compounds, ranging from peptides, polyketides, indoles, terpenes, acetogenins, and phenols to volatile halogenated hydrocarbons [73]. Halogenation often provides these compounds with interesting key features [74].

Three new chlorinated compounds, including two propenylphenol derivatives, chlorophenol A and B (**108** and **109**), and one benzofuran derivative, chlorophenol C (**110**), were isolated from the mangrove endophytic fungus *Amorosia* sp. SCSIO 41026. 7-Chloro-3,4-dihydro-6,8-dihydroxy-3-methylisocoumarine (**111**) and 2,4-dichloro-3-hydroxy-5-methoxytoluene (**112**) were obtained as new natural products [57]. Compounds **52**, **53**, **55**, and **56** were obtained and identified from the fermented rice cultures of a mangrove endophytic

fungus *Penicillium sclerotiorum* ZJHJJ-18 [42]. One brominated (**61**) and two iodinated cytochalasins (**62** and **64**) were isolated from the mangrove-derived fungus *Phomopsis* sp. QYM-13 treated with 3% NaBr or 3% KI in potato liquid medium [45]. A new benzoquinone, guxiumasperone A (**92**), was isolated from the mangrove endophytic fungus *Aspergillus* QG1a [51].

Two new chlorinated metabolites, 8-chlorine-5-hydroxy-2,3-dimethyl-7-methoxychromone (**124**) and 3,4-dichloro-1H-pyrrole-2,5-dione (**125**), were isolated from the mangrove sediment-derived fungus *Mollisia* sp. SCSIO41409 [75]. A new trithiodiketopiperazine derivative, adametizine C (**140**), was isolated from the mangrove sediment-derived fungus *Penicillium ludwigii* SCSIO 41408 [63]. Chlorinated compounds **146**–**149** and **151**–**153** were isolated from the culture broth of the mangrove-derived fungus, *Penicillium sclerotiorum* HY5, by various chromatographic methods [64].

4. Bioactivity

Natural products have been relevant sources for drug discovery and the development of medicines since ancient times. Newman and Cragg showed that from January 1981 to September 2019, at least 1881 new drugs were approved worldwide for the treatment of all types of diseases, and among them, 75.38% (1418) were derived from natural products [76,77]. Among the 165 compounds mentioned in this paper, 75 compounds (45.5%) had biological activity, including cytotoxicity, antibacterial activity, anti-inflammatory activity, antioxidant activity, and other activities (active compounds here refer to compounds that are specifically active in the articles reviewed, and some of the weakly active compounds are not counted). Cytotoxic compounds accounted for 37.3% of the active compounds and 17% of the total compounds (Figure 6). It is worth mentioning that compounds **45**, **108**, **109**, **120**, **135**, and **138** have multiple activities at the same time [40,59,63,75].

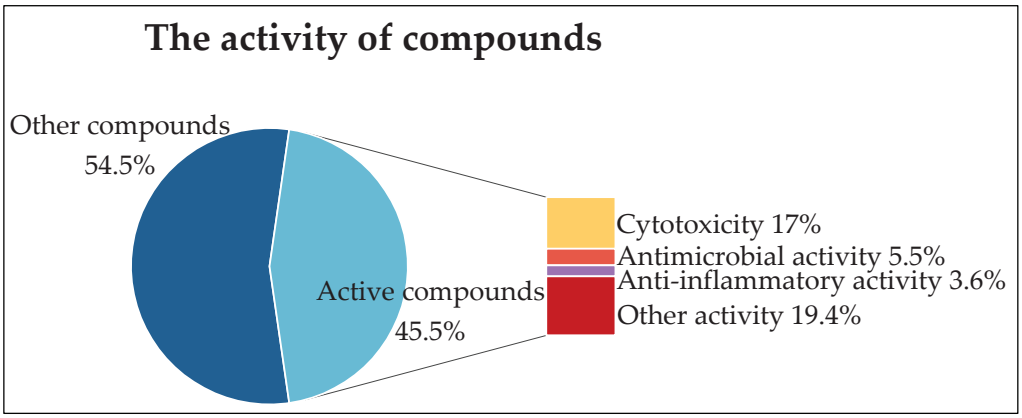

Figure 6. The activity of compounds.

The activity of endophytic fungal-derived compounds **1**–**112** is shown in Table 1. Then, the activity of other compounds (**113**–**165**) will be discussed next.

A variety of bioactive screens revealed polyketide derivative (**113**) to have obvious antifungal activity at 10 μmol L^{-1}, exhibiting obvious inhibition against phosphodiesterase 4 (PDE4) with an inhibitory rate of 49.7%, and **114** displayed moderate cytotoxicity against cell lines A549 and WPMY-1. Compounds **115** and **116** showed potential to inhibit acetylcholinesterase (AChE) by an enzyme activity test, as well as in silico docking analysis [59]. Peniditerpenoid A (**118**) inhibited lipopolysaccharide-induced NF-κB with an IC_{50} value of 11 μmol L^{-1} and further effectively prevented RANKL-induced osteoclast differentiation in bone marrow macrophages [69]. Compounds (**121**–**123**) possessed mild antifungal activity against *Aspergillus niger*, *Penicillium italicum*, *Candida albicans*, and *Saccharomyces cerevisiae* [60]. Compound **125** showed antimicrobial activities against several pathogenic fungi and bacteria, and antiproliferative activities against two human prostate cancer cell lines (IC_{50} values 2.77 to 9.60 μmol L^{-1}) [63]. Compound phomenone B (**130**) showed

moderate activity against *Bacillus subtilis*, with an MIC value of 6.25 μmol L^{-1} [72]. Compound **133** showed inhibitory activities against tumor cell lines of AGS, BEL-7402, HepG2, B16, and BIU87 with IC_{50} values ranging from 5.14 to 66.38 μmol L^{-1} [70]. Compound **137** displayed potent cytotoxicity against murine melanoma (B16) cells, human breast adenocarcinoma (MCF-7) cells, and human hepatocellular carcinoma (HepG2) cells at 50.0 μmol L^{-1} with inhibitory ratios of 82.7%, 75.1%, and 95.9%, respectively [62]. In a variety of bioactivity screenings, compound **140** showed cytotoxicity against prostate cancer cell line 22Rv1. Adametizine C (**140**), with the strongest inhibitory activity against RANKL-induced osteoclast differentiation in bone marrow macrophage cells at 10 μmol L^{-1}, was suggested to be the promising lead compound for the treatment of osteoclast-related diseases [63]. Compounds **149** and **150** exhibited potent phytotoxicity against the growth of radicle and plumule on *Amaranthus retroflexus* L., with EC_{50} values ranging from 234.87 to 320.84 μmol L^{-1} [64]. New peniprenylphenol A (**156**) was found to have antimicrobial activity against human pathogenic methicillin-resistant *Staphylococcus aureus* (MRSA), *Escherichia coli*, and *Candida albicans* with MIC values of 6, 13, and 13μg mL^{-1}, respectively [66]. Compound **157** showed strong cell proliferation inhibitory activity against nasopharyngeal carcinoma cell lines TW03 and 5-8F, and the semi-inhibitory concentration (half-inhibitory concentration, IC_{50}) was 2.7 μmol L^{-1} and 9.2 μmol L^{-1}, respectively [67]. Compounds **162**, **163,** and **165** exhibited moderate inhibitory effects against α-glucosidase with IC_{50} values in the range of 24.65–312.25 μmol L^{-1} [71].

Among these compounds, compounds **50**–**52** exhibited stronger inhibitory effects on LPS-induced NO production in RAW264.7 macrophage cells than that of the positive control indomethacin and had no toxicity towards macrophage RAW 264.7 at 50 μmol L^{-1} [42]. This means azaphilone derivatives from mangrove fungi have a good chance of contributing to the discovery of potential anti-inflammatory agents. Compound **113** showed obvious antifungal activities, especially against *F. graminearum*, *F. oxysporum*, and *R. solani*, with MIC values of 6.25–12.5 μg mL^{-1}, having the potential to be further developed into antifungal drugs [59]. Compounds **3**, **18**, **34**, **35**, **61**, **92**, **93**, **97**, **125**, and **137** have significant cytotoxic activity against selected tumor cells and have potential to be further developed into anticancer drugs [28,33,37,44,51,53,62,75], which deserve further attention. Compound **133** demonstrated highly selective inhibitory action towards AGS cells, specifically by arresting their cell cycle progression at the G2 phase and triggering apoptosis in a precise, dose-responsive manner [70]. This finding underscores the potential of Compound **133** as a promising lead candidate for the development of therapeutic strategies aimed at treating gastric adenocarcinoma.

4.1. Cytotoxicity

Cancer is the leading cause of death and an important barrier to increasing life expectancy around the world [78]. Currently, there is a great demand for new oncological therapies that reduce or do not cause severe adverse effects to patients, providing an improvement in quality of life. In this context, several studies seek new antitumor molecules from natural sources, attempting to reduce treatment costs, increase specificity, and decrease the side effects [79]. Various tumor cell lines from human and animal sources have been useful and applied for in vitro cytotoxicity and in vivo studies of the anticancer potential of natural products, whether by the academy or by pharmaceutical companies [76]. In this paper, 28 compounds showed cytotoxicity, accounting for 17% of the total compounds.

4.2. Antimicrobial Activity

Antimicrobial activity refers to the ability of a drug to inhibit or kill pathogenic microorganisms to treat infectious diseases. Antimicrobials include antibiotics, antifungals, and antivirals that kill microorganisms or inhibit their growth and reproduction by blocking key physiological functions of bacteria, fungi, or viruses. Compounds **45**, **114**–**118**, and **125** showed moderate antimicrobial activity [40,60].

4.3. Anti-Inflammatory Activity

Inflammation is an innate immunity that is the biological response of human tissues to various harmful stimuli. It is known to be a normal bodily defense mechanism that is activated in the event of injury, exposure to pollutants, radioactive materials, poisons, and allergens, as well as infection by various substances such as microorganisms, viruses, etc. Natural products play an important role in human health in the prevention and treatment of inflammation. Compounds **45**, **57**–**59**, **72**, **76**, and **81** showed anti-inflammatory activity [40,43,45,48].

4.4. Antioxidant Activity

Because of restriction on synthetic antioxidants due to their carcinogenicity, interest has increased considerably in finding naturally occurring antioxidants for use in foods, cosmetics, or medicine materials to replace the synthetic ones [80]. Among them, compounds **6**–**10**, **26**, and **31** had significant antioxidant activity [30,35,36].

5. Discussion

The microbial diversity within mangrove ecosystems is exceptionally rich and varied, harboring significant biotechnological potential. In a comprehensive review spanning 2021 to the present, we have examined the discovery of 165 novel secondary metabolites derived from 41 distinct microbial strains. Over the past four years, this research has unveiled 82 polyketides, 44 nitrogen-containing compounds, 16 terpenoids, and 23 halogenated compounds. Notably, some of the halogenated and nitrogen-containing compounds are also polyketides. Thus, polyketides dominate the metabolic landscape of mangrove-derived strains, while halogenated compounds also constitute a notable proportion. In terms of functional activity, nearly half of these secondary metabolites exhibit one or more biological activities, underscoring their potential as a foundation and roadmap for the discovery of novel drug leads.

However, our observation reveals that in recent years, there has been a notable surge in research endeavors focusing on the secondary metabolites of fungi, whereas a comparative scarcity of studies has emerged concerning the secondary metabolites of actinomycetes and bacteria. Given this disparity, it is prudent to redirect our attention and invest more efforts towards the exploration of actinomycetes and bacteria, as their secondary metabolites hold immense potential for scientific discovery and practical applications.

Over the past four years, we have witnessed a notable trend in the discovery of new natural products. In 2021, six related articles reported a total of nine novel natural products. This number significantly increased in 2022, with 22 articles yielding an impressive 90 new natural products. In 2023, while still substantial, the number of articles declined to 11, documenting 46 new natural products. From January to May 2024, we observed five articles contributing 20 new natural products (exclusively counting articles dedicated to the discovery of novel natural products). This analysis highlights that 2022 witnessed the highest number of new natural products discovered, closely followed by 2023 (as depicted in Figure 7). One plausible explanation for this surge in 2022 could be attributed to the outbreak of the pandemic, which restricted human mobility and activities, potentially allowing researchers to dedicate more time and energy to their research endeavors, ultimately leading to a proliferation of publications.

With the swift advancements in synthetic biology technologies, including genome mining and enzyme catalysis, researchers are empowered with an arsenal of tools. These tools facilitate computational excavation of genetic data, enabling seamless correlations with known secondary metabolites, and a wealth of reviews document their utility and applications [81]. Furthermore, the incorporation of enzymes in natural product synthesis holds immense potential to revolutionize and streamline overall synthetic processes [82]. These innovative techniques can be seamlessly integrated into the exploration of mangrove microorganism-derived natural products, thereby accelerating the discovery of marine drugs originating from mangroves.

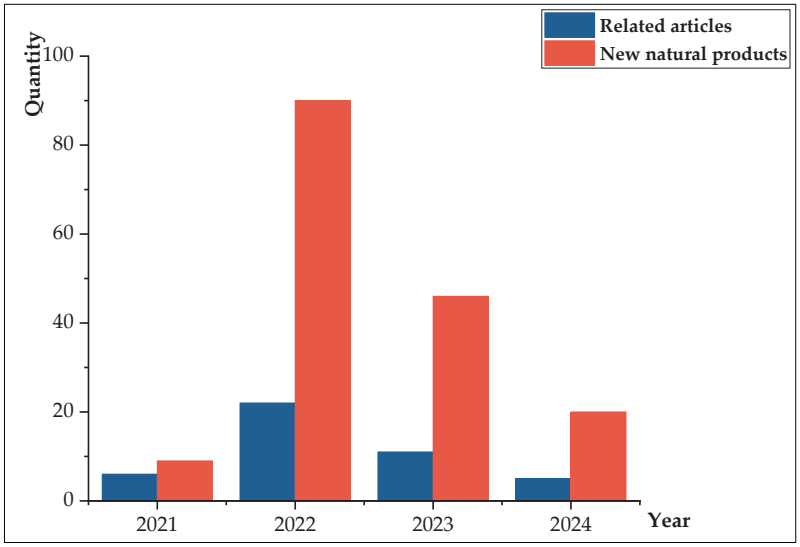

Figure 7. The number of relevant articles and new natural products in recent years.

Natural products have long been instrumental in advancing human health and wellbeing, particularly in the realm of cancer prevention and treatment strategies. With advancements in laboratory technology and enhanced capabilities for strain isolation, researchers are increasingly empowered to extract and purify bioactive compounds. However, to fully harness the therapeutic potential of these compounds, it is imperative to deepen our understanding of their mechanisms of action within living organisms and cells. Furthermore, rigorous research is needed to validate the efficacy of these active compounds as potential novel drugs and lead structures for disease management, thereby fostering the development of innovative therapeutic interventions.

Author Contributions: Y.Y. wrote the manuscript, Z.W. and D.X. collected data, L.Z. revised the manuscript, F.K. and Q.W. supervised and revised the manuscript. All authors have read and agreed to the published version of the manuscript.

Funding: Our project was supported by the Specific Research Project of Guangxi for Research Bases and Talents (AD22035018), Guangxi Natural Science Foundation under Grant (2021GXNSFBA075036), the National Natural Science Foundation of China (No. 82360699), 2021 University-Level Scientific Research Projects of Guangxi Minzu University (2021 MDKJ003), the Talent Scientific Research Initiation Project of Guangxi Minzu University (2021KJQD09), the Xiangsi Lake Youth Innovation Team Project of Guangxi Minzu University (2021RSCXSHQN01), the Natural Science Foundation of Hainan Province (822QN488), and the Hainan Province Clinical Medical Center (QWYH202175).

Conflicts of Interest: The authors declare no conflicts of interest.

References

1. Thatoi, H.; Behera, B.C.; Mishra, R.R.; Dutta, S.K. Biodiversity and biotechnological potential of microorganisms from mangrove ecosystems: A review. *Ann. Microbiol.* **2013**, *63*, 1–19. [CrossRef]
2. Kathiresan, K.; Bingham, B.L. Biology of mangroves and mangrove ecosystems. *Adv. Mar. Biol.* **2001**, *40*, 81–251.
3. Chen, S.; Cai, R.; Liu, Z.; Cui, H.; She, Z. Secondary metabolites from mangrove-associated fungi: Source, chemistry and bioactivities. *Nat. Prod. Rep.* **2022**, *39*, 560–595. [CrossRef]
4. Hastilestari, B.R.; Syahidah, D.; Riyanti, E.I.; Alfiansah, Y.R. Below tropical coastal land ecosystems: Composition and functional diversity of microbial community across mangroves and paddy field. In *Microbiome Drivers of Ecosystem Function*; Academic Press: Cambridge, MA, USA, 2024; pp. 281–309.
5. Pietra, F. Secondary metabolites from marine microorganisms: Bacteria, protozoa, algae and fungi. Achievements and prospects. *Nat. Prod. Rep.* **1997**, *14*, 453–464. [CrossRef]
6. Newman, D.J. Natural products as leads to potential drugs: An old process or the new hope for drug discovery? *J. Med. Chem.* **2008**, *51*, 2589–2599. [CrossRef] [PubMed]

7. Zhao, J.X.; Yue, J.M. Frontier studies on natural products: Moving toward paradigm shifts. *Sci. China Chem.* **2023**, *66*, 928–942. [CrossRef]
8. Hong, K.; Gao, A.-H.; Xie, Q.-Y.; Gao, H.G.; Zhuang, L.; Lin, H.-P.; Yu, H.-P.; Li, J.; Yao, X.-S.; Goodfellow, M.; et al. Actinomycetes for marine drug discovery isolated from mangrove soils and plants in China. *Mar. Drugs* **2009**, *7*, 24–44. [CrossRef]
9. Dias, A.C.F.; Andreote, F.D.; Dini-Andreote, F.; Lacava, P.T.; Sá, A.L.B.; Melo, I.S.; Azevedo, J.L.; Araújo, W.L. Diversity and biotechnological potential of culturable bacteria from Brazilian mangrove sediment. *World J. Microbiol. Biotechnol.* **2009**, *25*, 1305–1311. [CrossRef]
10. Blunt, J.W.; Copp, B.R.; Keyzers, R.A.; Munro, M.H.; Prinsep, M.R. Marine natural products. *Nat. Prod. Rep.* **2014**, *31*, 160–258. [CrossRef]
11. Blunt, J.W.; Copp, B.R.; Keyzers, R.A.; Munro, M.H.; Prinsep, M.R. Marine natural products. *Nat. Prod. Rep.* **2015**, *32*, 116–211. [CrossRef] [PubMed]
12. Blunt, J.W.; Copp, B.R.; Keyzers, R.A.; Munroa, M.H.; Prinsepd, M.R. Natural product reports. *Nat. Prod. Rep.* **2016**, *33*, 382–431. [CrossRef]
13. Blunt, J.W.; Copp, B.R.; Keyzers, R.A.; Munro, M.H.; Prinsep, M.R. Marine natural products. *Nat. Prod. Rep.* **2017**, *34*, 235–294. [CrossRef]
14. Braga, A.F.V.; Rosário, M.S.D.; Gomes, J.B.N.; Monteiro, C.D.A.; Farias, F.A.; Rodrigues Filho, E.; Cantanhede Filho, A.J. Antimicrobial Potential of Soil/Sediment Mangrove Associated Fungi: A Review. *J. Braz. Chem. Soc.* **2024**, *35*, e-20240032. [CrossRef]
15. Wu, M.J.; Xu, B.; Guo, Y.W. Unusual secondary metabolites from the mangrove ecosystems: Structures, bioactivities, chemical, and bio-syntheses. *Mar. Drugs* **2022**, *20*, 535. [CrossRef] [PubMed]
16. Law, J.W.-F.; Law, L.N.-S.; Letchumanan, V.; Tan, L.T.-H.; Wong, S.H.; Chan, K.-G.; Ab Mutalib, N.-S.; Lee, L.-H. Anticancer drug discovery from microbial sources: The unique mangrove streptomycetes. *Molecules* **2020**, *25*, 5365. [CrossRef] [PubMed]
17. Shearer, C.A.; Descals, E.; Kohlmeyer, B.; Kohlmeyer, J.; Marvanová, L.; Padgett, D.; Porter, D.; Raja, H.A.; Schmit, J.P.; Thorton, H.A.; et al. Fungal biodiversity in aquatic habitats. *Biodivers. Conserv.* **2007**, *16*, 49–67. [CrossRef]
18. Assami Doi, S.; Bartelochi Pinto, A.; Carolina Canali, M.; Raquel Polezel, D.; Merguizo Chinellato, R.A.; de Oliveira, A.J.F.C. Density and diversity of filamentous fungi in the water and sediment of Araçá bay in São Sebastião, São Paulo, Brazil. *Biota Neotrop. (Ed. Em Iingles)* **2018**, *18*, e20170416.
19. Thatoi, H.; Behera, B.C.; Mishra, R.R. Ecological role and biotechnological potential of mangrove fungi: A review. *Mycology* **2013**, *4*, 54–71. [CrossRef]
20. Holguin, G.; Vazquez, P.; Bashan, Y. The role of sediment microorganisms in the productivity, conservation, and rehabilitation of mangrove ecosystems: An overview. *Biol. Fertil. Soils* **2001**, *33*, 265–278. [CrossRef]
21. Ali, S.; Khan, A.L.; Ali, L.; Rizvi, T.S.; Khan, S.A.; Hussain, J.; Hamayun, M.; Al-Harrasi, A. Enzyme inhibitory metabolites from endophytic *Penicillium citrinum* isolated from *Boswellia sacra*. *Arch. Microbiol.* **2017**, *199*, 691–700. [CrossRef]
22. Chávez, R.; Fierro, F.; García-Rico, R.O.; Vaca, I. Filamentous fungi from extreme environments as a promising source of novel bioactive secondary metabolites. *Front. Microbiol.* **2015**, *6*, 903. [CrossRef] [PubMed]
23. Eccleston, G.P.; Brooks, P.R.; Kurtböke, D.I. The occurrence of bioactive micromonosporae in aquatic habitats of the Sunshine Coast in Australia. *Mar. Drugs* **2008**, *6*, 243–261. [CrossRef]
24. Huang, H.; Lv, J.; Hu, Y.; Fang, Z.; Zhang, K.; Bao, S. Micromonospora *rifamycinica* sp. nov., a novel actinomycete from mangrove sediment. *Int. J. Syst. Evol. Microbiol.* **2008**, *58*, 17–20. [CrossRef] [PubMed]
25. Chen, B.T.; Liang, Z.Y.; Wen, Z.C.; Guo, Z.K.; Xu, J. Research Progress on Bioactive Products from Mangrove-Derived Endophytic Fungi. *J. Hainan Norm. Univ. (Nat. Sci. Ed.)* **2022**, *39*, 373–385. (In Chinese) [CrossRef]
26. Heinig, U.; Scholz, S.; Jennewein, S. Getting to the bottom of Taxol biosynthesis by fungi. *Fungal Divers.* **2013**, *60*, 161–170. [CrossRef]
27. Nguyen, H.T.; Kim, S.; Yu, N.H.; Park, A.R.; Yoon, H.; Bae, C.; Yeo, J.H.; Kim, I.S.; Kim, J. Antimicrobial activities of an oxygenated cyclohexanone derivative isolated from *Amphirosellinia nigrospora* JS-1675 against various plant pathogenic bacteria and fungi. *J. Appl. Microbiol.* **2019**, *126*, 894–904. [CrossRef] [PubMed]
28. Guo, Z.; Chen, B.; Chen, D.; Deng, X.; Yuan, J.; Zhang, S.; Xiong, Z.; Xu, J. New Isocoumarin and Pyrone Derivatives from the Chinese Mangrove Plant Rhizophora mangle-Associated Fungus *Phomopsis* sp. DHS-11. *Molecules* **2023**, *28*, 3756. [CrossRef]
29. Chen, B.T.; Wu, W.C.; Zhou, D.D.; Deng, X.L.; Zhang, S.Q.; Yuan, J.Z.; Xu, J.; Guo, Z. Bioactive components of endophytic fungi from two Hainan mangrove plants. *J. Shenzhen Univ. Sci. Eng.* **2022**, *39*, 245–252. (In Chinese) [CrossRef]
30. Zou, G.; Li, T.; Yang, W.; Sun, B.; Chen, Y.; Wang, B.; Ou, Y.; Yu, H.; She, Z. Antioxidative indenone and benzophenone derivatives from the mangrove-derived fungus *Cytospora heveae* NSHSJ-2. *Mar. Drugs* **2023**, *21*, 181. [CrossRef]
31. Li, K.L.; Dai, Y.; She, J.L.; Zeng, Y.B.; Dai, H.F.; Ou, S.L.; Zhou, X.F.; Liu, Y.H. Bisabolanoic acid A, a new polychiral sesquiterpene with AChE inhibitory activity from a mangrove-derived fungus *Colletotrichum* sp. *J. Asian Nat. Prod. Res.* **2022**, *24*, 88–95. [CrossRef]
32. Feng, Z.; Zhang, X.; Wu, J.; Wei, C.; Feng, T.; Zhou, D.; Wen, Z.; Xu, J. Immunosuppressive cytochalasins from the mangrove endophytic fungus *Phomopsis asparagi* DHS-48. *Mar. Drugs* **2022**, *20*, 526. [CrossRef]

33. Feng, T.; Wei, C.; Deng, X.; Chen, D.; Wen, Z.; Xu, J. Epigenetic manipulation induced production of immunosuppressive chromones and cytochalasins from the mangrove endophytic fungus *Phomopsis asparagi* DHS-48. *Mar. Drugs* **2022**, *20*, 616. [CrossRef]
34. Zhou, J.; Zheng, D.Y.; Xu, J. Two new polyketides from endophytic fungus *Pestalotiopsis* sp. HQD-6 isolated from the Chinese mangrove plant *Rhizophora mucronata*. *J. Asian Nat. Prod. Res.* **2022**, *24*, 52–58. [CrossRef] [PubMed]
35. Cai, J.; Zhu, X.C.; Zeng, W.N.; Wang, B.; Luo, Y.P.; Liu, J.; Chen, M.-J.; Li, G.-Y.; Huang, G.-L.; Chen, G.-Y.; et al. Talaromarins A–F: Six new isocoumarins from mangrove-derived fungus *Talaromyces flavus* TGGP35. *Mar. Drugs* **2022**, *20*, 361. [CrossRef]
36. Cai, J.; Zhou, X.; Wang, B.; Zhang, X.; Luo, M.; Huang, L.; Wang, R.; Chen, Y.; Li, X.; Luo, Y.; et al. Bioactive polyketides and meroterpenoids from the mangrove-derived fungus *Talaromyces flavus* TGGP35. *Front. Microbiol.* **2024**, *15*, 1342843. [CrossRef]
37. Chen, Y.; Wang, G.; Yuan, Y.; Zou, G.; Yang, W.; Tan, Q.; Kang, W.; She, Z. Metabolites with cytotoxic activities from the mangrove endophytic fungus *Fusarium* sp. 2ST2. *Front. Chem.* **2022**, *10*, 842405. [CrossRef] [PubMed]
38. Zou, R.; Wei, C.; Zhang, X.; Zhou, D.; Xu, J. Alkaloids from endophytic fungus *Aspergillus fumigatus* HQD24 isolated from the Chinese mangrove plant *Rhizophora mucronata*. *Nat. Prod. Res.* **2022**, *36*, 5069–5073. [CrossRef]
39. Huang, D.Y.; Nong, X.H.; Zhang, Y.Q.; Xu, W.; Sun, L.Y.; Zhang, T.; Chen, G.-Y.; Han, C.-R. Two new 2, 5-diketopiperazine derivatives from mangrove-derived endophytic fungus *Nigrospora camelliae-sinensis* S30. *Nat. Prod. Res.* **2022**, *36*, 3651–3656. [CrossRef] [PubMed]
40. Jia, H.; Wu, L.; Liu, R.; Li, J.; Liu, L.; Chen, C.; Li, J.; Zhang, K.; Liao, J.; Long, Y. Penifuranone A: A Novel Alkaloid from the Mangrove Endophytic Fungus *Penicillium crustosum* SCNU-F0006. *Int. J. Mol. Sci.* **2024**, *25*, 5032. [CrossRef]
41. Yin, Y.; Yang, W.; Chen, T.; Tan, Q.; Zou, G.; Zang, Z.; Li, J.; Wang, B.; She, Z. Cytosporones W and X: Two mutually converting epimers from a mangrove endophytic fungus *Diaporthe* sp. ZJHJYZ-1. *ACS Omega* **2023**, *8*, 26628–26634. [CrossRef]
42. Jiang, H.; Cai, R.; Zang, Z.; Yang, W.; Wang, B.; Zhu, G.; Yuan, J.; She, Z. Azaphilone derivatives with anti-inflammatory activity from the mangrove endophytic fungus *Penicillium sclerotiorum* ZJHJJ-18. *Bioorg. Chem.* **2022**, *122*, 105721. [CrossRef]
43. Long, K.Y.; Dai, D.C.; Zheng, C.J.; Wang, Y.T.; Song, X.M.; Chen, X.; Zhou, X.-M.; Chen, G.-Y. Three new long-chain polyenes from the mangrove-derived fungus *Penicillium herquei* JX4. *J. Asian Nat. Prod. Res.* **2023**, *25*, 422–428. [CrossRef]
44. Chen, Y.; Yang, W.; Zou, G.; Wang, G.; Kang, W.; Yuan, J.; She, Z. Cytotoxic bromine-and iodine-containing cytochalasins produced by the mangrove endophytic fungus *Phomopsis* sp. QYM-13 using the OSMAC approach. *J. Nat. Prod.* **2022**, *85*, 1229–1238. [CrossRef]
45. Wang, G.; Yin, Z.; Wang, S.; Yuan, Y.; Chen, Y.; Kang, W. Diversified polyketides with anti-inflammatory activities from mangrove endophytic fungus *Daldinia eschscholtzii* KBJYZ-1. *Front. Microbiol.* **2022**, *13*, 900227. [CrossRef] [PubMed]
46. Wang, Y.; Zhong, Z.; Zhao, F.; Zheng, J.; Zheng, X.; Zhang, K.; Huang, H. Two new pyrone derivatives from the mangrove-derived endophytic fungus *Aspergillus sydowii*# 2B. *Nat. Prod. Res.* **2022**, *36*, 3872–3878.
47. Guo, S.; Zhou, H.; Huang, X.; Peng, S.; Li, J.; Ding, B.; Tao, Y.; Huang, H. New glucosidated indole-quinazoline alkaloids from mangrove endophytic fungus *Aspergillus fumigatus* SAl12. *Nat. Prod. Res.* **2023**, 1–6. [CrossRef] [PubMed]
48. Zhang, W.; Hao, L.; Qin, X.; Huang, J.; Yang, R.; Li, J.; Huang, X. A new lactone from mangrove endophytic fungus *Aspergillus* sp. GXNU-A9. *Nat. Prod. Res.* **2023**, *37*, 417–423. [CrossRef] [PubMed]
49. Qin, F.; Luo, L.; Liu, Y.C.; Bo, X.L.; Wu, F.R.; Wang, F.F.; Tan, M.J.; Wei, Y.Q.; Dou, X.B.; Wang, C.Y.; et al. Diisoprenyl-cyclohexene-type meroterpenoids from a mangrove endophytic fungus *Aspergillus* sp. GXNU-Y65 and their anti-nonalcoholic steatohepatitis activity in AML12 cells. *Phytochemistry* **2024**, *218*, 113955. [CrossRef] [PubMed]
50. Xiao, Z.E.; Huang, X.S.; Wei, W.X.; Lu, W.L.; Tan, Z.; Liu, Y.H. Anti-inflammatory secondary metabolites from a Beihai mangrove endophytic fungus *Aspergillus* sp. GXIMD00016. *Acta Sci. Nat. Univ. Sunyatseni/Zhongshan Daxue Xuebao* **2022**, *61*, 69–73. (In Chinese) [CrossRef]
51. Bo, X.; Zhao, Y.; Qin, F.; Wu, F.; Tan, M.; Ju, S.; Song, Z.; Li, W.; He, F.; Wei, Y.; et al. Cytotoxic metabolites from the mangrove endophytic fungus *Aspergillus* sp. GXNU QG1a. *Nat. Prod. Res.* **2024**, 1–8. [CrossRef]
52. Tan, M.; Xu, X.; Zhang, W.; Wu, F.; Bo, X.; Qin, F.; Ju, S.; Song, Z.; Yang, T.; Li, J.; et al. Isolation and insecticidal activities of new cyclic peptides from mangrove endophytic fungus *Aspergillus* sp. GXNU-4QQY1a. *Fitoterapia* **2023**, *171*, 105693. [CrossRef]
53. Yuan, Y.; Wang, G.; She, Z.; Chen, Y.; Kang, W. Metabolites isolated from the mangrove endophytic fungus *Didymella* sp. CYSK-4 and their cytotoxic activities. *Fitoterapia* **2023**, *171*, 105692. [CrossRef] [PubMed]
54. Li, T.; Yang, W.; Chen, T.; Ouyang, H.; Liu, Y.; Wang, B.; Yu, H.; She, Z. Five secondary metabolites from mangrove endophytic fungus *Fusarium. proliferatum* NSD-1. *J. Mol. Struct.* **2024**, *1302*, 137434. [CrossRef]
55. Wang, B.; Nong, X.H.; Zeng, W.N.; Li, S.S.; Li, G.Y.; Liu, J.; Huang, G.L.; Zheng, C.J. Study on bioactive secondary metabolites from the mangrove-derived fungus *Penicillium verruculosum* TGM14. *Chem. Nat. Compd.* **2022**, *58*, 812–815. [CrossRef]
56. Gan, Y.M.; Xia, J.L.; Zhao, L.Y.; Liu, K.; Tang, Z.Z.; Huang, B.Y.; Liu, Y.-H.; Gao, C.-H.; Bai, M. Two new isocoumarins isolated from a mangrove-derived *Penicillium* sp. *Phytochem. Lett.* **2022**, *50*, 21–24. [CrossRef]
57. Ren, X.; Chen, C.; Ye, Y.; Xu, Z.; Zhao, Q.; Luo, X.; Liu, Y.; Guo, P. Anti-inflammatory compounds from the mangrove endophytic fungus *Amorosia* sp. SCSIO 41026. *Front. Microbiol.* **2022**, *13*, 976399. [CrossRef]
58. Hertweck, C. The biosynthetic logic of polyketide diversity. *Angew. Chem. Int. Ed.* **2009**, *48*, 4688–4716. [CrossRef]
59. Peng, B.; Cai, J.; Xiao, Z.; Liu, M.; Li, X.; Yang, B.; Fang, W.; Huang, Y.-Y.; Chen, C.; Zhou, X.; et al. Bioactive Polyketides and Benzene Derivatives from Two Mangrove Sediment-Derived Fungi in the Beibu Gulf. *Mar. Drugs* **2023**, *21*, 327. [CrossRef]

60. Wu, M.D.; Chen, J.J.; Cheng, M.J. Secondary metabolites with antifungal activities from mangrove derived fungus *Monascus purpureus* WMD2424. *Mar. Drugs* **2023**, *21*, 200. [CrossRef] [PubMed]
61. Lu, X.; Zhang, M.; Qiu, Y.; Liu, X.; Wang, C.; Chen, J.; Zhang, H.; Wei, B.; Yu, Y.; Ying, Y.; et al. α-Glucosidase inhibitors from two mangrove-derived actinomycetes. *Molecules* **2023**, *28*, 3822. [CrossRef] [PubMed]
62. Huo, R.; Zhang, J.; Niu, S.; Liu, L. New prenylated indole diketopiperazine alkaloids and polyketides from the mangrove-derived fungus *Penicillium* sp. *Front. Mar. Sci.* **2022**, *9*, 1097594. [CrossRef]
63. Cai, J.; Wang, X.; Yang, Z.; Tan, Y.; Peng, B.; Liu, Y.; Zhou, X. Thiodiketopiperazines and alkane derivatives produced by the mangrove sediment–derived fungus *Penicillium ludwigii* SCSIO 41408. *Front. Microbiol.* **2022**, *13*, 857041. [CrossRef] [PubMed]
64. Wang, W.; Wang, M.; Wang, X.B.; Li, Y.Q.; Ding, J.L.; Lan, M.X.; Gao, X.; Zhao, D.L.; Zhang, C.S.; Wu, G.X. Phytotoxic azaphilones from the mangrove-derived fungus *Penicillium sclerotiorum* HY5. *Front. Microbiol.* **2022**, *13*, 880874. [CrossRef] [PubMed]
65. Hung, J.; Ying, C.H.E.N.; Yanchun, H.E.; Bin, Y.A.N.G. Secondary metabolites from the mangrove soil derived fungus *Xylariaceae* sp. SCSIO41212. *J. Holist. Integr. Pharm.* **2022**, *3*, 230–235. [CrossRef]
66. Newaz, A.W.; Yong, K.; Yi, W.; Wu, B.; Zhang, Z. Antimicrobial metabolites from the Indonesian mangrove sediment-derived fungus *Penicillium chrysogenum* sp. ZZ1151. *Nat. Prod. Res.* **2023**, *37*, 1702–1708. [CrossRef] [PubMed]
67. Huang, Y.Y.; Li, Z.; Pan, X.L.; Huang, Y.L.; Hu, W.J.; Li, F.; Wang, Q.Z.; Huang, S.S.; Zhou, X.Y.; Wen, W.S. Screening of Mangrove Soil Bacteria Producing in Vitro Anti-na sopharyngeal Carcinoma Substance and Analysis of Its Active Component. *Guangxi Sci.* **2022**, *29*, 846–853. (In Chinese) [CrossRef]
68. Naito, T. Development of new synthetic reactions for nitrogen-containing compounds and their application. *Chem. Pharm. Bull.* **2008**, *56*, 1367–1383. [CrossRef]
69. Cai, J.; Li, M.; Chen, C.; Yang, B.; Gao, C.; Liu, Y.; Luo, X.; Tan, Y.; Zhou, X. Peniditerpenoids A and B: Oxidized Indole Diterpenoids with Osteoclast Differentiation Inhibitory Activity from a Mangrove-Sediment-Derived *Penicillium* sp. *J. Nat. Prod.* **2024**, *87*, 1401–1406. [CrossRef] [PubMed]
70. Niu, S.; He, J.; Huang, S.; Wu, S.; Zeng, L.; Wang, J.; Hong, B.; Chen, Z. Phaeosphamides A and B, cytotoxic cyclodecadepsipeptides from the mangrove-derived fungus *Phaeosphaeriopsis* sp. S296. *Mar. Drugs* **2022**, *20*, 591. [CrossRef]
71. Lu, P.; Shi, Y.; Zhang, J.; Hong, K.; Xue, Y.; Liu, L. New prenylated indole-benzodiazepine-2, 5-diones with α-glucosidase inhibitory activities from the mangrove-derived *Aspergillus spinosus*. *Int. J. Biol. Macromol.* **2024**, *257*, 128808. [CrossRef]
72. Wu, Q.; Chang, Y.; Che, Q.; Li, D.; Zhang, G.; Zhu, T. Citreobenzofuran D–F and phomenone A–B: Five novel sesquiterpenoids from the mangrove-derived fungus *Penicillium* sp. HDN13-494. *Mar. Drugs* **2022**, *20*, 137. [CrossRef]
73. Butler, A.; Sandy, M. Mechanistic considerations of halogenating enzymes. *Nature* **2009**, *460*, 848–854. [CrossRef]
74. Cabrita, M.T.; Vale, C.; Rauter, A.P. Halogenated compounds from marine algae. *Mar. Drugs* **2010**, *8*, 2301–2317. [CrossRef]
75. Cai, J.; Wang, X.; Gan, X.; Zhou, Q.; Luo, X.; Yang, B.; Liu, Y.; Ratnasekera, D.; Zhou, X. New chlorinated metabolites and antiproliferative polyketone from the mangrove sediments-derived fungus *Mollisia* sp. SCSIO41409. *Mar. Drugs* **2022**, *21*, 32. [CrossRef]
76. Conrado, R.; Gomes, T.C.; Roque, G.S.C.; De Souza, A.O. Overview of bioactive fungal secondary metabolites: Cytotoxic and antimicrobial compounds. *Antibiotics* **2022**, *11*, 1604. [CrossRef]
77. Newman, D.J.; Cragg, G.M. Natural products as sources of new drugs over the nearly four decades from 01/1981 to 09/2019. *J. Nat. Prod.* **2020**, *83*, 770–803. [CrossRef]
78. Bray, F.; Laversanne, M.; Weiderpass, E.; Soerjomataram, I. The ever-increasing importance of cancer as a leading cause of premature death worldwide. *Cancer* **2021**, *127*, 3029–3030. [CrossRef]
79. Somarelli, J.A.; Boddy, A.M.; Gardner, H.L.; DeWitt, S.B.; Tuohy, J.; Megquier, K.; Sheth, M.U.; Hsu, S.D.; Thorne, J.L.; London, C.A.; et al. Improving cancer drug discovery by studying cancer across the tree of life. *Mol. Biol. Evol.* **2020**, *37*, 11–17. [CrossRef]
80. Jain, C.; Khatana, S.; Vijayvergia, R. Bioactivity of secondary metabolites of various plants: A review. *Int. J. Pharm. Sci. Res.* **2019**, *10*, 494–504.
81. Ziemert, N.; Alanjary, M.; Weber, T. The evolution of genome mining in microbes—A review. *Nat. Prod. Rep.* **2016**, *33*, 988–1005. [CrossRef] [PubMed]
82. Friedrich, S.; Hahn, F. Opportunities for enzyme catalysis in natural product chemistry. *Tetrahedron* **2015**, *71*, 1473–1508. [CrossRef]

marine drugs

MDPI

Review

Chemical Constituents and Biological Activities of *Bruguiera* Genus and Its Endophytes: A Review

Xiongming Luo [1,2,*,†], Xiaohong Chen [1,2,†], Lingli Zhang [1,2], Bin Liu [1,2], Lian Xie [1], Yan Ma [2,3], Min Zhang [2,3] and Xiaobao Jin [2,3,*]

[1] School of Life Sciences and Biopharmaceutics, Guangdong Pharmaceutical University, Guangzhou 510006, China; cxh2sky@163.com (X.C.); gdpu_zll@163.com (L.Z.); vert2222@163.com (B.L.); chain1009@163.com (L.X.)
[2] Guangdong Provincial Key Laboratory of Pharmaceutical Bioactive Substances, Guangdong Pharmaceutical University, Guangzhou 510006, China; mayan@gdpu.edu.cn (Y.M.); zhangminlala@126.com (M.Z.)
[3] School of Basic Medical Sciences, Guangdong Pharmaceutical University, Guangzhou 510006, China
* Correspondence: qxjun312xx@gdpu.edu.cn (X.L.); jinxf2001@163.com (X.J.)
† These authors contributed equally to this work.

Abstract: The genus *Bruguiera*, a member of the Rhizophoraceae family, is predominantly found in coastal areas as a mangrove plant, boasting a rich and diverse community of endophytes. This review systematically compiled approximately 496 compounds derived from both the *Bruguiera* genus and its associated endophytes, including 152 terpenoids, 17 steroids, 16 sulfides, 44 alkaloids and peptides, 66 quinones, 68 polyketides, 19 flavonoids, 38 phenylpropanoids, 54 aromatic compounds, and 22 other compounds. Among these, 201 compounds exhibited a spectrum of activities, including cytotoxicity, antimicrobial, antioxidant, anti-inflammatory, antiviral, antidiabetic, insecticidal and mosquito repellent, and enzyme inhibitory properties, etc. These findings provided promising lead compounds for drug discovery. Certain similar or identical compounds were found to be simultaneously present in both *Bruguiera* plants and their endophytes, and the phenomenon of their interaction relationship was discussed.

Keywords: *Bruguiera*; endophyte; chemical constituents; bioactivities; interaction relationship

1. Introduction

Mangroves thriving in tropical and subtropical coastal regions, estuaries, and mudflats represent unique plant communities. Globally, these mangrove plants host a diverse distribution of 84 species belonging to 24 genera and 16 families [1]. The Rhizophoraceae family, in particular, encompasses approximately four genera, with *Bruguiera* being one of them [2]. Currently, the *Bruguiera* genus comprises six species, including *Bruguiera cylindrica*, *B. exaristata*, *B. gymnorrhiza*, *B. hainessi*, *B. parviflora*, and *B. sexangula*, which are mainly distributed along the coasts of Asia, the islands of the eastern Pacific Ocean, and the coasts of Oceania, and one variety *B. sexangula var. rhynchopetala*, found in the Hainan and Guangdong provinces of China [2–4]. It has been reported that *B. gymnorrhiza*, *B. cylindrica*, *B. sexangula*, and *B. parviflora*, have undergone pharmacological validation for their role as traditional medicinal plants [5]. Among these, *B. gymnorrhiza* stands out as the most extensively used for traditional purposes. In diverse regions such as the Sundarbans, the Pichavaram and Pichavaram forests of India, Guangxi province of China, South Andaman Island, Selangor of Malaysia, Indonesia, and the Comoros of Mauritius, inhabitants leverage different components of *B. gymnorrhiza* to address various health conditions [5]. For example, the bark and leaf were employed for treating diarrhea, malaria, fevers, burns, diabetes, liver disorders, and intestinal worms [6,7]. The root was found to have applications in the treatment of diabetes and hyperlipidemias [8]. The fruit is utilized for managing conditions like shingles, eye diseases, and diarrhea [9]. Additionally, the

bark of *B. cylindrica* demonstrates efficacy in treating hemorrhages and ulcers [10], while the bark of *B. parviflora* has been utilized in diabetes treatment [5].

In 1966, Loder and Russell first reported the isolation of a new tropane alkaloid brugine from the stem bark of *B. sexangula* [11]. In 2008, Wu et al. conducted the first comprehensive review of natural products from true mangrove flora worldwide, encompassing their sources, chemistries, and bioactivities [3]. In 2014, Zheng et al. compiled 38 chemical constituents of the *Bruguiera* genus up to 2010 [12]. Subsequently, in 2018, Xie et al. conducted a literature search spanning from 1972 to 2017, providing an overview of the chemical compositions and biological activities of *B. gymnorrhiza* [13]; however, certain inaccuracies were identified. In 2021, Chen et al. summarized 1387 secondary metabolites from fungi associated with mangroves, covering the period from 1989 to 2020, detailing their sources, chemistries, and biological activities [14]. Our research team has undertaken partial studies on the isolation and activity screening of secondary metabolites from mangrove plants and marine microorganisms [15–19]. Currently, we are engaged in relevant research on the isolation and activity screening of secondary metabolites from *Bruguiera* plants and their endophytes.

The ongoing isolation endeavors for plants belonging to this genus are predominantly centered around four specific species: *B. gymnorrhiza*, *B. cylindrica*, *B. sexangula*, and *B. sexangula var. rhynchopetala*. A total of 167 secondary metabolites have been unearthed, with a unique class of sulfur-containing compounds discovered particularly in *B. gymnorrhiza*. Starting from 2018, the isolation of novel compounds from plants within the *Bruguiera* genus has encountered escalating challenges, and the enthusiasm for research in this area has gradually diminished. However, there is a current research focus on the secondary metabolites produced by endophytes within the *Bruguiera* genus.

The unique habitat of mangroves has nurtured a rich resource of fungi, bacteria, actinomycetes, and other microorganisms, particularly mangrove associated fungi, which constitute the second largest group of marine fungi [14,20]. These fungi play a crucial role in regulating the mangrove ecosystem, and produce unique structural and diverse bioactive secondary metabolites [14]. Since 2007, researchers have demonstrated considerable interest in the exploration of structurally novel and bioactive compounds derived from endophytes of mangrove genus *Bruguiera*. These endophytes, comprising fungi, bacteria, and actinomycetes, are predominantly sourced from various plant components, including branch, leaf, stem, bark, root, hypocotyl, and inner tissue. To better exploit the medicinal potential of microbial resources, researchers have extensively cultured and isolated endophytic fungi within the *Bruguiera* genus, conducting analyses on both their secondary metabolites and biological activities. Through a compilation of the relevant literature, it was revealed that these endophytes comprise 34 fungi strains, belonging to 19 genera (strains), namely *Aspergillus* (4), *Cladosporium* (1), *Clonostachys* (1), *Daldinia* (2), *Epicoccum* (1), *Fusarium* (1), *Gloesporium* (1), *Nigrospora* (1), *Nectria* (1), *Peniophora* (1), *Penicillium* (10), *Pestalotiopsis* (2), *Pseudolagarobcasidium* (1), *Phomopsis* (1), *Phyllosticta* (1), *Rhytidhysteron* (1), *Stemphylium* (1), *Trichoderma* (1), and *Xylaria* (2), along with four actinomycetes, affiliated with the genus *Streptomyces* (4). The above 38 strains of endophytes were derived from *B. gymnorrhiza* (63.2%), *B. sexangula var. rhynchopetala* (21.0%), *B. sexangula* (13.2%), and *B. parviflora* (2.6%).

Currently, 337 secondary metabolites have been found from the endophytes of the *Bruguiera* genus. Some of these compounds exhibit rare structural features and demonstrate significant bioactivity. For example, in the study by Zhang et al. [21], four novel 12-membered macrocyclic lactone compounds (**179–182**) with sulfur substitution at C-2 were obtained from the endophytic fungus *Cladosporium cladosporioides* MA-299, isolated from the leaves of *B. gymnorrhiza*, and the compounds exhibited notable antimicrobial activity against aquatic bacteria (*Edwardsiella tarda* and *Edwardsiella ictarda*) and plant pathogens (*Bipolaris sorokiniana*, *Colletotrichum glecosporioides*, *Fusarium oxysporum* f. sp. *cucumerinum*, and *Physalospora piricola* Nose). Additionally, Xu et al. [22] got a range of structurally diverse ansamycin compounds, named divergolides A–D (**329–332**), from the

endophytic actinomycete *Streptomyces sp.* in *B. gymnorrhiza*, offering a detailed analysis of the polyketide synthase domain, which not only validated the stereochemical integrity of divergolides, but also yielded valuable insights into the formation mechanisms of the diverse aromatic chromophores. Evidently, endophytes of *Bruguiera* genus plants emerge as a promising reservoir for acquiring structurally novel compounds.

Research indicates that there is no significant distinction in marine fungal natural products obtained from different ecological niches [23]. In-depth exploration of understudied microbial phyla, particularly those unique to specific environments, is more likely to unveil structurally novel biologically active compounds [24]. Clearly, there is still a substantial knowledge gap in the current exploratory research on endophytic bacteria and actinomycetes within the *Bruguiera* genus, necessitating further in-depth investigation. Simultaneously, a significant amount of current research employs similar isolation and cultivation techniques targeting microorganisms of the same genus, leading to the production of structurally similar or the known compounds during the processes of microbial culture and secondary metabolite isolation [25]. Therefore, to extract a more diverse array of unique natural products from endophytes within the *Bruguiera* genus, we should adopt a targeted approach. This involves the targeted isolation of strains, guided by early genomic sequencing to inform strain selection, and innovations in culture media and cultivation techniques [25].

This review encompasses the relevant literature describing the chemical composition and biological activities of *Bruguiera* genus plants and their endophytes until 30 December 2023. It summarizes approximately 496 compounds, of which 201 exhibit biological activity. Of particular note, during the process of the literature organization, it was observed that certain compounds—such as cytochalasin D, zygosporin D, 2,6-dimethoxy-1,4-benzoquinone, scopoletin, and so on—either coexist in both plants and their endophytic fungi or play a crucial regulatory role in the interaction between plants and endophytic fungi. The noteworthy discovery will be further explored and discussed below.

2. Chemical Composition of *Bruguiera* Genus Plants and Their Endophytes

The secondary metabolites of *Bruguiera* genus plants and their endophytes demonstrate a diverse array (Figure 1), comprising terpenoids (30.7%), steroids (3.4%), sulfur-containing compounds (3.2%), alkaloids and peptides (8.9%), quinones (13.3%), polyketides (13.7%), flavonoids (3.8%), phenylpropanoids (7.7%), aromatic compounds (10.9%), and other compounds (4.4%).

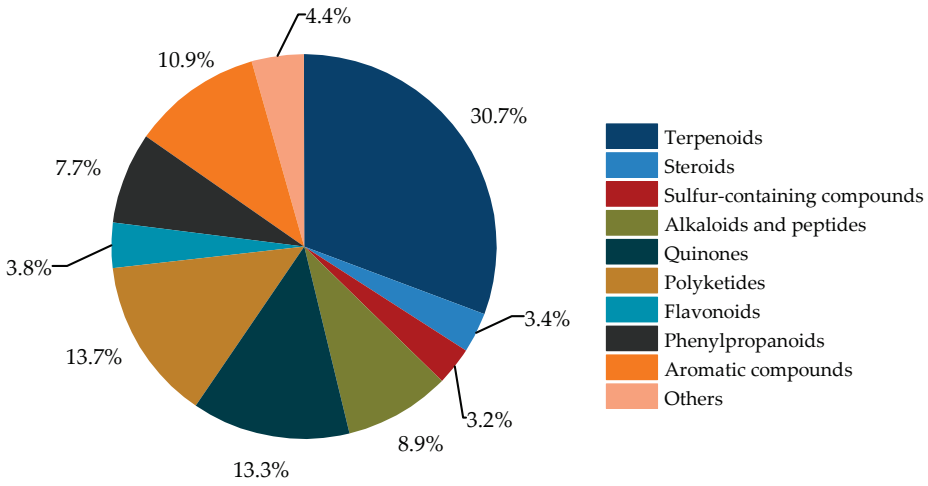

Figure 1. Classification of secondary metabolites from plants of *Bruguiera* genus and their endophytes.

2.1. Terpenoids

Terpenoids constitute the largest category of chemical constituents in both *Bruguiera* genus plants and their endophytes, totaling 152 compounds. This diverse group includes

2 monoterpenes, 56 sesquiterpenes, 28 diterpenes, 4 sesterterpenes, 40 triterpenes, and 22 meroterpenes. Monoterpenes, sesterterpenes, and meroterpenes are exclusively found in endophytic fungi. Diterpenes are isolated only from *Bruguiera* plants, which suggests the potential absence or inhibition of the biosynthetic pathway for these compounds in their endophytes.

2.1.1. Monoterpenes

In the context of *Bruguiera* genus plants and their endophytes, the occurrence of monoterpenoid compound is infrequent. Only Xu et al. [26] isolated two antibacterially active monoterpenoid derivatives (Figure 2), (3*R*,4*R*,6*R*,7*S*)-7-hydroxyl-3,7-dimethyloxabicyclo[3.3.1]nonan-2-one (**1**) and (3*R*,4*R*)-3-(7-methylcyclohexenyl)-propanoic acid (**2**), from the fermentation product of *Pestalotiopsis foedan*, an endophytic fungus found in the branch of *B. sexangula*. While a variety of monoterpenes, such as trans-β-ocimene and linalool, are present in the essential oils of *Bruguiera* plants like the flower of *B. gymnorrhiza* [27], researchers have seldom conducted isolation studies on this particular fraction of crude extracts.

2.1.2. Sesquiterpenes

In the *Bruguiera* genus and their endophytes, the biosynthetic pathway for sesquiterpenoids is exclusively present in both *B. gymnorrhiza* plant and its endophytes, having the production of 56 sesquiterpenoid compounds (**3–58**, Table 1 and Figure 2). In a study by Wibowo et al. [28,29], a total of 28 (nor)sesquiterpens (**8–35**) were isolated from the endophytic fungus *Pseudolagarobasidium acaciicola* in the roots of *B. gymnorrhiza*. Compound **8** is a novel tricyclic norsesquiterpene with a unique acaciicolane skeleton featuring a 6/5/5 ring system. Compounds **24–26** are identified as new spirobicyclic (nor)sesquiterpenes, characterized by a spiroacaciicolane skeleton with a 5/6 fused spirobicyclic ring system [28,29]. (Nor)sesquiterpenoid compounds (**27–29**, **35**) are found as new nor-chamigrane endoperoxides [28,29]. Additionally, compounds **9–11** and **12–23** possess a novel 6/5/6 tricyclic ring system and a 6/6 spirobicyclic structure, respectively [29].

Ding and colleagues [30–33] identified five types of sesquiterpenes from two endophytic actinomycetes, *Streptomyces sp.* GT2002/1503 and *Streptomyces sp.* JMRC:ST027706, isolated from the stems of *B. gymnorrhiza*. These compounds encompass indolosesquiterpenes (**44–45**), plant-derived caryolanes (**46–48**), geosmins (**49–52**), plant-like eudesmanes (**53–55**), and plant-like cadinanes (**56–58**). Significantly, among these, compound **53** demonstrated noteworthy broad antimicrobial activity and also emerged as a principal constituent in the essential oil derived from the aromatic grass *Cymbopogon distans*, which may play a pivotal role as an active ingredient in the medicinal plant *C. distans* [32]. Nevertheless, there exists a plausible suspicion that this compound may also be produced by *Streptomyces sp.* JMRC:ST027706 in a manner to the plant's defense response when the host *B. gymnorrhiza* plant is subjected to pathogenic threats. This implies a potential collaborative mechanism where the endophytic actinomycete aids the host plant in bolstering its resistance against diseases. Moreover, the discovery of oxygenated geosmins is interesting, as it has brought to light the potential presence of enzymes within the endophytic actinomycetes capable of modifying geosmin oxidizing the decalin core structure found in geosmin and analogous terpenoids [32]. This revelation not only expands our understanding but also introduces a promising prospect for employing biotechnological strategies to harness these enzymes for geosmin degradation.

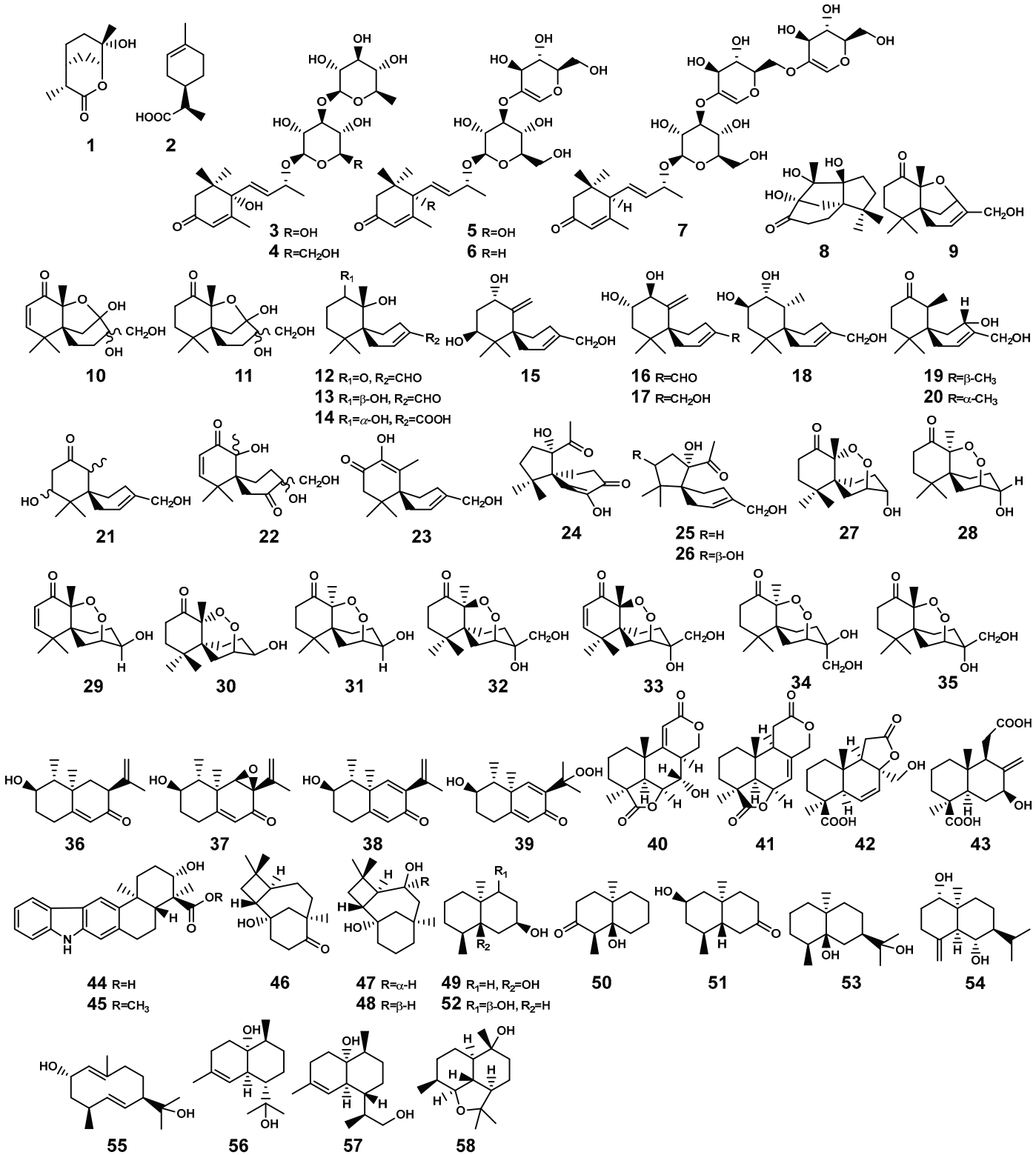

Figure 2. Monoterpenes (**1**–**2**) and sesquiterpenes (**3**–**58**) isolated from *Bruguiera* genus plants and their endophytes.

Table 1. Sesquiterpenes isolated from *Bruguiera* genus plants and their endophytes.

No.	Compound	Source	Reference
3	(*S*)-4-hydroxy-3,5,5-trimethyl-4-((*R*,*E*)-3-(((2*R*,3*R*,4*S*,5*S*,6*S*)-3,5,6-trihydroxy-4-(((2*S*,3*R*,4*S*,5*S*,6*R*)-3,4,5-trihydroxy-6methyltetrahydro-2*H*-pyran-2-yl)oxy)tetrahydro-2*H*-pyran-2-yl)oxy)but-1-en-1-yl)cyclohex-2-en-1-one	*B. gymnorrhiza*, leaf	[34]
4	(*S*)-4-((*R*,*E*)-3-(((2*R*,3*R*,4*S*,5*R*,6*R*)-3,5-dihydroxy-6-(hydroxymethyl)-4-(((2*S*,3*R*,4*S*,5*S*,6*R*)-3,4,5-trihydroxy-6-methyltetrahydro-2*H*-pyran-2-yl)oxy)tetrahydro-2H-pyran-2-yl)oxy)but-1-en-1-yl)-4-hydroxy-3,5,5-trimethylcyclohex-2-en-1-one	*B. gymnorrhiza*, leaf	[34]
5	(*S*)-4-((*R*,*E*)-3-(((2*R*,3*R*,4*S*,5*R*,6*R*)-4-(((2*R*,3*S*,4*S*)-3,4-dihydroxy-2-(hydroxymethyl)-3,4-dihydro-2*H*-pyran-5-yl)oxy)-3,5-dihydroxy-6-(hydroxymethyl)tetrahydro-2*H*-pyran-2-yl)oxy)but-1-en-1-yl)-4-hydroxy-3,5,5-trimethylcyclohex-2-en-1-one	*B. gymnorrhiza*, leaf	[34]
6	(*R*)-4-((*R*,*E*)-3-(((2*R*,3*R*,4*S*,5*R*,6*R*)-4-(((2*R*,3*S*,4*S*)-3,4-dihydroxy-2-(hydroxymethyl)-3,4-dihydro-2*H*-pyran-5-yl)oxy)-3,5-dihydroxy-6-(hydroxymethyl)tetrahydro-2*H*-pyran-2-yl)oxy)but-1-en-1-yl)-3,5,5-trimethylcyclohex-2-en-1-one	*B. gymnorrhiza*, leaf	[34]
7	(*R*)-4-((*R*,*E*)-3-(((2*R*,3*R*,4*S*,5*R*,6*R*)-4-(((2*R*,3*S*,4*S*)-2-((((2*R*,3*S*,4*S*)-3,4-dihydroxy-2-(hydroxymethyl)-3,4-dihydro-2*H*-pyran-5-yl)oxy)methyl)-3,4-dihydroxy-3,4-dihydro-2H-pyran-5-yl)oxy)-3,5-dihydroxy-6-(hydroxymethyl)tetrahydro-2*H*-pyran-2-yl)oxy)but-1-en-1-yl)-3,5,5-trimethylcyclohex-2-en-1-one	*B. gymnorrhiza*, leaf	[34]
8	Acaciicolin A	*P. acaciicola* (the root of *B. gymnorrhiza*, endophytic fungus)	[28]
9	Acaciicolide A	*P. acaciicola* (the root of *B. gymnorrhiza*, endophytic fungus)	[29]
10	Acaciicolide B	*P. acaciicola* (the root of *B. gymnorrhiza*, endophytic fungus)	[29]
11	Acaciicolide C	*P. acaciicola* (the root of *B. gymnorrhiza*, endophytic fungus)	[29]
12	Acaciicolinol A	*P. acaciicola* (the root of *B. gymnorrhiza*, endophytic fungus)	[29]
13	Acaciicolinol B	*P. acaciicola* (the root of *B. gymnorrhiza*, endophytic fungus)	[29]
14	Acaciicolinol C	*P. acaciicola* (the root of *B. gymnorrhiza*, endophytic fungus)	[29]
15	Acaciicolinol D	*P. acaciicola* (the root of *B. gymnorrhiza*, endophytic fungus)	[29]
16	Acaciicolinol E	*P. acaciicola* (the root of *B. gymnorrhiza*, endophytic fungus)	[29]
17	Acaciicolinol F	*P. acaciicola* (the root of *B. gymnorrhiza*, endophytic fungus)	[29]
18	Acaciicolinol G	*P. acaciicola* (the root of *B. gymnorrhiza*, endophytic fungus)	[29]
19	Acaciicolinol H	*P. acaciicola* (the root of *B. gymnorrhiza*, endophytic fungus)	[29]

Table 1. *Cont*.

No.	Compound	Source	Reference
20	Acaciicolinol I	*P. acaciicola* (the root of *B. gymnorrhiza*, endophytic fungus)	[29]
21	Acaciicolinol J	*P. acaciicola* (the root of *B. gymnorrhiza*, endophytic fungus)	[29]
22	Acaciicolinol K	*P. acaciicola* (the root of *B. gymnorrhiza*, endophytic fungus)	[29]
23	Acaciicolinol L	*P. acaciicola* (the root of *B. gymnorrhiza*, endophytic fungus)	[29]
24	Spiroacaciicolide A	*P. acaciicola* (the root of *B. gymnorrhiza*, endophytic fungus)	[28]
25	Spiroacaciicolide B	*P. acaciicola* (the root of *B. gymnorrhiza*, endophytic fungus)	[29]
26	Spiroacaciicolide C	*P. acaciicola* (the root of *B. gymnorrhiza*, endophytic fungus)	[29]
27	3-epi-Steperoxide A	*P. acaciicola* (the root of *B. gymnorrhiza*, endophytic fungus)	[28]
28	3-epi-merulin A	*P. acaciicola* (the root of *B. gymnorrhiza*, endophytic fungus)	[29]
29	(3*S*,4*R*,6a*S*,10a*R*)-4-hydroxy-7,7,10a-trimethyl-5,6,7,10a-tetrahydro-3*H*-3,6a-methanobenzo[c] [1,2] dioxocin-10(4*H*)-one	*P. acaciicola* (the root of *B. gymnorrhiza*, endophytic fungus)	[29]
30	Steperoxide A	*P. acaciicola* (the root of *B. gymnorrhiza*, endophytic fungus)	[28]
31	Merulin A	*P. acaciicola* (the root of *B. gymnorrhiza*, endophytic fungus)	[29]
32	Merulin B	*P. acaciicola* (the root of *B. gymnorrhiza*, endophytic fungus)	[28]
33	Merulin C	*P. acaciicola* (the root of *B. gymnorrhiza*, endophytic fungus)	[28]
34	Merulin D	*P. acaciicola* (the root of *B. gymnorrhiza*, endophytic fungus)	[29]
35	7-epi-merulin B	*P. acaciicola* (the root of *B. gymnorrhiza*, endophytic fungus)	[29]
36	Petasol	*B. gymnorrhiza*	[35]
37	Sporogen AO1	*B. gymnorrhiza*	[35]
38	6-dehydropetasol	*B. gymnorrhiza*	[35]
39	3α-hydroxy-11-peroxyl-eremophila-6,9-dien-8-one	*B. gymnorrhiza*	[35]
40	Botryosphaerin F	*Aspergillus terreus* No. GX7-3B (the branch of *B. gymnorrhiza*, endophytic fungus)	[36]
41	13,14,15,16-tetranorlabd-7-ene-19,6b:12,17-diolide	*A. terreus* No. GX7-3B (the branch of *B. gymnorrhiza*, endophytic fungus)	[36]
42	Botryosphaerin B	*A. terreus* No. GX7-3B (the branch of *B. gymnorrhiza*, endophytic fungus)	[36]
43	LLZ1271β	*A. terreus* No. GX7-3B (the branch of *B. gymnorrhiza*, endophytic fungus)	[36]
44	Xiamycin	*Streptomyces sp.* GT2002/1503 (the stem of *B. gymnorrhiza*, endophytic actinomycete)	[30]

Table 1. *Cont*.

No.	Compound	Source	Reference
45	Methyl ester of xiamycin	*Streptomyces sp.* GT2002/1503 (the stem of *B. gymnorrhiza*, endophytic actinomycete)	[30]
46	Bacaryolane A	*Streptomyces sp.* JMRC:ST027706 (the stem of *B. gymnorrhiza*, endophytic actinomycete)	[31]
47	Bacaryolane B	*Streptomyces sp.* JMRC:ST027706 (the stem of *B. gymnorrhiza*, endophytic actinomycete)	[31]
48	Bacaryolane C	*Streptomyces sp.* JMRC:ST027706 (the stem of *B. gymnorrhiza*, endophytic actinomycete)	[31]
49	7*R*-hydroxygeosmin	*Streptomyces sp.* JMRC:ST027706 (the stem of *B. gymnorrhiza*, endophytic actinomycete)	[32]
50	3-oxogeosmin	*Streptomyces sp.* JMRC:ST027706 (the stem of *B. gymnorrhiza*, endophytic actinomycete)	[32]
51	2*R*-hydroxy-7-oxogeosmin	*Streptomyces sp.* JMRC:ST027706 (the stem of *B. gymnorrhiza*, endophytic actinomycete)	[32]
52	5-deoxy-7β,9β-dihydroxygeosmin	*Streptomyces sp.* JMRC:ST027706 (the stem of *B. gymnorrhiza*, endophytic actinomycete)	[32]
53	(4*S*,5*S*,7*R*,10*S*)-4β,10α-eudesmane-5β,11-diol	*Streptomyces sp.* JMRC:ST027706 (the stem of *B. gymnorrhiza*, endophytic actinomycete)	[32]
54	(1*S*,5*S*,6*S*,7*S*,10*S*)-10α-eudesm-4(15)-ene-1α,6α-diol	*Streptomyces sp.* JMRC:ST027706 (the stem of *B. gymnorrhiza*, endophytic actinomycete)	[32]
55	1(10)*E*,5*E*-germacradiene-2,11-diol	*Streptomyces sp.* JMRC:ST027706 (the stem of *B. gymnorrhiza*, endophytic actinomycete)	[32]
56	(+)-11-hydroxy-epicubenol	*Streptomyces sp.* JMRC:ST027706 (the stem of *B. gymnorrhiza*, endophytic actinomycete)	[33]
57	(+)-12-hydroxy-epicubenol	*Streptomyces sp.* JMRC:ST027706 (the stem of *B. gymnorrhiza*, endophytic actinomycete)	[33]
58	5,11-epoxy-10-cadinanol	*Streptomyces sp.* JMRC:ST027706 (the stem of *B. gymnorrhiza*, endophytic actinomycete)	[33]

2.1.3. Diterpenoids

Diterpenoids are a class of compounds derived from the precursor (geranylgeranyl diphosphate, GGPP) [37]. The diversity of diterpenoids in plants playing important roles in plant development, stress resistance, and interactions with environmental microorganisms, depends on the various skeletons biosynthesized by terpene synthases and the substrate promiscuity of cytochrome P450 monooxygenases (P450s), along with other post-modification enzymes [38]. In the genus *Bruguiera*, researchers have isolated five different skeletal types of diterpenoid (Table 2 and Figure 3), namely *ent*-pimarane (**79**–**82**), isopi-

marane (**83**–**84**), *ent*-beyerane (**85**–**86**), *ent*-kaurane (**62**–**78**), and *ent*-gibberellane (**59**–**61**), with the key intermediate pimarane in their biosynthesis.

Table 2. Diterpenoids isolated from *Bruguiera* genus plants and their endophytes.

No.	Compound	Source	Reference
59	Gibbererllin A3	*B. gymnorrhiza*, fruit	[39]
60	Gibbererllin A4	*B. gymnorrhiza*, fruit	[39]
61	Gibbererllin A7	*B. gymnorrhiza*, fruit	[39]
62	Steviol	*B. gymnorrhiza*, root bark	[40]
63	Methyl-*ent*-kaur-9(11)-en-13,17-epoxy-16-hydroxy-19-oate	*B. gymnorrhiza*, root bark; *B. sexangula var. rhynchopetala*, stem	[40,41]
64	*ent*-kaur-16-en-13-hydroxy-19-al	*B. gymnorrhiza*, root bark and stem	[40,42]
65	*ent*-kaur-16-en-13,19-diol	*B. gymnorrhiza*, root bark and stem	[40,42]
66	13,16α,17-trihydroxy-*ent*-9(11)-kaurene-19-oic acid	*B. gymnorrhiza*, stem	[42]
67	16α,17-dihydroxy-*ent*-9(11)-kaurene-19-al	*B. gymnorrhiza*, stem; *B. sexangula var. rhynchopetala*, stem	[41,42]
68	17-chloro-13,16β-dihydroxy-*ent*-kauran-19-al	*B. gymnorrhiza*, stem	[42]
69	Methyl-16α,17-dihydroxy-*ent*-kauran-19-oate	*B. gymnorrhiza*, stem	[42]
70	16α,17-dihydroxy-*ent*-9(11)-kauren-19-oic acid	*B. gymnorrhiza*, stem	[42]
71	Methyl-16α,17-dihydroxy-*ent*-9(11)-kauren-19-oate	*B. gymnorrhiza*, stem; *B. sexangula var. rhynchopetala*, stem	[41,42]
72	16α,17-dihydroxy-*ent*-kauran-19-al	*B. gymnorrhiza*, stem	[42]
73	16αH-17-hydroxy-*ent*-kauran-19-oic acid	*B. gymnorrhiza*, stem	[42]
74	16αH-17,19-*ent*-kaurane-diol	*B. gymnorrhiza*, stem	[42]
75	16-*ent*-kauren-19-ol	*B. gymnorrhiza*, stem	[42]
76	(16*R*)-13,17-epoxy-16-hydroxy-*ent*-kaur-9(11)-en-19-al	*B. sexangula var. rhynchopetala*, stem	[41]
77	16,17-dihydroxy-19-nor-*ent*-kaur-9(11)-en-3-one	*B. sexangula var. rhynchopetala*, stem	[41]
78	Ceriopsin F	*B. sexangula var. rhynchopetala*, stem	[41]
79	1β,15(*R*)-*ent*-pimar-8(14)-en-1,15,16-triol	*B. gymnorrhiza*, root bark and stem; *B. sexangula var. rhynchopetala*, stem	[40,41,43]
80	*ent*-8(14)-pimarene-15*R*,16-diol	*B. gymnorrhiza*, stem	[43]
81	*ent*-8(14)-pimarene-1α,15*R*,16-triol	*B. gymnorrhiza*, stem	[43]
82	(5*R*,9*S*,10*R*,13*S*,15*S*)-*ent*-8(14)-pimarene-1-oxo-15*R*,16-diol	*B. gymnorrhiza*, stem	[43]
83	15(*S*)-isopimar-7-en-15,16-diol	*B. gymnorrhiza*, root bark and stem	[40,43]
84	Isopimar-7-ene-1β, 15*S*, 16-triol	*B. gymnorrhiza*, stem	[43]
85	(4*R*,5*S*,8*R*,9*R*,10*S*,13*S*)-*ent*-17-hydroxy-16-oxobeyeran-19-al	*B. gymnorrhiza*, stem; *B. sexangula var. rhynchopetala*, stem	[41,42]
86	17-hydroxy-16-oxobeyer-9(11)-en-19-al	*B. sexangula var. rhynchopetala*, stem	[41]

2.1.4. Sesterpenoids

Most sesterpenoids are sourced from marine organisms, with approximately 15% of these compounds having been isolated from plants [44]. Currently, no such compounds have been identified in *Bruguiera* plants, emphasizing the need for further exploration in this area. Only Liu et al. [45] reported the discovery of two tricyclic sesterterpenes, fusaprolifin A and fusaprolifin B (**87–88**) with brine-shrimp lethality activity, and other two sesterterpenes, terpestacin and fusaproliferin (**89–90**), which isolated from the endophytic fungus *Fusarium proliferatum* MA-84 associated with *B. sexangula* plant (Figure 3).

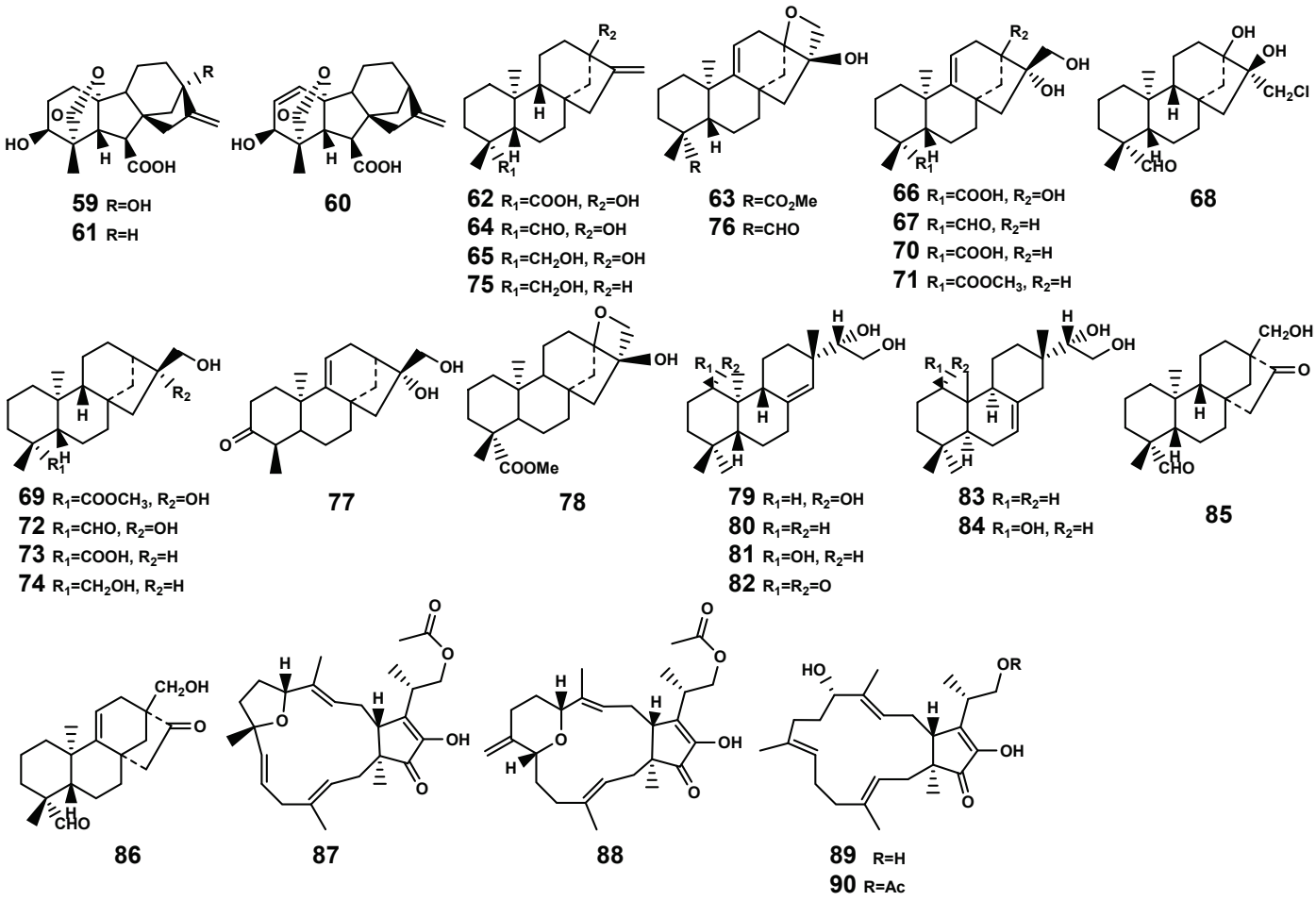

Figure 3. Diterpenes (**59**–**86**) and sesterterpenes (**87**–**90**) isolated from *Bruguiera* genus plants and their endophytes.

2.1.5. Triterpenoids

In the *Bruguiera* plants and their endophytic fungi, triterpenoids (**91**–**130**, Table 3 and Figure 4) constitute a primary class of compounds. Distinguished by variations in carbon ring structures, there are tetracyclic triterpenoids, such as dammarane-type (**91**–**93**) and lanostane-type (**94–98**). Additionally, pentacyclic triterpenoids are present, including oleanane-type (**99**–**104**), ursane-type (**105**–**107**), lupane-type (**108–117**), and other types (**118–130**).

Table 3. Triterpenoids isolated from *Bruguiera* genus plants and their endophytes.

No.	Compound	Source	Reference
91	Bruguierin A	*B. gymnorrhiza*, flower	[46]
92	Bruguierin B	*B. gymnorrhiza*, flower	[46]
93	Bruguierin C	*B. gymnorrhiza*, flower	[46]
94	Sexangulic acid	*B. sexangula*, stem	[47]
95	11-oxo-12α-acetoxy-4,4-dimethyl-24-methylene-5α-cholesta-8,14-diene-2α,3β-diol	*Penicillium sp.* J41221 (*B. sexangula var. rhynchopetala*, endophytic fungus)	[48]
96	12α-acetoxy-4,4-dimethyl-24-methylene-5α-cholesta-8-momoene-3β,11β-diol	*Penicillium sp.* J41221 (*B. sexangula var. rhynchopetala*, endophytic fungus)	[48]
97	12α-acetoxy-4,4-dimethyl-24-methylene-5α-cholesta-8,14-diene-3β,11β-diol	*Penicillium sp.* J41221 (*B. sexangula var. rhynchopetala*, endophytic fungus)	[48]
98	12α-acetoxy-4,4-dimethyl-24-methylene-5α-cholesta-8,14-diene-2α,3β,11β-triol	*Penicillium sp.* J41221 (*B. sexangula var. rhynchopetala*, endophytic fungus)	[48]
99	Gymnorhizol	*B. gymnorrhiza*, stem and leaf	[49]
100	β-amyrin	*B. gymnorrhiza*, leaf	[50]
101	Oleanolic acid	*B. gymnorrhiza*, leaf	[50]
102	(15α)-15-hydroxysoyasapogenol B	*Pestalotiopsis clavispora* (*B. sexangula*, endophytic fungus)	[51]
103	(7β,15α)-7,15-dihydroxysoyasapogenol B	*P. clavispora* (*B. sexangula*, endophytic fungus)	[51]
104	(7β)-7,29-dihydroxysoyasapogenol B	*P. clavispora* (*B. sexangula*, endophytic fungus)	[51]
105	α-amyrin	*B. gymnorrhiza*, leaf	[50]
106	Ursolic acid	*B. gymnorrhiza*, leaf;	[50]
107	Corosolic acid	*B. parviflora*, leaf	[52]
108	Lupeol	*B. gymnorrhiza*, stem and leaf *B. cylindrica*, fruit and hypocotyl *B. parviflora*, fruit and leaf	[50,52–55]
109	Lupenone	*B. gymnorrhiza*, stem and leaf *B. cylindrica*, fruit and hypocotyl *B. parviflora*, fruit	[53–55]
110	3-(*Z*)-caffeoyllupeol	*B. parviflora*, fruit	[54]
111	3β-*E*-caffeoyllupeol	*B. parviflora*, fruit; *B. cylindrica*, fruit and hypocotyl	[54,55]
112	3α-*E*-coumaroyllupeol	*B. cylindrica*, fruit and hypocotyl	[55]
113	3α-*Z*-coumaroyllupeol	*B. cylindrica*, fruit and hypocotyl	[55]
114	3β-*E*-coumaroyllupeol	*B. parviflora*, fruit; *B. cylindrica*, fruit and hypocotyl	[54,55]
115	3β-*Z*-coumaroyllupeol	*B. cylindrica*, fruit and hypocotyl	[55]
116	3α-lupeol	*B. cylindrica*, fruit and hypocotyl	[55]
117	Betulinic acid	*B. parviflora*, leaf	[52]
118	3α-feruloyltaraxerol dichloromethane solvate	*B. cylindrica*, fruit	[56]
119	3α-*E*-feruloyltaraxerol	*B. cylindrica*, fruit	[57]
120	3α-*Z*-feruloyltaraxerol	*B. cylindrica*, fruit	[57]
121	3β-*E*-feruloyltaraxerol	*B. cylindrica*, fruit	[57]
122	3β-*Z*-feruloyltaraxerol	*B. cylindrica*, fruit	[57]
123	3α-*E*-coumaroyltaraxerol	*B. cylindrica*, fruit	[57]

Table 3. *Cont.*

No.	Compound	Source	Reference
124	3*α*-*Z*-coumaroyltaraxerol	*B. cylindrica*, fruit	[57]
125	3*α*-taraxerol	*B. cylindrica*, fruit	[57]
126	3*β*-taraxerol	*B. cylindrica*, fruit and leaf	[57,58]
127	14-taraxeren-3-one	*B. gymnorrhiza*, stem and leaf	[53]
128	3*α*-*E*-caffeoyltaraxerol	*B. cylindrica*, fruit and hypocotyl	[55]
129	3*β*-(*Z*)-coumaroyltaraxerol	*B. cylindrica*, leaf	[58]
130	3*β*-(*E*)-coumaroyltaraxerol	*B. cylindrica*, leaf	[58]

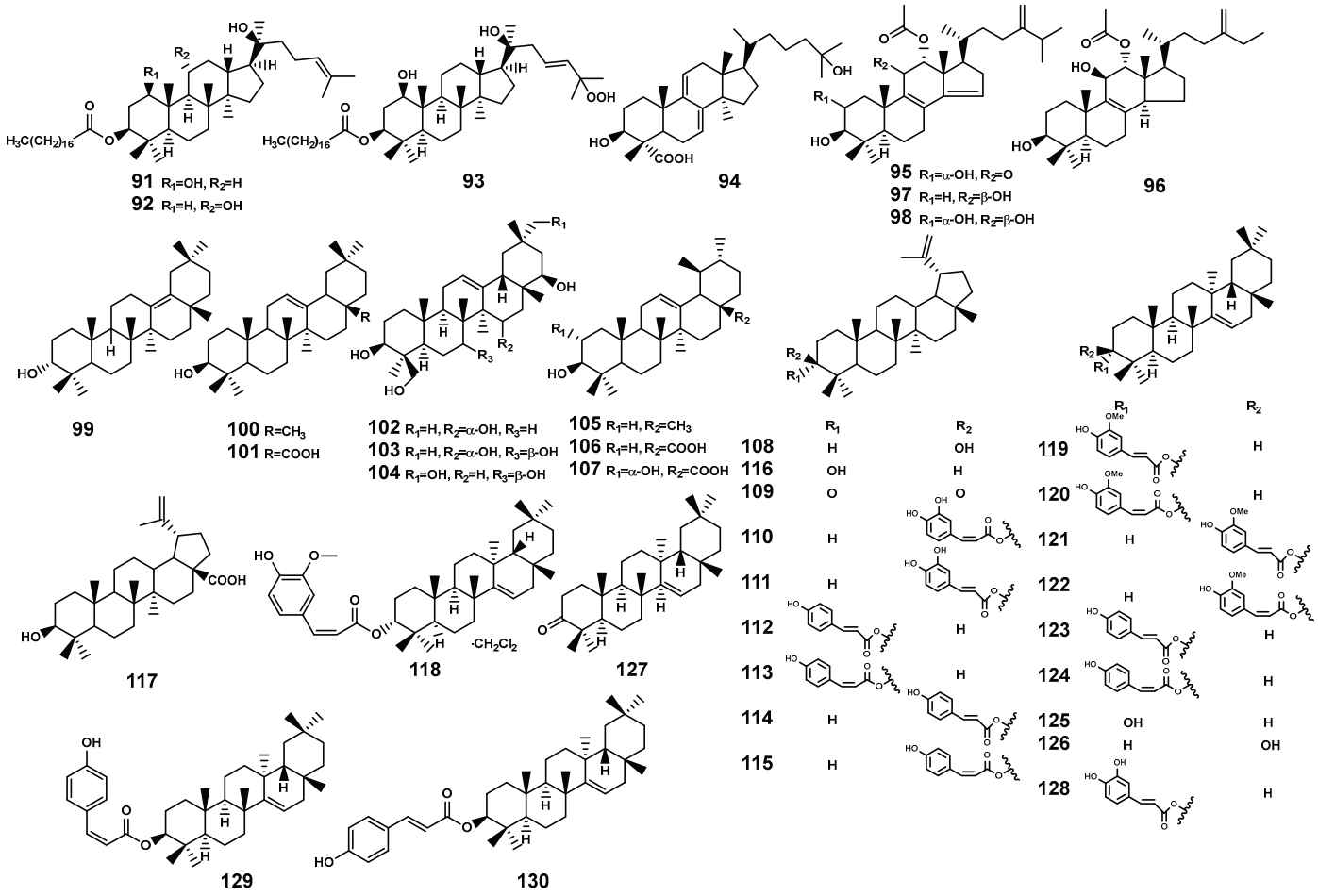

Figure 4. Triterpenoids (**91**–**130**) isolated from *Bruguiera* genus plants and their endophytes.

2.1.6. Meroterpenoids

Meroterpenoids as secondary metabolites arising from hybrid terpenoid biosynthetic pathways, are characterized by the combination of terpenoid and non-terpenoid segments [59]. Based on their non-terpenoid starting moieties, these compounds were categorized into four classes: polyketide–terpenoids, indole–terpenoids, shikimate–terpenoids, and miscellaneous meroterpenoids [59]. This review summarized 22 meroterpenoids (Table 4 and Figure 5) isolated from the endophytic fungi found in *B. gymnorrhiza*, *B. sexangula*, and *B. sexangula var. rhynchopetala*. These meroterpenoids have been classified as shikimate-meroterpenoids of the tricycloalternarene type (**149**–**152**) and polyketide-meroterpenoids (**131**–**148**), which contain tetraketide moieties derived from 3,5-dimethylors

ellinic acid (**131**–**143**) and 6-methylsalicylic acid (**144**), and hexaketide moiety (**145**–**148**), respectively.

Table 4. Meroterpenoids isolated from *Bruguiera* genus plants and their endophytes.

No.	Compound	Source	Reference
131	Dehydroaustin	*Penicillium citrinum* HL-5126 (the leaf of *B. sexangula var. rhynchopetala*, endophytic fungus)	[60]
132	11β-acetoxyisoaustinone	*P. citrinum* HL-5126 (the leaf of *B. sexangula var. rhynchopetala*, endophytic fungus) *Penicillium sp.* TGM112 (*B. sexangula var. rhynchopetala*, fungus);	[60,61]
133	Austinol	*P. citrinum* HL-5126 (the leaf of *B. sexangula var. rhynchopetala*, endophytic fungus); *Penicillium sp.* TGM112 (*B. sexangula var. rhynchopetala*, fungus)	[60,61]
134	Penicianstinoid A	*Penicillium sp.* TGM112 (*B. sexangula var. rhynchopetala*, fungus)	[61]
135	Penicianstinoid B	*Penicillium sp.* TGM112 (*B. sexangula var. rhynchopetala*, fungus)	[61]
136	Furanoaustinol	*Penicillium sp.* TGM112 (*B. sexangula var. rhynchopetala*, fungus)	[61]
137	1,2-dihydro-7-hydroxydehydroaustin	*Penicillium sp.* TGM112 (*B. sexangula var. rhynchopetala*, fungus)	[61]
138	7-hydroxydehydroaustin	*Penicillium sp.* TGM112 (*B. sexangula var. rhynchopetala*, fungus)	[61]
139	Dehydroaustinol	*Penicillium sp.* TGM112 (*B. sexangula var. rhynchopetala*, fungus)	[61]
140	Austin	*Penicillium sp.* TGM112 (*B. sexangula var. rhynchopetala*, fungus)	[61]
141	Penicianstinoid C	*Penicillium sp.* TGM112 (*B. sexangula var. rhynchopetala*, fungus)	[62]
142	Penicianstinoid D	*Penicillium sp.* TGM112 (*B. sexangula var. rhynchopetala*, fungus)	[62]
143	Penicianstinoid E	*Penicillium sp.* TGM112 (*B. sexangula var. rhynchopetala*, fungus)	[62]
144	Nectrianolin D	*Clonostachys rosea* B5–2 and *Nectria pseudotrichia* B69–1 (the branch of *B. gymnorrhiza*, endophytic fungus)	[63]
145	Furanocochlioquinol	*C. rosea* B5–2 and *N. pseudotrichia* B69–1 (the branch of *B. gymnorrhiza*, endophytic fungus)	[63]
146	Furanocochlioquinone	*C. rosea* B5–2 and *N. pseudotrichia* B69–1 (the branch of *B. gymnorrhiza*, endophytic fungus)	[63]
147	Nectripenoid B	*C. rosea* B5–2 and *N. pseudotrichia* B69–1 (the branch of *B. gymnorrhiza*, endophytic fungus)	[63]
148	Cochlioquinone D	*C. rosea* B5–2 and *N. pseudotrichia* B69–1 (the branch of *B. gymnorrhiza*, endophytic fungus)	[63]
149	Guignardone A	*Phyllosticta capitalensis* (the hypocotyl of *B. sexangula*, endophytic fungus)	[64]
150	12-hydroxylated guignardone A	*P. capitalensis* (the hypocotyl of *B. sexangula*, endophytic fungus)	[64]
151	Guignardone J	*P. capitalensis* (the hypocotyl of *B. sexangula*, endophytic fungus)	[64]
152	Guignardone M	*P. capitalensis* (the hypocotyl of *B. sexangula*, endophytic fungus)	[64]

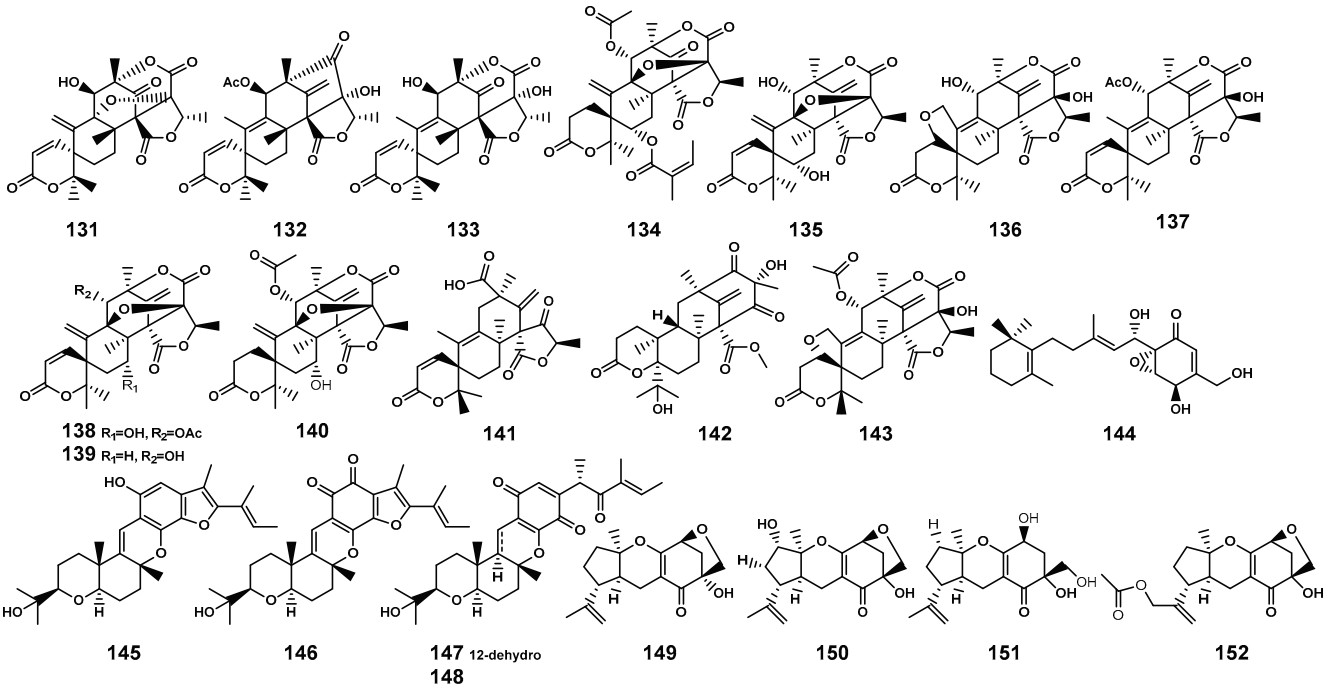

Figure 5. Meroterpenoids (**131**–**152**) isolated from *Bruguiera* genus plants and their endophytes.

2.2. Steroids

In plants and fungi, squalene serves as a precursor that undergoes oxidation catalyzed by squalene epoxidase to generate ox1idosqualene [65]. The further cyclization of oxidized squalene, catalyzed by oxidosqualene cyclases, leads to the biosynthesis of sterols representing a significant downstream structural derivative in the biosynthesis of triterpenoids [65]. Currently, 17 steroids (Table 5 and Figure 6) have been identified in the *Bruguiera* plants and their endophytic fungi. These compounds encompass three types: cholestrol (**153**), stigmastanol (**154–158**), and ergosterol (**159–169**), specifically noting the significance of two ergostanes (**168–169**) with a rearranged tetracyclic skeleton.

Table 5. Steroids isolated from *Bruguiera* genus plants and their endophytes.

No.	Compound	Source	Reference
153	Cholesterol	*B. gymnorrhiza*, leaf; *Penicillium thomi* (the root of *B. gymnorrhiza*, endophytic fungus);	[50,66]
154	Stigmasterol	*B. gymnorrhiza*, leaf	[50]
155	Sitosterol	*B. gymnorrhiza*, leaf; *P. thomi* (the root of B. gymnorrhiza, endophytic fungus); *B. cylindrica*, leaf	[50,58,66]
156	Stigmast-7-en-3β-ol	*B. gymnorrhiza*, leaf	[50]
157	*β*-daucosterol	*B. gymnorrhiza*, stem and leaf;	[53]
158	*β*-sitosteryl linoleate	*Phomopsis longicolla* HL-2232 (the leaf of *B. sexangula var. rhynchopetala*, endophytic fungus)	[67]
159	Ergosterol	*Penicillium sclerotiorum* (the inner bark of *B. gymnorrhiza*, endophytic fungus);	[68]
160	Campesterol	*B. gymnorrhiza*, leaf	[50]
161	3*β*,5*α*-dihydroxy-(22*E*,24*R*)-ergosta-7,22-dien-6-one	*A. terreus* No. GX7-3B (the branch of *B. gymnorrhiza*, endophytic fungus)	[69]

Table 5. *Cont.*

No.	Compound	Source	Reference
162	3*β*,5*α*,14*α*-trihydroxy-(22*E*,24*R*)-ergosta-7,22-dien-6-one	*A. terreus* No. GX7-3B (the branch of *B. gymnorrhiza*, endophytic fungus)	[69]
163	NGA0187	*A. terreus* No. GX7-3B (the branch of *B. gymnorrhiza*, endophytic fungus); *Penicillium sp.* GD6 (the stem bark of *B. gymnorrhiza*, endophytic fungus)	[69,70]
164	11-O-acetyl-NGA0187	*Penicillium sp.* GD6 (the stem bark of *B. gymnorrhiza*, endophytic fungus)	[70]
165	Ergosta-7,22-diene-3*β*,5*α*,6*β*-triol	*P. thomi* (the root of *B. gymnorrhiza*, endophytic fungus); *Penicillium sp.* J41221 (*B. sexangula var. rhynchopetala*, endophytic fungus); *P. longicolla* HL-2232 (the leaf *B. sexangula var. rhynchopetala*, endophytic fungus)	[48,66,67]
166	(3*β*,5*α*,6*β*,22*E*)-6-methoxyergosta-7,22-diene-3,5-diol	*Penicillium sp.* J41221 (*B. sexangula var. rhynchopetala*, endophytic fungus);	[48]
167	(22*E*)-5*α*,8*α*-epidioxyergosta-6,22-dien-3*β*-ol	*P. sclerotiorum* (the inner bark of *B. gymnorrhiza*, endophytic fungus); *P. longicolla* HL-2232 (the leaf *B. sexangula var. rhynchopetala*, endophytic fungus)	[67,68]
168	Cyclocitrinol	*Penicillium sp.* GD6 (the stem bark of *B. gymnorrhiza*, endophytic fungus)	[70]
169	Fortisterol	*P. longicolla* HL-2232 (the leaf *B. sexangula var. rhynchopetala*, endophytic fungus)	[67]

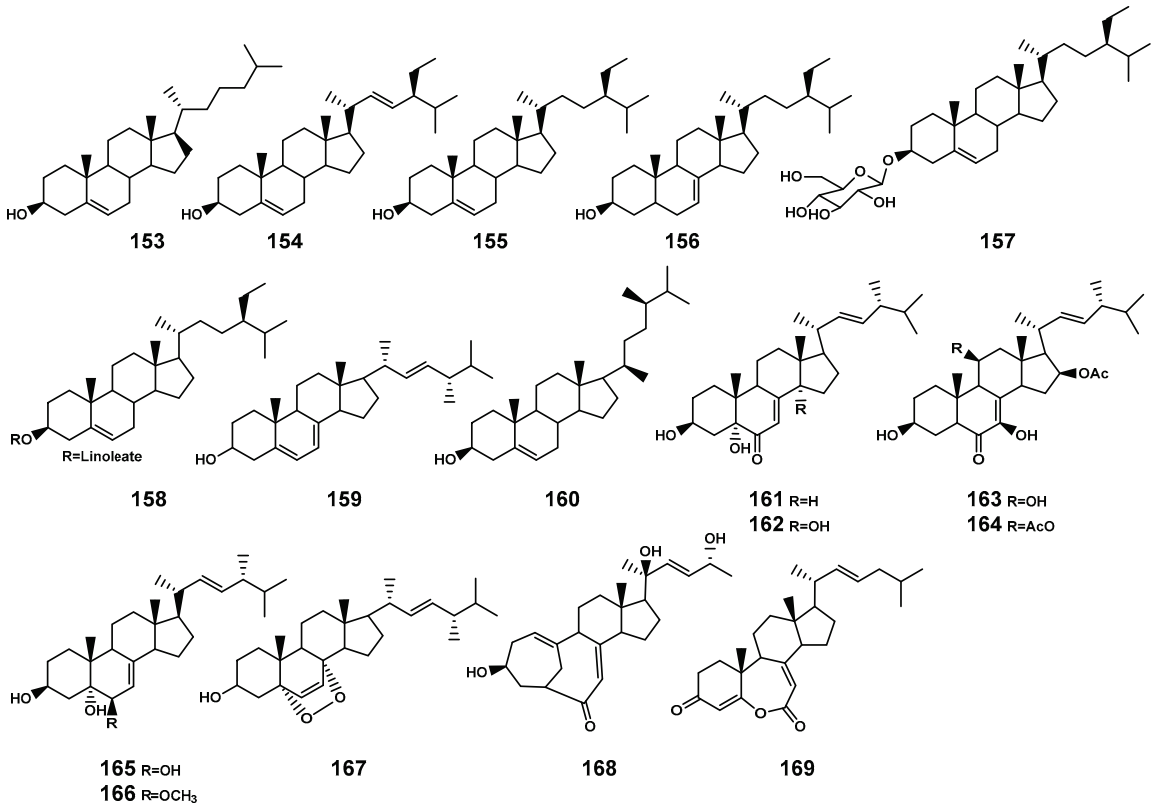

Figure 6. Steroids (**153**–**169**) isolated from *Bruguiera* genus plants and their endophytes.

2.3. Sulfides

Sulfur-containing natural products are predominantly isolated from plants of the Alliaceae family or bacteria, with relatively fewer sulfur compounds being separated from fungi [71]. Now, this paper summarizes a total of 16 sulfur-containing compounds (Table 6 and Figure 7) from the *Bruguiera* genus of Rhizophoraceae family and their endophytes. Within the plants *B. gymnorrhiza*, *B. sexangula var. rhynchopetala*, and *B. cylindrica*, a class of (poly)disulfide compounds (**170–178**) has been found. These compounds belong to a characteristic type of compounds found in mangrove ecosystem of the *Bruguiera* genus, and exhibit a proposed unique biosynthetic pathway (Figure 8) [41,72]. Previous research indicates that sulfides play a crucial role in plant defense against various pathogens and pests [73]. Dahibhate et al. [74] discovered that a mixture of brugierol and isobrugierol exhibited inhibitory activity against *Pseudomonas aeruginosa* by reducing the formation of virulence biofilms controlled by the quorum sensing system, lowering the level of virulence factors, thereby attenuating the pathogenicity of the bacterium against *Bruguiera* plants. Simultaneously, Zhang et al. [21,75] cultured and isolated the endophytic fungus *C. cladosporioides* MA-299 from the leaves of *B. gymnorrhiza*, obtaining seven sulfur-containing 12-membered macrocyclic lactones (**179–185**). The potential biosynthetic pathway of these compounds is illustrated in Figure 9, with the precursor cladocladosin A featuring the bicyclo 5/9 ring system. These compounds (**179–185**) demonstrate activity against aquatic pathogens and plant-pathogenic fungi [21,75], thereby assisting *B. gymnorrhiza* leaves in resisting microbial pathogen invasion.

Table 6. Sulfides isolated from *Bruguiera* genus plants and their endophytes.

No.	Compound	Source	Reference
170	(-)-3,4-dihydro-3-hydroxy-7-methoxy-2*H*-1,5-benzodithiepine-6,9-dione	*B. sexangula var. rhynchopetala*, stem	[41]
171	1,2-dithiolane	*B. gymnorrhiza*, stem and leaf; *B. cylindrica*, stem and bark	[76,77]
172	Brugierol	*B. gymnorrhiza*, stem, leaf, and flower; *B. sexangula var. rhynchopetala*, stem; *B. cylindrica*, stem and bark	[41,72,76–79]
173	Isobrugierol	*B. gymnorrhiza*, stem, leaf and flower; *B. sexangula var. rhynchopetala*, stem; *B. cylindrica*, stem and bark	[41,72,76–79]
174	Bruguiesulfurol	*B. gymnorrhiza*, flower	[72,79,80]
175	Trans-3,3′-dihydroxy-1,5,1′,5′-tetrathiacyclodecane	*B. gymnorrhiza*, stem and leaf	[80]
176	Cis-3,3′-dihydroxy-1,5,1′,5′-tetrathiacyclodecane	*B. gymnorrhiza*, stem and leaf	[80]
177	Gymnorrhizol	*B. gymnorrhiza*, stem, leaf and flower;	[72,76,80]
178	Neogymnorrhizol	*B. gymnorrhiza*, stem, leaf and flower	[72,80]
179	Thiocladospolide A	*C. cladosporioides* MA-299 (the leaf of *B. gymnorrhiza*, endophytic fungus)	[21]
180	Thiocladospolide B	*C. cladosporioides* MA-299 (the leaf of *B. gymnorrhiza*, endophytic fungus)	[21]
181	Thiocladospolide C	*C. cladosporioides* MA-299 (the leaf of *B. gymnorrhiza*, endophytic fungus)	[21]
182	Thiocladospolide D	*C. cladosporioides* MA-299 (the leaf of *B. gymnorrhiza*, endophytic fungus)	[21]

Table 6. *Cont*.

No.	Compound	Source	Reference
183	Pandangolide 3	*C. cladosporioides* MA-299 (the leaf of *B. gymnorrhiza*, endophytic fungus)	[21]
184	Thiocladospolide F	*C. cladosporioides* MA-299 (the leaf of *B. gymnorrhiza*, endophytic fungus)	[75]
185	Thiocladospolide G	*C. cladosporioides* MA-299 (the leaf of *B. gymnorrhiza*, endophytic fungus)	[75]

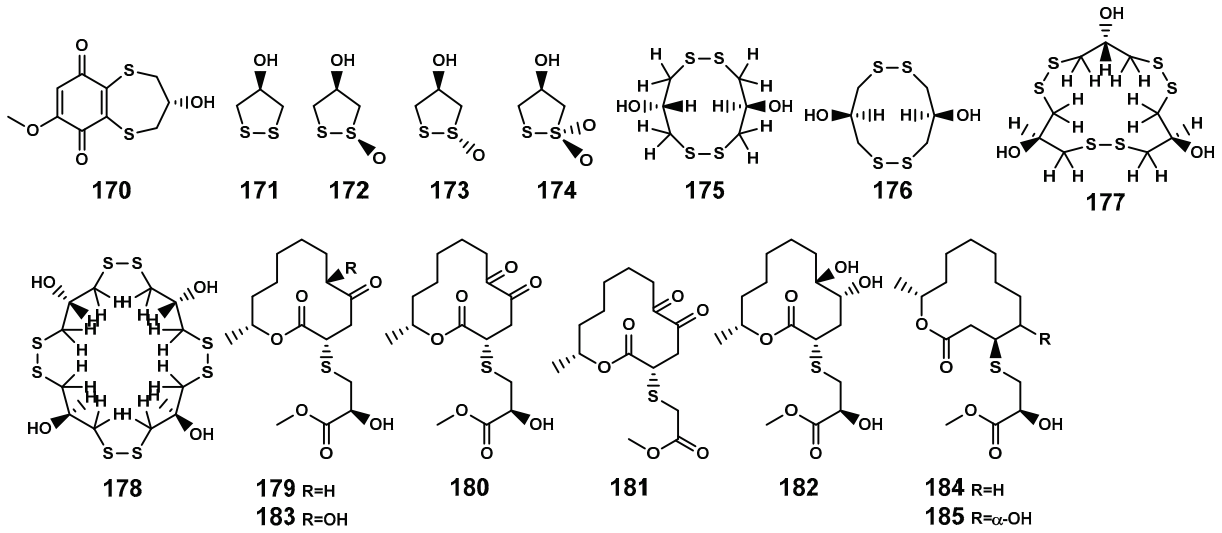

Figure 7. Sulfides (**170**–**185**) isolated from *Bruguiera* genus plants and their endophytes.

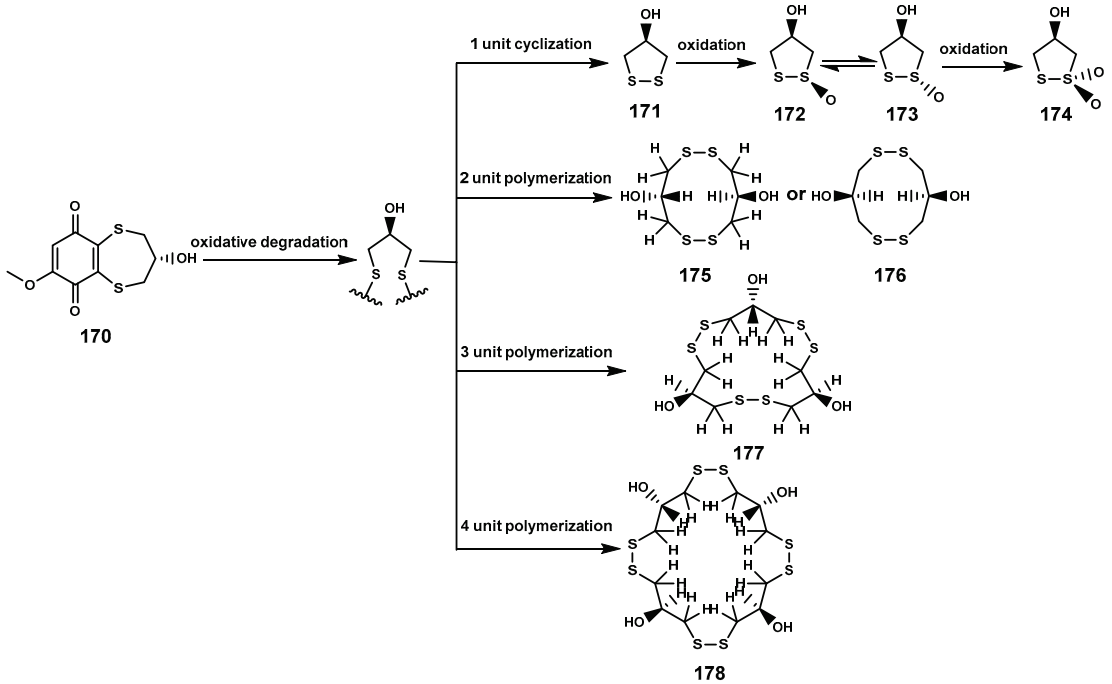

Figure 8. The proposed biosynthetic pathway of disulfide compounds (**170**–**178**).

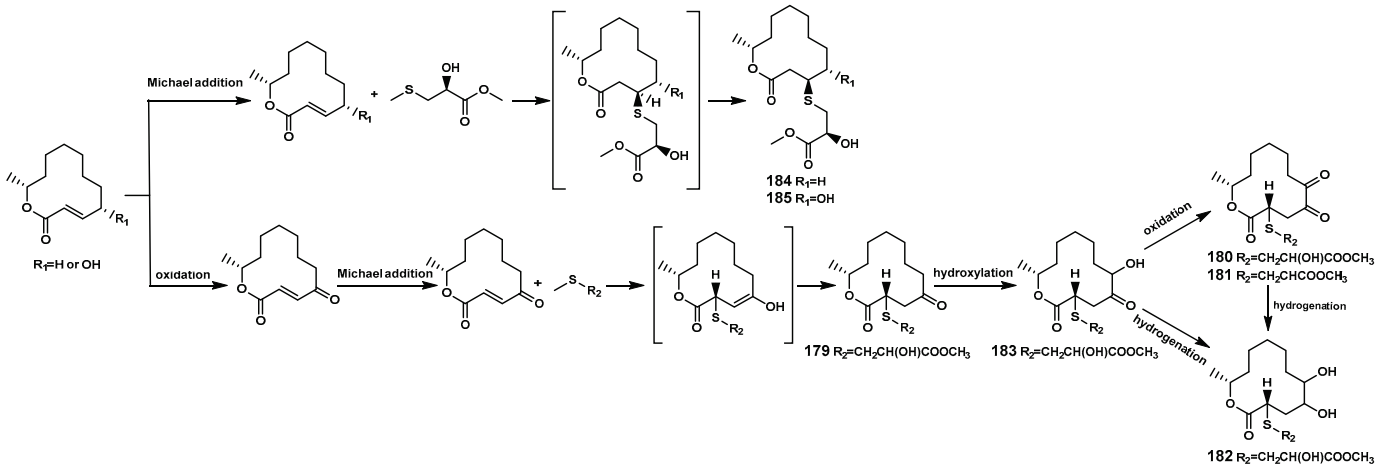

Figure 9. The proposed biosynthetic pathway of sulfur-containing 12-membered macrocyclic lactones (**179**–**185**).

2.4. Alkaloids and Peptides

Alkaloids constitute a class of naturally occurring organic compounds with at least one nitrogen atom, primarily derived from amino acids. They typically exhibit complex cyclic structures, with some playing crucial roles in plant defense mechanisms [81]. Currently, researchers have identified 33 alkaloids (Table 7 and Figure 10) with different types from *B. gymnorrhiza* plant and endophytic fungi in *B. gymnorrhiza* and *B. sexangula var. rhynchopetala*, including amine (**186**) and amide types (**187**–**191**), indole (**192–193**), pyrimidine (**194**) and purine types (**195–196**), tropane (**197**), pyrrolidine (**198**), pyrrolizidine (**199**), quinazoline (**200**–**201**), quinoline (**202–204**), benzodiazepine (**205**), diketopiperazine (**206–211**), and cyclohexylideneacetonitrile derivatives (**212**–**218**). Studies indicate a significant correlation between endophytes and alkaloid [82]. Among the alkaloid-producing endophytic fungi, 66% belong to the *Penicillium* genus, and 75% of the alkaloids isolated from endophytic fungi are derived from the *Penicillium* genus. Clearly, within the endophytic communities of *Bruguiera*, the *Penicillium* genus likely serves as the dominant producer of alkaloids. Additionally, Li et al. [68] isolated a 7-membered 2,5-dioxopiperazine alkaloid (+)-cyclopenol (**205**), from an endophytic fungus *Penicillium sclerotiorum* in the inner bark of *B. gymnorrhiza*. In the terrestrial plant *Garcinia atroviridis*, the endophytic fungus *P. sclerotiorum* produces azaphilone-type derivatives [83]. (-)-cyclopenol, which shares a biosynthetic pathway similar to **205**, was also isolated from terrestrial soil *Penicillium* genus [68,84]. This suggests that the mechanism of (+)-cyclopenol production may be associated with the unique habitat of mangroves.

Compounds **219**–**229** (Table 7 and Figure 10) are peptides derived from endophytic fungi found in *B. gymnorrhiza* and *B. sexangula var. rhynchopetala*, including cyclic dipeptides (**219**–**225**), depsipeptide (**226**), cyclic tetrapeptide (**227**), and lumazines (**228**–**229**).

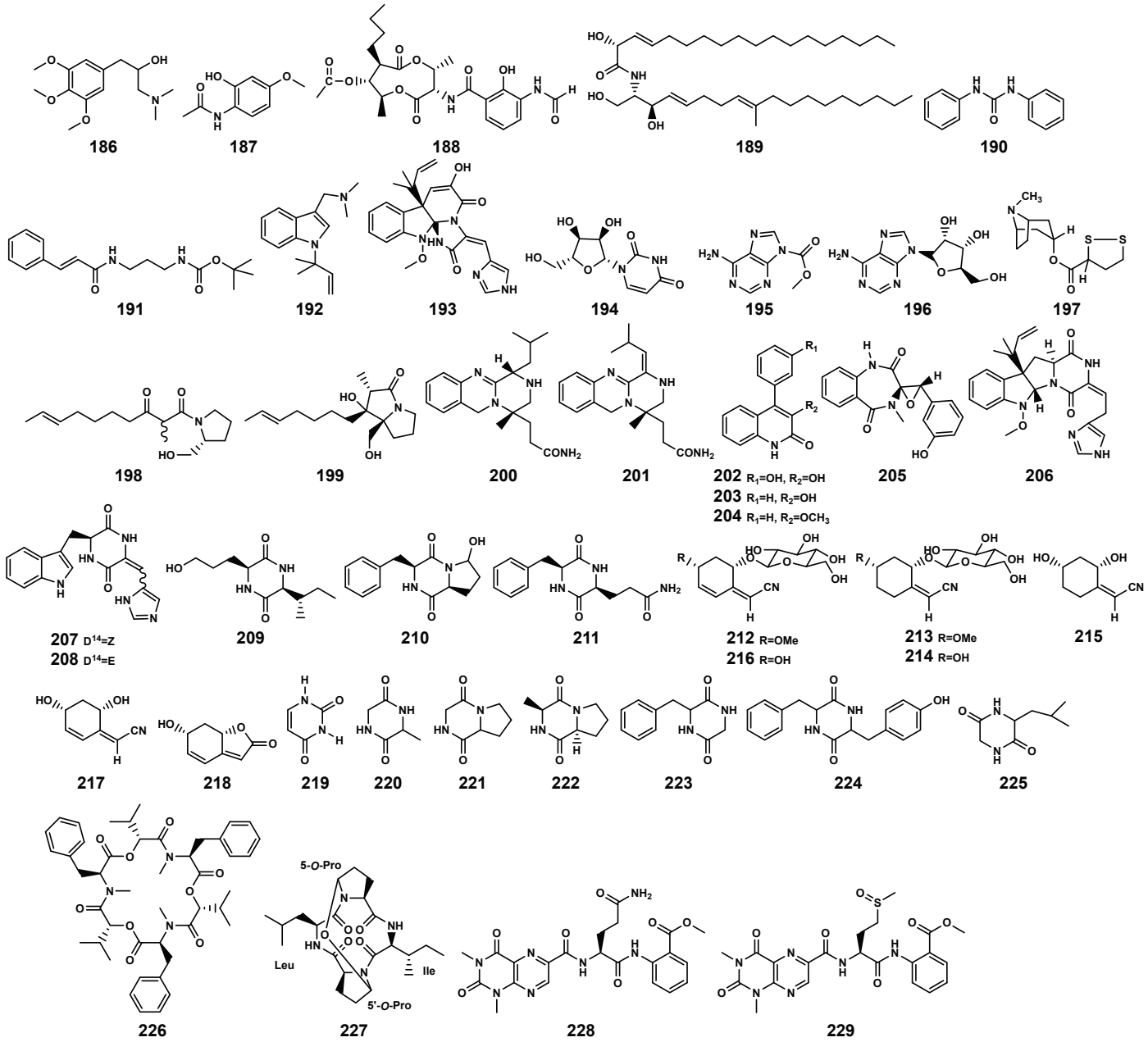

Figure 10. Alkaloids (**186**–**218**) and peptides (**219**–**229**) isolated from *Bruguiera* genus plants and their endophytes.

Table 7. Alkaloids and Peptides isolated from *Bruguiera* genus plants and their endophytes.

No.	Compound	Source	Reference
186	Gymnorrhizin A	*B. gymnorrhiza*, hypocotyl	[85]
187	N-(2-hydroxy-4-methoxyphenyl)acetamide	*P. thomi* (the root of *B. gymnorrhiza*, endophytic fungus)	[66]
188	Antimycin A18	*Streptomyces albidoflavus* 107A-01824 (the leaf of *B. gymnorrhiza*, endophytic actinomycete)	[86]
189	(2*S*,2′*R*,3*R*,4*E*,8*E*,3′*E*)-2-(2′-hydroxy-3′-octadecenoylamino)-9-methyl-4,8-octadecadiene-l,3-diol	*P. longicolla* HL-2232 (the leaf *B. sexangula var. rhynchopetala*, endophytic fungus)	[67]

Table 7. *Cont*.

No.	Compound	Source	Reference
190	N,N′-diphenyl urea	*P. longicolla* HL-2232 (the leaf *B. sexangula var. rhynchopetala*, endophytic fungus)	[67]
191	(*E*)-tert-butyl(3-cinnamamidopropyl)carbamate	*P. citrinum* HL-5126 (*B. sexangula var. rhynchopetala*, endophytic fungus)	[87]
192	3-(dimethylaminomethyl)-1-(1,1-dimethyl-2-propenyl)indole	*P. sclerotiorum* (the inner bark of *B. gymnorrhiza*, endophytic fungus)	[68]
193	Meleagrin	*Penicillium sp.* GD6 (the stem bark of *B. gymnorrhiza*, endophytic fungus)	[88]
194	Uridine	*P. longicolla* HL-2232 (the leaf *B. sexangula var. rhynchopetala*, endophytic fungus)	[67]
195	6-aminopurine-9-carboxylic acid methyl ester	*P. longicolla* HL-2232 (the leaf *B. sexangula var. rhynchopetala*, endophytic fungus)	[67]
196	Adenine riboside	*P. longicolla* HL-2232 (the leaf *B. sexangula var. rhynchopetala*, endophytic fungus)	[67]
197	Brugine	*B. sexangula*, stem bark; *B. cylindrica*, stem and bark	[11,77,89]
198	Scalusamide A	*Penicillium sp.* GD6 (the stem bark of *B. gymnorrhiza*, endophytic fungus)	[88]
199	Penibruguieramine A	*Penicillium sp.* GD6 (the stem bark of *B. gymnorrhiza*, endophytic fungus)	[88]
200	Anacine	*P. sclerotiorum* (the inner bark of *B. gymnorrhiza*, endophytic fungus)	[68]
201	Aurantiomide C	*P. sclerotiorum* (the inner bark of *B. gymnorrhiza*, endophytic fungus)	[68]
202	Viridicatol	*P. sclerotiorum* (the inner bark of *B. gymnorrhiza*, endophytic fungus)	[68]
203	Viridicatin	*P. sclerotiorum* (the inner bark of *B. gymnorrhiza*, endophytic fungus)	[68]
204	3-O-methylviridicatin	*P. sclerotiorum* (the inner bark of *B. gymnorrhiza*, endophytic fungus)	[68]
205	(+)-Cyclopenol	*P. sclerotiorum* (the inner bark of *B. gymnorrhiza*, endophytic fungus)	[68]
206	Roquefortine F	*Penicillium sp.* GD6 (the stem bark of *B. gymnorrhiza*, endophytic fungus)	[88]
207	Penilloid A	*Penicillium sp.* GD6 (the stem bark of *B. gymnorrhiza*, endophytic fungus)	[90]
208	Cyclo(dehydrohistidyl-L-tryptophyl)	*Penicillium sp.* GD6 (the stem bark of *B. gymnorrhiza*, endophytic fungus)	[90]
209	5*S*-hydroxynorvalines-Ile	*Penicillium sp.* GD6 (the stem bark of *B. gymnorrhiza*, endophytic fungus)	[90]
210	3*S*-hydroxylcyclo(*S*-Pro-*S*-Phe)	*Penicillium sp.* GD6 (the stem bark of *B. gymnorrhiza*, endophytic fungus)	[90]
211	Cyclo(*S*-Phe-*S*-Gln)	*Penicillium sp.* GD6 (the stem bark of *B. gymnorrhiza*, endophytic fungus)	[90]
212	Menisdurin B	*B. gymnorrhiza*, hypocotyl	[91]
213	Menisdurin C	*B. gymnorrhiza*, hypocotyl	[91]
214	Menisdurin D	*B. gymnorrhiza*, hypocotyl	[91]

Table 7. *Cont.*

No.	Compound	Source	Reference
215	Menisdurin E	*B. gymnorrhiza*, hypocotyl	[91]
216	Menisdurin	*B. gymnorrhiza*, hypocotyl	[91]
217	Coclauril	*B. gymnorrhiza*, hypocotyl	[91]
218	Menisdaurilide	*B. gymnorrhiza*, hypocotyl	[91]
219	Uracil	*P. thomi* (the root of *B. gymnorrhiza*, endophytic fungus)	[66]
220	Cyclo-(Ala-Gly)	*P. thomi* (the root of *B. gymnorrhiza*, endophytic fungus); *Penicillium citrinum* ZD6 (the stem of *B. gymnorrhiza*, endophytic fungus)	[66,92]
221	Cyclo-(Pro-Gly)	*P. thomi* (the root of *B. gymnorrhiza*, endophytic fungus)	[66]
222	Cyclo-(Ala-Pro)	*P. thomi* (the root of *B. gymnorrhiza*, endophytic fungus)	[66]
223	3-benzylpiperazine-2,5-dione	*Gloesporium sp.* (*B. gymnorrhiza*, endophytic fungus)	[93]
224	3-benzyl-6-(4-hydroxybenzyl) piperazine-2,5-dione	*Gloesporium sp.* (*B. gymnorrhiza*, endophytic fungus)	[93]
225	3-(2-methylpropyl)-2,5-piperazinedione	*Gloesporium sp.* (*B. gymnorrhiza*, endophytic fungus)	[93]
226	Beauvericin	*A. terreus* No. GX7-3B (the branch of *B. gymnorrhiza*, endophytic fungus)	[69]
227	5,5′-epoxy-MKN-349A	*Penicillium sp.* GD6 (the stem bark of *B. gymnorrhiza*, endophytic fungus)	[70]
228	Aspergilumamide A	*Aspergillus sp.* 33241 (*B. sexangula var. rhynchopetala*, fungus)	[94]
229	Penilumamide	*Aspergillus sp.* 33241 (*B. sexangula var. rhynchopetala*, fungus)	[94]

2.5. Quinones

Plants are the primary producers of quinones [95], but in *Bruguiera* genus plants and their endophytes, 87.5% of quinones originate from endophytic fungi. The identified quinones (Table 8 and Figure 11) include benzoquinones (**230–231**), naphthalenes (**232–242**), naphthalenones (**243**–**246**), naphthofurans (**247**–**248**), naphthoquinones (**249**–**256**), xanthones (**257**–**266**), and anthraquinones (**267**–**295**). Among these, 41.2% of quinones sourced from endophytic fungi exhibit antibacterial activity. Studies have shown that fungi can commonly reduce 2,6-dimethoxy-1,4-benzoquinone (**230**) to hydroquinones, and some fungi showed effects of quinone-dependent polymer polystyrene sulfonate degradation, contributing to driving fungi to utilize the redox cycling of quinones for biodegradation in the ecological environment [96]. In plant immunity, quinone-related molecules could play a role as pathogen- or danger-associated molecular patterns [95]. The series of evidence underscores the ecological significance of quinone substances.

Table 8. Quinones isolated from *Bruguiera* genus plants and their endophytes.

No.	Compound	Source	Reference
230	2,6-dimethoxy-1,4-benzoquinone	*B. sexangula var. rhynchopetala*, stem	[41]
231	2-chloro-5-methoxy-3-methylcyclohexa-2,5-diene-1,4-dione	*Xylaria cubensis* PSU-MA34 (the branch of *B. parviflora*, endophytic fungus)	[97]
232	Palmarumycins BG1	*B. gymnorrhiza*, stem and leaf	[98]
233	Palmarumycins BG2	*B. gymnorrhiza*, stem and leaf	[98]
234	Palmarumycins BG3	*B. gymnorrhiza*, stem and leaf	[98]
235	Palmarumycins BG4	*B. gymnorrhiza*, stem and leaf	[98]
236	Palmarumycins BG5	*B. gymnorrhiza*, stem and leaf	[98]

Table 8. *Cont.*

No.	Compound	Source	Reference
237	Palmarumycins BG6	*B. gymnorrhiza*, stem and leaf	[98]
238	Palmarumycins BG7	*B. gymnorrhiza*, stem and leaf	[98]
239	Preussomerin BG1	*B. gymnorrhiza*, stem and leaf	[98]
240	8-methoxy-1-naphthol	*Daldinia eschscholtzii* PSU-STD57 (the leaf of *B. gymnorrhiza*, endophytic fungus)	[99]
241	1,8-dimethoxynaphthalene	*D. eschscholtzii* PSU-STD57 (the leaf of *B. gymnorrhiza*, endophytic fungus); *Daldinia eschscholtzii* HJ001 (*B. sexangula var. rhynchopetala*, endophytic fungus)	[99,100]
242	Nigronatthaphenyl	*Nigrospora sphaerica* (the mature leaf of *B. gymnorrhiza*, endophytic fungus)	[101]
243	(3*S*)-3,8-dihydroxy-6,7-dimethyl-*α*-tetralone	*D. eschscholtzii* PSU-STD57 (the leaf of *B. gymnorrhiza*, endophytic fungus)	[99]
244	Isosclerone	*D. eschscholtzii* PSU-STD57 (the leaf of *B. gymnorrhiza*, endophytic fungus); *X. cubensis* PSU-MA34 (the branch of *B. parviflora*, endophytic fungus)	[97,99]
245	(4*S*)-3,4-dihydro-4,8-dihydroxy-l(2*H*)-naphthalenoe	*P. citrinum* HL-5126 (the leaf of *B. sexangula var. rhynchopetala*, endophytic fungus)	[102]
246	Regiolone	*P. capitalensis* (the hypocotyl of *B. sexangula*, endophytic fungus)	[64]
247	1,3,8-trimethoxynaphtho[9–c]furan	*D. eschscholtzii* HJ004 (the stem of *B. sexangula var. rhynchopetala*, endophytic fungus)	[103]
248	4-O-methyl eleutherol	*D. eschscholtzii* HJ004 (the stem of *B. sexangula var. rhynchopetala*, endophytic fungus)	[103]
249	8-hydroxy-2-[1-hydroxyethyl]-5,7-dimethoxynaphtho[2,3-b] thiophene-4,9-dione	*A. terreus* No. GX7-3B (the branch of *B. gymnorrhiza*, endophytic fungus)	[69]
250	Anhydrojavanicin	*A. terreus* No. GX7-3B (the branch of *B. gymnorrhiza*, endophytic fungus)	[69]
251	8-O-methylbostrycoidin	*A. terreus* No. GX7-3B (the branch of *B. gymnorrhiza*, endophytic fungus)	[69]
252	8-O-methyljavanicin	*A. terreus* No. GX7-3B (the branch of *B. gymnorrhiza*, endophytic fungus)	[69]
253	Botryosphaerone D	*A. terreus* No. GX7-3B (the branch of *B. gymnorrhiza*, endophytic fungus)	[69]
254	6-ethyl-5-hydroxy-3,7-dimethoxynaphthoquinone	*A. terreus* No. GX7-3B (the branch of *B. gymnorrhiza*, endophytic fungus)	[69]
255	5-hydroxy-2-methoxy-6,7-dimethyl-1,4-naphthoquinone	*D. eschscholtzii* HJ004 (the stem of *B. sexangula var. rhynchopetala*, endophytic fungus)	[103]
256	5-hydroxy-2-methoxynaphtho[9–c] furan-1,4-dione	*D. eschscholtzii* HJ004 (the stem of *B. sexangula var. rhynchopetala*, endophytic fungus)	[103]
257	Incarxanthone A	*Peniophora incarnata* Z4 (*B. gymnorrhiza*, endophytic fungus)	[104]
258	Incarxanthone B	*P. incarnata* Z4 (*B. gymnorrhiza*, endophytic fungus)	[104]
259	Incarxanthone C	*P. incarnata* Z4 (*B. gymnorrhiza*, endophytic fungus)	[104]
260	Incarxanthone D	*P. incarnata* Z4 (*B. gymnorrhiza*, endophytic fungus)	[104]
261	Incarxanthone E	*P. incarnata* Z4 (*B. gymnorrhiza*, endophytic fungus)	[104]
262	Incarxanthone F	*P. incarnata* Z4 (*B. gymnorrhiza*, endophytic fungus)	[104]
263	2,8-Dihydroxyvertixanthone	*P. incarnata* Z4 (*B. gymnorrhiza*, endophytic fungus)	[104]
264	Globosuxanthone B	*P. incarnata* Z4 (*B. gymnorrhiza*, endophytic fungus)	[104]
265	4-chloro-1-hydroxy-3-methoxy-6-methyl-8-methoxycarbonyl-xanthen-9-one	*P. citrinum* HL-5126 (*B. sexangula var. rhynchopetala*, endophytic fungus)	[105]
266	Chloroisosulochrin dehydrate	*P. citrinum* HL-5126 (*B. sexangula var. rhynchopetala*, endophytic fungus)	[105]

Table 8. *Cont.*

No.	Compound	Source	Reference
267	Emodin	*P. citrinum* ZD6 (the stem of *B. gymnorrhiza*, endophytic fungus)	[92]
268	Auxarthrol C	*Stemphylium sp.* 33231 (*B. sexangula var. rhynchopetala*, endophytic fungus)	[106]
269	Macrosporin-2-O-(6′-acetyl)-*α*-D-glucopyranoside	*Stemphylium sp.* 33231 (*B. sexangula var. rhynchopetala*, endophytic fungus)	[106]
270	Macrosporin	*Stemphylium sp.* 33231 (*B. sexangula var. rhynchopetala*, endophytic fungus)	[106]
271	Macrosporin-7-O-sulfate	*Stemphylium sp.* 33231 (*B. sexangula var. rhynchopetala*, endophytic fungus)	[106]
272	2-O-acetylaltersolanol B	*Stemphylium sp.* 33231 (*B. sexangula var. rhynchopetala*, endophytic fungus)	[106]
273	Altersolanol A	*Stemphylium sp.* 33231 (*B. sexangula var. rhynchopetala*, endophytic fungus)	[106]
274	Altersolanol B	*Stemphylium sp.* 33231 (*B. sexangula var. rhynchopetala*, endophytic fungus); *P. longicolla* HL-2232 (the leaf of *B. sexangula var. rhynchopetala*, endophytic fungus)	[106,107]
275	Altersolanol C	*Stemphylium sp.* 33231 (*B. sexangula var. rhynchopetala*, endophytic fungus)	[106]
276	2-O-acetylaltersolanol L	*Stemphylium sp.* 33231 (*B. sexangula var. rhynchopetala*, endophytic fungus)	[106]
277	Altersolanol L	*Stemphylium sp.* 33231 (*B. sexangula var. rhynchopetala*, endophytic fungus)	[106]
278	Ampelanol	*Stemphylium sp.* 33231 (*B. sexangula var. rhynchopetala*, endophytic fungus)	[106]
279	Tetrahydroaltersolanol B	*Stemphylium sp.* 33231 (*B. sexangula var. rhynchopetala*, endophytic fungus)	[106]
280	Dihydroaltersolanol A	*Stemphylium sp.* 33231 (*B. sexangula var. rhynchopetala*, endophytic fungus)	[106]
281	Alterporriol T	*Stemphylium sp.* 33231 (*B. sexangula var. rhynchopetala*, endophytic fungus)	[106]
282	Alterporriol U	*Stemphylium sp.* 33231 (*B. sexangula var. rhynchopetala*, endophytic fungus)	[106]
283	Alterporriol V	*Stemphylium sp.* 33231 (*B. sexangula var. rhynchopetala*, endophytic fungus)	[106]
284	Alterporriol W	*Stemphylium sp.* 33231 (*B. sexangula var. rhynchopetala*, endophytic fungus)	[106]
285	Alterporriol A	*Stemphylium sp.* 33231 (*B. sexangula var. rhynchopetala*, endophytic fungus)	[106]
286	Alterporriol B	*Stemphylium sp.* 33231 (*B. sexangula var. rhynchopetala*, endophytic fungus)	[106]
287	Alterporriol D	*Stemphylium sp.* 33231 (*B. sexangula var. rhynchopetala*, endophytic fungus)	[106]
288	Alterporriol E	*Stemphylium sp.* 33231 (*B. sexangula var. rhynchopetala*, endophytic fungus)	[106]
289	Alterporriol C	*Stemphylium sp.* 33231 (*B. sexangula var. rhynchopetala*, endophytic fungus)	[106]
290	Alterporriol N	*Stemphylium sp.* 33231 (*B. sexangula var. rhynchopetala*, endophytic fungus)	[106]
291	Alterporriol R	*Stemphylium sp.* 33231 (*B. sexangula var. rhynchopetala*, endophytic fungus)	[106]
292	Alterporriol Q	*Stemphylium sp.* 33231 (*B. sexangula var. rhynchopetala*, endophytic fungus)	[106]
293	2′-acetoxy-7-chlorocitreorosein	*P. citrinum* HL-5126 (*B. sexangula var. rhynchopetala*, endophytic fungus)	[105]

Table 8. *Cont.*

No.	Compound	Source	Reference
294	Citreorosein	*P. citrinum* HL-5126 (*B. sexangula var. rhynchopetala*, endophytic fungus)	[105]
295	MT-1	*P. citrinum* HL-5126 (*B. sexangula var. rhynchopetala*, endophytic fungus)	[105]

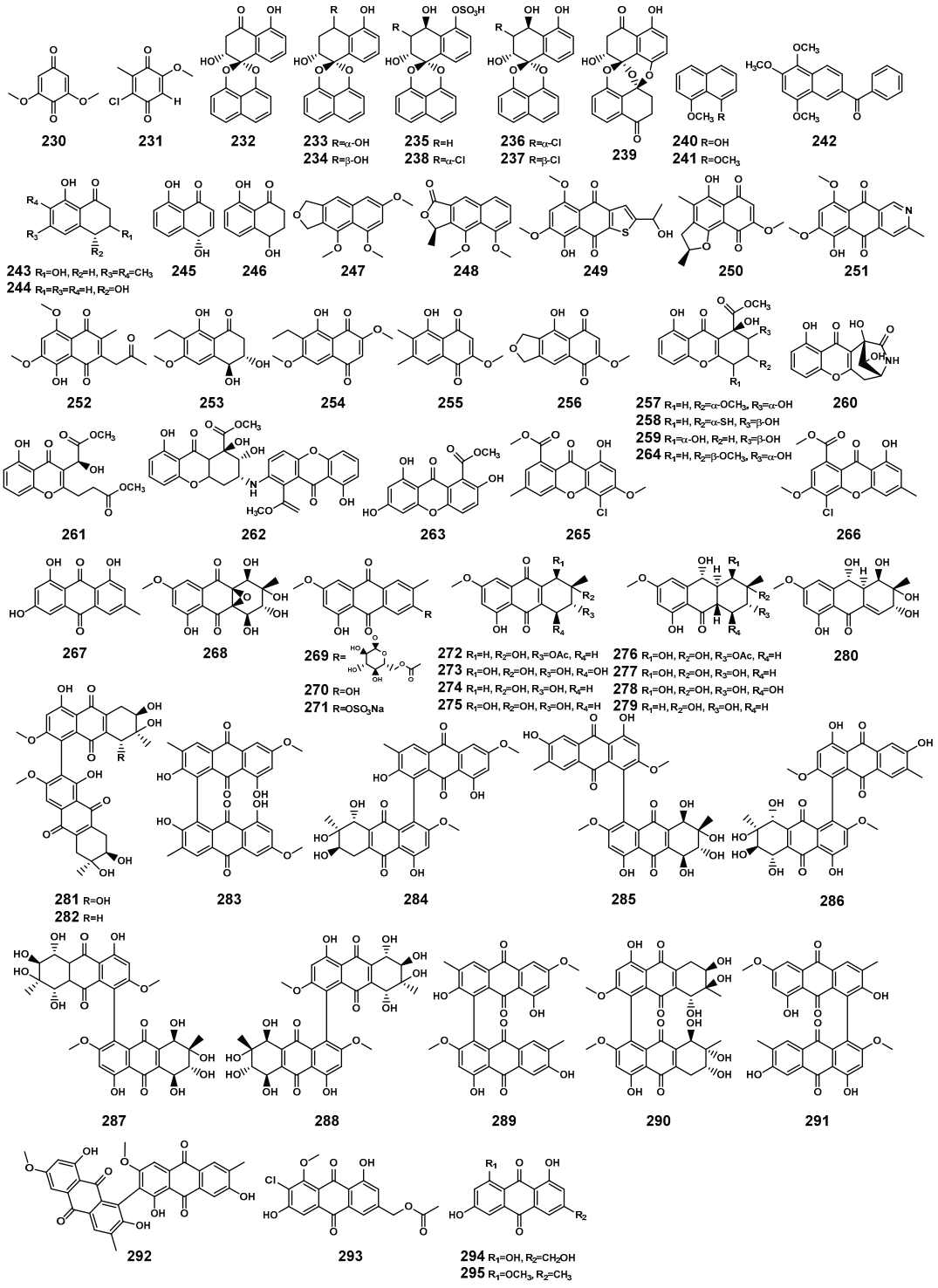

Figure 11. Quinones (**230**–**295**) isolated from *Bruguiera* genus plants and their endophytes.

2.6. Polyketides

In the genus *Bruguiera* and its endophytes, polyketides primarily exhibit antibacterial and cytotoxic activities, predominantly sourced from endophytes of the *Bruguiera* genus. These polyketides (Table 9 and Figure 12) encompass various types, including cytochalasins (**296**–**314**), phenols (**315**–**328**), ansamycins (**329**–**336**), 12-membered macrolides (**337**–**341**), α-pyrone (**342–346**), chromanone (**347**), furanones (**348–354**), sorbicillinoids (**355**–**362**), and benzofuranones (**363**). Supratman et al. [108] isolated (-)-dihydrovertinolide (**352**) from endophytic fungus *C. rosea* B5-2 obtained from the branch of *B. gymnorrhiza*. The compound **352** exhibited no antibacterial activity but demonstrated phytotoxicity to lettuce seedlings (*Lactuca sativa* L.) [108]. This effect may enhance the competitive abilities of *B. gymnorrhiza* with other plants in terms of nutrients and space [109], contributing to the reinforcement of *B. gymnorrhiza* plant defense mechanisms. It could serve as a lead compound for the development of potential bioherbicides.

Table 9. Polyketides isolated from *Bruguiera* genus plants and their endophytes.

No.	Compound	Source	Reference
296	Cytochalasin D	*B. gymnorrhiza*; *Xylaria arbuscula* GZS74 (the fruit of *B. gymnorrhiza*, endophytic fungus) *X. cubensis* PSU-MA34 (the branch of *B. parviflora*, endophytic fungus)	[35,97,110]
297	Zygosporin D	*B. gymnorrhiza*; *X. arbuscula* GZS74 (the fruit of *B. gymnorrhiza*, endophytic fungus)	[35,110]
298	[11]-cytochalasa-5(6),13-diene-1,21-dione-7,18-dihydroxy-16,18-dimethyl-10-phenyl(7*S**,13*E*,16*S**,18*R**)	*D. eschscholtzii* HJ001 (*B. sexangula var. rhynchopetala*, endophytic fungus)	[100]
299	[11]-cytochalasa-6(12),13-diene-1,21-dione-7,18-dihydroxy16,18-dimethyl-10-phenyl-(7*S**,13*E*,16*S**,18*R**)	*D. eschscholtzii* HJ001 (*B. sexangula var. rhynchopetala*, endophytic fungus)	[100]
300	Arbuschalasins A	*X. arbuscula* GZS74 (the fruit of *B. gymnorrhiza*, endophytic fungus)	[110]
301	Arbuschalasins B	*X. arbuscula* GZS74 (the fruit of *B. gymnorrhiza*, endophytic fungus)	[110]
302	Arbuschalasins C	*X. arbuscula* GZS74 (the fruit of *B. gymnorrhiza*, endophytic fungus)	[110]
303	Arbuschalasins D	*X. arbuscula* GZS74 (the fruit of *B. gymnorrhiza*, endophytic fungus)	[110]
304	Cytochalasin Q	*X. arbuscula* GZS74 (the fruit of *B. gymnorrhiza*, endophytic fungus)	[110]
305	12-hydroxylcytochalasin Q	*X. arbuscula* GZS74 (the fruit of *B. gymnorrhiza*, endophytic fungus)	[110]
306	Cytochalasin D-13,14-epoxid	*X. arbuscula* GZS74 (the fruit of *B. gymnorrhiza*, endophytic fungus)	[110]
307	19,20-epoxycytochalasin D	*X. arbuscula* GZS74 (the fruit of *B. gymnorrhiza*, endophytic fungus)	[110]
308	Cytochalasin O	*X. arbuscula* GZS74 (the fruit of *B. gymnorrhiza*, endophytic fungus)	[110]
309	Cytochalasin P	*X. arbuscula* GZS74 (the fruit of *B. gymnorrhiza*, endophytic fungus)	[110]

Table 9. *Cont*.

No.	Compound	Source	Reference
310	Cytochalasin C	*X. arbuscula* GZS74 (the fruit of *B. gymnorrhiza*, endophytic fungus)	[110]
311	Deacetylcytochalasin C	*X. arbuscula* GZS74 (the fruit of *B. gymnorrhiza*, endophytic fungus)	[110]
312	6,7-dihydro-7-oxo-cytochalasin C	*X. arbuscula* GZS74 (the fruit of *B. gymnorrhiza*, endophytic fungus)	[110]
313	6,7-dihydro-7-oxo-deacetylcytochalasin C	*X. arbuscula* GZS74 (the fruit of *B. gymnorrhiza*, endophytic fungus)	[110]
314	19, 20-epoxycytochalasin C	*X. arbuscula* GZS74 (the fruit of *B. gymnorrhiza*, endophytic fungus)	[110]
315	1,10-dihydroxy-8-methyldibenz[b, e] oxepin-6,11-dione	No. GX4-1B (the branch of *B. gymnorrhiza*, endophytic fungus)	[111]
316	1,10-dihydroxy-dibenz[b, e]oxepin-6,11-dione	No. GX4-1B (the branch of *B. gymnorrhiza*, endophytic fungus)	[111]
317	2-deoxy-sohirnone C	*Penicillium sp.* GD6 (the stem bark of *B. gymnorrhiza*, endophytic fungus)	[90]
318	Sohirnone A	*Penicillium sp.* GD6 (the stem bark of *B. gymnorrhiza*, endophytic fungus)	[90]
319	3,4-dihydroxybenzoic acid	*P. capitalensis* (the hypocotyl of *B. sexangula*, endophytic fungus)	[64]
320	Penibenzophenone A	*P. citrinum* HL-5126 (*B. sexangula var. rhynchopetala*, endophytic fungus)	[87]
321	Penibenzophenone B	*P. citrinum* HL-5126 (*B. sexangula var. rhynchopetala*, endophytic fungus)	[87]
322	Sulochrin	*P. citrinum* HL-5126 (*B. sexangula var. rhynchopetala*, endophytic fungus)	[87]
323	Sorbicillin	*Trichoderma reesei* SCNU-F0042 (the fresh bark of *B. gymnorrhiza*, endophytic fungus)	[112]
324	Asterric acid	*P. citrinum* HL-5126 (*B. sexangula var. rhynchopetala*, endophytic fungus)	[87]
325	N-butyl asterrate	*P. citrinum* HL-5126 (*B. sexangula var. rhynchopetala*, endophytic fungus)	[87]
326	8-O-methylnodulisporin F	*D. eschscholtzii* HJ004 (the stem of *B. sexangula var. rhynchopetala*, endophytic fungus)	[103]
327	Nodulisporin H	*D. eschscholtzii* HJ004 (the stem of *B. sexangula var. rhynchopetala*, endophytic fungus)	[103]
328	Epicoccolide A	*Epicoccum nigrum* MLY-3 (the leaf of *B. gymnorrhiza*, endophytic fungus)	[113]
329	Divergolide A	*Streptomyces sp.* (*B. gymnorrhiza*, endophytic bacteria)	[22]
330	Divergolide B	*Streptomyces sp.* (*B. gymnorrhiza*, endophytic bacteria)	[22]
331	Divergolide C	*Streptomyces sp.* (*B. gymnorrhiza*, endophytic bacteria)	[22]
332	Divergolide D	*Streptomyces sp.* (*B. gymnorrhiza*, endophytic bacteria)	[22]
333	Divergolide E	*Streptomyces sp.* (*B. gymnorrhiza*, endophytic bacteria)	[22]
334	Divergolide F	*Streptomyces sp.* (*B. gymnorrhiza*, endophytic bacteria)	[22]
335	Divergolide G	*Streptomyces sp.* (*B. gymnorrhiza*, endophytic bacteria)	[22]
336	Divergolide H	*Streptomyces sp.* (*B. gymnorrhiza*, endophytic bacteria)	[22]

Table 9. *Cont*.

No.	Compound	Source	Reference
337	Seco-patulolide C	*C. cladosporioides* MA-299 (the leaf of *B. gymnorrhiza*, endophytic fungus)	[21]
338	5*R*-hydroxyrecifeiolide	*C. cladosporioides* MA-299 (the leaf of *B. gymnorrhiza*, endophytic fungus)	[114]
339	5*S*-hydroxyrecifeiolide	*C. cladosporioides* MA-299 (the leaf of *B. gymnorrhiza*, endophytic fungus)	[114]
340	Pandangolide 1	*C. cladosporioides* MA-299 (the leaf of *B. gymnorrhiza*, endophytic fungus)	[114]
341	Cladocladosin A	*C. cladosporioides* MA-299 (the leaf of *B. gymnorrhiza*, endophytic fungus)	[75]
342	Verrucosidin	*P. sclerotiorum* (the inner bark of *B. gymnorrhiza*, endophytic fungus)	[68]
343	Acetylchrysopyrone B	*T. reesei* SCNU-F0042 (the fresh bark of *B. gymnorrhiza*, endophytic fungus)	[112]
344	Saturnispol H	*T. reesei* SCNU-F0042 (the fresh bark of *B. gymnorrhiza*, endophytic fungus)	[112]
345	Infectopyrone A	*Stemphylium sp.* 33231 (the leaf *B. sexangula var. rhynchopetala*, endophytic fungus)	[106]
346	Infectopyrone B	*Stemphylium sp.* 33231 (the leaf *B. sexangula var. rhynchopetala*, endophytic fungus)	[106]
347	6,8-dihydroxy-5-methoxy-3-methyl-1*H*-isochromen-1-one	*P. capitalensis* (the hypocotyl of *B. sexangula*, endophytic fungus)	[64]
348	*ent*-cladospolide F	*C. cladosporioides* MA-299 (the leaf of *B. gymnorrhiza*, endophytic fungus)	[114]
349	Cladospolide G	*C. cladosporioides* MA-299 (the leaf of *B. gymnorrhiza*, endophytic fungus)	[114]
350	Cladospolide H	*C. cladosporioides* MA-299 (the leaf of *B. gymnorrhiza*, endophytic fungus)	[114]
351	Iso-cladospolide B	*C. cladosporioides* MA-299 (the leaf of *B. gymnorrhiza*, endophytic fungus)	[114]
352	(-)-dihydrovertinolide	*C. rosea* B5-2 (the branch of *B. gymnorrhiza*, endophytic fungus)	[108]
353	(-)-vertinolide	*C. rosea* B5-2 (the branch of *B. gymnorrhiza*, endophytic fungus)	[108]
354	Xenofuranone B	*P. capitalensis* (the hypocotyl of *B. sexangula*, endophytic fungus)	[64]
355	14-hydroxybislongiquinolide	*T. reesei* SCNU-F0042 (the fresh bark of *B. gymnorrhiza*, endophytic fungus)	[112]
356	20-hydroxybislongiquinolide	*T. reesei* SCNU-F0042 (the fresh bark of *B. gymnorrhiza*, endophytic fungus)	[112]
357	14, 20-dihydroxybislongiquinolide	*T. reesei* SCNU-F0042 (the fresh bark of *B. gymnorrhiza*, endophytic fungus)	[112]
358	Bislongiquinolide	*T. reesei* SCNU-F0042 (the fresh bark of *B. gymnorrhiza*, endophytic fungus)	[112]
359	Trichodimerol	*T. reesei* SCNU-F0042 (the fresh bark of *B. gymnorrhiza*, endophytic fungus)	[112]
360	Bisorbicillinolide	*T. reesei* SCNU-F0042 (the fresh bark of *B. gymnorrhiza*, endophytic fungus)	[112]

Table 9. *Cont*.

No.	Compound	Source	Reference
361	Saturnispol B	*T. reesei* SCNU-F0042 (the fresh bark of *B. gymnorrhiza*, endophytic fungus)	[112]
362	Bisvertinolone	*T. reesei* SCNU-F0042 (the fresh bark of *B. gymnorrhiza*, endophytic fungus)	[112]
363	Penicitrinone acetate	*Penicillium sp.* B21 (the leaf *B. sexangula var. rhynchopetala*, endophytic fungus)	[115]

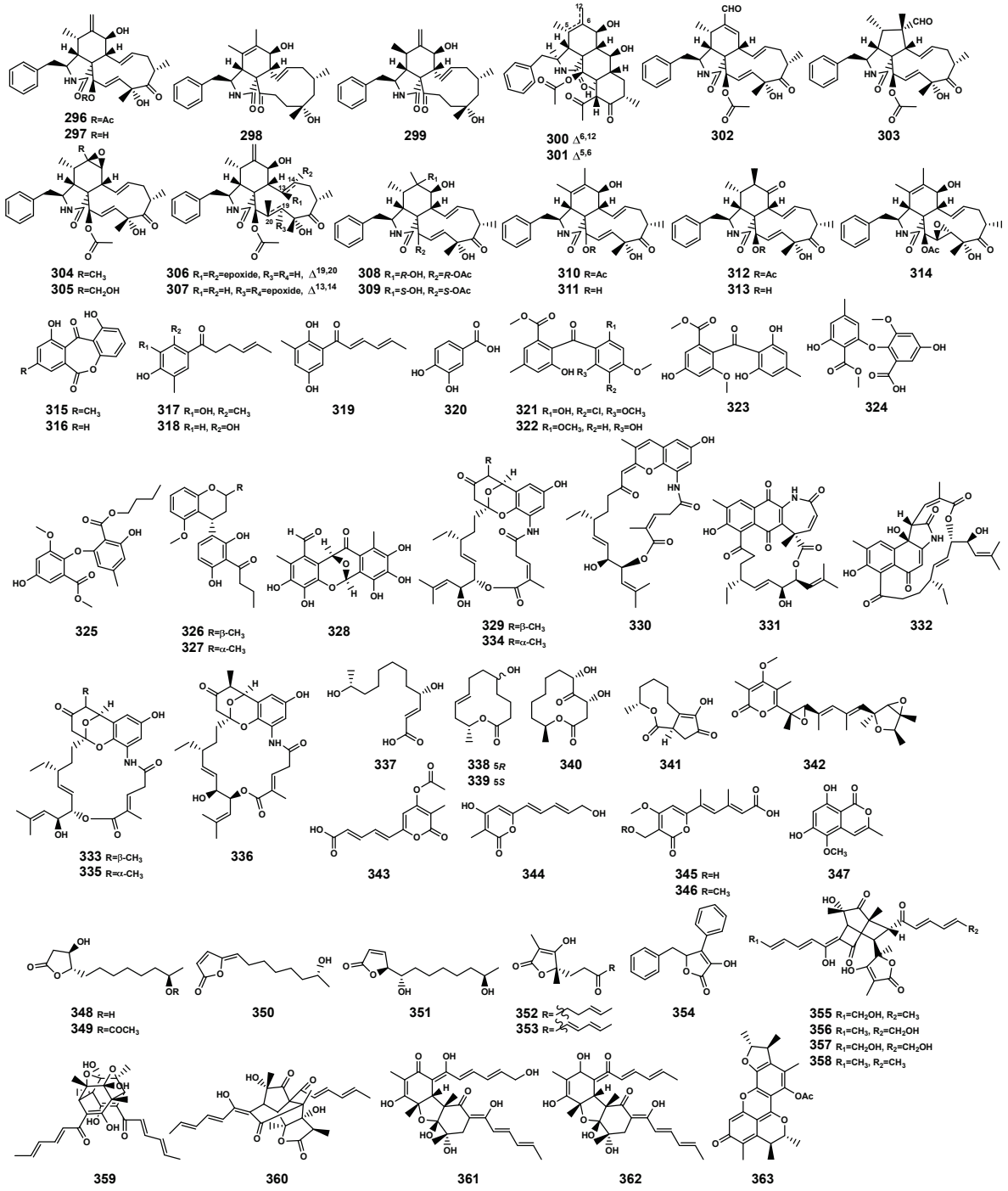

Figure 12. Polyketides (**296**–**363**) isolated from *Bruguiera* genus plants and their endophytes.

2.7. Flavonoids

Flavonoids are commonly present in the organs of plants, participating in the plant's response to environmental stressors [116]. Currently, in the genus *Bruguiera* and its endophytes, flavonoid (Table 10 and Figure 13) primarily originates from *B. gymnorrhiza* plants, including flavones (**364–367**), flavone glycosides (**372–375**), and flavonol glycosides (**376–381**). In the *B. parviflora* plant, dihydroflavonol (**368**) and flavonol (**369–371**) have been identified. Additionally, WU et al. [117] isolated a novel aurone glycoside compound (*Z*)-7,4′-dimethoxy-6-hydroxy-aurone-4-O-*β*-glucopyranoside (**382**) from the endophytic fungus *Penicillium citrinum* associated with *B. gymnorrhiza*, exhibiting significant neuroprotective activity.

Table 10. Flavonoids isolated from *Bruguiera* genus plants and their endophytes.

No.	Compound	Source	Reference
364	3′,4′,5′-trihydroxy-7-hydroxy-5-methoxyflavone	*B. gymnorrhiza*, leaf	[118,119]
365	Gramrione	*B. gymnorrhiza*, stem and leaf	[53,119]
366	3′,4′,5,7-tetrahydroxy methylflavone	*B. gymnorrhiza*, stem and leaf	[53]
367	5,7-dihydroxy-2-[3-hydroxy-4,5-dimethoxy-phenyl]-chromen-4-one	*B. gymnorrhiza*, leaf	[120]
368	Taxifolin	*B. parviflora*, leaf	[52]
369	Quercetin	*B. parviflora*, leaf	[52]
370	Myricetin	*B. parviflora*, leaf	[52]
371	Kaempferol	*B. parviflora*, leaf	[52]
372	Luteolin 5-methyl ether 7-O-*β*-D-glucopyranoside	*B. gymnorrhiza*, leaf	[119]
373	7,4′-dihydroxy-5,3′-dimethoxyflavone 7-O-*β*-D-glucopyranoside	*B. gymnorrhiza*, leaf	[119]
374	7,4′,5′-trihydroxy-5,3′-dimethoxyflavone 7-O-*β*-D- glucopyranoside	*B. gymnorrhiza*, leaf	[119]
375	7,4′-dihydroxy-5-methoxyflavone 7-O-*β*-D-glucopyranoside	*B. gymnorrhiza*, leaf	[119]
376	Quercetin-3-O-*β*-D-glucopyranoside	*B. gymnorrhiza*, stem and leaf	[53,119]
377	Astragalin	*B. gymnorrhiza*, stem and leaf	[53]
378	Rutin	*B. gymnorrhiza*, stem and leaf; *B. parviflora*, leaf	[52,53,119]
379	Kaempferol 3-O-rutinoside	*B. gymnorrhiza*, leaf	[119]
380	Myricetin 3-O-rutinoside	*B. gymnorrhiza*, leaf	[119]
381	Brugymnoside A	*B. gymnorrhiza*, hypocotyl	[121]
382	(Z)-7,4′-dimethoxy-6-hydroxy-aurone-4-O-*β*-glucopyranoside	*P. citrinum* (*B. gymnorrhiza*, endophytic fungus)	[117]

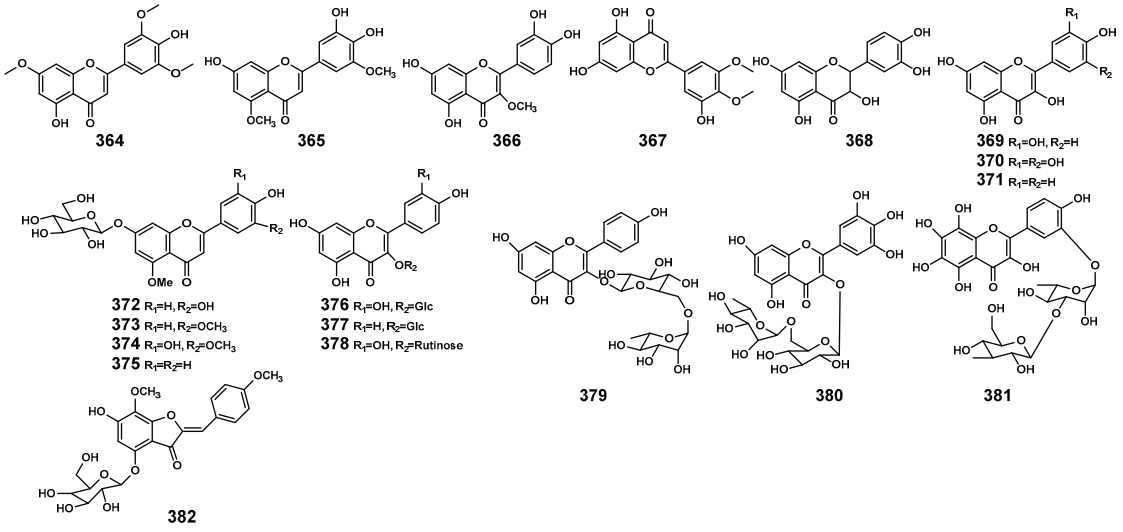

Figure 13. Flavonoids (**364–382**) isolated from *Bruguiera* genus plants and their endophytes.

2.8. Phenylpropanoids

The 38 phenylpropanoids (Table 11 and Figure 14) include phenylpropanoic acid (**383**), coumarins (**384–385**) and isocoumarins (**386**–**409**), and lignans (**410**–**420**). Among these, isocoumarins and lignans are the main compounds, originating from endophytic fungi associated with the *Bruguiera* genus and *Bruguiera* plants, respectively. Previous research has indicated that plant-derived coumarins have the potential to resist infections in both plants and animals [122], particularly scopoletin (**384**). When different plant species are exposed to multiple pathogens such as bacteria, fungi, oomycetes, and viruses, it can lead to the accumulation of **384**, thereby enhancing their resistance to diseases [123]. So, compound **384** in *B. gymnorrhiza* plants may serve as a crucial participant in the plant's chemical defense strategy against various pathogen invasions, contributing to the plant's ability to resist diseases.

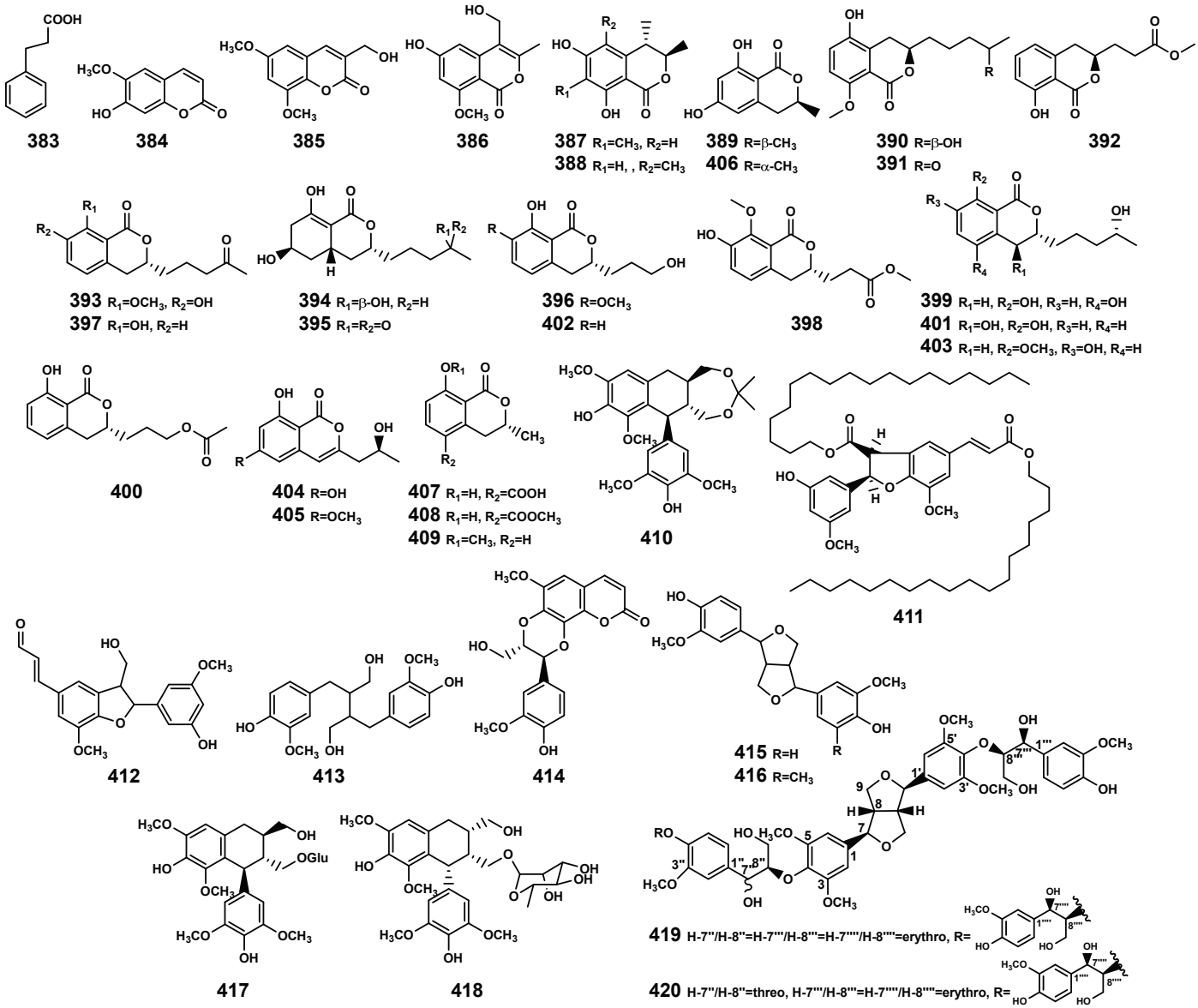

Figure 14. Phenylpropanoids (**383**–**420**) isolated from *Bruguiera* genus plants and their endophytes.

Table 11. Phenylpropanoids isolated from *Bruguiera* genus plants and their endophytes.

No.	Compound	Source	Reference
383	3-phenylpropanoic acid	*Gloesporium sp.* (*B. gymnorrhiza*, endophytic fungus)	[93]
384	Scopoletin	*B. gymnorrhiza*, hypocotyl	[124]
385	3-hydroxymethyl-6,8-dimethoxycoumarin	No. GX4-1B (the branch of *B. gymnorrhiza*, endophytic fungus)	[111]
386	6-hydroxy-4-hydroxymethyl-8-methoxy-3- methylisocoumarin	No. GX4-1B (the branch of *B. gymnorrhiza*, endophytic fungus)	[111]
387	(3*R**,4*S**)-6,8-dihydroxy-3,4,7-trimethylisocoumarin	*Penicillium sp.* 091402 (the root of *B. sexangula*, endophytic fungus)	[125]
388	(3*R*,4*S*)-6,8-dihydroxy-3,4,5-trimethylisocoumarin	*Penicillium sp.* 091402 (the root of *B. sexangula*, endophytic fungus)	[125]
389	€-6-hydroxymellein	*P. citrinum* HL-5126 (the leaf of *B. sexangula var. rhynchopetala*, endophytic fungus	[102]
390	Penicimarin G	*P. citrinum* HL-5126 (the leaf of *B. sexangula var. rhynchopetala*, endophytic fungus	[60]
391	Penicimarin H	*P. citrinum* HL-5126 (the leaf of *B. sexangula var. rhynchopetala*, endophytic fungus	[60]
392	Penicimarin I	*P. citrinum* HL-5126 (the leaf of *B. sexangula var. rhynchopetala*, endophytic fungus	[60]
393	Aspergillumarin A	*P. citrinum* HL-5126 (the leaf of *B. sexangula var. rhynchopetala*, endophytic fungus; *Penicillium sp.* TGM112 (*B. sexangula var. rhynchopetala*, fungus)	[60,61]
394	Peniciisocoumarin A	*Penicillium sp.* TGM112 (*B. sexangula var. rhynchopetala*, fungus)	[61]
395	Peniciisocoumarin B	*Penicillium sp.* TGM112 (*B. sexangula var. rhynchopetala*, fungus)	[61]
396	Peniciisocoumarin C	*Penicillium sp.* TGM112 (*B. sexangula var. rhynchopetala*, fungus)	[61]
397	Peniciisocoumarin D	*Penicillium sp.* TGM112 (*B. sexangula var. rhynchopetala*, fungus)	[61]
398	Peniciisocoumarin E	*Penicillium sp.* TGM112 (*B. sexangula var. rhynchopetala*, fungus)	[61]
399	Peniciisocoumarin F	*Penicillium sp.* TGM112 (*B. sexangula var. rhynchopetala*, fungus)	[61]
400	Peniciisocoumarin G	*Penicillium sp.* TGM112 (*B. sexangula var. rhynchopetala*, fungus)	[61]
401	Peniciisocoumarin H	*Penicillium sp.* TGM112 (*B. sexangula var. rhynchopetala*, fungus)	[61]
402	(*R*)-3-(3-hydroxypropyl)-8-hydroxy-3,4-dihydroisocoumarin	*Penicillium sp.* TGM112 (*B. sexangula var. rhynchopetala*, fungus)	[61]
403	Penicimarin C	*Penicillium sp.* TGM112 (*B. sexangula var. rhynchopetala*, fungus)	[61]
404	(-)-Orthosporin	*D. eschscholtzii* HJ004 (the stem of *B. sexangula var. rhynchopetala*, endophytic fungus)	[103]
405	Diaporthin	*D. eschscholtzii* HJ004 (the stem of *B. sexangula var. rhynchopetala*, endophytic fungus)	[103]
406	6-hydroxymellein	*D. eschscholtzii* HJ004 (the stem of *B. sexangula var. rhynchopetala*, endophytic fungus)	[103]

Table 11. *Cont.*

No.	Compound	Source	Reference
407	(*R*)-(-)-5-Carbonylmellein	*X. cubensis* PSU-MA34 (the branch of *B. parviflora*, endophytic fungus)	[97]
408	(*R*)-(-)-5-Methoxycarbonylmellein	*X. cubensis* PSU-MA34 (the branch of *B. parviflora*, endophytic fungus)	[97]
409	(*R*)-(-)-Mellein methyl ether	*X. cubensis* PSU-MA34 (the branch of *B. parviflora*, endophytic fungus)	[97]
410	Brugunin A	*B. gymnorrhiza*, branch	[126]
411	Brugnanin	*B. gymnorrhiza*, stem bark	[127]
412	Balanophonin	*B. gymnorrhiza*, hypocotyl	[124]
413	Secoisolariciresinol	*B. gymnorrhiza*, hypocotyl	[124]
414	Cleomiscosin A	*B. gymnorrhiza*, hypocotyl	[124]
415	Pinoresinol	*B. gymnorrhiza*, hypocotyl	[124]
416	Medioresinol	*B. gymnorrhiza*, hypocotyl	[124]
417	Lyoniresinol-3α-O-β-D-glucopyranosides	*B. gymnorrhiza*, hypocotyl	[124]
418	Aryl-tetralin lignan rhamnoside	*B. gymnorrhiza*, leaf	[119]
419	Rhyncosides E	*B. sexangula var. rhynchopetala*, stem	[128]
420	Rhyncosides F	*B. sexangula var. rhynchopetala*, stem	[128]

2.9. Aromatic Compounds

The aromatic compounds (Table 12 and Figure 15) are prevalent in both plants and endophytic fungi secondary metabolites. The majority of the aromatic compounds summarized in this study are phenolic-related aromatic compounds. Previous reports have highlighted the crucial role of phenolic compounds in plants' defense against various biotic and abiotic stresses [129]. In mangrove plants, some compounds have been identified as substrates of fungal metabolism or (and) signals of plant origin, such as compounds **431**, **435**, and **436**. Additionally, there are other types of aromatic compounds present, including biphenyl derivatives (**451–453**), (iso) benzopyrans (**454–458**), chromones (**459–465**), (iso) benzofurans (**467–468**), and (iso) benzofuranones (**471–474**), among others.

Table 12. Aromatic compounds isolated from *Bruguiera* genus plants and their endophytes.

No.	Compound	Source	Reference
421	Bruguierol A	*B. gymnorrhiza*, stem	[130]
422	Bruguierol B	*B. gymnorrhiza*, stem	[130]
423	Bruguierol C	*B. gymnorrhiza*, stem	[130]
424	1-(3-hydroxyphenyl)-hexane-2,5-diol	*B. gymnorrhiza*, stem	[130]
425	Bruguierol D	*B. gymnorrhiza*, branch	[126]
426	2,3-dimethoxy-5-propylphenol	*B. gymnorrhiza*, branch	[126]
427	Phenol A	*Penicillium sp.* 091402 (the root of *B. sexangula*, endophytic fungus)	[125]
428	3,4,5-trimethyl-1,2-benzenediol	*Penicillium sp.* 091402 (the root of *B. sexangula*, endophytic fungus)	[125]
429	Tyrosol	*D. eschscholtzii* PSU-STD57 (the leaf of *B. gymnorrhiza*, endophytic fungus)	[99]

Table 12. *Cont.*

No.	Compound	Source	Reference
430	3-hydroxy-4-methoxybenzoic acid	*B. gymnorrhiza*, hypocotyl	[131]
431	4-hydroxybenzoic acid	*B. gymnorrhiza*, hypocotyl	[131]
432	4-methoxybenylacetic acid	*B. gymnorrhiza*, hypocotyl	[131]
433	Di-(2-entylhexyl) phthalate	*B. gymnorrhiza*, hypocotyl	[131]
434	Dibutylphthalate	*B. gymnorrhiza*, hypocotyl; *P. thomi* (the root of *B. gymnorrhiza*, endophytic fungus)	[66,131]
435	Methyl caffeate	*B. gymnorrhiza*, hypocotyl	[131]
436	Methyl 3,5-dihydroxybenzoate	*B. gymnorrhiza*, hypocotyl	[131]
437	(*S*)-3-(3′,5′-dihydroxy-2′,4′-methylphenyl) butan-2-one	*Penicillium sp.* 091402 (the root of *B. sexangula*, endophytic fungus)	[125]
438	1-(2,6-dihydroxyphenyl)butan-1-one	*D. eschscholtzii* PSU-STD57 (the leaf of *B. gymnorrhiza*, endophytic fungus); *P. citrinum* HL-5126 (the leaf of *B. sexangula var. rhynchopetala*, endophytic fungus); *D. eschscholtzii* HJ001 (*B. sexangular var. rhynchopetala*, endophytic fungus)	[99,100,102]
439	1-(2-methoxyphenyl)butan-1-one	*P. longicolla* HL-2232 (the leaf of *B. sexangula var. rhynchopetala*, endophytic fungus)	[107]
440	Deoxyphomalone	*E. nigrum* MLY-3 (the leaf of *B. gymnorrhiza*, endophytic fungus)	[113]
441	Phomalone	*E. nigrum* MLY-3 (the leaf of *B. gymnorrhiza*, endophytic fungus)	[113]
442	Procyanidin	*B. parviflora*, bark	[132]
443	3-(3,4-dihydroxyphenyl)-7,8-dihydroxyhexahydro-6*H*-pyrano[2,3-b][1,4]dioxine-6-carboxylic acid	*B. gymnorrhiza*, leaf	[34]
444	2-(((3,4-dihydroxy-6-methyltetrahydro-2*H*-pyran-2-yl)oxy)methyl)-6-(3,4-dihydroxybenzyl)tetrahydro-2*H*-pyran-3,4,5-triol	*B. gymnorrhiza*, leaf	[34]
445	7,8-dihydroxy-3-(4-hydroxy-3-methoxyphenyl)-2-(hydroxymethyl)hexahydro-6*H*-pyrano[2,3-b][1,4]dioxine-6-carboxylic acid	*B. gymnorrhiza*, leaf	[34]
446	3-(3,4-dimethoxyphenyl)-7,8-dihydroxy-2-(hydroxymethyl)hexahydro-6*H*-pyrano[2,3-b][1,4]dioxine-6-carboxylic acid	*B. gymnorrhiza*, leaf	[34]
447	Rhyncosides A	*B. sexangula var. rhynchopetala*, stem	[128]
448	Rhyncosides B	*B. sexangula var. rhynchopetala*, stem	[128]
449	Rhyncosides C	*B. sexangula var. rhynchopetala*, stem	[128]
450	Rhyncosides D	*B. sexangula var. rhynchopetala*, stem	[128]
451	4′,5-dihydroxy-2,3-dimethoxy-4-(hydroxypropyl)-biphenyl	*P. thomi* (the root of *B. gymnorrhiza*, endophytic fungus)	[66]
452	5,5′-dimethoxybiphenyl-2,2′-diol	*P. longicolla* HL-2232 (the leaf of *B. sexangula var. rhynchopetala*, endophytic fungus)	[107]

Table 12. *Cont.*

No.	Compound	Source	Reference
453	6,6′-dimethoxybiphenyl-2,2′-diol	*P. longicolla* HL-2232 (the leaf of *B. sexangula var. rhynchopetala*, endophytic fungus)	[107]
454	3-(3-hydro-xybutyl)-1,1-dimethylisochroman-6,8-diol	*B. gymnorrhiza*, stem	[130]
455	(3*R*,4*S*)-6,8-dihydroxy-3,4,5,7-tetramethylisochroman	*Penicillium sp.* 091402 (the root of *B. sexangula*, endophytic fungus)	[125]
456	(1*S*,3*R*,4*S*)-1-(4′-hydroxylphenyl)-3,4-dihydro-3,4,5-trimethyl-1*H*-2-benzopyran-6,8-diol	*P. citrinum* (*B. gymnorrhiza*, endophytic fungus)	[117]
457	(2*R**,4*R**)-3,4-dihydro-5-methoxy-2-methyl-2*H*-1-benzopyran-4-ol	*P. citrinum* HL-5126 (the leaf of *B. sexangula var. rhynchopetala*, endophytic fungus)	[102]
458	(2*R**,4*R**)-3,4-dihydro-4-methoxy-2-methyl-2*H*-1-benzopyran-4-ol	*P. citrinum* HL-5126 (the leaf of *B. sexangula var. rhynchopetala*, endophytic fungus)	[102]
459	2-(2′*S*-hydroxypropyl)-5-methyl-7-hydroxychromone	*P. longicolla* HL-2232 (the leaf *B. sexangula var. rhynchopetala*, endophytic fungus)	[67]
460	5,7-dihydroxy-2-propylchromone	*P. citrinum* HL-5126 (the leaf of *B. sexangula var. rhynchopetala*, endophytic fungus)	[102]
461	Rhytidchromone A	*R. rufulum* (the leaf of *B. gymnorrhiza*, endophytic fungus)	[133]
462	Rhytidchromone B	*R. rufulum* (the leaf of *B. gymnorrhiza*, endophytic fungus)	[133]
463	Rhytidchromone C	*R. rufulum* (the leaf of *B. gymnorrhiza*, endophytic fungus)	[133]
464	Rhytidchromone D	*R. rufulum* (the leaf of *B. gymnorrhiza*, endophytic fungus)	[133]
465	Rhytidchromone E	*R. rufulum* (the leaf of *B. gymnorrhiza*, endophytic fungus)	[133]
466	Alternariol 5-O-methyl ether	*P. longicolla* HL-2232 (the leaf of *B. sexangula var. rhynchopetala*, endophytic fungus)	[107]
467	2-acetyl-7-methoxybenzofuran	*D. eschscholtzii* HJ004 (the stem of *B. sexangula var. rhynchopetala*, endophytic fungus)	[103]
468	4,6-dihydroxy-5-methoxy-7-methyl-1,3-dihydroisobenzofuran	*E. nigrum* MLY-3 (the leaf of *B. gymnorrhiza*, endophytic fungus)	[113]
469	Furobenzotropolone A	*E. nigrum* MLY-3 (the leaf of *B. gymnorrhiza*, endophytic fungus)	[113]
470	Furobenzotropolone B	*E. nigrum* MLY-3 (the leaf of *B. gymnorrhiza*, endophytic fungus)	[113]
471	3-hydroxyepicoccone B	*E. nigrum* MLY-3 (the leaf of *B. gymnorrhiza*, endophytic fungus)	[113]
472	4,6-dihydroxy5-methoxy-7-methylphthalide	*E. nigrum* MLY-3 (the leaf of *B. gymnorrhiza*, endophytic fungus)	[113]
473	4,5,6-trihydroxy-7-methyl-3*H*-isobenzofuran-1-one	*E. nigrum* MLY-3 (the leaf of *B. gymnorrhiza*, endophytic fungus)	[113]
474	Sparalide C	*E. nigrum* MLY-3 (the leaf of *B. gymnorrhiza*, endophytic fungus)	[113]

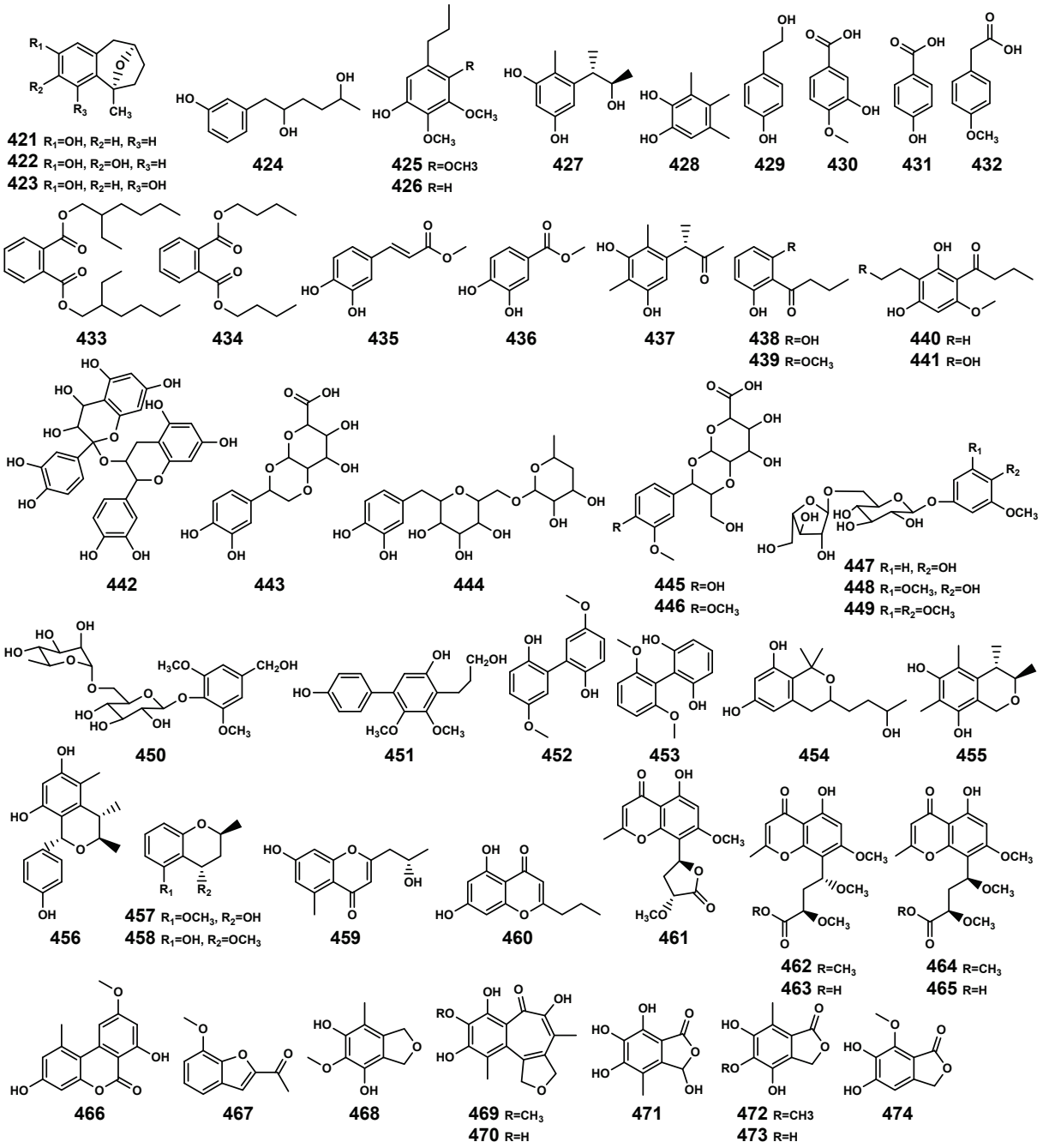

Figure 15. Aromatic compounds (**421–474**) isolated from *Bruguiera* genus plants and their endophytes.

2.10. Other Compounds

Apart from the previously mentioned compounds, fatty acids (**475–486**), 2H-pyran-2-ones (**487–490**), alcohols (**491–493**), and additional ones (**494–496**) were also identified (Table 13 and Figure 16). Specifically, the secondary metabolite **495**, originating from the endophytic fungus *Aspergillus terreus*, was discovered for the first time in the ripe fruits of *Garcinia cowa* [134,135]. It belonged to polyprenylated benzoylphloroglucinols with a unique tetracyclo[7.3.3.3^{3,11}.0^{3,7}]tetradecane-2,12,14-trione skeleton, and exhibited significant anti-inflammatory and alpha-glucosidase inhibition activities [135].

Table 13. Other compounds isolated from *Bruguiera* genus plants and their endophytes.

No.	Compound	Source	Reference
475	(9*Z*,12*Z*,15*Z*)-6,8,11-trihydroxyoctadeca-9,12,15-trienoic acid	*B. gymnorrhiza*, leaf	[34]
476	(9*E*,12*Z*)-6,8,11-trihydroxyoctadeca-9,12-dienoic acid	*B. gymnorrhiza*, leaf	[34]
477	(*E*)-6,8,12-trihydroxyoctadec-9-enoic acid	*B. gymnorrhiza*, leaf	[34]
478	8,12-dihydroxyhexadecanoic acid	*B. gymnorrhiza*, leaf	[34]
479	Tetradeca-5,8-dienoic acid	*S. albidoflavus* 107A-01824 (the leaf of *B. gymnorrhiza*, endophytic actinomycete)	[136]
480	Clonostach acids A	*C. rosea* B5-2 (the branch of *B. gymnorrhiza*, endophytic fungus)	[108]
481	Clonostach acids B	*C. rosea* B5-2 (the branch of *B. gymnorrhiza*, endophytic fungus)	[108]
482	Clonostach acids C	*C. rosea* B5-2 (the branch of *B. gymnorrhiza*, endophytic fungus)	[108]
483	Succinic acid	*P. thomi* (the root of *B. gymnorrhiza*, endophytic fungus)	[66]
484	Xylacinic acid A	*X. cubensis* PSU-MA34 (the branch of *B. parviflora*, endophytic fungus)	[97]
485	Xylacinic acid B	*X. cubensis* PSU-MA34 (the branch of *B. parviflora*, endophytic fungus)	[97]
486	2-Hexylidene-3-methyl succinic acid 4-methyl ester	*X. cubensis* PSU-MA34 (the branch of *B. parviflora*, endophytic fungus)	[97]
487	Prolipyrone A	*Fusarium proliferatum* MA-84 (the inner tissue of *B. sexangula*, endophytic fungus)	[45]
488	Prolipyrone B	*F. proliferatum* MA-84 (the inner tissue of *B. sexangula*, endophytic fungus)	[45]
489	Prolipyrone C	*F. proliferatum* MA-84 (the inner tissue of *B. sexangula*, endophytic fungus)	[45]
490	Gibepyrone D	*F. proliferatum* MA-84 (the inner tissue of *B. sexangula*, endophytic fungus)	[45]
491	Erythritol	*P. citrinum* ZD6 (the stem of *B. gymnorrhiza*, endophytic fungus)	[92]
492	Mannitol	*P. citrinum* ZD6 (the stem of *B. gymnorrhiza*, endophytic fungus)	[92]
493	Eicosanol	*B. cylindrica*, leaf	[58]
494	(2*R*,3*R*,4*S*,5*R*,6*R*)-4-(((4*R*,5*S*,6*R*)-4-hydroxy-5-methoxy-6-methyltetrahydro-2H-pyran-3-yl)oxy)-6-(hydroxymethyl)tetrahydro-2*H*-pyran-2,3,5-triol	*B. gymnorrhiza*, leaf	[34]
495	Cowabenzophenone A	*A. terreus* (*B. gymnorrhiza*, endophytic fungus)	[135]
496	(±)-1-monopalmitin	*P. thomi* (the root of *B. gymnorrhiza*, endophytic fungus)	[66]

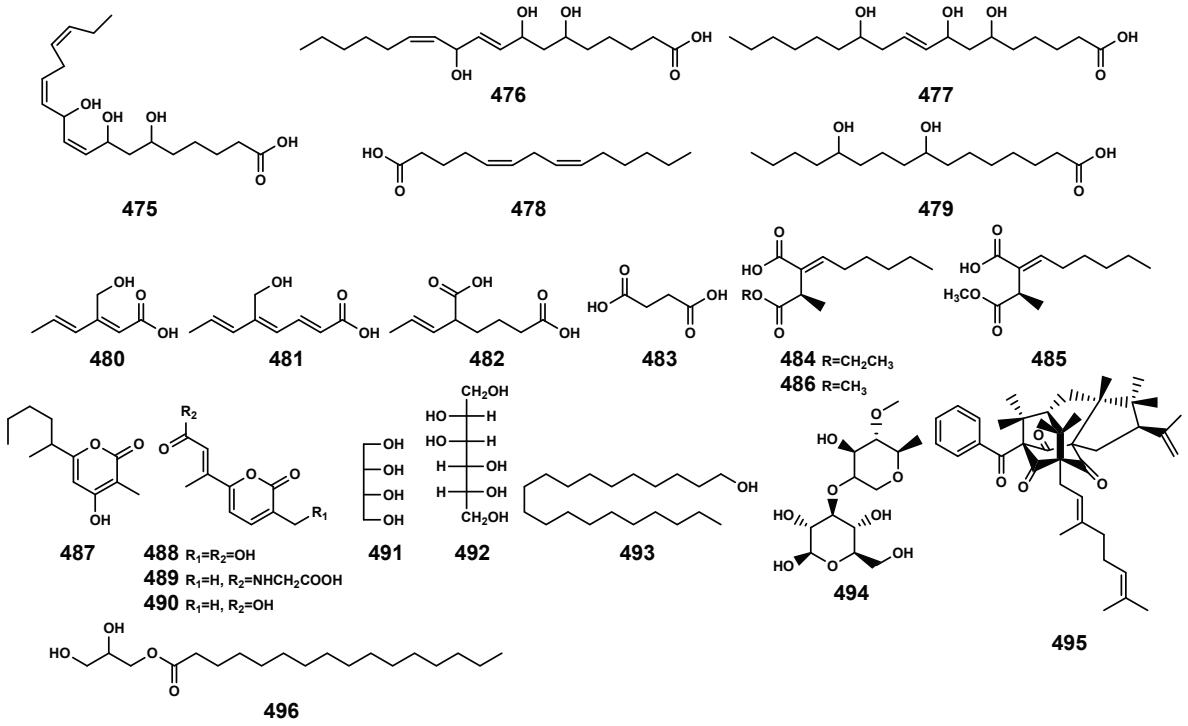

Figure 16. Other compounds (**475–496**) isolated from *Bruguiera* genus plants and their endophytes.

3. Bioactivities

3.1. Cytotoxic Activity

Cytotoxic activity stands out as a pharmacological attribute of secondary metabolites derived from *Bruguiera* genus plants and their associated endophytes. The n-butanol extract from *B. gymnorrhiza* showed antitumor activity against A-549 and HL-60 [76]. Methanol extract of *B. gymnorrhiza* displayed selective cytotoxicity against breast ductal carcinoma cells (MDA-MB-435S) with IC_{50} 1.38 mg/mL [137]. Leaves extract of *B. sexangula* demonstrated inhibitory effect on the proliferation of gastric cancer cells in both in vitro and in vivo studies [138]. Qayoom et al. [139] utilized network pharmacology methods and unveiled that brugine (**197**) possesses significant anti-breast cancer activity, exerting its effects through various pathways such as the calcium signaling pathway, cAMP signaling pathway, PI3K-Akt pathway, and others. Additionally, anticancer compounds have been identified in *B. gymnorrhiza* plants and the endophytic fungi of both *B. gymnorrhiza* and *B. sexangula var. rhynchopetala*. The lethality assay using brine shrimp (*Artemia salina* L.) reveals significant cytotoxicity in *B. gymnorrhiza* extracts and certain compounds [9,140]. Table 14 provides a summary of the cytotoxic activity of monomeric compounds.

Table 14. Cytotoxic activity of the compounds isolated from *Bruguiera* genus and its endophytes.

Compound	Cell Lines/Brine Shrimp	Effects	References
Acaciicolide B (**10**)	cytotoxic activity against MOLT-3 and HL-60 cancer cells;	IC_{50} values of 165.04 and 159.05 μM	[29]
3-epi-Steperoxide A (**27**)	cytotoxic activity against MOLT-3, HuCCA-1, A549, HepG2, HL-60, MDA-MB-231, T47D, and HeLa cancer cell lines;	IC_{50} values range of 0.68–3.71 μg/mL	[28]
Steperoxide A (**30**)	cytotoxic activity against MOLT-3, HuCCA-1, A549, HepG2, HL-60, MDA-MB-231, T47D, and HeLa cancer cell lines;	IC_{50} values range of 0.67–5.25 μg/mL	[28]
Merulin A (**31**)	cytotoxic activity against HuCCA-1, A549, MOLT-3, HepG2, HL-60, MDA-MB-231, T47D, Hela and MRC-5 cell lines;	IC_{50} values range of 15.20–76.97 μM	[29]

Table 14. *Cont.*

Compound	Cell Lines/Brine Shrimp	Effects	References
Merulin B (**32**)	cytotoxic activity against MOLT-3, A549, HepG2, HL-60, MDA-MB-231, and T47D cell lines;	IC_{50} values range of 11.94–49.08 μg/mL	[28]
Merulin C (**33**)	cytotoxic activity against HL-60 cancer cells; cytotoxic activity against MOLT-3, HuCCA-1, A549, HepG2, MDA-MB-231, T47D, and HeLa cell lines;	IC_{50} value of 0.08 μg/mL; IC_{50} values range of 0.19–3.75 μg/mL	[28]
Merulin D (**34**)	cytotoxic activity against HuCCA-1, A549, MOLT-3, HepG2, HL-60, MDA-MB-231, T47D, Hela and MRC-5 cell lines;	IC_{50} values range of 18.31–154.51 μM	[29]
7-epi-merulin B (**35**)	cytotoxic activity against HuCCA-1, A549, MOLT-3, HepG2, HL-60, MDA-MB-231, T47D, and MRC-5 cell lines;	IC_{50} values range of 0.28–37.46 μM	[29]
Botryosphaerin F (**40**)	cytotoxic activity against MCF-7 and HL-60 cancer cells;	IC_{50} values of 4.49 and 3.43 μM	[36]
13,14,15,16-tetranorlabd-7-ene-19,6b:12,17-diolide (**41**)	cytotoxic activity against MCF-7 and HL-60 cancer cells;	IC_{50} values of 2.79 and >30 μM	[36]
Botryosphaerin B (**42**)	cytotoxic activity against MCF-7 and HL-60 cancer cells;	IC_{50} values of 17.60 and >30 μM	[36]
LLZ1271*β* (**43**)	cytotoxic activity against MCF-7 and HL-60 cancer cells;	IC_{50} values of >30 and 0.60 μM	[36]
Ent-kaur-16-en-13-hydroxy-19-al (**64**)	cytotoxic activities against L-929, K562 and HeLa cell lines;	GI_{50}/CC_{50} values of 11.5, 10.5 and 42.3 μg/mL	[42]
Ent-kaur-16-en-13,19-diol (**65**)	cytotoxic activities against L-929, K562 and HeLa cell lines;	GI_{50}/CC_{50} values of 50.0, 50.0 and 50.0 μg/mL	[42]
17-chloro-13,16*β*-dihydroxy-*ent*-kauran-19-al (**68**)	cytotoxic activities against L-929, K562 and HeLa cell lines;	GI_{50}/CC_{50} values of 50.0, 29.2 and 38.2 μg/mL	[42]
Methyl-16*α*,17-dihydroxy-*ent*-kauran-19-oate (**69**)	cytotoxic activities against L-929, K562 and HeLa cell lines;	GI_{50}/CC_{50} values of 39.5, 27.7 and 40.5 μg/mL	[42]
Methyl-16*α*,17-dihydroxy-*ent*-9(11)-kauren-19-oate (**71**)	cytotoxic activities against L-929, K562 and HeLa cell lines;	GI_{50}/CC_{50} values of 41.9, 26.7 and 38.7 μg/mL	[42]
16*α*,17-dihydroxy-*ent*-kauran-19-al (**72**)	cytotoxic activities against L-929, K562 and HeLa cell lines;	GI_{50}/CC_{50} values of 50.0, 50.0 and 50.0 μg/mL	[42]
16*α*H-17-hydroxy-*ent*-kauran-19-oic acid (**73**)	cytotoxic activities against L-929, K562 and HeLa cell lines;	GI_{50}/CC_{50} values of 42.4, 32.8 and 43.0 μg/mL	[42]
16*α*H-17,19-*ent*-kaurane-diol (**74**)	cytotoxic activities against L-929, K562 and HeLa cell lines;	GI_{50}/CC_{50} values of 12.8, 13.6 and 35.7 μg/mL	[42]
16-*ent*-kauren-19-ol (**75**)	cytotoxic activities against L-929, K562 and HeLa cell lines;	GI_{50}/CC_{50} values of 18.2, 6.8 and 32.8 μg/mL	[42]
(5*R*,9*S*,10*R*,13*S*,15*S*)-*ent*-8(14)-pimarene-1-oxo-15*R*,16-diol (**82**)	cytotoxic activities against L-929 cell lines;	IC_{50} value of 9.8 μg/mL	[43]
15(*S*)-isopimar-7-en-15,16-diol (**83**)	cytotoxic activities against K562 cell lines;	IC_{50} value of 7.0 μg/mL	[43]
(4*R*,5*S*,8*R*,9*R*,10*S*,13*S*)-*ent*-17-hydroxy-16-oxobeyeran-19-al (**85**)	cytotoxic activities against L-929, K562 and HeLa cell lines;	GI_{50}/CC_{50} values of 45.4, 50.0 and 37.7 μg/mL	[42]
Sexangulic acid (**94**)	anti-tumour activity against A-549 and HL60 cell lines;	moderate in vitro cytotoxicity at 5 μg/mL	[47]
3*α*-*Z*-feruloyltaraxerol (**120**)	cytotoxic activities against NCI-H187 cell lines;	IC_{50} value of 12.2 μg/mL	[57]
3*α*-*Z*-coumaroyltaraxerol (**124**)	cytotoxic activities against NCI-H187 cell lines;	IC_{50} value of 20.0 μg/mL	[57]
3*β*-(*Z*)-coumaroyltaraxerol (**129**)	cytotoxic against Neuro 2A cell lines	IC_{50} value of 75.76 μM	[58]
Nectrianolin D (**144**)	cytotoxic against HL-60 cell lines;	IC_{50} value of 10.16 μM	[63]
Furanocochlioquinol (**145**)	cytotoxic against HL-60 cell lines;	IC_{50} value of 0.47 μM	[63]
Furanocochlioquinone (**146**)	cytotoxic against HL-60 cell lines;	IC_{50} value of 0.63 μM	[63]
Nectripenoid B (**147**)	cytotoxic against HL-60 cell lines;	IC_{50} value of 0.93 μM	[63]
Cochlioquinone D (**148**)	cytotoxic against HL-60 cell lines;	IC_{50} value of 1.61 μM	[63]

Table 14. *Cont.*

Compound	Cell Lines/Brine Shrimp	Effects	References
3*β*,5*α*-dihydroxy-(22*E*,24*R*)-ergosta-7,22-dien-6-one (**161**)	cytotoxic against MCF-7, A549, Hela and KB cell lines;	IC_{50} values of 4.98, 1.95, 0.68 and 1.50 μM	[69]
3*β*,5*α*,14*α*-trihydroxy-(22*E*,24*R*)-ergosta-7,22-dien-6-one (**162**)	cytotoxic against MCF-7, A549, Hela and KB cell lines;	IC_{50} values of 25.4, 27.1, 24.4 and 19.4 μM	[69]
Meleagrin (**193**)	cytotoxic against MCF-7, A549, Hela and KB cell lines;	IC_{50} values of 9.7 and 8.3 μM	[88]
Uridine (**194**)	cytotoxic against B16F10, A549, HL60 and MCF-7 cell lines;	IC_{50} values of 16.7, 8.6, 15.9 and 31.9 μmol/L	[67]
6-aminopurine-9-carboxylic acid methyl ester (**195**)	cytotoxic against B16F10, A549, HL60 and MCF-7 cell lines;	IC_{50} values of 29.0, 21.2, 4.1 and 14.9 μmol/L	[67]
Adenine riboside (**196**)	cytotoxic against B16F10, A549, HL60 and MCF-7 cell lines;	IC_{50} values of 18.2, 12.5, 14.4 and 26.2 μmol/L	[67]
Cyclo-(Ala-Gly) (**220**)	cytotoxic against K562, HepG2 and HT29 cell lines;	IC_{50} values of 18.1, 9.5, and 10.3 μM	[66]
Cyclo-(Pro-Gly) (**221**)	cytotoxic against K562, HepG2 and HT29 cell lines;	IC_{50} values of 17.6, >50 and 10.8 μM	[66]
Cyclo-(Ala-Pro) (**222**)	cytotoxic against K562, HepG2 and HT29 cell lines;	IC_{50} values of 9.6, 13.6, and 20.1 μM	[66]
Beauvericin (**226**)	cytotoxic against HL60 and A549 cell lines;	IC_{50} values of 2.02, 0.8, 1.14 and 1.10 μM	[69]
Palmarumycins BG5 (**236**)	cytotoxic against MCF-7 and HL-60 cell lines;	IC_{50} values of 7.6 and 1.9 μM	[98]
Nigronatthaphenyl (**242**)	cytotoxic against HCT 116 colon cell line;	IC_{50} value of 9.62 μM	[101]
Incarxanthone B (**258**)	cytotoxicity against A375, MCF-7 and HL-60 cell lines;	IC_{50} values of 8.6, 6.5, and 4.9 μM	[104]
Cytochalasin D (**296**)	cytotoxic against KB cell lines;	IC_{50} value of 3.99 μg/mL	[97]
Zygosporin D (**297**)	cytotoxic against HCT15 cell lines;	IC_{50} value of 13.5 μM	[110]
12-hydroxylcytochalasin Q (**305**)	cytotoxic against HCT15 cell lines;	IC_{50} value of 13.4 μM	[110]
Penibenzophenone B (**321**)	cytotoxic against A549 cell lines;	IC_{50} value of 15.7 μg/mL	[87]
Asterric acid (**324**)	cytotoxic against Hela cell lines;	IC_{50} value of 21.6 μg/mL	[87]
Scopoletin (**384**)	cytotoxic against Hela, A435, A549 and K562 cell lines;	IC_{50} values of 764.7, 593.4, 290.2 and 487.7 μg/mL	[124]
(3*R**,4*S**)-6,8-dihydroxy-3,4,7-trimethylisocoumarin (**387**)	cytotoxic against K562 cell lines;	IC_{50} value of 18.9 μg/mL	[125]
Brugnanin (**411**)	cytotoxic against CNE-1 nasopharyngeal carcinoma cell lines;	IC_{50} value of 5.72×10^{-4} M	[127]
Secoisolariciresinol (**413**)	cytotoxic against Hela, A435, A549 and K562 cell lines;	IC_{50} values of 571.5, 397.5, 323.0 and 768.8 μg/mL	[124]
Lyoniresinol-3*α*-O-*β*-D-glucopyranosides (**417**)	cytotoxic against Hela, A435, A549 and K562 cell lines;	IC_{50} values of 328.8, 455.5, 209.3 and 361.9 μg/mL	[124]
3,4,5-trimethyl-1,2-benzenediol (**428**)	cytotoxic against SGC-7901 cell lines;	IC_{50} value of 36.0 μg/mL	[125]
Dibutylphthalate (**434**)	cytotoxic against K562, HepG2 and HT29 cell lines;	IC_{50} values of 17.3, 15.2, and 11.1 μM	[66]
4′,5-dihydroxy-2,3-dimethoxy-4-(hydroxypropyl)-biphenyl (**451**)	cytotoxic against K562, HepG2 and HT29 cell lines;	IC_{50} values of 10.1, 12.2 and 8.9 μM	[66]
Rhytidchromone A (**461**)	cytotoxic against MCF-7 and Kato-3 cell lines;	IC_{50} values of 19.3 and 23.3 μM	[133]
Rhytidchromone B (**462**)	cytotoxic against Kato-3 cell lines;	IC_{50} value of 21.4 μM	[133]
Rhytidchromone D (**464**)	cytotoxic against Kato-3 cell lines;	IC_{50} value of 16.8 μM	[133]
Rhytidchromone E (**465**)	cytotoxic against MCF-7 and Kato-3 cell lines;	IC_{50} values of 17.7 and 16.0 μM	[133]
Cowabenzophenone A (**495**)	cytotoxic against HCT 116 colon cell line;	IC_{50} value of 10.1 μM	[135]
Fusaprolifin A (**87**)	The lethality activity against brine shrimp;	lethality rate of 49.5%, at 100 mg/mL	[45]
Fusaprolifin B (**88**)	The lethality activity against brine shrimp;	lethality rate of 9.6%, at 100 mg/mL	[45]
Macrosporin-2-O-(6′-acetyl)-α-D-glucopyranoside (**269**)	The lethality activity against brine shrimp;	LD_{50} value of 10 μM	[106]

3.2. Antimicrobial Activity

Previous studies have indicated that crude extracts of *B. gymnorrhiza* exhibit substantial antibacterial activity against a range of bacteria, including the fungal pathogen *Candida albicans* and bacterial pathogens, such as *Micrococcus sp.*, *Staphylococcus aureus* (MTCC 3160), *Klebsiella pneumoniae* (MTCC 4030), *Escherichia coli* (MTCC 42), *E. coli* (NX, AMP, OF resistant strain) [141]. Bibi Sadeer et al. [142] found that ethyl acetate extract of *B. gymnorrhiza* twig, when used in combination with streptomycin and ciprofloxacin, respectively, potentiates their inhibitory effects against MRSA and *P. aeruginosa*. Ethyl acetate extracts obtained from mature leaves, immature leaves, and the bark of *B. sexangula* reveal antibacterial properties against *S. aureus* [143]. Currently, numerous compounds isolated from *B. gymnorrhiza* and endophytes of plants (*B. gymnorrhiza*, *B. sexangula*, *B. sexangula var. rhynchopetala*, and *B. parviflora*) have shown considerable antibacterial activity, as presented in Table 15.

Table 15. Antimicrobial activity of the compounds isolated from *Bruguiera* genus and its endophytes.

Compound	Pathogen	Effect	Reference
(3*R*,4*R*,6*R*,7*S*)-7-hydroxyl-3,7-dimethyl-oxabicyclo[3.3.1]nonan-2-one (**1**)	*B. cinerea*, and *P. nicotianae*	3.1 and 6.3 μg/mL	[26]
(3*R*,4*R*)-3-(7-methylcyclohexenyl)-propanoic acid (**2**)	*C. albicans*, *B. cinerea*, and *P. nicotianae*	50, 3.1 and 6.3 μg/mL	[26]
7*R*-hydroxygeosmin (**49**)	*B. subtilis*, *E. coli* and *P. aeruginosa*	weak activities	[32]
3-oxogeosmin (**50**)	*B. subtilis*, *P. aeruginosa* and VRE	weak activities	[32]
(4*S*,5*S*,7*R*,10*S*)-4*β*,10*α*-eudesmane-5*β*,11-diol (**53**)	*B. subtilis*, *S. aureus*, *E. coli*, *P. aeruginosa*, MRSA, VRE, *M. vaccae*, *S. salmonicolor* and *P. notatum*	broad antimicrobial activities	[32]
11-oxo-12*α*-acetoxy-4,4-dimethyl-24-methylene-5*α*-cholesta-8,14-diene-2*α*,3*β*-diol (**95**)	*S. aureus*, *B. subtilis*, *E. coli*, *M. luteus*, *M. tetragenus*, *S. albus* and *B. cereus*	>20, >20, 9.76, >20, >20, 9.76 and 9.76 μmol/L	[48]
12*α*-acetoxy-4,4-dimethyl-24-methylene-5*α*-cholesta-8-momoene-3*β*,11*β*-diol (**96**)	*S. aureus*, *B. subtilis*, *E. coli*, *M. luteus*, *M. tetragenus*, *S. albus* and *B. cereus*	5, 10, 5, >20, 5, 10 and 10 μmol/L	[48]
12*α*-acetoxy-4,4-dimethyl-24-methylene-5*α*-cholesta-8,14-diene-2*α*,3*β*,11*β*-triol (**98**)	*S. aureus*, *B. subtilis*, *E. coli*, *M. luteus*, *M. tetragenus*, *S. albus* and *B. cereus*	4.86, 9.72, 4.86, 9.72, 4.86, >20 and >20 μmol/L	[48]
Dehydroaustin (**131**)	*S. epidermidis*, *S. aureus*, *E. coli*, *B. cereus* and *V. alginolyticus*	20, >20, >20, >20 and >20 μM	[60]
11*β*-acetoxyisoaustinone (**132**)	*S. epidermidis*, *S. aureus*, *E. coli*, *B. cereus* and *V. alginolyticus*	20, >20, >20, >20 and >20 μM	[60]
Austinol (**133**)	*S. epidermidis*, *S. aureus*, *E. coli*, *B. cereus* and *V. alginolyticus*	10, >20, >20, 20 and >20 μM	[60]
Guignardone A (**149**)	*P. aeruginosa*, and MRSA	25, and 25 μg/mL	[64]
Guignardone J (**151**)	*P. aeruginosa*, and MRSA	50, and 50 μg/mL	[64]
BG138 (a mixture of brugierol **172** and isobrugierol **173**)	*P. aeruginosa*	32 μg/mL	[74]
Thiocladospolide A (**179**)	*E. tarda*, *E. ictarda* and *C. glecosporioides*	1, 8 and 2 μg/mL	[21]
Thiocladospolide B (**180**)	*C. glecosporioides*, *P. piricola* Nose and *F. oxysporum* f. sp. *Cucumerinum*	2, 32 and 1 μg/mL	[21]
Thiocladospolide C (**181**)	*C. glecosporioides*, *P. piricola* Nose and *F. oxysporum* f. sp. *Cucumerinum*	1, 32 and 32 μg/mL	[21]
Thiocladospolide D (**182**)	*E. ictarda*, *C. glecosporioides*, *P. piricola* Nose and *F. oxysporum* f. sp. *Cucumerinum*	1, 1, 32 and 1 μg/mL	[21]

Table 15. *Cont.*

Compound	Pathogen	Effect	Reference
Pandangolide 3 (**183**)	*C. glecosporioides* and *B. sorokiniana*	2 and 8 μg/mL	[21]
Thiocladospolide F (**184**)	*E. coli*, *E. tarda*, *P. aeruginosa*, *V. anguillarum*, *F. oxysporum* f. sp. *Momodicae*, *P. digitatum* and *H. maydis*	16, 1.0, 4.0, 2.0, 32, 32 and 8.0 μg/mL	[75]
Thiocladospolide G (**185**)	*E. coli*, *E. tarda*, *V. anguillarum*, *F. oxysporum* f. sp. *Momodicae*, *P. digitatum* and *H. maydis*	16, 2.0, 2.0, 16, 16 and 4.0 μg/mL	[75]
Antimycin A18 (**188**)	plant pathogenic fungi: *C. lindemuthianum*, *B. cinerea*, *A. solani* and *M. grisea*	the minimum concentration values to show inhibition zone on plates were 0.01, 0.06, 0.03 and 0.20 μg/mL	[86]
Penibruguieramine A (**199**)	*S. aureus*	20 μg/mL	[88]
Cyclo-(Ala-Gly) (**220**)	*B. subtilis*	400 μg/mL	[92]
2-Chloro-5-methoxy-3-methylcyclohexa-2,5-diene-1,4-dione (**231**)	*SA* and *MRSA*	equal MIC values of 128 μg/mL	[97]
8-methoxy-1-naphthol (**240**)	*S. aureus*, MRSA and *M. gypseum*	200 μg/mL	[99]
1,8-dimethoxynaphthalene (**241**)	*S. aureus*, MRSA and *M. gypseum*	200 μg/mL	[99]
Nigronatthaphenyl (**242**)	*B. subtilis*, *B. subtilis* TISTR 088, *B. cereus TISTR 688*, *S. aureus*, *E. coli*, MRSA, *C. albicans*, *P. aeruginosa*, *C. gloeosporioides* and *A. niger*	4, 4, 2, 4, 2, 2, 2, 2, 4 and 8 μg/mL	[101]
(3*S*)-3,8-Dihydroxy-6,7-dimethyl-*α*-tetralone (**243**)	*S. aureus*, MRSA *and M. gypseum*	200 μg/mL	[99]
Isosclerone (**244**)	*S. aureus*, MRSA and *M. gypseum*	200 μg/mL	[99]
1,3,8-trimethoxynaphtho[9-c]furan (**247**)	*S. aureus*, MRSA and *B. cereus*	>25, >25 and 12.5 μg/mL	[103]
5-hydroxy-2-methoxy-6,7-dimethyl-1,4-naphthoquinone (**255**)	*B. cereus*	12.5 μg/mL	[103]
Chloroisosulochrin dehydrate (**266**)	MRSA, *S. aureus*, *E. coli*, *B. cereus*, *V. alginolyticus* and *V. parahaemolyticus*	with the same MIC value of 50 Mm	[105]
Emodin (**267**)	*B. subtilis* and *P. aeruginosa*	25 and 100 μg/mL	[92]
Auxarthrol C (**268**)	*E. coli*	9.8 μM	[106]
Macrosporin (**270**)	*M. tetragenus*, *E. coli*, *S. albus*, *S. aureus* and *B. subtilis*	7.8, 3.9, 3.9, 3.9 and 3.9 μM	[106]
2-O-acetylaltersolanol B (**272**)	*M. tetragenus*, *E. coli* and *S. aureus*	4.6, 4.6 and 9.2 μM	[106]
Altersolanol A (**273**)	*M. tetragenus*, *E. coli*, *S. aureus* and *B. subtilis*	8.2, 4.1, 2.07 and 4.1 μM	[106]
Altersolanol B (**274**)	*V. parahaemolyticus* and *V. anguillarum*; *M. tetragenus*, *S. aureus*, *K. rhizophila*, and *B. subtilis*	2.5 and 5 μg/mL; 7.8, 7.8, 7.8 and 7.8 μM	[106,107]
Altersolanol C (**275**)	*B. subtilis*	8.8 μM	[106]
Tetrahydroaltersolanol B (**279**)	*E. coli*	7.3 μM	[106]
Alterporriol U (**282**)	*B. cereus*	8.3 μM	[106]
Alterporriol V (**283**)	*B. cereus*	8.1 μM	[106]
Alterporriol B (**286**)	*B. cereus*	7.9 μM	[106]
Alterporriol D (**287**)	*E. coli*, *B. cereus* and *S. aureus*	7.5, 10.0 and 5.0 μM	[106]
Alterporriol E (**288**)	*E. coli* and *B. cereus*	5.0 and 2.50 μM	[106]
Alterporriol C (**289**)	*B. cereus*	8.9 μM	[106]
2′-acetoxy-7-chlorocitreorosein (**293**)	*S. aureus* and *V. parahaemolyticus*	22.8 and 10 μM	[105]
Citreorosein (**294**)	*S. aureus*, *E. coli*, *B. cereus*, *V. alginolyticus* and *V. parahaemolyticus*	22.8, 50, 50, 50 and 50 μM	[105]
MT-1 (**295**)	MRSA, *S. aureus*, *E. coli*, *B. cereus*, *V. alginolyticus* and *V. parahaemolyticus*	with the same MIC value of 50 Mm	[105]

Table 15. *Cont.*

Compound	Pathogen	Effect	Reference
[11]-cytochalasa-5(6),13-diene-1,21-dione-7,18-dihydroxy-16,18-dimethyl-10-phenyl(7*S**,13*E*,16*S**,18*R**) (**298**)	*E. coli*, *S. aureus*, *B. cereus*, *V. parahaemolyticus* and *V. alginolyticus*	with the same MIC value of 50 μg/mL	[100]
2-deoxy-sohirnone C (**317**)	MRSA	80 μg/mL	[90]
3,4-dihydroxybenzoic acid (**319**)	*P. aeruginosa*, *E. faecalis*, MRSA, *E. coli* and *C. albicans*	25, 25, 25, 12.5 and 25 μg/mL	[64]
8-O-methylnodulisporin F (**326**)	*S. aureus*, MRSA and *B. cereus*	6.25, 12.5 and 6.25 μg/mL	[103]
Nodulisporin H (**327**)	*S. aureus*, MRSA and *B. cereus*	12.5, 12.5 and 6.25 μg/mL	[103]
5*R*-hydroxyrecifeiolide (**338**)	*E. ictarda* and *P. aeruginosa*	32 and 32 μg/mL	[114]
5*S*-hydroxyrecifeiolide (**339**)	*G. cingulate*	16 μg/mL	[114]
Pandangolide 1 (**340**)	*S. aureus*, *E. ictarda*, *G. cingulate* and *P. aeruginosa*	32, 4.0, 1.0 and 32 μg/mL	[114]
Cladocladosin A (**341**)	*E. tarda*, *V. anguillarum*, *F. oxysporum* f. sp. *Momodicae*, *P. digitatum* and *H. maydis*	2.0, 4.0, 32, 32 and 8.0 μg/mL	[75]
Infectopyrone A (**345**)	*S. albus*, *E. coli*, *B. subtilis*, *M. tetragenus* and *M. luteus*	5.0, 2.5, 10.0, 10.0 and 10.0 μg/mL	[106]
Infectopyrone B (**346**)	*S. albus*, *E. coli*, *M. tetragenus* and *M. luteus*	10.0, 2.5, 10.0 and 10.0 μg/mL	[106]
6,8-dihydroxy-5-methoxy-3-methyl-1H-isochromen-1-one (**347**)	*P. aeruginosa*, and MRSA	50, and 50 μg/mL	[64]
Ent-cladospolide F (**348**)	*S. aureus*, *E. ictarda* and *P. aeruginosa*	8.0, 16 and 64 μg/mL	[114]
Cladospolide G (**349**)	*E. coli*, *G. cingulate*, *B. sorokiniana* and *F. oxysporum* f. sp. *Cucumerinum*	32, 1.0, 32 and 1.0 μg/mL	[114]
Iso-cladospolide B (**351**)	*E. coli*, *E. tarda*, *E. ictarda* and *G. cingulate*	32, 32, 16 and 64 μg/mL	[114]
Penicimarin G (**390**)	*S. epidermidis*, *S. aureus*, *E. coli*, *B. cereus* and *V. alginolyticus*	20, 20, 20, 20 and 20 μM	[60]
Penicimarin H (**391**)	*S. epidermidis*, *S. aureus*, *E. coli*, *B. cereus* and *V. alginolyticus*	10, 20, >20, 20 and 20 μM	[60]
Bruguierol A (**421**)	*M. vaccae* and *C. albicans*	25 and 50 μg/mL	[130]
Bruguierol B (**422**)	*M. vaccae* and *C. albicans*	25 and 50 μg/mL	[130]
Bruguierol C (**423**)	*S. aureus*, *M. luteus*, *E. faecalis*, *E. coli*, *M. vaccae* and *C. albicans*	12.5, 12.5, 12.5, 12.5, 12.5 and 50 μg/mL	[130]
Tyrosol (**429**)	*S. aureus*, MRSA and *M. gypseum*	200 μg/mL	[99]
1-(2,6-dihydroxyphenyl)butan-1-one (**438**)	*S. aureus*, MRSA and *M. gypseum*; *B. subtilis*, *B. cereus* and *M. tetragenus*	200 μg/mL; 6.94 μM	[99]
5,5′-dimethoxybiphenyl-2,2′-diol (**452**)	*V. parahaemolyticus*	10 μg/mL	[107]
2-(2′*S*-hydroxypropyl)-5-methyl-7-hydroxychromone (**459**)	*E. coli*	5 μg/mL	[67]
Erythritol (**491**)	*B. subtilis*	50 μg/mL	[58]
Cowabenzophenone A (**495**)	*B. subtilis*, *S. aureus*, *E. coli*, MRSA, *C. albicans*, *P. aeruginosa* and *C. gloeosporioides*	1, 2, 4, 4, 4, 2 and 2 μg/mL	[135]

Abbreviations: *A. niger* = *Aspergillus niger*; *A. solani* = *Alternaria solani*; *B. cereus* = *Bacillus cereus*; *B. subtilis* = *Bacillus subtilis*; *B. cinerea* = *Botrytis cinerea*; *C. gloeosporioides* = *Colletotrichum gloeosporioides*; *C. lindemuthianum* = *Colletotrichum lindemuthianum*; *E. faecalis* = *Enterococcus faecalis*; *E. coli* = *Escherichia coli*; *F. oxysporum* f. sp. *Momodicae* = *Fusarium oxysporum* f. sp. *Momodicae*; *G. cingulate* = *Glomerella cingulate*; *H. maydis* = *Helminthosporium maydis*; *K. rhizophila* = *Kocuria rhizophila*; MRSA = methicillin-resistant *Staphylococcus aureus*; *M. grisea* = *Magnaporth grisea*; *M. luteus* = *Micrococcus luteus*; *M. tetragenus* = *Micrococcus tetragenus*; *M. gypseum* = *Microsporum gypseum*; *M. vaccae* = *Mycobacterium vaccae*; *P. digitatum* = *Penicillium digitatum*; *P. notatum* = *Penicillium notatum*; *P. nicotianae* = *Phytophthora nicotianae*; *S. albus* = *Staphylococcus albus*; *S. epidermidis* = *Staphylococcus epidermidis*; *V. anguillarum* = *Vibrio anguillarum*; *S. salmonicolor* = *Sporobolomyces salmonicolor*; VRE = vancomycin-resistant *Enterococcus*; *V. alginolyticus* = *Vibrio alginolyticus*; *V. anguillarum* = *Vibrio anguillarum*; *V. parahaemolyticus* = *Vibrio parahaemolyticus*.

3.3. Antioxidant Activity

Studies have revealed significant antioxidant activity in extracts derived from *B. gymnorrhiza*, *B. sexangula*, and *B. cylindrica* [10,144,145]. The antioxidant and polyphenol-rich leaves of *B. gymnorrhiza* can exert hepatoprotective effects by ameliorating liver tissue injury [7]. Condensed tannins from *B. gymnorrhiza* possessed notable anti-tyrosinase and antioxidant capabilities, effectively inhibiting browning reactions in fresh-cut lotus roots [146]. Ethanol extract of *B. sexangula* leaves had antioxidant and melanin inhibition activities without skin irritation [145]. In the in vitro antioxidant activity studies, compounds **469**, **470**, **471**, **472**, **473**, **468**, and **328** showed DPPH radical scavenging activity with IC_{50} values of 57.6, 26.5, 29.3, 85.2, 16.5, 53.1, and 14.7 μM, and ABTS radical scavenging activity with IC_{50} values of 46.4, 29.2, 23.7, 43.1, 23.3, 24.0, and 18.8 μM, respectively [113]. Yao et al. [121] conducted the cellular antioxidant assay and identified that compound **381** exhibited antioxidant activity with an EC_{50} value of 11.79 μM. Compound **382** exhibited effective neuroprotective activity against 1-methyl-4-phenylpyridinium-induced oxidative damage in PC12 cells, and its mechanism involved inhibiting apoptosis in PC12 cells through the mitochondrial pathway [117]. It also attenuated oxidative stress and inflammatory responses induced by lipoteichoic acid in embryonic rat heart cells (H9c2) [147].

3.4. Anti-Inflammatory Activity

Studies have indicated the anti-inflammatory activity in extracts from plants within the *Bruguiera* genus, such as *B. gymnorrhiza*, *B. sexangula*, and *B. parviflora*, as well as endophytic fungi associated with *B. gymnorrhiza*. Chen et al. [148] conducted research revealing that aqueous extract of *B. gymnorrhiza* leaves can alleviate dextran sulfate sodium (DSS)-induced ulcerative colitis by inhibiting of NF-κB activation and modulating the gut microbiota. Subsequently, Lin et al. [149] observed that aqueous extracts from *B. gymnorrhiza* fruit also exhibited a protective effect against DSS-induced ulcerative colitis, and the mechanism may be associated with the attenuation of inflammation, activation of the Keap1/Nrf2 signaling pathway, and modulation of the gut microbiota. Furthermore, Zhang et al. [150] reported that methanol extracts of *B. gymnorrhiza* fruits mitigate inflammation in gastric injury by activating the NF-κB pathway, thus conferring gastroprotective effects. Moreover, consumption of *B. gymnorrhiza* fruits has been shown to ameliorate systemic inflammations in obesity, increase circulating satiety hormones, reduce lipid profiles, elevate short-chain fatty acids levels, and promote weight loss [151]. Eldeen et al. [152] discovered that metabolites obtained from *B. cylindrica* possessed inhibitory effects on pro-inflammatory enzymes, including 5-lipoxygenase, cyclooxygenase, and acetylcholinesterase, and on the growth of an induced rheumatoid arthritis synovial fibroblasts. According to reports, compound **367** may serve as the potential primary anti-inflammatory substance in *B. gymnorrhiza* leaves through various possible mechanisms, such as regulation of oxidative stress, suppression of arachidonic acid metabolism, and downregulation of pro-inflammatory cytokines by inhibiting NF-κB [120]. Ukwatta et al. [101,135] employed a cell-based assay for THP-1 cytokine-release assay to quantify the anti-inflammatory activity of compounds **242** and **495**, showcasing IC_{50} values of 6.2 μM and 12.1 μg/mL, respectively. Furthermore, compounds **368**, **369**, **370**, **378**, and **371** from *B. parviflora* leaves exhibited significant inhibitory effects on the inflammatory response of the RAW 264.7 cells induced by lipopolysaccharide with a range of NO production between 11.77 and 13.92 μM, at the concentration of 100 μg/mL [52].

3.5. Antiviral Activity

Hou et al. [153]detected that endophytic fungal strains (GXIMD07366, GXIMD07616, GXIMD07384, GXIMD07550, GXIMD07445X) from *B. gymnorrhiza* have anti-hepatitis B virus (HBV) activity. At a concentration of 125 μg/mL, their extracts significantly reduced the HBV-DNA levels in the supernatant of HepG2.2.15 cells, and the inhibition rates were 51%, 47%, 63%, 52%, and 47%, respectively. Compounds **212–218** derived from the hypocotyls of *B. gymnorrhiza* displayed moderate anti-HBV activity [91]. Furthermore, the

compound **186** exhibited anti-HBV activity, with IC_{50} values of 4.37 mmol/L for HbsAg and 4.89 mmol/L for HBeAg, and therapeutic indices of 2.68 and 2.40 [85]. In addition to anti-HBV activity, compound **44** showed selective anti-HIV activity [30]. It is worth noting that the compound **356** demonstrated moderate antiviral activity against the pathogen SARS-CoV-2, the causative agent of COVID-19, with an EC_{50} value of 29.0 μM [112]. Aqueous extracts from the roots and fruits of *B. gymnorrhiza* inhibited Zika virus (ZIKV) infection at non-cytotoxic concentrations [154]. Moreover, *B. cylindrica*-synthesized AgNP, at a concentration of 30 μg/mL, significantly suppressed the production of dengue viral E protein and downregulated the expression of dengue viral E gene in Vero cells [155].

3.6. Antidiabetic Activity

The decoctions of both roots and leaves of *B. gymnorrhiza* have demonstrated varying degrees of antidiabetic activity, ranging from low to moderate efficacy [156]. *B. gymnorrhiza* leaf extracts displayed inhibitory effects on α-glucosidase, with an IC_{50} value of 2.670 mg/mL [144]. Extracts derived from *B. cylindrica* leaves contained antidiabetic components, and the ethanol extract of which was considered potential sources of novel bioactive compounds for treating type 2 diabetes [157,158]. Notably, several compounds, including **108**, **117**, **107**, **368**, **369**, **370**, **378**, **371**, and **467** exhibited significant α-glucosidase inhibitory activity, with IC_{50} values ranging from 1.1 to 98.0 μg/mL (better than the positive control acarbose) [52,103]. Compounds **242**, **256**, and **495** also show α-glucosidase inhibitory activity, with IC_{50} values of 6.9 μM, 5.7 μg/mL, and 7.8 μM, respectively [101,103,135]. Additionally, through in vitro bioactivity assays, it was found that compounds **177** and **174** exhibited significant inhibitory activity against the target molecule associated with type II diabetes, human protein tyrosine phosphatase 1B (PTP1B), with IC_{50} values of 14.9 and 17.6 μM, respectively [72,80,159].

3.7. Insecticidal and Mosquito Repellent Activity

Currently, in the *Bruguiera* genus and its endophytes, researchers have primarily investigated the anti-plasmodial, anti-*Caenorhabditis elegans*, and mosquito-repellent activities. Bai et al. [61] identified insecticidal activity in meroterpenoids and isocoumarin compounds obtained from the fungus *Penicillium sp*. TGM112, isolated from *B. sexangula var. rhynchopetala*. Compounds **133**, **134**, **135**, **137**, **140**, **141**, **143**, **394**, **395**, **398**, **399**, and **401** showed insecticidal activity against newly hatched larvae of *Helicoverpa armigera* Hubner, with IC_{50} values ranging from 50 to 200 μg/mL [61,62]. Compounds **133**, **134**, **135**, **136**, **137**, **138**, and **139** displayed anti-*C. elegans* activity, with EC_{50} values ranging from 9.4 to 38.2 μg/mL [61]. These types of compounds are expected to be potential candidates for effective and low-toxicity novel biopesticides [62]. The leaf and hypocotyl extracts of *B. cylindrica* exhibited in vitro antiplasmodial activities, with IC_{50} values of 173.75 and 74.81 μg/mL, respectively [160,161]. And compound **110** showed anti-malarial activity, with an EC_{50} value of 8.6 mg/mL [54]. Compound **364** significantly reduced the lifespan of *C. elegans* [118]. Compound **479** displays good nematocidal activity [136]. Compound **495** had anti-filarial activity, with MIC, IC_{50}, and LC_{50} values of 0.358, 0.708, and 3.89 mg/mL, respectively [135]. Murugan et al. [155] discovered that *B. cylindrica*-synthesized AgNP had mosquito larvicidal properties and effectively reduced the populations of *Aedes aegypti* larvae and pupae when applied at low doses.

3.8. Enzyme Inhibitory Activity

Homhual et al. [46,79] discovered that in stably transfected HepG2 cells, compounds **91–93** and **172–174** from the flowers of *B. gymnorrhiza* activated antioxidant response elements (ARE) luciferase activity, with respective EC_{50} values were 7.8, 9.4, 15.7, 3.7, 1.8, and 56.7 μM. Compounds **91**, **172**, and **173** were found to inhibit phorbol ester-induced NF-κB luciferase activity, with IC_{50} values of 1.4, 85.0, and 14.5 μM, respectively [46,79]. Compounds **91** and **172** also exhibited inhibitory effects on cyclooxygenase-2 (COX-2) activity, with IC_{50} values of 0.37 and 6.1 μM, respectively [46,79]. In vitro bioactivity

tests revealed that compounds **126**, **129**, **130**, **163**, **226**, **250**, and **251** significantly inhibited α-acetylcholinesterase (AChE) with IC_{50} values of 84.26, 5.28, 12.00, 1.89, 3.09, 2.01, and 6.71 μM, respectively [58,69]. Compound **348** demonstrated potent activity against acetylcholinesterase, with an IC_{50} value of 40.26 μM [114].

3.9. Other Activities

In addition to the aforementioned biological activities, it has also been reported to possess analgesic, anti-diarrheal, anti-hemolytic activities, and various other pharmacological effects.

The extracts from *B. gymnorrhiza* stem, leaf, and hypocotyl have demonstrated significant analgesic and anti-diarrheal effects [144,162]. When administered at doses of 250 and 500 mg/kg body weight, the leaf and hypocotyl extracts exhibited a remarkable inhibitory effect on castor oil-induced diarrhea mice [144]. Moreover, *B. cylindrica* extracts have shown the ability to inhibit H_2O_2-induced hemolysis of bovine erythrocytes [10]. The methanol extract of *B. gymnorrhiza* also exhibited anti-hemolytic activity with an IC_{50} value of 311.28 μg/mL [9]. Extracts from *B. gymnorrhiza*, prepared using different solvents (n-hexane, ethyl acetate, n-butanol, and an aqueous phase), and from leaves of different ages (senescent, mature, and young leaves), exhibited significant inhibitory effects on algae growth [34,163].

4. Interactions between *Bruguiera* Genus and Its Endophytes

Plants constitute a complex ecological community, engaging in symbiotic relationships with endophytic fungi, wherein they coexist and evolve together over an extended period [164]. Recent study has reported that the endophytic *Streptomyces parvulus* VCCM 22513 from *B. gymnorrhiza* exhibited significant adaptive responses to abiotic environmental stressors, including antioxidation, salt tolerance, and degradation of aromatic compounds [165]. Moreover, through the review of the literature, it has been observed that both the *Bruguiera* genus and its associated endophytes produce similar or closely related secondary metabolites, including cholesterol (**153**), cytochalasin D (**296**), zygosporin D (**297**), and dibutylphthalate (**434**). This phenomenon may be attributed to the fact that the plants flourish in high-salinity and waterlogged environments. In response to the complex environmental stresses, endophytes associated with *Bruguiera* genus have evolved similar signaling pathways to their host counterparts, enabling information exchange [164,166,167]. This allows the endophytes to elicit defense responses akin to those of the *Bruguiera* genus plants, consequently, synthesize the shared metabolites.

In the genus *Bruguiera* and its endophytic fungi, cytochalasins (**296–314**) were isolated from various sources, including *B. gymnorrhiza* (**296–297**), endophytic fungus *Xylaria arbuscula* GZS74 from *B. gymnorrhiza* (**296–297**, **300–314**), endophytic fungus *Daldinia eschscholtzii* HJ001 from *B. sexangula var. rhynchopetala* (**298–299**), and endophytic fungus *Xylaria cubensis* PSU-MA34 from *B. parviflora* (**296**). Cytochalasins are typically derived from the *Xylaria* genus of endophytic fungi [168]. Structurally, they consist of a highly substituted isoindolone ring, featuring a benzyl group at C-3 and fused to an 11- to 14-membered macrocyclic ring [169]. According to their structure–activity relationship, one of the significant toxic structural features of cytochalasins is the presence of a complete perihydroisoindolyl-1-one motif fused to either a [11] or a [13] carbocyclic or a [14] lactone macrocycle ring [169]. Additionally, the C7-OH group may also exhibit toxicity depending on the crop species, sensitivity, and type of cytochalasins [169]. Compound **296** exhibits inhibitory activity against plant pathogens such as *Botrytis cinerea* (at a concentration of 25 μg/disc) [170], *Cladosporium cladosporioides* (at a concentration of 10 μg/mL) [171], *C. sphaerospermum* (at a concentration of 25 μg/mL) [171], and *C. gloeosporioides* (MIC value of 2.46 μmol/mL) [168]. Compound **297** effectively inhibits the shoot elongation of rice seedlings [172]. Compounds **307** and **314** both display nonspecific moderate phytotoxicity against monocotyledonous plant bentgrass and dicotyledonous plant lettuce [173]. Evidently, endophytic fungi of the *Bruguiera* genus aid in plant growth competition and de-

fense against plant pathogens by producing cytochalasins with phytotoxic and antifungal activities, thereby providing protection for *Bruguiera* species' growth.

Simultaneously, existing research confirms that dibutylphthalate (**434**), a secondary metabolite derived from the *B. gymnorrhiza* plant and its endophytic fungus *Penicillium thomi*, also serves as the primary active metabolite of endophyte *Bacillus sp.* KL5 from the plant *Rumex dentatus*, exhibits significant antagonistic activity against plant pathogens *Fusarium oxysporum* and *Verticillium dahliae*, making it a promising candidate for the prevention and control of postharvest diseases Fusarium root rot in potato [174]. Compound **434** may therefore also contribute to bolstering the *B. gymnorrhiza* plant's resilience against plant pathogens.

In addition to the shared compounds mentioned above, specific secondary metabolites have been identified in *Bruguiera* genus plants and their endophytes that play crucial roles in promoting plant growth and development, as well as enhancing the plant's resistance to both biotic and abiotic stresses, like 2,6-dimethoxy-1,4-benzoquinone (**230**), scopoletin (**384**), erythritol (**491**), and mannitol (**492**).

According to the research analysis by Laohavisit et al. [95], quinone molecules may serve as pathogen or danger-associated molecular patterns, such as 2,6-dimethoxy-1,4-benzoquinone (**230**). This quinone signal is perceived by leucine-rich-repeat receptor-like kinases, triggering the expression of defense-related genes and immune responses against bacterial pathogens [95]. Compound **230** produced by host plants can also act as an inducing factor for the development of root parasitic plant absorbers, potentially playing a regulatory role during the parasitic process of these plants [175].

Scopoletin (**384**), as a crucial component in the plant's natural immune response, plays a role in resisting the invasion of pathogenic microorganisms and promoting the proliferation of beneficial microbes [123]. In healthy plant leaves, due to the instability and toxicity of scopoletin, it is converted into the glycosylated form, scopolin, by glucosyltransferases, then transferred intracellularly and stored in vacuoles, with their accumulation typically maintained at low levels [123]. Upon activation of the leaf defense system by pathogens (fungi, bacteria, and viruses, etc.) or elicitors (flg22, MYB15, MPK3, etc.), scopolin is released from the vacuoles in infected tissues [123,176]. It is then converted to scopoletin by β-glucosidases, leading to an increase in scopoletin production [176]. This, in turn, exhibits antimicrobial activity and clears H_2O_2 in infected tissues to prevent cell death [176]. The level of disease resistance is correlated with the extent and timing of scopoletin accumulation [177]. The toxic effects of scopoletin may be attributed to the presence of methoxy (-OCH_3) and hydroxy (-OH) groups on the benzene ring [123]. Upon glycosylation, scopoletin is confined by the cell wall, limiting its toxicity [178]. Depending on the environmental conditions, scopolin and scopoletin in tissues of *B. gymnorrhiza* plant can mutually convert within cells, thereby regulating the level of scopoletin to aid in resisting pathogen invasion.

The compound erythritol (**491**) with antibacterial activity, is one of the main chemical components of the endophytic fungus *Lasiodiplodia pseudotheobromae* APR5 [179], and it is also produced by the endophytic fungus *P. citrinum* ZD6 within the stems of the Chinese medicinal plant *B. gymnorrhiza* [92]. The endophytic fungus *L. pseudotheobromae* APR5, originating from the host plant *Andrographis paniculata*, effectively inhibits the growth of plant pathogenic fungi [179]. Moreover, it produces the plant hormone IAA (indole-3-acetic acid) and iron carrier, promoting the growth and development of the host plant and enhancing its resistance to adverse environmental conditions [179]. Furthermore, the genus *Penicillium* has been confirmed to enhance the resistance of host plants to both biotic and abiotic stresses [180]. As a major member of endophytic fungi within the *Bruguiera* genus, *Penicillium* (26.3%) undoubtedly plays a crucial role in conferring resistance to pathogenic fungal invasion in *Bruguiera* genus plants.

Mannitol (**492**) is present in *B. gymnorrhiza* plant and its endophytic fungus *P. citrinum* ZD6 [92], serving as both an osmoprotectant and an antioxidant against oxidative stress [181]. However, research suggests that fungal pathogens also secrete mannitol, playing a role in fungal pathogenicity [181]. Mannitol can protect fungal pathogens against

plant defense mechanisms based on reactive oxygen [182]. Given the complexity of the existing interactions, the specific mechanisms underlying these processes have not been elucidated as of now.

In summary, utilizing secondary metabolites as a starting point for research, exploring the interactive relationships between the *Bruguiera* genus plants and their endophytic fungi presents an intriguing direction. To delve deeper into the mechanisms underlying the interaction between *Bruguiera* plants and their endophytic fungi, modern "omics" tools, including genome sequencing, comparative genomics, microarrays, next-generation sequencing, metagenomics, metatranscriptomics, and others, can be integrated with various systems biology techniques to explore the role of endophytic fungi in the ecology of *Bruguiera* plants [183].

5. Conclusions

The *Bruguiera* genus encompasses a diverse range of plant species housing a wide array of endophytic fungal communities. These organisms are prolific producers of secondary metabolites, which manifest extensive pharmacological effects. Many compounds derived from these sources have demonstrated notable biological activities. Despite the discovery of numerous pharmacological effects, a more comprehensive investigation into the underlying mechanisms is still imperative. The presence of certain compounds in both plants and their endophytes suggests the potential for further exploration into the interaction mechanisms between *Bruguiera* plants and their endophytic fungi. Future research endeavors can be directed towards developing highly active lead compounds with therapeutic potential from the *Bruguiera* genus and its endophytes.

Author Contributions: Conceptualization, X.C., X.L. and X.J.; writing—original draft preparation, X.C. and L.Z.; writing—review and editing, X.C. and X.L.; visualization, B.L., L.X. and M.Z.; resources, X.L., X.J. and Y.M., X.L. and X.C. contributed equally to this paper. All authors have read and agreed to the published version of the manuscript.

Funding: This research was funded by the National Natural Science Foundation of China, grant number 31670349, and the Young Scientists Fund of the National Natural Science Foundation of China, grant number 81802678.

Institutional Review Board Statement: Not applicable.

Data Availability Statement: No new data were created or analyzed in this study. Data sharing is not applicable to this article.

Acknowledgments: We would like to express our gratitude to Jun Wu from Guangdong Medical University for his guidance and assistance in writing this paper.

Conflicts of Interest: The authors declare no conflicts of interest.

References

1. Wang, B.S.; Liang, S.C.; Zhang, W.Y.; Zan, Q.J. Mangrove flora of the world. *Acta Bot. Sin.* **2003**, *45*, 644–653.
2. Lin, P. Distribution of mangrove species. *Sci. Silvae Sin.* **1987**, *23*, 481–490.
3. Wu, J.; Xiao, Q.; Xu, J.; Li, M.Y.; Pan, J.Y.; Yang, M.H. Natural products from true mangrove flora: Source, chemistry and bioactivities. *Nat. Prod. Rep.* **2008**, *25*, 955–981. [CrossRef] [PubMed]
4. Wang, L.L.; Zhang, X.; Wang, J.S.; Shen, X.X.; Tang, L.L.; Li, R.L. Utilization Status and Development Countermeasures of Mangrove Medicinal Resources in the Marine-Terrestrial Interlaced Zone. *Acta Sci. Nat. Univ. Pekin.* **2023**, *59*, 704–718.
5. Bibi, S.N.; Fawzi, M.M.; Gokhan, Z.; Rajesh, J.; Nadeem, N.; Kannan, R.R.R.; Albuquerque, R.D.D.G.; Pandian, S.K. Ethnopharmacology, Phytochemistry, and Global Distribution of Mangroves—A Comprehensive Review. *Mar. Drugs* **2019**, *17*, 231. [CrossRef] [PubMed]
6. Haq, M.; Sani, W.; Hossain, A.B.M.S.; Taha, R.M.; Monneruzzaman, K.M. Total phenolic contents, antioxidant and antimicrobial activities of *Bruguiera gymnorrhiza*. *J. Med. Plants Res.* **2011**, *5*, 4112–4118.
7. Sur, T.K.; Hazra, A.; Hazra, A.K.; Bhattacharyya, D. Antioxidant and hepatoprotective properties of Indian Sunderban mangrove *Bruguiera gymnorrhiza* L. leave. *J. Basic Clin. Pharm.* **2016**, *7*, 75–79. [CrossRef] [PubMed]
8. Karimulla, S.; Kumar, B.P. Anti diabetic and Anti hyperlipidemic activity of bark of *Bruguiera gymnorrhiza* on streptozotocin induced diabetic rats. *Asian J. Pharm. Sci. Technol.* **2011**, *1*, 4–7.

9. Karim, M.A.; Islam, M.A.; Islam, M.M.; Rahman, M.S.; Sultana, S.; Biswas, S.; Hosen, M.J.; Mazumder, K.; Rahman, M.M.; Hasan, M.N. Evaluation of antioxidant, anti-hemolytic, cytotoxic effects and anti-bacterial activity of selected mangrove plants (*Bruguiera gymnorrhiza* and *Heritiera littoralis*) in Bangladesh. *Clin. Phytosci.* **2020**, *6*, 8. [CrossRef]
10. Krishnamoorthy, M.; Sasikumar, J.M.; Shamna, R.; Pandiarajan, C.; Sofia, P.; Nagarajan, B. Antioxidant activities of bark extract from mangroves, *Bruguiera cylindrica* (L.) Blume and *Ceriops decandra* Perr. *Indian J. Pharmacol.* **2011**, *43*, 557–562.
11. Loder, J.W.; Russell, G.B. Tropine 1,2-dithiolane-3-carboxylate, a new alkaloid from *Bruguiera sexangula*. *Tetrahedron Lett.* **1966**, *51*, 6327–6329. [CrossRef] [PubMed]
12. Zheng, C.J.; Wang, D.N.; Ming, X.C.; Li, W.; Han, B.; Zhao, J.; Huang, G.L. Recent Advances of Chemical Constituents of Genus *Bruguiera*. *Guangdong Chem. Ind.* **2014**, *41*, 45–46,50.
13. Xie, L.H.; Hou, X.T.; Deng, J.G.; Wei, L.Y.; Xia, Z.S.; Du, Z.C. Research Progress on Chemical Constituents and Pharmacological Effect of *Bruguiera gymnorrhiza*. *Chin. J. Exp. Tradit. Med. Formulae* **2018**, *24*, 225–234.
14. Chen, S.H.; Cai, R.L.; Liu, Z.M.; Cui, H.; She, Z.G. Secondary metabolites from mangrove-associated fungi: Source, chemistry and bioactivities. *Nat. Prod. Rep.* **2021**, *39*, 560–595. [CrossRef] [PubMed]
15. Yin, H.; Zhang, S.; Luo, X.M.; Liu, Y.H. Preparative isolation and purification of two benzoxazinoid glucosides from *Acanthus ilicifolius* L. by high-speed counter-current chromatography. *J. Chromatogr. A* **2008**, *1205*, 177–181. [CrossRef]
16. Gao, C.H.; Tian, X.P.; Qi, S.H.; Luo, X.M.; Wang, P.; Zhang, S. Antibacterial and antilarval compounds from marine gorgonian-associated bacterium *Bacillus amyloliquefaciens* SCSIO 00856. *J. Antibiot.* **2010**, *63*, 191–193. [CrossRef] [PubMed]
17. Liu, J.X.; Luo, M.Q.; Xia, M.; Wu, Q.; Long, S.M.; Hu, Y.H.; Gao, G.C.; Yao, X.L.; He, M.; Su, H.X.; et al. Marine Compound Catunaregin Inhibits Angiogenesis through the Modulation of Phosphorylation of Akt and eNOS in vivo and in vitro. *Mar. Drugs* **2014**, *12*, 2790–2801. [CrossRef]
18. Tang, H.; Ge, H.; Chen, Z.B.; Luo, X.M.; Su, F.J.; Liang, Y.B.; Li, Z.Y.; Wu, J.G.; Yang, Q.; Zeng, L.J.; et al. Micrometam C Protects against Oxidative Stress in Inflammation Models in Zebrafish and RAW264.7 Macrophages. *Mar. Drugs* **2015**, *13*, 5593–5605. [CrossRef]
19. Liu, B.; Jin, X.B.; Chen, X.H.; Wang, X.; Zhang, W.B.; Luo, X.M. Two New Lactam Derivatives from *Micromelum falcatum* (Lour.) Tan. with Brine Shrimp Larvae Toxicity. *Molecules* **2023**, *28*, 7157. [CrossRef]
20. Jia, S.L.; Chi, Z.; Liu, G.L.; Hu, Z.; Chi, Z.M. Fungi in mangrove ecosystems and their potential applications. *Crit. Rev. Biotechnol.* **2020**, *40*, 852–864. [CrossRef]
21. Zhang, F.Z.; Li, X.M.; Yang, S.Q.; Meng, L.H.; Wang, B.G. Thiocladospolides A−D, 12-Membered Macrolides from the Mangrove-Derived Endophytic Fungus *Cladosporium cladosporioides* MA-299 and Structure Revision of Pandangolide 3. *J. Nat. Prod.* **2019**, *82*, 1535–1541. [CrossRef] [PubMed]
22. Xu, Z.L.; Baunach, M.; Ding, L.; Peng, H.Y.; Franke, J.; Hertweck, C. Biosynthetic Code for Divergolide Assembly in a Bacterial Mangrove Endophyte. *Chembiochem* **2014**, *15*, 1274–1279. [CrossRef] [PubMed]
23. Carroll, A.R.; Copp, B.R.; Davis, R.A.; Keyzers, R.A.; Prinsep, M.R. Marine natural products. *Nat. Prod. Rep.* **2021**, *38*, 362–413. [CrossRef] [PubMed]
24. Hernandez, A.; Nguyen, L.T.; Dhakal, R.; Murphy, B.T. The need to innovate sample collection and library generation in microbial drug discovery: A focus on academia. *Nat. Prod. Rep.* **2021**, *38*, 292–300. [CrossRef]
25. Voser, T.M.; Campbell, M.D.; Carroll, A.R. How different are marine microbial natural products compared to their terrestrial counterparts? *Nat. Prod. Rep.* **2022**, *39*, 7–19. [CrossRef] [PubMed]
26. Xu, D.; Zhang, B.Y.; Yang, X.L. Antifungal Monoterpene Derivatives from the Plant Endophytic Fungus *Pestalotiopsis foedan*. *Chem. Biodivers.* **2016**, *13*, 1422–1425. [CrossRef] [PubMed]
27. Azuma, H.; Toyota, M.; Asakawa, Y.; Takaso, T.; Tobe, H. Floral scent chemistry of mangrove plants. *J. Plant Res.* **2002**, *115*, 47–53. [CrossRef] [PubMed]
28. Wibowo, M.; Prachyawarakorn, V.; Aree, T.; Wiyakrutta, S.; Mahidol, C.; Ruchirawat, S.; Kittakoop, P. Tricyclic and Spirobicyclic Norsesquiterpenes from the Endophytic Fungus *Pseudolagarobasidium acaciicola*. *Eur. J. Org. Chem.* **2014**, *2014*, 3976–3980. [CrossRef]
29. Wibowo, M.; Prachyawarakorn, V.; Aree, T.; Mahidol, C.; Ruchirawat, S.; Kittakoop, P. Cytotoxic sesquiterpenes from the endophytic fungus *Pseudolagarobasidium acaciicola*. *Phytochemistry* **2016**, *122*, 126–138. [CrossRef] [PubMed]
30. Ding, L.; Münich, J.; Goerls, H.; Maier, A.; Fiebig, H.H.; Lin, W.H.; Hertweck, C. Xiamycin, a pentacyclic indolosesquiterpene with selective anti-HIV activity from a bacterial mangrove endophyte. *Bioorg. Med. Chem. Lett.* **2010**, *20*, 6685–6687. [CrossRef]
31. Ding, L.; Goerls, H.; Dornblut, K.; Lin, W.; Maier, A.; Fiebig, H.H.; Hertweck, C. Bacaryolanes A-C, Rare Bacterial Caryolanes from a Mangrove Endophyte. *J. Nat. Prod.* **2015**, *78*, 2963–2967. [CrossRef] [PubMed]
32. Ding, L.; Hertweck, C. Oxygenated Geosmins and Plant-like Eudesmanes from a Bacterial Mangrove Endophyte. *J. Nat. Prod.* **2020**, *83*, 2207–2211. [CrossRef] [PubMed]
33. Ding, L.; Görls, H.; Hertweck, C. Plant-like Cadinane Sesquiterpenes from an Actinobacterial Mangrove Endophyte. *Magn. Reson. Chem. MRC* **2021**, *59*, 34–42. [CrossRef] [PubMed]
34. Zhao, M.; Xiao, H.; Sun, D.; Duan, S.S. Investigation of the Inhibitory Effects of Mangrove Leaves and Analysis of Their Active Components on Phaeocystis globosa during Different Stages of Leaf Age. *Int. J. Environ. Res. Public Health* **2018**, *15*, 2434. [CrossRef] [PubMed]

35. Cai, Y.S.; Liu, H.L.; Gong, J.X.; Guo, Y.W. Chemical constituents of mangrove plant *Bruguiera gymnorrhiza*. *Chin. J. Mar. Drugs* **2011**, *30*, 15–18.
36. Deng, C.M.; Huang, C.H.; Wu, Q.L.; Pang, J.Y.; Lin, Y.C. A new sesquiterpene from the mangrove endophytic fungus *Aspergillus terreus* (No. GX7-3B). *Nat. Prod. Res.* **2013**, *27*, 1882–1887. [CrossRef] [PubMed]
37. Boncan, D.A.T.; Tsang, S.S.K.; Li, C.D.; Lee, I.H.T.; Lam, H.M.; Chan, T.F.; Hui, J.H.L. Terpenes and Terpenoids in Plants: Interactions with Environment and Insects. *Int. J. Mol. Sci.* **2020**, *21*, 7382. [CrossRef] [PubMed]
38. Shao, J.; Sun, Y.W.; Liu, H.L.; Wang, Y. Pathway elucidation and engineering of plant-derived diterpenoids. *Curr. Opin. Biotechnol.* **2021**, *69*, 10–16. [CrossRef] [PubMed]
39. Ganguly, S.N.; Sircar, S.M. Gibberellins from mangrove plants. *Phytochemistry* **1974**, *13*, 1911–1913. [CrossRef]
40. Subrahmanyam, C.; Rao, B.V.; Ward, R.S.; Hursthouse, M.B.; Hibbs, D.E. Diterpenes from the marine mangrove *Bruguiera gymnorhiza*. *Phytochemistry* **1999**, *51*, 83–90. [CrossRef]
41. Bao, S.Y.; Deng, Z.W.; Fu, H.Z.; Proksch, P.; Lin, W.H. Diterpenes and Disulfides from the Marine Mangrove Plant *Bruguiera sexangula var. rhynchopetala*. *Helv. Chim. Acta* **2005**, *88*, 2757–2763. [CrossRef]
42. Han, L.; Huang, X.S.; Sattler, I.; Dahse, H.M.; Fu, H.Z.; Lin, W.H.; Grabley, S. New Diterpenoids from the Marine Mangrove *Bruguiera gymnorrhiza*. *J. Nat. Prod.* **2004**, *67*, 1620–1623. [CrossRef] [PubMed]
43. Han, L.; Huang, X.S.; Sattler, I.; Dahse, H.M.; Fu, H.Z.; Grabley, S.; Lin, W.H. Three new pimaren diterpenoids from marine mangrove plant, *Bruguiera gymnorrhiza*. *Pharmazie* **2005**, *60*, 705–707. [CrossRef] [PubMed]
44. Guo, K.; Liu, Y.; Li, S.H. The untapped potential of plant sesterterpenoids: Chemistry, biological activities and biosynthesis. *Nat. Prod. Rep.* **2021**, *38*, 2293–2314. [CrossRef] [PubMed]
45. Liu, D.; Li, X.; Li, C.; Wang, B. Sesterterpenes and 2H-Pyran-2-ones (=α-Pyrones) from the Mangrove-Derived Endophytic Fungus *Fusarium proliferatum* MA-84. *Helv. Chim. Acta* **2013**, *96*, 437–444. [CrossRef]
46. Homhual, S.; Bunyapraphatsara, N.; Kondratyuk, T.; Herunsalee, A.; Chaukul, W.; Pezzuto, J.M.; Fong, H.H.S.; Zhang, H.J. Bioactive Dammarane Triterpenes from the Mangrove Plant *Bruguiera gymnorrhiza*. *J. Nat. Prod.* **2006**, *69*, 421–424. [CrossRef] [PubMed]
47. Li, L.A.; Huang, C.G.; Wang, C.Y.; Guo, Y.W. Sexangulic acid, a new cytotoxic triterpenoid from the Chinese mangrove *Bruguiera sexangula*. *Nat. Prod. Res.* **2010**, *24*, 1044–1049. [CrossRef] [PubMed]
48. Zheng, C.J.; Huang, G.L.; Tang, X.Z.; Wang, D.N.; Gong, X.L.; Zhang, Q.; Song, X.P.; Chen, G.Y. Secondary Metabolites and Antibacterial Activities of a *Bruguiera sexangula var. Rhynchopetala*-Derived Fungus *Penicillium* sp. (J41221). *Chin. J. Org. Chem.* **2014**, *34*, 1172–1176. [CrossRef]
49. Sarkar, A.; Ganguly, S.N. Gymnorhizol, a new triterpene alcohol from *Brugiera gymnorhiza*. *Chem. Informationsdienst* **1979**, *10*, 138.
50. Ghosh, A.; Misra, S.; Dutta, A.K.; Choudhury, A. Pentacyclic triterpenoids and sterols from seven species of mangrove. *Phytochemistry* **1985**, *24*, 1725–1727. [CrossRef]
51. Luo, D.Q.; Deng, H.Y.; Yang, X.L.; Shi, B.Z.; Zhang, J.Z. Oleanane-Type Triterpenoids from the Endophytic Fungus *Pestalotiopsis clavispora* Isolated from the Chinese Mangrove Plant *Bruguiera sexangula*. *Helv. Chim. Acta* **2011**, *94*, 1041–1047. [CrossRef]
52. Bui, T.T.; Nguyen, K.P.T.; Nguyen, P.P.K.; Le, D.T.; Nguyen, T.L. Anti-Inflammatory and α-Glucosidase Inhibitory Activities of Chemical Constituents from *Bruguiera parviflora* Leaves. *J. Chem.* **2022**, *2022*, 3049994. [CrossRef]
53. Li, F.; Li, X.M.; Wang, B.G. Chemical constituents of marine mangrove plant *Bruguiera gymnorrhiza*. *Mar. Sci.* **2010**, *34*, 24–27.
54. Chumkaew, P.; Kato, S.; Chantrapromma, K. A New Triterpenoid Ester from the Fruits of *Bruguiera parviflora*. *Chem. Pharm. Bull.* **2005**, *53*, 95–96. [CrossRef]
55. Karalai, C.; Laphookhieo, S. Triterpenoid Esters from *Bruguiera cylindrica*. *Aust. J. Chem.* **2005**, *58*, 556–559. [CrossRef]
56. Chantrapromma, S.; Fun, H.-K.; Razak, I.A.; Laphookhieo, S.; Karalai, C. Absolute configuration of 3-feruloyltaraxerol dichloromethane solvate. *Acta Cryst. E* **2003**, *59*, o1864–o1866. [CrossRef]
57. Laphookhieo, S.; Karalai, C.; Ponglimanont, C.; Chantrapromma, K. Pentacyclic Triterpenoid Esters from the Fruits of *Bruguiera cylindrica*. *J. Nat. Prod.* **2004**, *67*, 886–888. [CrossRef] [PubMed]
58. Kalappurakkal, V.N.; Bhattacharya, D.; Chakravarty, S.; Uppuluri, M.V. Isolation, Synthesis and AChE Inhibitory Potential of Some Novel Cinnamyl Esters of Taraxerol, the Major Metabolite of the Mangrove *Bruguiera cylindrica*. *Chem. Biodivers.* **2018**, *15*, e1800008. [CrossRef]
59. Jiang, M.; Wu, Z.; Liu, L.; Chen, S. The chemistry and biology of fungal meroterpenoids (2009–2019). *Org. Biomol. Chem.* **2020**, *19*, 1644–1704. [CrossRef]
60. Huang, G.L.; Zhou, X.M.; Bai, M.; Liu, Y.X.; Zhao, Y.L.; Luo, Y.P.; Niu, Y.Y.; Zheng, C.J.; Chen, G.Y. Dihydroisocoumarins from the Mangrove-Derived Fungus *Penicillium citrinum*. *Mar. Drugs* **2016**, *14*, 177. [CrossRef]
61. Bai, M.; Zheng, C.J.; Huang, G.L.; Mei, R.Q.; Wang, B.; Luo, Y.P.; Zheng, C.; Niu, Z.G.; Chen, G.Y. Bioactive Meroterpenoids and Isocoumarins from the Mangrove Derived Fungus *Penicillium* sp. TGM112. *J. Nat. Prod.* **2019**, *82*, 1155–1164. [CrossRef] [PubMed]
62. Bai, M.; Zheng, C.J.; Chen, G.Y. Austins-Type Meroterpenoids from a Mangrove-Derived *Penicillium* sp. *J. Nat. Prod.* **2021**, *84*, 2104–2110. [CrossRef] [PubMed]
63. Sofian, F.F.; Suzuki, T.; Supratman, U.; Harneti, D.; Maharani, R.; Salam, S.; Abdullah, F.F.; Koseki, T.; Tanaka, K.; Kimura, K.I.; et al. Cochlioquinone derivatives produced by coculture of endophytes, *Clonostachys rosea* and *Nectria pseudotrichia*. *Fitoterapia* **2021**, *155*, 105056. [CrossRef] [PubMed]

64. Xu, Z.Y.; Xiong, B.X.; Xu, J. Chemical Investigation Of Secondary Metabolites Produced By Mangrove Endophytic Fungus *Phyllosticta Capitalensis*. *Nat. Prod. Res.* **2019**, *35*, 1561–1565. [CrossRef] [PubMed]
65. Hillier, S.G.; Lathe, R. Terpenes, hormones and life: Isoprene rule revisited. *J. Endocrinol.* **2019**, *242*, R9–R22. [CrossRef] [PubMed]
66. Chen, G.; Zhu, Y.; Wang, H.Z.; Wang, S.J.; Zhang, R.Q. The metabolites of a mangrove endophytic fungus, *Penicillium thomi*. *J. Asian Nat. Prod. Res.* **2007**, *9*, 159–164. [CrossRef] [PubMed]
67. Song, X.M.; Zhou, X.M.; Li, X.B.; Zheng, C.J.; Huang, G.L.; Yu, Z.X.; Song, X.P.; Chen, G.Y. Secondary Metabolites of a *Bruguiera sexangula var. Rhynchopetala* Derived Fungus *Phomopsis longicolla* HL-2232. *Chin. J. Org. Chem.* **2015**, *35*, 2102–2107. [CrossRef]
68. Li, J.; Wang, J.; Jiang, C.S.; Li, G.; Guo, Y.W. (+)-Cyclopenol, a new naturally occurring 7-membered 2,5-dioxopiperazine alkaloid from the fungus *Penicillium sclerotiorum* endogenous with the Chinese mangrove *Bruguiera gymnorrhiza*. *J. Asian Nat. Prod. Res.* **2014**, *16*, 542–548. [CrossRef] [PubMed]
69. Deng, C.M.; Liu, S.X.; Huang, C.H.; Pang, J.Y.; Lin, Y.C. Secondary Metabolites of a Mangrove Endophytic Fungus Aspergillus terreus (No. GX7-3B) from the South China Sea. *Mar. Drugs* **2013**, *11*, 2616–2624. [CrossRef]
70. Zhou, Z.F.; Yang, X.H.; Liu, H.L.; Gu, Y.C.; Ye, B.P.; Guo, Y.W. A New Cyclic Peptide and a New Steroid from the Fungus Penicillium sp. GD6 Isolated from the Mangrove Bruguiera gymnorrhiza. *Helv. Chim. Acta* **2014**, *97*, 1564–1570. [CrossRef]
71. Liu, Z.M.; Li, M.Q.; Wang, S.; Huang, H.B.; Zhang, W.M. Sulfur-Containing Metabolites from Marine and Terrestrial Fungal Sources: Origin, Structures, and Bioactivities. *Mar. Drugs* **2022**, *20*, 765. [CrossRef] [PubMed]
72. Liu, H.L.; Shen, X.; Jiang, H.L.; Guo, Y.W. Structural Studies on an Unusual Novel Macrocyclic Polydisulfide from the Chinese Mangrove *Bruguiera gymnorrhiza*. *Chin. J. Org. Chem.* **2008**, *28*, 246–251.
73. Nwachukwu, I.D.; Slusarenko, A.J.; Gruhlke, M.C. Sulfur and Sulfur Compounds in Plant Defence. *Nat. Prod. Commun.* **2012**, *7*, 395–400. [CrossRef] [PubMed]
74. Dahibhate, N.L.; Shukla, S.K.; Kumar, K. A Cyclic Disulfide Diastereomer From Bioactive Fraction of *Bruguiera gymnorhiza* Shows Anti–*Pseudomonas aeruginosa* Activity. *Front. Pharmacol.* **2022**, *13*, 890790. [CrossRef] [PubMed]
75. Zhang, F.Z.; Li, X.M.; Meng, L.H.; Wang, B.G. Cladocladosin A, an unusual macrolide with bicyclo 5/9 ring system, and two thiomacrolides from the marine mangrove-derived endophytic fungus, *Cladosporium cladosporioides* MA-299. *Bioorg Chem.* **2020**, *101*, 103950. [CrossRef] [PubMed]
76. Sun, Y.Q.; Guo, Y.W. Gymnorrhizol, an unusual macrocyclic polydisulfide from the Chinese mangrove *Bruguiera gymnorrhiza*. *Tetrahedron Lett.* **2004**, *45*, 5533–5535. [CrossRef]
77. Kato, A.; Takahashi, J. A new naturally occurring 1,2-dithiolane from *Bruguiera cylindrica*. *Phytochem. Lett.* **1976**, *15*, 220–221. [CrossRef]
78. Kato, A.; Numata, M. Brugierol and Isobrugierol, trans- and cis-1,2-dithiolane-1-oxide, from *Brugiera conjugata*. *Tetrahedron Lett.* **1972**, *13*, 203–206. [CrossRef]
79. Homhual, S.; Zhang, H.J.; Bunyapraphatsara, N.; Kondratyuk, T.P.; Santarsiero, B.D.; Mesecar, A.D.; Herunsalee, A.; Chaukul, W.; Pezzuto, J.M.; Fong, H.H. Bruguiesulfurol, A New Sulfur Compound from *Bruguiera gymnorrhiza*. *Planta Med.* **2006**, *72*, 255–260. [CrossRef]
80. Huang, X.Y.; Wang, Q.; Liu, H.L.; Zhang, Y.; Xin, G.R.; Shen, X.; Dong, M.L.; Guo, Y.W. Diastereoisomeric macrocyclic polydisulfides from the mangrove *Bruguiera gymnorrhiza*. *Phytochemistry* **2009**, *70*, 2096–2100. [CrossRef]
81. Hashimoto, T.; Yamada, Y. Alkaloid Biogenesis: Molecular Aspects. *Annu. Rev. Plant Physiol. Plant Mol. Biol.* **1994**, *45*, 257–285. [CrossRef]
82. Lei, F.Y.; Liu, X.D.; Huang, H.N.; Fu, S.D.; Zou, K.; Zhang, S.F.; Zhou, L.; Zeng, J.G.; Liu, H.W.; Jiang, L.H.; et al. The Macleaya cordata Symbiont: Revealing the Effects of Plant Niches and Alkaloids on the Bacterial Community. *Front. Microbiol.* **2021**, *12*, 681210. [CrossRef] [PubMed]
83. Arunpanichlert, J.; Rukachaisirikul, V.; Sukpondma, Y.; Phongpaichit, S.; Tewtrakul, S.; Rungjindamai, N.; Sakayaroj, J. Azaphilone and Isocoumarin Derivatives from the Endophytic Fungus *Penicillium sclerotiorum* PSU-A13. *Chem. Pharm. Bull.* **2010**, *58*, 1033–1036. [CrossRef] [PubMed]
84. Bracken, A.; Pocker, A.; Raistrick, H. Studies in the biochemistry of microorganisms. 93. Cyclopenin, a nitrogen-containing metabolic product of *Penicillium cyclopium* Westling. *Biochem. J.* **1954**, *57*, 587–595. [CrossRef] [PubMed]
85. Chen, Z.Y.; Qu, C.H.; Lu, J.; Cheng, G.; Gao, C.H. A new antiviral alkaloid from the hypocotyl of *Bruguiera gymnorrhiza*. *Guihaia* **2016**, *36*, 236–239.
86. Yan, L.L.; Han, N.N.; Zhang, Y.Q.; Yu, L.Y.; Chen, J.; Wei, Y.Z.; Li, Q.P.; Tao, L.; Zheng, G.H.; Yang, S.E.; et al. Antimycin A18 produced by an endophytic *Streptomyces albidoflavus* isolated from a mangrove plant. *J. Antibiot.* **2010**, *63*, 259–261. [CrossRef] [PubMed]
87. Zheng, C.J.; Liao, H.X.; Mei, R.Q.; Huang, G.L.; Yang, L.J.; Zhou, X.M.; Shao, T.M.; Chen, G.Y.; Wang, C.Y. Two new benzophenones and one new natural amide alkaloid isolated from a mangrove-derived Fungus *Penicillium citrinum*. *Nat. Prod. Res.* **2018**, *33*, 1127–1134. [CrossRef]
88. Zhou, Z.F.; Kurtán, T.; Yang, X.H.; Mándi, A.; Geng, M.Y.; Ye, B.P.; Taglialatela-Scafati, O.; Guo, Y.W. Penibruguieramine A, a Novel Pyrrolizidine Alkaloid from the Endophytic Fungus *Penicillium* sp. GD6 Associated with Chinese Mangrove *Bruguiera gymnorrhiza*. *Org. Lett.* **2014**, *16*, 1390–1393. [CrossRef]
89. Kato, A. Brugine from *Bruguiera cylindrica*. *Phytochemistry* **1975**, *14*, 1458. [CrossRef]

90. Jiang, C.S.; Zhou, Z.F.; Yang, X.H.; Lan, L.F.; Gu, Y.C.; Ye, B.P.; Guo, Y.W. Antibacterial sorbicillin and diketopiperazines from the endogenous fungus *Penicillium* sp. GD6 associated Chinese mangrove *Bruguiera gymnorrhiza*. *Chin. J. Nat. Med.* **2018**, *16*, 358–365. [CrossRef]
91. Yi, X.X.; Deng, J.G.; Gao, C.H.; Hou, X.T.; Li, F.; Wang, Z.P.; Hao, E.W.; Xie, Y.; Du, Z.C.; Huang, H.X.; et al. Four New Cyclohexylideneacetonitrile Derivatives from the Hypocotyl of Mangrove (*Bruguiera gymnorrhiza*). *Molecules* **2015**, *20*, 14565–14575. [CrossRef] [PubMed]
92. Li, M.Y.; Chang, M.; Zhang, Q.H.; He, R.F.; Ye, B.P. The endophytic fungus strain ZD6 isolated from the stem of *Bruguiera gymnorrhiza* and the antibacterial activity of its metabolites. *Mycosystema* **2010**, *29*, 739–745.
93. Li, C.Y.; Chen, M.; Ding, W.J.; Lin, Y.C.; Zhou, S.N. Study on the Metabolites of Endophytic Fungus (*Gloesporium sp.*) Isolated from *Bruguiera gymnoihiza* Grown in the South China Sea. *J. South. China Agric. Univ.* **2008**, *29*, 122–124.
94. Zheng, C.J.; Wu, L.Y.; Li, X.B.; Song, X.M.; Niu, Z.G.; Song, X.P.; Chen, G.Y.; Wang, C.Y. Structure and Absolute Configuration of Aspergilumamide A, a Novel Lumazine Peptide from the Mangrove-Derived Fungus *Aspergillus* Sp. *Helv. Chim. Acta* **2015**, *98*, 368–373. [CrossRef]
95. Laohavisit, A.; Wakatake, T.; Ishihama, N.; Mulvey, H.; Takizawa, K.; Suzuki, T.; Shirasu, K. Quinone perception in plants via leucine-rich-repeat receptor-like kinases. *Nature* **2020**, *587*, 92–97. [CrossRef]
96. Krueger, M.C.; Bergmann, M.; Schlosser, D. Widespread ability of fungi to drive quinone redox cycling for biodegradation. *Fems Microbiol. Lett.* **2016**, *363*, fnw105. [CrossRef]
97. Klaiklay, S.; Rukachaisirikul, V.; Sukpondma, Y.; Phongpaichit, S.; Buatong, J.; Bussaban, B. Metabolites from the Mangrove-derived Fungus *Xylaria cubensis* PSU-MA34. *Arch. Pharm. Res.* **2012**, *35*, 1127–1131. [CrossRef] [PubMed]
98. Cai, Y.S.; Kurtán, T.; Miao, Z.H.; Mándi, A.; Komáromi, I.; Liu, H.L.; Ding, J.; Guo, Y.W. Palmarumycins BG1-BG7 and Preussomerin BG1: Establishment of Their Absolute Configurations Using Theoretical Calculations of Electronic Circular Dichroism Spectra. *J. Org. Chem.* **2011**, *76*, 1821–1830. [CrossRef]
99. Kongyen, W.; Rukachaisirikul, V.; Phongpaichit, S.; Sakayaroj, J. A new hydronaphthalenone from the mangrove-derived *Daldinia eschscholtzii* PSU-STD57. *Nat. Prod. Res.* **2015**, *29*, 1995–1999. [CrossRef]
100. Yang, L.J.; Liao, H.X.; Bai, M.; Huang, G.L.; Luo, Y.P.; Niu, Y.Y.; Zheng, C.J.; Wang, C.Y. One new cytochalasin metabolite isolated from a mangrove-derived fungus *Daldinia eschscholtzii* HJ001. *Nat. Prod. Res.* **2018**, *32*, 208–213. [CrossRef]
101. Ukwatta, K.M.; Lawrence, J.L.; Wijayarathna, C.D. The study of antimicrobial, anti-cancer, antiinflammatory and α-glucosidase inhibitory activities of Nigronapthaphenyl, isolated from an extract of *Nigrospora sphaerica*. *Mycology* **2019**, *10*, 222–228. [CrossRef] [PubMed]
102. Zheng, C.J.; Huang, G.L.; Xu, Y.; Song, X.M.; Yao, J.; Liu, H.; Wang, R.P.; Sun, X.P. A new benzopyrans derivatives from a mangrove-derived fungus *Penicillium citrinum* from the South China Sea. *Nat. Prod. Res.* **2015**, *30*, 821–825. [CrossRef]
103. Liao, H.X.; Shao, T.M.; Mei, R.Q.; Huang, G.L.; Zhou, X.M.; Zheng, C.J.; Wang, C.Y. Bioactive Secondary Metabolites from the Culture of the Mangrove-Derived Fungus *Daldinia eschscholtzii* HJ004. *Mar. Drugs* **2019**, *17*, 710. [CrossRef] [PubMed]
104. Li, S.J.; Jiao, F.W.; Li, W.; Zhang, X.; Yan, W.; Jiao, R.H. Cytotoxic Xanthone Derivatives from the Mangrove-Derived Endophytic Fungus *Peniophora incarnata* Z4. *J. Nat. Prod.* **2020**, *83*, 2976–2982. [CrossRef] [PubMed]
105. He, K.Y.; Zhang, C.; Duan, Y.R.; Huang, G.L.; Yang, C.Y.; Lu, X.R.; Zheng, C.J.; Chen, G.Y. New chlorinated xanthone and anthraquinone produced by a mangrove-derived fungus *Penicillium citrinum* HL-5126. *J. Antibiot.* **2017**, *70*, 823–827. [CrossRef]
106. Zhou, X.M.; Zheng, C.J.; Chen, G.Y.; Song, X.P.; Han, C.R.; Li, G.N.; Fu, Y.H.; Chen, W.H.; Niu, Z.G. Bioactive Anthraquinone Derivatives from the Mangrove-Derived Fungus *Stemphylium* sp. 33231. *J. Nat. Prod.* **2014**, *77*, 2021–2028. [CrossRef]
107. Li, X.B.; Chen, G.Y.; Liu, R.J.; Zheng, C.J.; Song, X.M.; Han, C.R. A new biphenyl derivative from the mangrove endophytic fungus *Phomopsis longicolla* HL-2232. *Nat. Prod. Res.* **2017**, *31*, 2264–2267. [CrossRef] [PubMed]
108. Supratman, U.; Suzuki, T.; Nakamura, T.; Yokoyama, Y.; Harneti, D.; Maharani, R.; Salam, S.; Abdullah, F.F.; Koseki, T.; Shiono, Y. New metabolites produced by endophyte *Clonostachys rosea* B5-2. *Nat. Prod. Res.* **2019**, *35*, 1525–1531. [CrossRef]
109. Macías-Rubalcava, M.L.; Garrido-Santos, M.Y. Phytotoxic compounds from endophytic fungi. *Appl. Microbiol. Biotechnol.* **2022**, *106*, 931–950. [CrossRef]
110. Su, J.H.; Wang, M.Q.; Li, Y.Z.; Lin, Y.S.; Gu, J.Y.; Zhu, L.P.; Yang, W.Q.; Jiang, S.Q.; Zhao, Z.X.; Sun, Z.H. Rare cytochalasans isolated from the mangrove endophytic fungus *Xylaria arbuscula*. *Fitoterapia* **2022**, *157*, 105124. [CrossRef]
111. Huang, H.B.; Li, Q.; Feng, X.J.; Chen, B.; Wang, J.; Liu, L.; She, Z.G.; Lin, Y.C. Structural elucidation and NMR assignments of four aromatic lactones from amangrove endophytic fungus (No. GX4-1B). *Magn. Reson. Chem. MRC* **2010**, *48*, 496–499. [CrossRef] [PubMed]
112. Li, J.L.; Chen, T.; Yu, J.C.; Jia, H.; Chen, C.; Long, Y.H. New Sorbicillinoids from the Mangrove Endophytic Fungus *Trichoderma reesei* SCNU-F0042. *Mar. Drugs* **2023**, *21*, 442. [CrossRef]
113. Zou, G.; Tan, Q.; Chen, Y.; Yang, W.C.; Zang, Z.M.; Jiang, H.M.; Chen, S.Y.; Wang, B.; She, Z.G. Furobenzotropolones A, B and 3-Hydroxyepicoccone B with Antioxidative Activity from Mangrove Endophytic Fungus *Epicoccum nigrum* MLY-3. *Mar. Drugs* **2021**, *19*, 395. [CrossRef]
114. Zhang, F.Z.; Li, X.M.; Li, X.; Yang, S.Q.; Meng, L.H.; Wang, B.G. Polyketides from the Mangrove-Derived Endophytic Fungus *Cladosporium cladosporioides*. *Mar. Drugs* **2019**, *17*, 296. [CrossRef]
115. Deng, P.F.; Luo, Y.P.; Niu, Y.Y.; Zheng, C.J.; Chen, G.Y.; Chen, J.; Ma, W.H. A New Penicitrinone Derivative from the Endophytic Fungus *Penicillium* sp. from *Bruguiera sexangula var. rhynchopetala*. *Chem. Nat. Compd.* **2016**, *52*, 810–812. [CrossRef]

116. Chen, S.; Wang, X.J.; Cheng, Y.; Gao, H.S.; Chen, X.H. A Review of Classification, Biosynthesis, Biological Activities and Potential Applications of Flavonoids. *Molecules* **2023**, *28*, 4982. [CrossRef]
117. Wu, Y.Z.; Qiao, F.; Xu, G.W.; Zhao, J.; Teng, J.F.; Li, C.; Deng, W.J. Neuroprotective metabolites from the endophytic fungus *Penicillium citrinum* of the mangrove *Bruguiera gymnorrhiza*. *Phytochem. Lett.* **2015**, *12*, 148–152. [CrossRef]
118. Hu, Y.O.; Ye, B.P.; Wang, D.Y. Study on the bioactivity of 3′,4′,5′-trihydroxy-7-hydroxy-5-methoxyflavone extracted from *Bruguiera gymnorrhiza* by *C.elegans*. *Chin. J. Mar. Drugs* **2007**, *26*, 20–26.
119. Panyadee, A.; Sahakitpichan, P.; Ruchirawat, S.; Kanchanapoom, T. 5-Methyl ether flavone glucosides from the leaves of *Bruguiera gymnorrhiza*. *Phytochem. Lett.* **2015**, *11*, 215–219. [CrossRef]
120. Barik, R.; Sarkar, R.; Biswas, P.; Bera, R.; Sharma, S.; Nath, S.; Karmakar, S.; Sen, T. 5,7-dihydroxy-2-(3-hydroxy-4, 5-dimethoxy-phenyl)-chromen-4-one-a flavone from *Bruguiera gymnorrhiza* displaying anti-inflammatory properties. *Indian. J. Pharmacol.* **2016**, *48*, 304–311.
121. Yao, J.E.; Shen, M.R.; Yi, X.X.; Yang, Y.; Gao, C.H. A New 8-Hydroxyquercetagetin Glycoside from the Hypocotyls of Mangrove *Bruguiera gymnorrhiza*. *Chem. Nat. Comp.* **2017**, *53*, 33–35. [CrossRef]
122. Borges, F.; Roleira, F.; Milhazes, N.; Santana, L.; Uriarte, E. Simple coumarins and analogues in medicinal chemistry: Occurrence, synthesis and biological activity. *Curr. Med. Chem.* **2005**, *12*, 887–916. [CrossRef]
123. Stringlis, I.A.; de Jonge, R.; Pieterse, C.M.J. The Age of Coumarins in Plant–Microbe Interactions. *Plant Cell Physiol.* **2019**, *60*, 1405–1419. [CrossRef]
124. Yi, X.X.; Gao, C.H.; He, B.J.; Chen, B. Study on phenylpropanoids from hypocotyls of the mangrove plant *Bruguiera gymnorrhiza*. *Guihaia* **2013**, *33*, 191–194.
125. Han, Z.; Mei, W.L.; Zhao, Y.X.; Deng, Y.Y.; Dai, H.F. A new cytotoxic isocoumarin from endophytic fungus *Penicillium sp.* 091402 of the mangrove plant *Bruguiera sexangula*. *Chem. Nat. Compd.* **2009**, *45*, 805–807. [CrossRef]
126. Han, L.; Huang, X.S.; Sattler, I.; Fu, H.Z.; Grabley, S.; Lin, W.H. Two new constituents from mangrove *Bruguiera gymnorrhiza*. *J. Asian Nat. Prod. Res.* **2007**, *9*, 327–331. [CrossRef] [PubMed]
127. Shang, S.S.; Long, S.J. Brugnanin, a new syn-2,3-dihydrobenzofuran neolignan dioate from the mangrove *Bruguiera gymnorrhiza*. *Chem. Nat. Compd.* **2008**, *44*, 186–189. [CrossRef]
128. Bao, S.; Ding, Y.; Deng, Z.; Proksch, P.; Lin, W. Rhyncosides A-F, phenolic constituents from the Chinese mangrove plant *Bruguiera sexangula var. rhynchopetala*. *Chem. Pharm. Bull.* **2007**, *55*, 1175–1180. [CrossRef]
129. Shalaby, S.; Horwitz, B.A. Plant phenolic compounds and oxidative stress: Integrated signals in fungal-plant interactions. *Curr. Genet.* **2015**, *61*, 347–357. [CrossRef]
130. Han, L.; Huang, X.S.; Sattler, I.; Moellmann, U.; Fu, H.Z.; Lin, W.H.; Grabley, S. New aromatic compounds from the marine mangrove *Bruguiera gymnorrhiza*. *Planta Med.* **2005**, *71*, 160–164. [CrossRef]
131. Gao, C.H.; Long, B.; Su, Z.W.; Yu, L.; Yan, D.M.; Wen, L.J.; He, B.J. Study on Aromatic Compounds from Hypocotyls of Mangrove *Bruguiera gymnorrhiza*. *J. Guangxi Acad. Sci.* **2015**, *31*, 28–31.
132. Seshadri, T.R.; Trikha, R.K. Procyanidin of *Bruguiera parviflora*. *Indian. J. Chem.* **1971**, *9*, 302–304.
133. Chokpaiboon, S.; Choodej, S.; Boonyuen, N.; Teerawatananond, T.; Pudhom, K. Highly oxygenated chromones from mangrove-derived endophytic fungus *Rhytidhysteron rufulum*. *Phytochemistry* **2016**, *122*, 172–177. [CrossRef]
134. Sriyatep, T.; Maneerat, W.; Sripisut, T.; Cheenpracha, S.; Machan, T.; Phakhodee, W.; Laphookhieo, S. Cowabenzophenones A and B, two new tetracyclo[7.3.3.33,11.03,7]tetradecane-2,12,14-trione derivatives, from ripe fruits of *Garcinia cowa*. *Fitoterapia* **2014**, *92*, 285–289. [CrossRef]
135. Ukwatta, K.M.; Lawrence, J.L.; Wijayarathne, C.D. Antimicrobial, anti-cancer, anti-filarial and antiinflammatory activities of Cowabenzophenone A extracted from the endophytic fungus *Aspergillus terreus* isolated from a mangrove plant *Bruguiera gymnorrhyza*. *Mycology* **2019**, *11*, 297–305. [CrossRef] [PubMed]
136. Tao, L.; Habden, X.; Han, N.N.; Yu, S.Y.; Yan, L.L.; Luan, Y.C.; Liu, S.W.; Guo, L.J.; Zhong, K.; Yu, L.Y.; et al. Separation, purification and structural identification of an active nematicidal component from the fermentation broth of Endophytic streptomyces I07A-01824 from Mangrove ecosystem. *Chin. Med. Biotechnol.* **2012**, *7*, 5–8.
137. Uddin, S.J.; Grice, I.D.; Tiralongo, E. Cytotoxic Effects of Bangladeshi Medicinal Plant Extracts. *Evid.-Based Complement. Altern. Med. Ecam.* **2011**, *2011*, 578092. [CrossRef] [PubMed]
138. Huang, M.Q.; Tao, G.L.; Tian, S.H.; Yang, Z.X.; Yao, M.Z.; Huang, L.; Fu, J. Inhibitory effect of *Bruguiera sexangula* leaves extract on gastric cancer cells proliferation and its acute toxicity in mice. *Chin. J. Mar. Drugs* **2018**, *37*, 39–44. [CrossRef] [PubMed]
139. Qayoom, H.; Alkhanani, M.; Almilaibary, A.; Alsagaby, S.A.; Mir, M.A. A network pharmacology-based investigation of brugine reveals its multi-target molecular mechanism against Breast Cancer. *Med. Oncol.* **2023**, *40*, 202. [CrossRef]
140. Hosen, M.Z.; Biswas, A.; Islam, M.R.; Hossain, S.J. Anti-Bacterial, Anti-Diarrheal, and Cytotoxic Activities of Edible Fruits in the Sundarbans Mangrove Forest of Bangladesh. *Prev. Nutr. Food Sci.* **2021**, *26*, 192–199. [CrossRef]
141. Acharya, S.; Patra, D.K.; Pradhan, C.; Mohapatra, P.K. Anti-bacterial, anti-fungal and anti-oxidative properties of different extracts of *Bruguiera gymnorrhiza* L. (Mangrove). *Eur. J. Integr. Med.* **2020**, *36*, 101140. [CrossRef]
142. Sadeer, N.B.; Sinan, K.I.; Cziáky, Z.; Jeko, J.; Zengin, G.; Jeewon, R.; Abdallah, H.H.; Rengasamy, K.R.R.; Mahomoodally, M.F. Assessment of the Pharmacological Properties and Phytochemical Profile of *Bruguiera gymnorhiza* (L.) Lam Using In Vitro Studies, In Silico Docking, and Multivariate Analysis. *Biomolecules* **2020**, *10*, 731. [CrossRef] [PubMed]

143. Abeysinghe, P.D. Antibacterial Activity of some Medicinal Mangroves against Antibiotic Resistant Pathogenic Bacteria. *Indian. J. Pharm. Sci.* **2010**, *72*, 167–172. [CrossRef] [PubMed]
144. Golder, M.; Sadhu, S.K.; Biswas, B.; Islam, T. Comparative pharmacologic profiles of leaves and hypocotyls of a mangrove plant: *Bruguiera gymnorrhiza*. *Adv. Tradit. Med.* **2020**, *20*, 395–403. [CrossRef]
145. Tao, G.L.; Yang, F.; Tian, S.H.; Huang, L.; Huang, M.Q. The antioxidative and melanin-inhibitory effects of alcohol extract of *Bruguiera sexangula* leaves. *Chin. J. Mar. Drugs* **2019**, *38*, 59–63.
146. Liu, X.L.; Chen, T.; Wang, Q.; Liu, J.A.; Lu, Y.H.; Shi, Y. Structure Analysis and Study of Biological Activities of Condensed Tannins from *Bruguiera gymnorhiza* (L.) Lam and Their Effect on Fresh-Cut Lotus Roots. *Molecules* **2021**, *26*, 1369. [CrossRef] [PubMed]
147. Song, Q.; Xie, X.G.; Hu, Z.; Xue, J.Y.; Zhang, S.L.; Xie, X.M. (Z)-7,4'-dimethoxy-6-hydroxy-aurone-4-O-β-glucopyranoside attenuates lipoteichoic acid-induced damage in rat cardiomyoblast cells. *J. Int. Med. Res.* **2020**, *48*, 300060519889716. [CrossRef] [PubMed]
148. Chen, J.F.; Luo, D.D.; Lin, Y.S.; Liu, Y.H.; Wu, J.Z.; Yi, X.Q.; Wu, Y.; Zhang, Q.; Gao, C.J.; Cai, J.; et al. Aqueous extract of *Bruguiera gymnorrhiza* leaves protects against dextran sulfate sodium induced ulcerative colitis in mice via suppressing NF-κB activation and modulating intestinal microbiota. *J. Ethnopharmacol.* **2020**, *251*, 112554. [CrossRef] [PubMed]
149. Lin, Y.S.; Zheng, X.H.; Chen, J.F.; Luo, D.D.; Xie, J.H.; Su, Z.R.; Huang, X.Q.; Yi, X.Q.; Wei, L.; Cai, J.; et al. Protective Effect of *Bruguiera gymnorrhiza* (L.) Lam. Fruit on Dextran Sulfate Sodium-Induced Ulcerative Colitis in Mice: Role of Keap1/Nrf2 Pathway and Gut Microbiota. *Front. Pharmacol.* **2020**, *10*, 1602. [CrossRef]
150. Zhang, X.; Mai, J.-H.; Gao, Z.-W.; Wang, L.-L.; Emran, T.B. *Bruguiera gymnorrhiza* (L.) Lam. Fruit Accelerates Healing in Gastric Injury via the Regulation of the NF-κB Pathway. *Evid.-Based Complement. Altern. Med.* **2022**, *2022*, 1046712. [CrossRef]
151. Amalia, R.; Pramono, A.; Afifah, D.N.; Noer, E.R.; Muniroh, M.; Kumoro, A.C. Mangrove fruit (*Bruguiera gymnorhiza*) increases circulating GLP-1 and PYY, modulates lipid profiles, and reduces systemic inflammation by improving SCFA levels in obese wistar rats. *Heliyon* **2022**, *8*, e10887. [CrossRef] [PubMed]
152. Eldeen, I.M.S.; Ringe, J.; Ismail, N. Inhibition of Pro-inflammatory Enzymes and Growth of an Induced Rheumatoid Arthritis Synovial Fibroblast by *Bruguiera cylindrica*. *Int. J. Pharmacol.* **2019**, *15*, 916–925. [CrossRef]
153. Hou, S.S.; Liang, C.Y.; Gao, C.H.; Jiang, C.P.; Tang, Q.Q.; Liu, Y.H.; Yi, X.X. Species diversity and anti-hepatitis B virus activity of culturable bacteria isolated from the habitat of *Bruguiera gymnorrhiza*. *Guihaia* **2023**, *43*, 616–625.
154. Bibi Sadeer, N.; Haddad, J.G.; Oday Ezzat, M.; Desprès, P.; Abdallah, H.H.; Zengin, G.; Uysal, A.; El Kalamouni, C.; Gallo, M.; Montesano, D.; et al. *Bruguiera gymnorhiza* (L.) Lam. at the Forefront of Pharma to Confront Zika Virus and Microbial Infections—An In Vitro and In Silico Perspective. *Molules* **2021**, *26*, 5768. [CrossRef] [PubMed]
155. Murugan, K.; Dinesh, D.; Paulpandi, M.; Althbyani, A.D.; Subramaniam, J.; Madhiyazhagan, P.; Wang, L.; Suresh, U.; Kumar, P.M.; Mohan, J.; et al. Nanoparticles in the fight against mosquito-borne diseases: Bioactivity of *Bruguiera cylindrica*-synthesized nanoparticles against dengue virus DEN-2 (in vitro) and its mosquito vector *Aedes aegypti* (Diptera: Culicidae). *Parasitol. Res.* **2015**, *114*, 4349–4361. [CrossRef] [PubMed]
156. Bibi Sadeer, N.; Sinan, K.I.; Cziáky, Z.; Jekő, J.; Zengin, G.; Jeewon, R.; Abdallah, H.H.; AlDhaheri, Y.; Eid, A.H.; Mahomoodally, M.F. Towards the Pharmacological Validation and Phytochemical Profiling of the Decoction and Maceration of *Bruguiera gymnorhiza* (L.) Lam.—A Traditionally Used. *Molules* **2022**, *27*, 2000. [CrossRef] [PubMed]
157. Pitchaipillai, R.; Ponniah, T. In Vitro Antidiabetic Activity of Ethanolic Leaf Extract of *Bruguiera cylindrica* L.—Glucose Uptake by Yeast Cells Method. *IBBJ* **2016**, *2*, 171–175.
158. Revathi, P.; Jeyaseelan, S.C.; Subramanian, P.; Manickavasagam, S.; Prabhu, N. A comparative mechanism of antidiabetic role of various extracts of *Bruguriera cylindrica* L leaves. *World J. Pharm. Pharm. Sci.* **2015**, *4*, 1168–1176.
159. Gong, J.X.; Shen, X.; Yao, L.G.; Jiang, H.L.; Krohn, K.; Guo, Y.W. Total Synthesis of Gymnorrhizol, an Unprecedented 15-Membered Macrocyclic Polydisulfide from the Chinese Mangrove *Bruguiera gymnorrhiza*. *Org. Lett.* **2007**, *9*, 1715–1716. [CrossRef]
160. Ravikumar, S.; Inbaneson, S.J.; Suganthi, P.; Gnanadesigan, M. In vitro antiplasmodial activity of ethanolic extracts of mangrove plants from South East coast of India against chloroquine-sensitive *Plasmodium falciparum*. *Parasitol. Res.* **2011**, *108*, 873–878. [CrossRef]
161. Ravikumar, S.; Inbaneson, S.J.; Suganthi, P.; Venkatesan, M.; Ramu, A. Mangrove plants as a source of lead compounds for the development of new antiplasmodial drugs from South East coast of India. *Parasitol. Res.* **2011**, *108*, 1405–1410. [CrossRef] [PubMed]
162. Mahmud, I.; Zilani, M.N.H.; Biswas, N.N.; Bokshi, B. Bioactivities of *Bruguiera gymnorrhiza* and profiling of its bioactive polyphenols by HPLC-DAD. *Clin. Phytoscience* **2017**, *3*, 11. [CrossRef]
163. Sun, Z.W.; Tian, F.; An, M.; Duan, S.S. Inhibitive effects of organic solvent extracts from mangrove plant *Bruguiera gymnorrhiza* on *Phaeocystis globosa*. *Ecol. Sci.* **2012**, *31*, 245–251.
164. Cui, J.L.; Guo, S.X.; Xiao, P.G. Interaction between endophytes and host plant and the role of endophytes in genuineness analysis of medicinal plant. *Acta Pharm. Sin.* **2017**, *52*, 214–221.
165. Quach, N.T.; Vu, T.H.N.; Bui, T.L.; Le, T.T.X.; Nguyen, T.T.A.; Ngo, C.C.; Phi, Q.-T. Genomic and physiological traits provide insights into ecological niche adaptations of mangrove endophytic *Streptomyces parvulus* VCCM 22513. *Ann. Microbiol.* **2022**, *72*, 27. [CrossRef]

166. Ma, Q.; Lei, R.F.; Abudourousuli, D.; Aosiman, M.; Rouzi, Z.; An, D.D. Research Progress on the Symbiotic Metabolic of Endophytes and Plants Under Stress. *Biotechnol. Bull.* **2021**, *37*, 153–161.
167. Liu, Y.L.; Qin, Y.Y.; Zheng, H.L. Research Progresses of Water Logging Tolerance and High Saline Adaptation of Mangrove Plants. *J. Xiamen Univ. (Nat. Sci.)* **2017**, *56*, 314–322.
168. Elias, L.M.; Fortlzamp, D.; Sartori, S.B.; Ferreira, M.C.; Gomes, L.H.; Azevedo, J.L.; Montoya, Q.V.; Rodrigues, A.; Ferreira, A.G.; Lira, S.P. The potential of compounds isolated from *Xylaria* spp. as antifungal agents against anthracnose. *Braz. J. Microbiol.* **2018**, *49*, 840–847. [CrossRef] [PubMed]
169. Zhang, Q.; Xiao, J.; Sun, Q.Q.; Qin, J.C.; Pescitelli, G.; Gao, J.M. Characterization of Cytochalasins from the Endophytic *Xylaria* sp. and Their Biological Functions. *J. Agric. Food Chem.* **2014**, *62*, 10962–10969. [CrossRef]
170. Betina, V.; Mičeková, D.; Němec, P. Antimicrobial Properties of Cytochalasins and Their Alteration of Fungal Morphology. *Microbiology* **1972**, *71*, 343–349. [CrossRef]
171. Prasain, J.K.; Ueki, M.; Stefanowicz, P.; Osada, H. Rapid screening and identification of cytochalasins by electrospray tandem mass spectrometry. *J. Mass Spectrom. JMS* **2002**, *37*, 283–291. [CrossRef] [PubMed]
172. Fujii, Y.; Tani, H.; Ichinoe, M.; Nakajima, H. Zygosporin D and Two New Cytochalasins Produced by the Fungus *Metarrhizium anisopliae*. *J. Nat. Prod.* **2000**, *63*, 132–135. [CrossRef] [PubMed]
173. Kumarihamy, M.; Ferreira, D.; Croom, E.M.; Sahu, R.; Tekwani, B.L.; Duke, S.O.; Khan, S.; Techen, N.; Nanayakkara, N.P.D. Antiplasmodial and Cytotoxic Cytochalasins from an Endophytic Fungus, *Nemania* sp. UM10M, Isolated from a Diseased *Torreya taxifolia* Leaf. *Molecules* **2019**, *24*, 777. [CrossRef] [PubMed]
174. Ntemafack, A.; Chouhan, R.; Kapoor, N.; Kumar, A.; Dhiman, S.K.; Manhas, R.S.; Chaubey, A.; Hassan, Q.P.; Gandhi, S.G. Protective effect of *Bacillus* species associated with *Rumex dentatus* against postharvest soil borne disease in potato tubers and GC–MS metabolite profile. *Arch. Microbiol.* **2022**, *204*, 583. [CrossRef] [PubMed]
175. Cui, S.; Wakatake, T.; Hashimoto, K.; Saucet, S.B.; Toyooka, K.; Yoshida, S.; Shirasu, K. Haustorial Hairs Are Specialized Root Hairs That Support Parasitism in the Facultative Parasitic Plant *Phtheirospermum japonicum*. *Plant Physiol.* **2016**, *170*, 1492–1503. [CrossRef]
176. Chong, J.; Baltz, R.; Schmitt, C.; Beffa, R.; Fritig, B.; Saindrenan, P. Downregulation of a pathogen-responsive tobacco UDP-Glc:phenylpropanoid glucosyltransferase reduces scopoletin glucoside accumulation, enhances oxidative stress, and weakens virus resistance. *Plant Cell* **2002**, *14*, 1093–1107. [CrossRef] [PubMed]
177. Garcia, D.; Sanier, C.; Macheix, J.J.; D'Auzac, J. Accumulation of scopoletin in *Hevea brasiliensis* infected by *Microcyclus ulei* (P. Henn.) V.ARX and evaluation of its fungitoxicity for three leaf pathogens of rubber tree. *Physiol. Mol. Plant Pathol.* **1995**, *47*, 213–223. [CrossRef]
178. Rauckman, B.S.T.; Mary, Y.; Johnson, J.V.; Roth, B. 2,4-Diamino-5-benzylpyrimidines and analogs as antibacterial agents. 10. 2,4-Diamino-5-(6-quinolylmethyl)- and -[(tetrahydro-6-quinolyl)methyl]pyrimidine derivatives. Further specificity studies. *J. Med. Chem.* **1989**, *32*, 1927–1935. [CrossRef] [PubMed]
179. Segaran, G.; Sathiavelu, M. Fungicidal and plant growth-promoting traits of *Lasiodiplodia pseudotheobromae*, an endophyte from *Andrographis paniculata*. *Front. Plant Sci.* **2023**, *14*, 1125630. [CrossRef]
180. Khan, I.H.; Javaid, A. DNA cleavage of the fungal pathogen and production of antifungal compounds are the possible mechanisms of action of biocontrol agent *Penicillium italicum* against *Macrophomina phaseolina*. *Mycologia* **2022**, *114*, 24–34. [CrossRef]
181. Patel, T.K.; Williamson, J.D. Mannitol in Plants, Fungi, and Plant–Fungal Interactions. *Trends Plant Sci.* **2016**, *21*, 486–497. [CrossRef] [PubMed]
182. Jennings, D.B.; Ehrenshaft, M.; Pharr, D.M.; Williamson, J.D. Roles for mannitol and mannitol dehydrogenase in active oxygen-mediated plant defense. *Proc. Natl. Acad. Sci. USA* **1998**, *95*, 15129–15133. [CrossRef] [PubMed]
183. Kaul, S.; Sharma, T.; Dhar, M.K. "Omics" Tools for Better Understanding the Plant-Endophyte Interactions. *Front. Plant Sci.* **2016**, *7*, 955. [CrossRef] [PubMed]

MDPI AG
Grosspeteranlage 5
4052 Basel
Switzerland
Tel.: +41 61 683 77 34

Marine Drugs Editorial Office
E-mail: marinedrugs@mdpi.com
www.mdpi.com/journal/marinedrugs

Academic Open
Access Publishing

mdpi.com

ISBN 978-3-7258-8562-6